# Cortisol synthesis by primary human keratinocytes

Hannen, Rosalind Francesca

# Cortisol Synthesis by Primary Human Keratinocytes

**Rosalind Francesca Hannen**

Queen Mary University of London

Doctorate of Philosophy

**Abstract**

Cortisol analogues have been used to treat skin disorders, such as psoriasis and atopic dermatitis, for over 50 years but the ability of normal human keratinocytes to synthesise cortisol has not been reported. Keratinocytes are capable of *de novo* cholesterol synthesis, they express P450 enzymes that are required for steroidogenesis and can metabolise androgens and estrogens. In addition, steroidogenic acute regulatory protein (StAR) that controls the rate determining step of acute steroidogenesis has been identified in the epidermis. The aim of this thesis was to identify *de novo* cortisol steroidogenesis by keratinocytes and investigate the function of cortisol in keratinocytes *in vitro*.

Normal epidermis was shown to express three cholesterol transporters that are associated with promoting steroid synthesis; StAR was identified in the basal layer, metastatic lymph node 64 (MLN64) in the suprabasal layers and translocator protein (TSPO) was detected throughout the epidermal layers. In addition, the nuclear receptor DAX1, a negative regulator of StAR, was identified in the cytoplasm of cells that form normal epidermis. Comparatively, the expression of these proteins was altered in psoriasis and atopic dermatitis, where DAX1 was localised to the nucleus of most diseased tissue and StAR was not detected. This suggests that acute steroid synthesis is ablated in these hyperproliferative skin conditions.

The ability of normal primary human keratinocytes to synthesise cortisol was investigated. Radioimmunoassay demonstrated keratinocytes were capable of *de novo* pregnenolone synthesis, which was promoted with the cortisol analogue dexamethasone (dex). Interestingly, 25-hydroxycholesterol, which bypasses StAR, did not further enhance steroid synthesis. This suggests that there is an alternative rate determining step of steroid synthesis in cultured primary keratinocytes. Thin layer chromatography demonstrated keratinocytes could metabolise pregnenolone to progesterone and progesterone to cortisol. Progesterone metabolism to cortisol was also confirmed with liquid chromatography/mass spectroscopy.

Dex was shown to maintain keratinocyte viability and was implicated in promoting cellular redox potential. Since redox potential is a critical regulator of steroidogenesis, this observation could provide a mechanism for dex-induced pregnenolone synthesis in cultured keratinocytes. These observations led to a hypothesis that local cortisol synthesis functions to regulate cellular redox potential to prevent cell death as part of a positive feedback system. Therefore, this thesis has identified the cortisol steroidogenic pathway in primary human keratinocytes and a potential functional mechanism for the pathway.

**Statement of copyright**



**Declaration**

The work contained in this thesis is the independent work of the author (except where stated) with advice and guidance from the supervisors Professor Jacky Burrin and Professor Mike Philpott.

## Abstracts

**R.F. Hannen**, A.E. Michael, M.P. Philpott, A.J. Clark, J.M. Burrin. Cortisol Synthesis by Primary Human Keratinocytes; Implications for Skin Biology. 91st Annual Meeting ENDO 09, Washington DC, 10-13th June 2009. Poster presentation.

**Hannen R.F**., Michael A.E., Burrin J., Philpott M. Cortisol synthesis and regulation of proliferation in keratinocytes. *Journal of Investigative Dermatology* (2008) 128: S139, Kyoto, Japan. Poster presentation.

**Hannen R.F.**, Michael A.E., Burrin J., Philpott M. StAR role for glucocorticoid synthesis in keratinocytes. BSID Annual Meeting, University of Oxford, 7-9th April 2008. Oral communication.

**Hannen R.**, Michael A., Burrin J., Philpott M. Human skin and keratinocytes express cholesterol transporters and primary keratinocytes are capable of metabolising progesterone into cortisol. 37th Annual Meeting of the European Society of Dermatological Research. Zurich, Switzerland, 5th-8th September 2007. Poster presentation.

## Awards

Oral Presentation Prize winner, ICMS Graduate School Day, Queen Mary's, May 2008.

Oral Presentation Prize winner, BSID Annual Meeting, University of Oxford, 7-9 April 2008.

Travel Award, BSID Annual Meeting, University of Oxford, 7-9 April 2008.

**Contents**

**Figures**

**Tables**

**Abbreviations**

| | |
|---|---|
| 3βHSD | 3β-hydroxysteroid dehydrogenase |
| 11βHSD | 11β-hydroxysteroid dehydrogenase |
| 6PGDH | 6-phospho-gluconate dehydrogenase |
| ACTH | Adrenal corticotrophic hormone |
| AD | Atopic dermatitis |
| AF2 | Transcription activation function 2 |
| AHC | X-linked adrenal hypoplasia congenital |
| AKAP | A-kinase anchoring protein |
| ANOVA | Analysis of variance |
| ANT | Adenine nucleotide carrier |
| APC | Alloplycocyanin |
| ATF2 | Activating transcription factor 2 |
| BSA | Bovine serum albumin |
| BrdU | Bromodeoxyuridine |
| CAH | Congenital adrenal hyperplasia |
| cAMP | Cyclic adenosine monophosphate |
| CCHCRI | Coiled-coil alpha helical rod protein |
| cDNA | Complementary deoxyribonucleic acid |
| CDSN | Corneodesmosin |
| C/EBPβ | CCAAT/enhancer binding protein |
| CHAPS | 3-[(3-cholamidopropyl)dimethylammonio]-1-propanesulfonate |
| CRH | Corticotrophic releasing hormone |
| CRE | cAMP response element |
| CREB | cAMP-response element binding protein |
| CREM | cAMP-responsive element modulator |
| CRH | Corticotrophin releasing hormone |
| $CO_2$ | Carbon dioxide |
| CYP | Cytochrome P450 enzyme |
| DAPI | 4',6-diamidion-2-phenylindole dihydrochloride |
| dATP | Deoxyadenosine 5'-triphosphate |

| | |
|---|---|
| DAX1 | Dosage-sensitive sex reversal, adrenal hypoplasia critical region, on chromosome X, gene 1 |
| DBD | DNA binding domain |
| DBI | Diazapam binding inhibitor |
| dCTP | Deoxycytosine 5'-triphosphate |
| DEPC | Diethyl-pyrocarbonate |
| DED | Depidermalised dermis |
| Dex | Dexamethasone |
| DF | Differential filter |
| dGTP | Deoxyguanine 5'-triphosphate |
| DHEA | Dehydroepiandrosterone |
| DHT | Dihydrotestosterone |
| DMEM | Dulbecco's Modified Eagle Media |
| DMSO | Diethyl sulphoxide |
| DNA | Deoxyribonucleic acid |
| DOC | Deoxycorticosterone |
| dTTP | Deoxythymine 5'-triphosphate |
| DTT | Dithiothreitol |
| DUSP1 | Dual specificity phosphatase 1 |
| ECL | Electrochemiliuminescence |
| EDTA | Ethylenediaminetetraacetic acid |
| EGF | Epidermal growth factor |
| ELISA | Enzyme-linked immunosorbent assay |
| ER | Endoplasmic reticulum |
| ERK1/2 | Extracellular signal-related kinases |
| ETC | Electron transport chain |
| FACS | Fluorescent Activated Cell Sorter |
| FAD | Flavin adenine dinucleotide |
| FBS | Foetal bovine serum |
| FCS | Foetal calf serum |
| FDXR | Ferrodoxin reductase |
| FDX | Ferrodoxin |
| FLG | Filaggrin |

| | |
|---|---|
| FITC | Fluorescin isothiocyanate |
| FMN | Flavin mononucleotide |
| GAPDH | Glyceraldehyde-3-phosphate dehydrogenase |
| G6PDH | Glucose-6-phosphate dehydrogenase |
| GC | Glucocorticoid |
| G6P | Glucose-6-phosphate |
| GR | Glucocorticoid receptor |
| h | Hour |
| HCl | Hydrochloric acid |
| HPA | Hypothalamic pituitary adrenal |
| H6PDH | Hexose-6-phosphate dehydrogenase |
| HPLC | High performance liquid chromatography |
| HRP | Horseradish peroxidase |
| HSD | Hydroxysteroid dehydrogenase |
| ICAD | Inhibitor of caspase 3 related DNase |
| IFNγ | Interferon gamma |
| IgG | Immunoglobulin G |
| IL-1 | Interleukin 1 |
| IL-6 | Interleukin 6 |
| IMM | Inner mitochondrial membrane |
| ITS | Insulin, transferring, sodium selenite |
| JNK | Jun N-terminal Kinase |
| K | Ketoconazole |
| KDM | Keratinocyte defined media |
| KLF4 | Kruppel-like factor 4 |
| LCAH | Lipoid congenital adrenal hyperplasia |
| LC-MS | Liquid Chromatography-Mass Spectrometry |
| LH | Leutinising hormone |
| M | Molar |
| MAPK | Mitogen-activated protein kinase |
| MBq | Megabecquerel |
| MEK | Mitogen-activated protein kinase kinase |
| $MgCl_2$ | Magnesium chloride |

| | |
|---|---|
| MOPS | 3-(N-Morpholino)propanesulfonic acid |
| min | Minute |
| MLN64 | Metastatic Lymphnode 64 |
| μM | Micromolar |
| mM | Millimolar |
| MPK1 | MAPK phosphatase 1 |
| MPTP | Mitochondrial permeability transition pore |
| mRNA | Messenger ribonucleic acid |
| MTT | 3-(4,5-dimethylthiazol-2-yl)-2,5-diphenyl tetrazolium bromide |
| NaCl | Sodium chloride |
| $NAD^+$ | Nicotinamide adenine dinucleotide (oxidised form) |
| NADH | Nicotinamide adenine dinucleotide (reduced form) |
| $NADP^+$ | Nicotinamide adenine dinucleotide phosphate (oxidised form) |
| NADPH | Nicotinamide adenine dinucleotide phosphate (reduced form) |
| Nf-ATP | Nuclear factor of activated T-cell protein |
| $(NH_4)_2SO_4$ | Ammonium sulphate |
| nM | Nanomolar |
| NR | Nuclear receptor |
| OD | Optical density |
| OH | Hydroxy |
| OMM | Outer mitochondrial membrane |
| PAGE | Polyacrilamide gel electrophoresis |
| PAP7 | PBR associated protein |
| PBS | Phosphate buffered saline |
| PBR | Peripheral benzodiazapine receptor |
| PCP | Phosphate carrier protein |
| PCR | Polymerase chain reaction |
| PI | Propidium idodide |
| PKA | Protein kinase A |
| PKAR1α | cAMP-dependent PKA regulatory subunit 1alpha |
| PKC | Protein kinase C |
| pmol | Picomole |
| PMSF | Phenazine methosulfate |

| | |
|---|---|
| POMC | Pro-opiomelanocortin |
| POR | P450 oxidoreductase |
| PPP | Pentose phosphate pathway |
| PS | Phosphatidylserine |
| PSORSI | Psoriasis susceptibility locus |
| Rf | Retention factor |
| RIA | Radioimmunoassay |
| RNA | Ribonucleic acid |
| ROS | Reactive oxygen species |
| RT | Reverse transcriptase |
| RT-PCR | Reverse transcription-polymerase chain reaction |
| RXR | Retinoid X receptor |
| SCID | Severe combined immunodeficiency |
| SD | Standard deviation |
| SDS | Sodium dodecyl sulphate |
| sec | Second |
| SEM | Standard error mean |
| SF1 | Steroidogenic factor 1 |
| StAR | Steroidogenic acute regulatory protein |
| START | StAR-related lipid transfer |
| STAT1 | Signal Transducers and Activators of Transcription 1 |
| SULT2B1 | Sulfotransferase type 2 isoform B1 |
| T | Trilostane |
| TAE | Tris-acetate ethylediamine-tetra-acetic acid |
| TBS-T | Tris-buffered saline-tween |
| TEWL | Trans-epidermal water loss |
| TGMI | Transglutaminase 1 |
| TLC | Thin layer chromatography |
| TNFα | Tumour Necrosis Factor-alpha |
| TSPO | Translocator protein |
| TUNEL | Terminal deoxynucleotidyl transferase dUTP nick end labelling |
| U.V. | Ultra violet |
| U.V.B. | Ultra violet type B |

| | |
|---|---|
| VDAC1 | Voltage-dependent anion channel 1 |

**Acknowledgments**

I would like to thank the following people, without whom this thesis would not have been possible: Professor Jacky Burrin (William Harvey Research Institute, London, U.K) and Professor Mike Philpott (Institute of Cell and Molecular Science, London, U.K) for their expert supervision and support; Tony Michael (St George's Medical School, London, U.K.) for his invaluable help with steroid assays and scientific discussion; Dr. Ranjit Bhogal (Unilver, Coleworth House, Bedford, U.K.) for her support at Unilever and help with organising LC-MS analysis; Dr. Thomas Behr (Unilver, Coleworth House, Bedford, U.K.) for analysing LC-MS samples; Dr. GaryWarnes (Institute of Cell and Molecular Science, London, U.K) for his expertise in FACS analysis; Dr. Anna Thomas (Institute of Cell and Molecular Science, London, U.K) for providing NEB-1 organotypic raft samples; Dr. Paul Bowden (Cardiff University, Cardiff, U.K.) and Dr. Catherine Harwood (Institute of Cell and Molecular Science, London, U.K), Dr. Wei-Li Di (Institute of Child Health, London, U.K.), Professor Arne Akbar (UCL, London, U.K.) and Professor David Kelsell (Institute of Cell and Molecular Science, London, U.K) for generously giving tissue sections of skin conditions; Dr. Alex Brown (Institute of Cell and Molecular Science, London, U.K) for cutting skin sections; The Genome Centre (Barts and The London, London U.K.) for sequencing PCR products. Finally I would like to thank Paul Caton for his patience and support throughout my PhD.

# Chapter 1. Introduction

## Introduction 1.1: Steroid synthesis

### 1.1.1 Sources of cholesterol, the precursor to steroids

Cholesterol is the precursor to all steroids. The basic four-carbon ringed cholesterol molecule can undergo sequential enzymatic modifications to produce thousands of unique steroid signalling molecules (basic pathway depicted in Figure 1.1). Most cells are capable of synthesising cholesterol *de novo* from acetate. Alternatively, cells obtain cholesterol from circulating lipoproteins or by release of intracellular esterified cholesterol lipid stores (Cherradi and Capponi, 1998). Due to the high lipophilic nature of steroids, these molecules do not accumulate within secretory cells and require continuous synthesis to maintain steroid output. Upon extracellular (e.g. trophic hormone) stimulation, cholesterol esters are hydrolysed and cholesterol is mobilised to the outer mitochondrial membrane for the first step of steroid synthesis (Cherradi and Capponi, 1998).

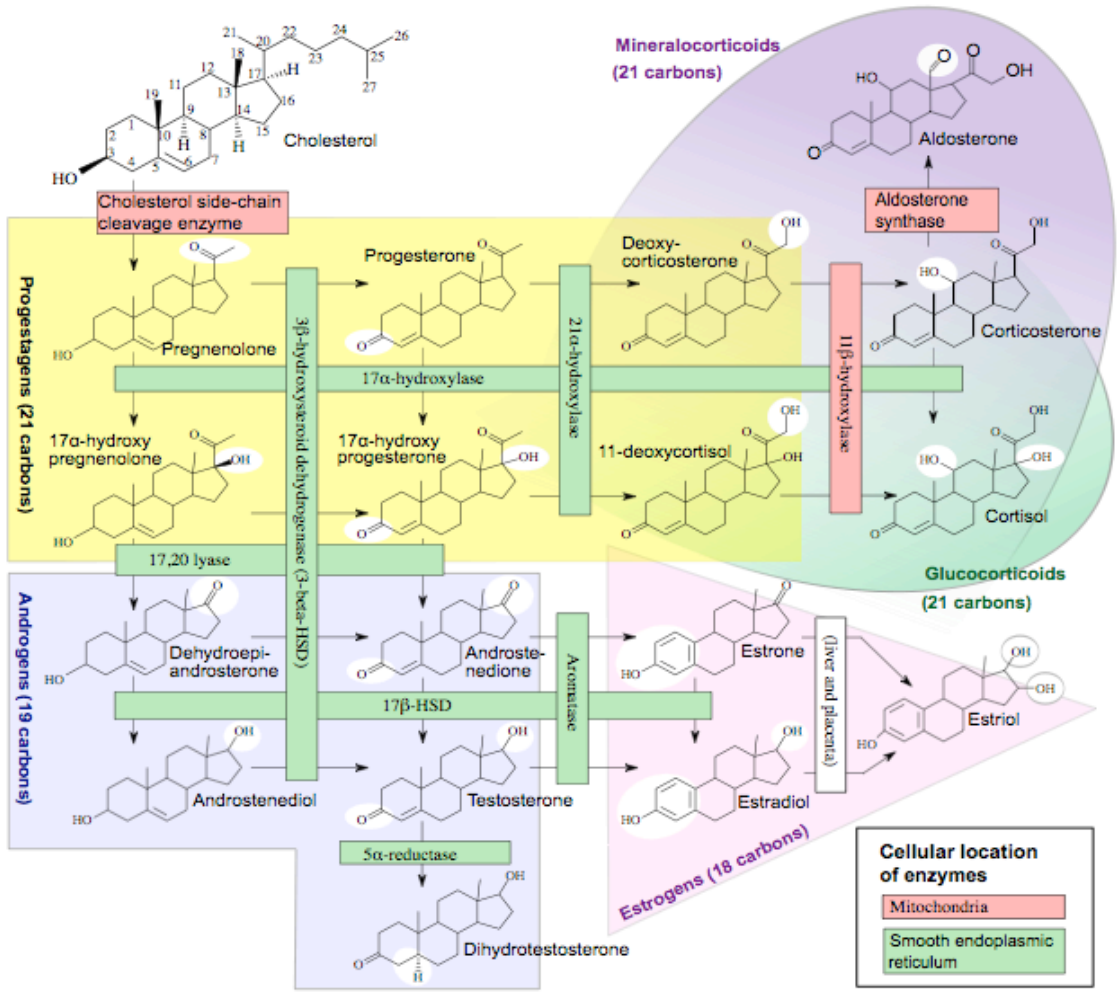


**Figure 1.1 Schematic of human steroidogenesis.** White highlights the site of chemical modification post enzymatic metabolism. (http://en.wikipedia.org/wiki/File:Steroidogenesis.svg).

### 1.1.2 Steroidogenic acute regulatory protein

Steroidogenic acute regulatory protein (StAR, also known as STARD1) is critical for delivering insoluble cholesterol across the aqueous inter-mitochondrial membrane space to initiate acute *de novo* steroid synthesis (Stocco, 2001a). The transport of cholesterol to the inner mitochondrial membrane (IMM) appears to be the rate determining step of steroid synthesis rather than the metabolism of cholesterol to pregnenolone (Iida et al., 1989; Stocco and Clark, 1996).

Early experiments demonstrated that acute steroid synthesis, induced by ACTH in adrenals and gonadotrophins in gonads, was blocked by chemical protein synthesis inhibitors such as cycloheximide (Cherradi and Capponi, 1998). This showed that acute steroidogenesis was dependent upon protein synthesis, which led to future investigations into protein synthesis inhibitor sensitive proteins that were associated with the induction of steroidogenesis. Using rat adrenal cells, a set of 30 kDa phosphoproteins were identified to be up regulated upon ACTH stimulation (Brownie et al., 1972). Rapid cessation of steroidogenesis was observed in MA-10 mouse Leydig cells treated with protein synthesis inhibitors (ortho-phenanthroline and carbonyl cyanide m-chlorophenylhydrazone), however the 30 kDa proteins were still found to be expressed in the mitochondria (Stocco and Sodeman, 1991). Instead, a labile 37 kDa precursor protein was identified. Decreased expression of the 37 kDa precursor protein corresponded with the reduction of steroidogenesis and the appearance of 32 and 30 kDa phosphoproteins in MA-10 Leydig cells treated with protein synthesis inhibitors (Stocco and Sodeman, 1991). Pulse-chase experiments identified the precursor-product relationship between 37 kDa, 32 kDa and 30 kDa proteins (Stocco and Sodeman, 1991). The direct link between the 37 kDa pre-protein and steroidogenesis was established by the isolation of cDNA that encoded the protein in MA-10 mouse Leydig cells (Clark et al., 1994). Sequence analysis identified the 37 kDa product as a novel protein and was called ‘steroidogenic acute regulatory protein’ (Clark et al., 1994).

Co-transfection of StAR and the P450 side chain cleavage system into non-steroidogenic COS-1 cells demonstrated that StAR could induce over a four-fold increase in pregnenolone synthesis (Sugawara et al., 1995). Further analysis of StAR

demonstrated that the 37 kDa precursor protein is expressed in the cytoplasm of cells and only activated upon phosphorylation of $Ser^{195}$, which targets the protein to the outer mitochondrial membrane (OMM) (Arakane et al., 1996). StAR is then processed to a 32 kDa intermediate, imported into mitochondria and cleaved to a 30 kDa inactive protein (Arakane et al., 1996).

Shortly after the identification of StAR, mutations in StAR were found to be the only cause of lipoid congenital adrenal hyperplasia (LCAH) (Bose et al., 1996; Sugawara et al., 1995; Tee et al., 1995). LCAH is a potentially fatal condition characterised by an almost complete inhibition of steroid synthesis. Patients with LCAH have abnormally high levels of ACTH and low levels of cortisol in their serum and a build up of esterified-cholesterol as lipid droplets in the adrenal glands (Bose et al., 1996; Sugawara et al., 1995; Tee et al., 1995). As a result, LCAH patients are unable to regulate salt or glucose levels. Despite the lack of steroid synthesis, LCAH patients were found to have normal steroidogenic enzyme activity. The discovery that cholesterol transport for steroidogenesis was inhibited due to loss of StAR function explained the cause for the absence of steroids in patients with LCAH (Bose et al., 1996; Sugawara et al., 1995; Tee et al., 1995).

Genetic analysis of patients with LCAH has identified thirty common mutations in StAR that have been used to aid mechanistic understanding of the StAR protein (Bose et al., 2000a; Roostaee et al., 2008). StAR is composed of two functional domains, an N-terminal 62 amino acid domain that provides the mitochondrial target sequence and a C-terminal StAR-related lipid transfer (START) domain (Christenson and Strauss, 2001). The START domain is critical for the binding and transfer of cholesterol and mutations that cause LCAH are predominantly located between exons 5 and 7 of this domain (Bose et al., 2000a).

The mutation F267Q is located in the C-terminal α-helix 4 region that lines the interface of the START domain cholesterol binding site (Roostaee et al., 2008). Thermodynamic stability analysis demonstrated that the F267Q mutation resulted in significantly diminished cholesterol binding capacity (Roostaee et al., 2008). This was coupled with an inhibition of pregnenolone synthesis when the F267Q mutant was transfected in Y-1

adrenal cells and MA-10 Leydig cells (Roostaee et al., 2008). Hence cholesterol must bind to StAR to initiate acute steroidogenesis.

Replacement of arginine by leucine at position 182 (R182L) is common in patients with LCAH from the Arab population (Bose et al., 1996). This mutation lies at the site of the hydrophobic core of StAR which is involved in binding and transferring cholesterol. Interestingly, the R182L mutant does not alter the binding capacity of cholesterol to StAR but rather the conformational flexibility of the protein (Bose et al., 2009). Wild type StAR was found to adopt a flexible form due to the accommodation of more water molecules whereas R182L mutant maintained a more rigid structure inhibiting its activity (Bose et al., 2009).

The precise molecular mechanism by which StAR enables cholesterol transport across the mitochondrial membranes is still under debate. It was first proposed that StAR could fuse the outer and inner mitochondrial membrane forming a bridge that hydrophobic cholesterol could cross (Clark et al., 1994; Stocco and Clark, 1996; Thomson, 2003). However, this inter-membrane shuttle model was questioned when cells that were transfected with StAR lacking the mitochondrial signalling domain were still able to induce steroid synthesis, even though StAR had not entered the organelle (Stocco, 2001b).

The molten globule hypothesis was proposed following the discovery that StAR partially unfolds and transitions to a molten globule state at low pH (below pH 4) (Bose et al., 1999). The phospholipids on the OMM may form an acidic microenvironment, increasing the flexibility of the StAR structure, allowing for the cholesterol binding site to be exposed (Bose et al., 1999). This corresponds with the data generated from thermodynamic activity of R182L versus wild-type StAR (Bose et al., 2009). Importantly, this hypothesis does not require StAR to contact the IMM to induce cholesterol transport.

The molton globule hypothesis is also supported by the observation that the 37 kDa StAR pre-protein is functionally active and exclusively resides on the OMM. However, mature 30 kDa StAR protein formed by cleavage of N-terminal amino acids resides in

the IMM and is functionally inactive (Arakane et al., 1996). Therefore import of StAR into the mitochondrial matrix has been described as a switch-off mechanism for terminating StAR activity (Arakane et al., 1996). Thus StAR is thought to be rapidly degraded once imported into the matrix compartment. Excessive accumulation of 30 kDa StAR in the cristae of the IMM can damage the mitochondria (Granot et al., 2007b). As a result, StAR has a short half-life and requires continual protein synthesis to maintain steroidogenic activity. Pulse-chase experiments of StAR-transfected COS-1 cells showed that newly imported 30 kDa StAR is degraded with a half life of 5 hours and that this degradation could be delayed with the protease inhibitor MG132 (Granot et al., 2007a; Granot et al., 2007b).

In addition to protease degradation, mitochondrial membrane potential (manipulated by changes in pH) can also regulate StAR activity (Granot et al., 2007b). Maintenance of the mitochondrial membrane potential is critical for steroid synthesis. Recently StAR was found to form a complex with voltage-dependent anion channel 1 (VDAC1) and phosphate carrier protein (PCP) (Bose et al., 2008). Absence of VDAC1 inhibited StAR-mediated pregnenolone synthesis (Bose et al., 2008). The majority of metabolites are thought to cross the mitochondrial membrane via VDAC proteins, therefore cholesterol could be transported into the mitochondria via VDAC1 channels upon activation with the StAR complex (Hodge and Colombini, 1997; Liu et al., 2006). Channel opening and closing of VDAC1 is sensitive to electron gradient, which may account for the sensitivity of steroidogenesis to mitochondrial membrane potential (Hodge and Colombini, 1997).

Other proteins are associated with StAR and VDAC1 to form a macromolecular signaling complex on the OMM for steroidogenesis. These include translocator protein (TSPO, also known as the peripheral benzodiazepine receptor or PBR (see section 1.4) and the PBR associated protein 7 (PAP7) which is thought to form an anchor for PBR interaction with cAMP-dependent PKA regulatory subunit 1a (PKAR1$\alpha$) (Bose et al., 2008; Liu et al., 2006).

Therefore cholesterol transport for steroidogenesis is a complex, highly coordinated event but the synthesis of StAR remains the critical step for initiating acute steroid

synthesis. Expression of StAR is initiated by trophic hormone signalling such as ACTH, LH or hCG. Upon binding to their respective receptors, these hormones initiate a cAMP second messenger response, causing protein kinase A (PKA) activation (Elias and Clark, 2000). Even though StAR mRNA transcription rapidly increases in the presence of cAMP, the human StAR promoter does not contain a consensus cAMP-responsive element (CRE) (Manna et al., 2009b). Instead, cAMP activates transcription factors such as CREB/CREM/ATF-2, Fos and Jun, and C/EBPβ, which promote the transcription of StAR (Manna et al., 2009b). These transcription factors contain a basic leucine zipper motif that can bind to StAR promotor regions to facilitate RNA polymerase II recruitment and initiate StAR transcription (Manna et al., 2009b).

Alternatively, StAR expression can be mediated by cAMP-independent mechanisms. This is thought to be particularly important for maintaining basal levels of StAR expression rather than acute StAR activation (Manna et al., 2006). A number of factors including insulin-like growth factor-I, epidermal growth factor (EGF), fibroblast growth factor, transforming growth factor alpha, interleukin-1, and colony-stimulating factor-1, increased the levels of StAR mRNA, StAR protein, and progesterone in mouse Leydig tumour cells (Manna et al., 2006). These factors promoted StAR protein to varying degrees but did not induce StAR phosphorylation and were not associated with fluctuations of cAMP signaling (Manna et al., 2006).

Therefore StAR is a tightly regulated protein essential for acute activation of steroidogenesis. However, other proteins have been implicated in contributing to steroid synthesis. These are metastatic lymph node 64 (MLN64) and the translocator protein (TSPO).

### 1.1.3 Metastatic lymph node 64

MLN64, also known as STARD3, was first identified as a gene up regulated in highly invasive breast cancers (Alpy et al., 2003). The protein was found to contain a C-terminal START domain, sharing 38% sequence homology and 60% amino acid similarity with the START domain of StAR (Watari et al., 1997). The START domain is a 210 amino acid region that provides a hydrophobic pocket capable of binding lipids

such as cholesterol oxysterols, phospholipids or ceramides depending on the specific START domain protein (Alpy and Tomasetto, 2005). To date, sixteen START domain proteins have been identified and both StAR and MLN64 are specific for regulating cholesterol transport (Alpy and Tomasetto, 2005).

The START domain of StAR is a highly flexible structure and forms aggregates at the concentration required for crystal formation, thus the structure has yet to be resolved (Tsujishita and Hurley, 2000). However, X-ray crystallography analysis of MLN64's START domain has increased the understanding of both MLN64 and StAR function and activity (Bose et al., 2000b). Crystallographic analysis of the MLN64 START domain revealed a nine-stranded twisted antiparallel β-sheet, 4 α-helices and 2-ohme loops (Tsujishita and Hurley, 2000). The β-sheets are arranged as a β-barrel forming a hydrophobic tunnel optimal for accommodating one cholesterol molecule (Tsujishita and Hurley, 2000). The $\alpha_4$-helix appears to form a lid for the cavity and access to the hydrophobic tunnel is dependent on the conformational changes of the $\alpha_4$-helix and connecting loops (Reitz et al., 2008). Photoaffinity labeling with [$^3$H]azocholestanol demonstrated that cholesterol preferentially interacts with one side of the START hydrophobic cavity in StAR but that cholesterol can interact with any side of the hydrophobic cavity in MLN64 (Reitz et al., 2008). This suggests that there could be differential cholesterol binding properties for StAR and MLN64 (Reitz et al., 2008). However, mutations of inactive StAR identified from LCAH patients correlated with conserved motifs identified in MLN64 (Watari et al., 1997).

Due to sequence homology and cholesterol binding capacity, MLN64 was investigated to see if it possessed StAR-like activity. MLN64 was shown to be able to induce cholesterol transport to promote pregnenolone synthesis in COS-1 cells co-transfected with the cytochrome P450 scc system (Watari et al., 1997). However, MLN64 could only increase steroid synthesis by two-fold whereas StAR induced a seven-fold increase in pregnenolone synthesis. Therefore, MLN64 has approximately 30% activity of StAR (Watari et al., 1997).

This functional evidence for MLN64-mediated steroidogenic activity supported the theory that MLN64 was responsible for steroid synthesis in the human placenta, a tissue

capable of steroidogenesis but lacking StAR expression (Sugawara et al., 1995; Watari et al., 1997). In placental trophoblasts, MLN64-mediated cholesterol transport was not regarded as the rate limiting step of steroid synthesis (Tuckey, 2005). Unlike acutely regulated StAR, MLN64 is constitutively active and could therefore supply a constant amount of cholesterol to the mitochondria for steroidogenesis to maintain the production of progesterone (Tuckey, 2005). Progesterone production by the placenta inhibits spontaneous abortion, 83% of miscarriages are associated with serum progesterone concentrations below a threshold level (Hahlin *et al*. 1990).

However, there is now substantial evidence suggesting that MLN64 is not directly responsible for cholesterol delivery enabling pregnenolone synthesis. This is because the protein was found to be exclusively located to the late endosomes, an organelle involved in the trafficking of cholesterol (Alpy et al., 2001; Holtta-Vuori et al., 2005). The N-terminal sequence for MLN64 differs greatly from the mitochondrial targeting sequence found in StAR, suggesting MLN64 functions in a different sub cellular compartment (Alpy et al., 2001). A mouse model with a targeted homozygous mutation in the MLN64 START domain failed to show any significant phenotype since the mice were viable, neurologically intact and fertile (Kishida et al., 2004). However, embryonic fibroblasts isolated from the mutant mice that were transfected with P450 scc system did show a reduction in testosterone (but not corticosterone) synthesis (Kishida et al., 2004). The authors concluded that MLN64 was largely dispensable for intracellular sterol trafficking but might play an upstream role in delivering cholesterol for steroidogenesis (Kishida et al., 2004).

Therefore the precise function of MLN64 remains elusive, however the protein does appear to be highly expressed in numerous hormone-dependent tumours such as some invasive breast carcinomas and high stage prostate cancer (Alpy et al., 2003; Stigliano et al., 2007). Both these tumours are associated with poor patient prognosis and are resistant to hormone therapy. Interestingly, a positive correlation for MLN64 and CYP17 gene expression was identified in neoplastic but not normal prostate tissue, suggesting a role for MLN64 in intraneoplastic autonomous steroidogenesis (Stigliano et al., 2007).

In addition, reduction of both MLN64 and StAR expression in human macrophages has been implicated in foam cell formation where cells are laden with cholesterol and cholesterol ester (Borthwick et al., 2009). Dysregulation of macrophage cholesterol homeostasis and foam cell formation leads to the development of atherosclerosis (Borthwick et al., 2009). In addition, dysregulation of cholesterol transport was associated with over-expression of hepatic MLN64 inducing liver damage in mice (Tichauer et al., 2007). Therefore, although the precise function of MLN64 has yet to be determined, it is likely that the protein plays a role in cholesterol homeostasis and could therefore influence steroid synthesis.

### 1.1.4 Translocator protein

The translocator protein (TSPO) functions to regulate steroid synthesis, cell proliferation, calcium flow, mitochondrial respiration, apoptosis, cellular immunity and malignancy (Gavish et al., 1999). These seemingly disparate biological activities can be accounted for due to the protein complexes formed by TSPO that interact with both StAR and the mitochondrial permeability transition pore (MPTP) (Veenman et al., 2007).

TSPO is a small 18 kDa protein originally described as the peripheral benzodiazepine receptor due to its binding site for the benzodiazepine diazepam (Braestrup and Squires, 1977). In addition to drug binding properties, TSPO also has a high affinity for cholesterol binding and is associated with cholesterol transport (Delavoie et al., 2003). TSPO is predominantly located on the outer mitochondrial membrane of steroidogenic cells but can also locate to the inner mitochondrial membrane, nuclei, Golgi apparatus, lysosomes, peroxisomes and plasma membrane in some cell types (Gavish et al., 1999). The density of TSPO expression is particularly high in classical steroidogenic tissues with the greatest expression in the adrenals, however, TSPO is ubiquitously expressed throughout all tissues, including the skin (Stoebner et al., 1999).

Numerous high affinity drug ligands have been used to assess the function of TSPO. These include the isoquinoline carboxiamide PK 11195, the PK 11195 nitrophenyl derivative PK 14105 and the benzodiazepine Ro5-4864. Photolabeled PK 14105

identified that TSPO forms a complex with at least two proteins, the voltage-dependent anion channel (VDAC, 32 kDa), and the adenine nucleotide carrier (ANT, 30 kDa)(Golani et al., 2001; McEnery et al., 1992). VDAC and ANT form part of the MPTP which is a critical mediator of apoptosis through regulation of cytochrome c release (Tsujimoto and Shimizu, 2000). TSPO is reported to regulate the opening and closing of VDAC, where VDAC opening leads to cytochrome C release into the cytoplasm, initiating caspase-dependent apoptosis.

In addition to mediating apoptosis, TSPO has been shown to be functionally coupled to steroidogenesis. Due to the high expression in steroidogenic tissue and co-localisation to the mitochondria, TSPO was assessed for its ability to regulate steroid synthesis (Gavish et al., 1999). Ligands for TSPO enhanced steroid production in Y-1 adrenocortical and MA-10 Leydig immortalised cells (Papadopoulos et al., 1990), as well as stimulating pregnenolone synthesis in brain mitochondrial preparations (Guarneri et al., 1992; Papadopoulos et al., 1992). Diazepam binding inhibitor (DBI, 10 kDa), a natural ligand for TSPO, is reported to be required for ACTH, hCG and luteinising hormone-activated steroid synthesis (Boujrad et al., 1996; Papadopoulos et al., 1991a; Papadopoulos et al., 1991b). TSPO is also reported to be capable of translocating cholesterol across the mitochondrial membranes in adrenocortical cells that could be enhanced with PK 11195 (Krueger and Papadopoulos, 1990). This suggests that TSPO is a facilitator of the rate-determining cholesterol transport step in steroid synthesis.

Despite the mounting evidence for TSPO regulation of steroidogenesis, it is unclear whether TSPO and StAR interact (Figure 1.2). Bioluminescence resonance energy transfer analysis did not identify any direct interaction of StAR with TSPO (Bogan et al., 2007). However, in a separate study fluorescence energy transfer analysis suggested co-localisation of TSPO with StAR (West et al., 2001). Recent studies have found that the two proteins form a complex via VDAC1 to coordinate steroidogenesis (Bose et al., 2008; Miller, 2007).

PBR can reside as a monomer or form polymeric clusters. The monomer is thought to bind cholesterol with greater efficacy whereas the polymers demonstrate high drug-

ligand binding affinity (Delavoie et al., 2003). In mouse Leydig cells, hCG induced rapid (15-30 s) cluster formation consisting of seven or more TSPO monomers (Boujrad et al., 1996). The fast rate of cluster formation is associated with the rapid induction of steroidogenesis by hCG in Leydig cells (Amri et al., 1996). Clusters develop through the formation of dityrosine covalent cross-linker bonds following U.V. exposure and subsequent ROS production (Delavoie et al., 2003). However, ROS is a by-product of steroidogenesis and may account for rapid cluster formation with hCG stimulation in Leydig cells (Delavoie et al., 2003).

Changes in cholesterol transport are associated with cancer progression, and increased TSPO expression is associated with increased severity of breast cancer (Hardwick et al., 1999). In addition there was a direct correlation with TSPO nuclear localisation and intensity with the severity of metastatic breast cancer cells lines (Hardwick et al., 1999). Therefore TSPO is now generating interest as an important protein for regulating cell viability, proliferation and apoptosis with implications in disease.

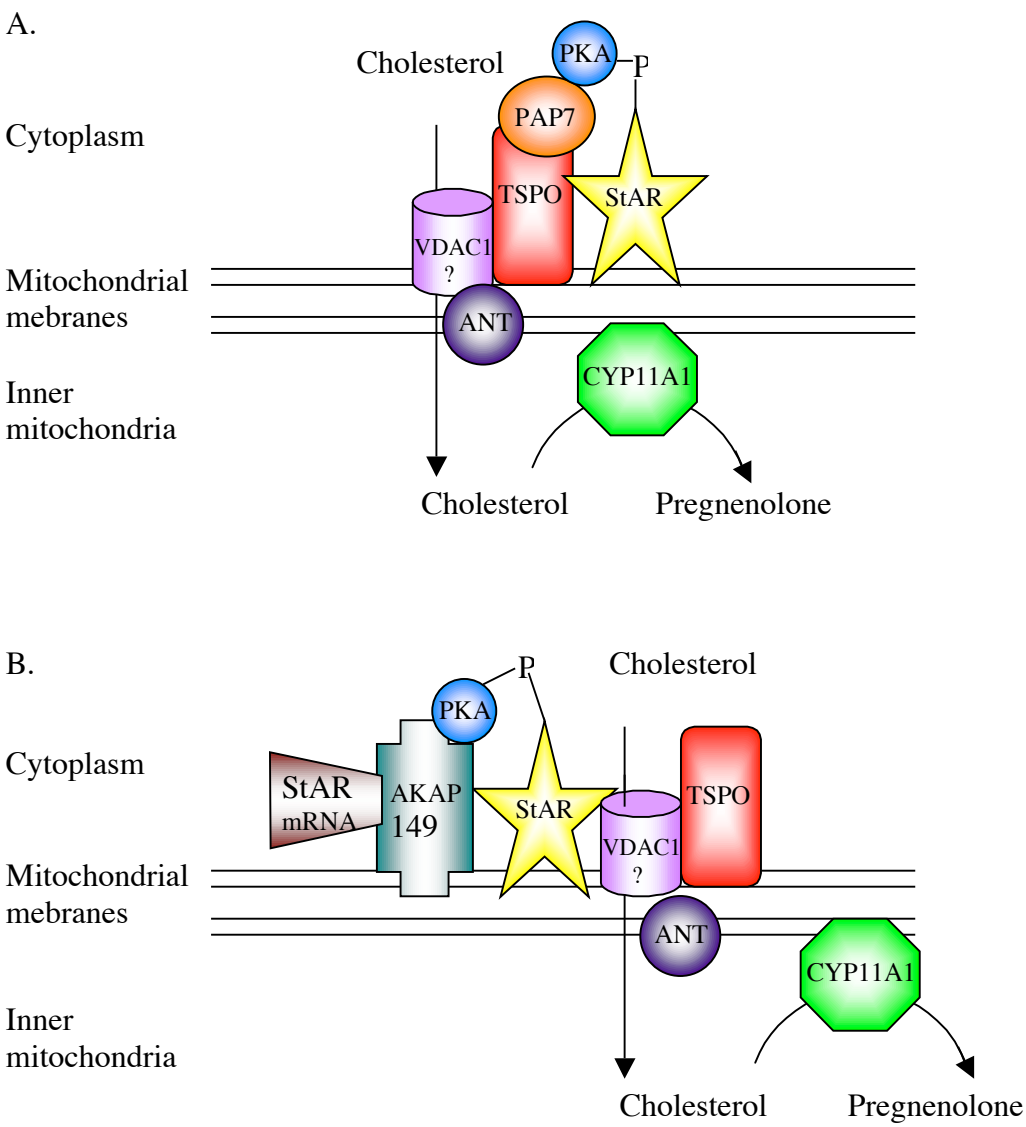


**Figure 1.2 Illustrations of cholesterol transport for steroid synthesis.**

(A) StAR associates with TSPO to facilitate acute steroidogenesis. TSPO interacts with PAP7 and PKA to maintain the active phosphorylated state of StAR. (B) StAR and TSPO do not directly interact but bind to VDAC1 to promote steroid synthesis. AKAP anchors StAR mRNA and PKA to the outer mitochondrial membrane, where StAR is translated *in situ* and rapidly activated by PKA phosphorylation. The precise mechanism of cholesterol transport across the mitochondrial membranes is not known but is currently thought to be regulated by VDAC1. Once cholesterol enters the inner mitochondrial membrane, the sterol is metabolised to pregnenolone by CYP11A1.

### 1.1.5 DAX1, a negative regulator of StAR

Dosage-sensitive sex-reversal, adrenal hypoplasia congenita, critical region on the X-linked chromosome, gene 1 (DAX1, gene name *NR0B1*) is a nuclear receptor (NR) that acts as a negative regulator of steroidogenesis (Zazopoulos et al., 1997). The essential role of DAX1 during development and regulation of subsequent steroid synthesis is exemplified by X-linked adrenal hypoplasia congenita (AHC). Loss of function or expression mutations of DAX1 in AHC prevents the inhibition of StAR and steroid synthesis (Zanaria et al., 1994). This leads to an abnormally early expression of genes involved in steroid production, impairing proliferation and adrenal zonation in the developing embryo (Lalli and Sassone-Corsi, 2003). Patients with AHC also have gonadal deficits including disorganised testes cords and hypogonadic hypogonadism. In contrast DAX1 gene duplication in males leads to dosage-sensitive male-to-female sex reversal (Ludbrook and Harley, 2004).

Members of the NR superfamily have conserved structural domains that separate them from other transcription factor families (Niakan and McCabe, 2005). These are an N-terminal DNA binding domain (DBD) and C-terminal ligand binding domain. DAX1 is unusual as its N-terminal domain does not resemble the canonical zinc-finger DNA binding domain making it distinct from all other NRs (Zazopoulos et al., 1997). Instead, in humans DAX1 has a unique 65-67 cysteine-rich amino acid sequence that repeats three and a half times and includes an LXXLL or NR-box motif (Suzuki et al., 2003). Unlike the N-terminus, the C-terminus of DAX1 does share sequence homology to other NR proteins such as the retinoid X receptor (RXR) (Niakan and McCabe, 2005). This region contains a transcriptional activation function 2 (AF2) ligand-binding domain, although currently there is no known ligand to induce DAX1 activity making it an orphan receptor (Niakan and McCabe, 2005).

As an NR, DAX1 can exert its steroidogenic repressor activities by inhibiting transcription of genes involved in the steroid response. For example, the DAX1 N-terminus recognises adenine-rich hairpin loop structures in the StAR promoter, preventing StAR transcription. DAX1 and SF-1 binding sites are close together on the promoter, suggesting allosteric inhibition by DAX1 of SF-1-StAR interaction. Indeed,

the expression pattern of DAX1 overlaps with SF-1 in specialised steroidogenic and reproductive tissue. SF-1 knockout mice suggests that SF-1 can control the transcription of the *Dax1* gene (Kawabe et al., 1999). Activation of the PKA and PKC second messenger response in mouse Leydig tumour cells inhibited DAX1-DNA binding interactions, leading to promotion of StAR expression and progesterone synthesis (Manna et al., 2009a). Interestingly, the DAX1 promoter site also contains an adenine-rich hairpin loop structure suggesting a self-regulating feedback system. In addition, DAX1 can act as a coregulatory protein suppressing the activity of other NRs, including *NR5A1* encoding SF1, the estrogen receptor (ER), androgen receptor (AR), progesterone receptor (PR) (Niakan and McCabe, 2005).

DAX1 can also function in the cytoplasm through protein-protein interaction. A single C200W mutation in the hinge region of the DAX1 was identified in a family with mild AHC phenotype (Bernard et al., 2006), leading to prevention of nuclear localisation of DAX1, shifting expression to the cytoplasm. Despite this, the patients still maintained 80% of wild-type activity (Bernard et al., 2006). Protein-protein interactions of DAX1 have been identified with SF1 and ER and DAX1 has been shown to antagonise AR and ER receptor dimerisation, as well as retinoic acid response element interaction with RXR (Niakan and McCabe, 2005). DAX1 can also recruit co-repressors, such as nuclear co-repressor and Alien, and shuttle mRNA back to the nucleus to prevent protein synthesis (Iyer and McCabe, 2004). Thus DAX1 acts as a master suppressor of steroid synthesis by interacting with the steroid pathway at many different levels.

### 1.1.6 Enzymes of steroid synthesis

Cytochrome P450 side chain cleavage enzyme (CYP11A1) catalyses the first step in steroid synthesis, metabolising cholesterol to pregnenolone (Storbeck et al., 2007). CYP11A1 is tightly associated but not integrated to the IMM. The CYP11A1 preprotein contains an N-terminal target sequence to deliver the protein to the surface of the IMM (Storbeck et al., 2007). This target sequence is then rapidly cleaved yielding the mature CYP11A1 protein by specific peptidases that are only found in the mitochondrial matrix of cells that express mitochondrial P450 enzymes (Storbeck et al., 2007).

CYP11A1 acts in a sequential three-step process where cholesterol undergoes 22-hydroxylation, 20-hydroxylation and then C20-C22 bond cleavage yielding pregnenolone and isocaproic acid (Storbeck et al., 2007). Each hydroxylation step requires two electrons to activate molecular oxygen that are provided by a mitochondrial steroid electron transport system (a distinct system from respiratory electron transport) (Lambeth et al., 1979). Electron transfer from NADPH to CYP11A1 is mediated via two soluble enzyme components, ferredoxin reductase (FDXR, also known as adrenodoxin reductase, a mono FAD single subunit protein) and ferredoxin (FDX, also known as adrenodoxin, an $Fe_2S_2$* protein) (Lambeth et al., 1979). NADPH directly reduces FDXR which in turn reduces FDX that then acts as an electron shuttle between FDXR and CYP11A1 (and other mitochondrial P450 enzymes). FDXR is specific for NADPH rather than NADH since the apparent $K_m$ values for these pyridine nucleotides are 1.82 μM and 5.56 mM respectively (Lambeth et al., 1976). In addition, *in vitro*, 1 NADH can only reduce the FDXR FAD moiety by 70%, whereas NADPH is 100% efficient (Lambeth et al., 1976).

Once CYP11A1 synthesises pregnenolone from cholesterol, pregnenolone is converted to progesterone by dehydrogenation of the 3β-hydroxyl group and Δ5 to Δ4 double bond isomerisation (Davies and MacKenzie, 2003). The enzyme 3β-hydroxysteroid dehydrogenase (3βHSD) was identified in 1951 to be responsible for the catalysis of this reaction (and all other steroid 3β-hydroxylations and Δ5 to Δ4 isomerisations) (Simard et al., 2005). In humans, two 3βHSD isoenzymes account for 3βHSD activity, where type I regulates 3βHSD activity in placenta and peripheral tissues, and type II predominantly regulates 3βHSD activity in the adrenal gland, ovary, and testis (Simard et al., 2005). Located to the membrane of both the ER and mitochondria, 3βHSD is dependent upon $NAD^+$ (Simard et al., 2005). A shift in 3βHSD localisation from the ER to the mitochondria in mouse ovaries was observed during the luteal phase of ovulation (Chapman et al., 2005). It has been proposed that this shift in localisation ensures high levels of progesterone production during the luteal phase, since $NAD^+$ cofactor availability is greater in the mitochondria relative to the ER (Chapman et al., 2005). The difference in subcellular localisation of 3βHSD could also aid the efficiency of steroidogenesis depending on the substrate. For example, mitochondrial 3βHSD can

interact with CYP11A1 to promote progesterone synthesis, whereas ER 3βHSD promotes DHEA metabolism (Simard et al., 2005).

The Δ5 to Δ4 isomerisation step is also thought to be conducted by 3βHSD since reduced $NAD^+$ (NADH) has been shown to induce a conformational change in 3βHSD that causes 3-oxo-Δ5-steroid isomerisation (Simard et al., 2005). However recent evidence has demonstrated that human alpha class glutathione transferase 3-3 (GSTA3-3) may regulate the isomerase part of the reaction (Johansson and Mannervik, 2001). GSTA3-3 was shown to be 230 times more efficient than 3βHSD at Δ5 to Δ4 steroid isomerisation and siRNA targeted inhibition of GSTA3-3 in adrenal whole cell extracts decreased progesterone production by 30% (Johansson and Mannervik, 2001; Raffalli-Mathieu et al., 2008).

An alternative pathway of pregnenolone metabolism is via CYP17. CYP17 is a 17-hydroxylase and 17,20 lyase enzyme that is regarded as the 'qualitative regulator' that determines which class of steroids are produced (Miller, 2005). For example, in the absence of 17,20 lyase activity, C21 17-deoxysteroids such as aldosterone are synthesised, but with 17,20 lyase activity C19 precursors of sex steroids are produced (Miller, 2005). The onset of 17,20 lyase activity is predominant in controlling the development of the adrenarche, inducing an increase of adrenal DHEA synthesis from aged 6-8 years that reaches its pinnacle level between 25-30 years in humans. The increase of DHEA synthesis is independent of serum concentrations of cortisol and ACTH (Miller, 2005).

Both 17-hydroxylase and 17,20 lyase reactions occur at the same, single active site of the enzyme but 17,20 lyase activity is regulated by electron flow from NADPH via P450 oxidoreductase (POR) to CYP17 (Miller, 2005). POR is required for both reactions however cytochrome $b_5$ selectively augments 17,20 lyase activity (Miller, 2005). The increase in cytochrome $b_5$ expression in the zona reticularis of the adrenals coordinates the onset of adrenarche. Kinetic analysis revealed that the 17,20 lyase activity of CYP17 is 30-fold greater for Δ5 substrates than Δ4, thus most androstendione synthesis proceeds via DHEA from 17-hydroxypregnenolone

metabolism rather than from 17-hydroxyprogesterone metabolism in humans (Miller, 2005).

The next step of cortisol synthesis is via CYP21 that acts as a 21-hyroxylase to synthesis 11-deoxycortisol from 17-hydroxyprogesterone. Similar to CYP17, this enzyme is located to the ER membrane and is dependent upon NADPH cofactor POR electron transport. CYP21 also regulates the formation of mineralocorticoids (e.g. aldosterone) by metabolising deoxycorticosterone to corticosterone as a precursor to aldosterone synthesis (Miller, 2005). The significance of CYP21 in glucocorticoid (GC) and mineralocorticoid synthesis is highlighted in two disorders, Addison's disease and congenital adrenal hyperplasia (CAH).

Addison's disease causes adrenocortical failure due to the production of autoimmunity auto-antibodies that are specific for CYP21 (Bratland et al., 2009). CAH also causes adrenocortical insufficiency and is one of the most common autosomal recessive inherited diseases affecting 1:5000-15000 live births (Trakakis et al., 2009). Approximately 90% of all CAH cases are due to mutations of CYP21 (as opposed to lipoid CAH that is due to StAR deficiency) (Trakakis et al., 2009). Interestingly, untreated infants with lipoid CAH may survive without treatment for several months, whereas patients with severe salt-wasting CAH do not (Miller, 2005). This is due to StAR-independent steroidogenesis that is not disrupted in lipoid CAH, however both acute (StAR-mediated) and background steroidogenesis of cortisol and aldosterone can be inhibited CYP21 mutations in CAH (Miller, 2005).

The 11-deoxycortisol product of CYP21 metabolism can then be used to synthesise cortisol. This is achieved by the 11β-hydroxylase activity of CYP11B1, a member of the same CYP11 gene family as CYP11A1. Similar to CYP11A1, the CYP11B1 enzyme is also expressed in the mitochondria and couples with NADPH to achieve cortisol synthesis in humans (Ishimura and Fujita, 1997). The activity of the two P450 enzymes are interlinked since the expression of CYP11A1 can promote CYP11B1 activity in recombinant yeast models (Cauet et al., 2001).

Another enzyme of the CYP11 family is CYP11B2, sharing 95% sequence homology to CYP11B1. CYP11B2 is also located at the IMM and is responsible for synthesising corticosterone, the precursor to aldosterone. Corticosterone rather than cortisol is the major GC in rodents. This is due to differences in the expression patterns where by the qualitative regulator CYP17 is expressed in the zona glomerulosa of rat adrenals but zona fasiculata of human adrenals (Miller, 2005). Thus the synthesis of cortisol is a divergent pathway from mineralocorticoid production in humans.

The concentration of cortisol in cells can be tightly regulated by 11βHSD activity, which exists as two distinct isoforms of 11βHSD, 11βHSD1 and 11βHSD2. Both isoforms are expressed in the ER but have different functions. 11βHSD2 is an $NAD^+$ dependent enzyme that rapidly deactivates cortisol to inactive cortisone. This enzyme is expressed in mineralocorticoid-sensitive cells, since cortisol can bind to mineralocorticoid receptors with the same affinity as GC receptors. In contrast, 11βHSD1 is a reversible NADPH dependent reaction that predominantly acts to oxidise cortisone to cortisol (Sherbet et al., 2007). Unlike most other HSD enzymes, 11βHSD1 uses NADPH cofactor generated from the intra-luminal hexose-6-phosphate dehydrogenase (H6PD) pathway in the ER (Hewitt et al., 2005). Disruption of 11βHSD1 due to an impairment of the H6PD activity and has recently been implicated in the pathogenesis of metabolic syndrome, highlighting the necessity of cofactor availability for steroid catalysis (Hewitt et al., 2005).

### 1.1.7 Cofactors, redox potential and cell viability

Cofactor availability is the driving force of steroid metabolism, determining the directional preference of HSD catalysis (unlike HSD enzymes, P450 reactions are considered mechanistically irreversible) (Sherbet et al., 2007). HSD enzymes appear to have unidirectional synthesis, however these enzymes are bidirectional with strong directional preference that is governed by cofactor availability. A pseudo-equilibrium state is reached that gives the apparent directional preference of the enzyme (Agarwal and Auchus, 2005). There are two key factors that ensure cofactors regulate the directional preference of HSD enzymes, these are cofactor concentration and binding kinetics. Free cofactor (NADPH and $NAD^+$) exceeds steroid substrate by several orders

of magnitude (mM versus nM), in addition, steroid enzyme kinetics require the cofactor to bind prior to the substrate (Agarwal and Auchus, 2005). Thus subtle changes in cofactor levels that can be tolerated by cells may dramatically alter the ability of the cells to synthesise steroids (Agarwal and Auchus, 2005).

Cofactor availability in the cell is controlled by the amount and type of metabolism together with oxygen supply (Agarwal and Auchus, 2005). The overall redox state of the cell is determined by the relative abundance of reducing (NADPH) and oxidising equivalents ($NAD^+$). Under optimal fuel and oxygen conditions, there is a high ratio of NADPH relative to $NADP^+$ and $NAD^+$ relative to NADH (Agarwal and Auchus, 2005).

The pentose phosphate pathway (PPP) is the principle process that maintains the cytosolic $NADP^+$/NADPH gradient by regenerating NADPH from $NADP^+$ during the oxidation of hydrocarbon substrates (Agarwal and Auchus, 2005). This provides a source of NADPH to most HSD enzymes for steroid metabolism. Two enzymes, glucose-6-phosphate dehydrogenase (G6PDH) and 6-phosphogluconate dehydrogenase (6PGDH), are key to the PPP pathway and utilise glucose-6-phosphate (G6P) from glucose to generate NADPH (Agarwal and Auchus, 2005). An alternative pathway for cytosolic NADPH production is via the citric acid cycle. All reactions for this cycle occur in the mitochondria and reduce $NAD^+$ to NADH, except for one step that in the cytoplasm where isocitrate dehydrogenase uses $NADP^+$ as an electron acceptor, creating NADPH in the process (Agarwal and Auchus, 2005). Another source of NADPH that is restricted to the lumen of the ER is generated by the hexose-6-phosphate dehydrogenase pathway (Agarwal and Auchus, 2005). Most enzymes that require NADPH from the ER rely on this local source of NADPH.

All NADPH is originally derived from $NAD^+$/NADH. $NAD^+$ is produced by the *de novo* pathway or the salvage pathway and under physiological conditions, cytosolic $NAD^+$ exceeds NADPH by approximately 700:1 (Ying, 2008). In contrast to NADPH, cells maintain the $NAD^+$/NADH gradient to favour the $NAD^+$ oxidised form. This is because electrons from NADH are constantly removed for use in the mitochondrial electron transport chain for ATP generation (Ying, 2008).

Interestingly, GC whose synthesis relies heavily on cofactor availability are able to influence cellular redox potential. GC have been shown to increase G6PDH in rat hepatocytes and adipose tissue, suggesting GC can influence cellular redox potential (Agarwal and Auchus, 2005). Cortisol has also been reported to promote NADPH reduction in the predominantly oxidative environment of the ER lumen (Piccirella et al., 2006). The ER lumen is considered to be a uniformly oxidising environment since the ratio of reduced to oxidised glutathione is 1-2:1 in the ER but 200:1 in the cytosol (Piccirella et al., 2006). This oxidising environment aids the protein folding and secretion function of the ER, however there are many intra-luminal ER reactions that require reducing equivalents. This includes 11βHSD1, which predominantly exhibits cortisone reductase activity *in vivo* but is also reported to oxidise cortisol *in vitro* (Piccirella et al., 2006). Addition of cortisone promoted $NADP^+$ oxidation in liver microsomes whereas cortisol enhanced NADPH reduction (Piccirella et al., 2006). Therefore, cortisol can promote 11βHSD1 to favour cortisone to cortisol formation, whereas cortisone may enhance the enzyme to favour cortisone formation (at least in an *in vitro* system). Increased NADPH levels in the ER following incubation with cortisol occurred due to upregulation of the hexose-6-phosphate pathway that was independent of glutathione reductase activity (Piccirella et al., 2006). Therefore, cortisol can change both cytosolic and ER redox potential to favour steroidogenesis and further cortisol synthesis.

The positive feedback effect of cortisol on steroidogenesis was identified in a study on granulosa cells. Cortisol promoted steroidogenesis in granulosa cells independently of StAR and steroid enzyme protein expression levels (Sasson et al., 2001). However no mechanism for this phenomenon was described in the paper and changes in cellular redox potential or cofactor availability were not measured. In addition, corticosterone deficiency was shown to inhibit testosterone synthesis in mice Leydig cells. Addition of corticosterone back to the system rescued the phenotype and increased expression of CYP11A1 and 17αHSD mRNA levels (Parthasarathy and Balasubramanian, 2008). Therefore, whilst GC can act via a negative feedback response to suppress the HPA access that ultimately down regulates steroidogenesis, GC also appear to be able to promote steroidogenesis. Indeed, GC have been described as having a biphasic response with respect to the regulation of neuronal plasticity by protecting cells and

preventing apoptosis at low concentration but inducing apoptosis at high concentration (Du et al., 2009). GC exerted these differential properties in neuronal cells by modulating cellular redox potential, calcium flux and Bcl-2 proteins (Du et al., 2009).

Maintaining cellular redox potential is pivotal to cell viability and prevention of apoptosis (Green and Reed, 1998). Changes in electron transport, loss of mitochondrial transmembrane potential, altered cellular oxidation-reduction, and participation of pro- and anti-apoptotic Bcl-2 family proteins are all key factors in the onset of apoptosis (Green and Reed, 1998). In a tissue-specific manner, cortisol can either inhibit or promote apoptosis (Viegas et al., 2008). Recently this function of cortisol has been attributed as an additional novel anti-inflammatory mechanism of GC. This is because GC predominantly induces apoptosis of haematopoietic cell such as monocytes, macrophages and T lymphocytes whilst protecting tissues such as mammary gland epithelial cells, endometrium, hepatocytes, ovarian follicular cells, fibroblasts and keratinocytes (Viegas et al., 2008). The mechanism for these opposing effects of cortisol are yet to be elucidated, though the steroid has been shown to have differential effects on Bcl-2 proteins that could account for the pro- and anti-apoptotic properties of GC (Viegas et al., 2008).

The seemingly disparate function of steroidogenesis and apoptosis are also linked via the TSPO protein (as described previously). TSPO is a ubiquitously expressed protein and could aid the transport of cholesterol for steroid synthesis in tissues that are not classically regarded as steroidogenic cells. Over the past few years, many non-classical endocrine cells such as retinal pigment epithelium (Zmijewski et al., 2007), astrocytes (Karri et al., 2007), the hair follicle (Ito et al., 2005), sebocytes (Chen et al., 2006) and dermal fibroblasts (Slominski et al., 2006) have been shown to possess steroidogenic capabilities (Table 1.1). In addition, many more tissues such as pancreatic cells (Morales et al., 2008) and chondrocytes (Takeuchi et al., 2007) have been shown to express StAR, TSPO and enzymes required for steroidogenesis. The function of local steroidogenesis and its necessity beyond the systemic endocrine system remains to be defined.

| Cell/tissue type and reference | Steroid measured | Concentration | Method of analysis |
|---|---|---|---|
| SEB1 sebocytes (Thiboutot et al., 2003) | 17OH pregnenolone | ~5pg/$10^6$ cells or ~2 pg $10^6$ cells without 10μM forskolin when treated with 22-OHcholesterol (5μM) for 48h. | RIA |
| Primary human keratinocytes (Milewich et al., 1988) | Pregnenolone and progesterone | No metabolism detected | Radiometric |
| HaCaT keratinocytes (Slominski et al., 2002) and (Rogoff et al., 2001) | Progesterone to deoxycorticosterone | Not applicable | Radiometric |
| Hair follicle (Ito et al., 2005) | Cortisol | ~10 μg/L by follicles treated with CRH (0.1 μM) and 10 μg/ml hydrocortisone; ~5 μg/ml by follicles treated with 10 μg/ml hydrocortisone over 6 days. | RIA |
| Primary human dermal fibroblasts (Slominski et al., 2006) | Cortisol | ~1 ng/ml untreated, ~4 ng/ml with progesterone (1 μM),~ 6 ng/ml with progesterone (1 μM) and ACTH (1 μM), cell density 1x$10^5$ in 24 well plate, 24 h. | RIA |
| Mesencephalon primary rat astrocytes (Karri et al., 2007) | Pregnenolone | ~20 pg/0.1ml extract, ~120 pg/ml with 1mM dbcAMP, 20 μM SU-10603 and 5 μM cyanoketone both over 24 h | RIA |
| Cerebellum primary rat astrocytes (Karri et al., 2007) | Pregnenolone | ~10 pg/0.1ml extract, ~100 pg/ml with 1mM dbcAMP, 20 μM SU-10603 and 5 μM cyanoketone both over 24 h | RIA |
| Rat heart (Silvestre et al., 1998) | Corticosterone | ~500 pg/mg protein from basal levels to 1500 pg/mg protein upon 3 h ACTH (10 nM) perfusion. | RIA |
| ARPE-19 (human retinal pigment epithelial cells) (Zmijewski et al., 2007) | Cortisol | ~5 ng/ml untreated or ~25 ng/ml with progesterone (10 μM) over 24 h, 500,000 cell per 10 cm Petri dish. | ELISA |

**Table 1.1 Summary of studies reporting pregnenolone, progesterone and/or cortisol synthesis and metabolism by non-classical steroidogenic tissue.**

## Introduction II: Steroid biology of the skin

### 1.2.1 The structure and function of the epidermis

The skin is an essential barrier that protects the body from the external environment. As such, the skin forms the primary defence from biological, chemical and U.V. radiation assault. In addition, this organ provides a vital role to protect the body from dehydration as well as aiding body temperature regulation.

The skin is composed of three layers, the epidermis (epithelial layer), the dermis (connective tissue) and the hypodermis (adipose tissue). The epidermis forms as a stratified layer of cells, which provides greater protection than a single monolayer (Eckert, 1989). Approximately 85% of the epidermis is made up of keratinocytes whilst the remaining cell components are melanocytes, Langerhans and Merkel cells. There are five distinct layers of the epidermis that are formed due to morphological changes that keratinocytes undergo as they differentiate (Figure 1.3). These are the basal layer, spinous layer, granular layer, transitional layer and cornified layer (Proksch et al., 2008).

The basal layer is the site of proliferating keratinocytes containing transient-amplifying keratinocytes and stem cells that maintain keratinocyte regeneration (Watt, 1998). The stem cells undergo a mitotic division to produce two daughter cells, one forms another stem cell to maintain the stem cell pool (approximately 10%), whilst the other forms a transient-amplifying cell that undergoes a limited number of cell divisions to generate the main basal layer (Watt, 1998). Approximately 80% of the basal layer comprises transient-amplifying cells. After completing the cell division cycles, the transient-amplifying cell enters differentiation (forming the remaining 10% of the basal population) and migrates through the epidermal layers starting with the spinous layer (Watt, 1998).

The spinous layer forms above the basal layer and derives its name from the spine-like morphology of the keratinocytes. The spines are formed by the development of

desmosome connections with neighbouring cells. Above the stratum spinosum is the granular layer. As the name suggests, keratinocytes in the granular layer exhibit keratohyalin granules that contain profilaggrin and lipid-filled lamellar granules (Eckert 1989).

Granular keratinocytes then transition from 'live' to 'dead' cells in the transition zone. This is a demanding metabolic process where all organelles are destroyed and lamellar granules fuse with the plasma membrane, releasing lipids into the extracellular space that leads to the formation of the cornified layer (Elias, 2005). The cornified layer is the site of terminal keratinocyte differentiation where keratinocytes flatten and lose approximately 70% of their dry weight. Keratins form 80% of the corneocytes that interlink with lipids to provide a waterproof barrier. Over time, the corneocytes are sloughed off as the skin regenerates. The transition from the basal layer to the stratum corneum takes between 12-24 days (Eckert 1989). The thickness of the epidermis is maintained through a delicate equilibrium between cell proliferation, cell differentiation, senescence and apoptosis (Doger et al., 2007). Aberrant regulation of one or all of these processes leads to barrier incompetence as seen in many skin diseases (Doger et al., 2007).

Keratinocyte differentiation for barrier formation is a complex event that can be defined by certain markers. Keratins are intermediate filaments that form a ring surrounding the nucleus and radiate out to desmosome junctions to provide a major structural network for the keratinocyte (Proksch et al., 2008). Keratin 5 (K5) and keratin 14 (K14) are associated with proliferating keratinocytes and are expressed exclusively in the basal layer of normal epidermis. An early marker of keratinocyte differentiation is the expression of keratin (K1) and keratin (K10) instead of K5 and K14, as detected in the spinous layer (Leigh et al., 1993). During conditions of hyper-proliferation such as lesional atopic dermatitis and psoriasis, K6 and K16 are expressed instead of K1 and K10 as well as inflammation-associated keratin (K17) (Jensen et al., 2004).

Filaggrins are filament associated-proteins that are essential for skin hydration and bind to keratin fibres to form a dense lipid-protein matrix. Profilaggrin is an insoluble phosphorylated protein containing multiple filaggrin repeats that accumulate in

keratohyalin granules (Markova et al., 1993). In late stages of differentiation, the protein is dephosphorylated and processed into individual filaggrin units that aligns keratins and lipids into a parallel plane to form the cornified layer of the epidermis (Markova et al., 1993). Loricrin is another critical component of the hydrophobic epidermal barrier that is linked together with disulphide bonds by the action of transglutaminase as part of cornification.

Calcium homeostasis is an important regulator of epidermal differentiation and can coordinate protein synthesis, including the activation of transglutaminase activity (Proksch et al., 2008). A healthy epidermis has a complex calcium gradient. The highest calcium level is in the granulosum which rapidly drops during cell transition to the stratum corneum due to high lipid and low water content of cornified keratinocytes (Proksch et al., 2008). Previously it was considered that a calcium gradient existed from basal (low calcium) to granulosum (high calcium) keratinocytes. However, electron probe microanalysis recently demonstrated that the calcium content of basal layer keratinocytes was higher than that of the lowest spinous cell layer in normal epidermis (Leinonen 2008). The epidermal calcium gradient is disrupted with barrier defects leading to abnormally low calcium content throughout the epidermis (Proksch et al., 2008).

Oxygen can also regulate keratinocyte differentiation. The skin is one of the few organs that can absorb atmospheric (21%) oxygen and levels as high as 17% $O_2$ have been measured in corneocytes whilst basal keratinocytes are exposed between 2-5% $O_2$ (Ngo et al., 2007). Primary keratinocytes cultured in 5% $O_2$ do not display altered proliferative rates but differentiation is profoundly suppressed (Ngo et al., 2007). Cells cultured at 2% $O_2$ showed decreased cell proliferation and differentiation rates but higher colony forming capacity (Ngo et al., 2007). Thus the oxygen gradient is proposed to act as a driving force between basal cell maintenance and keratinocyte differentiation.

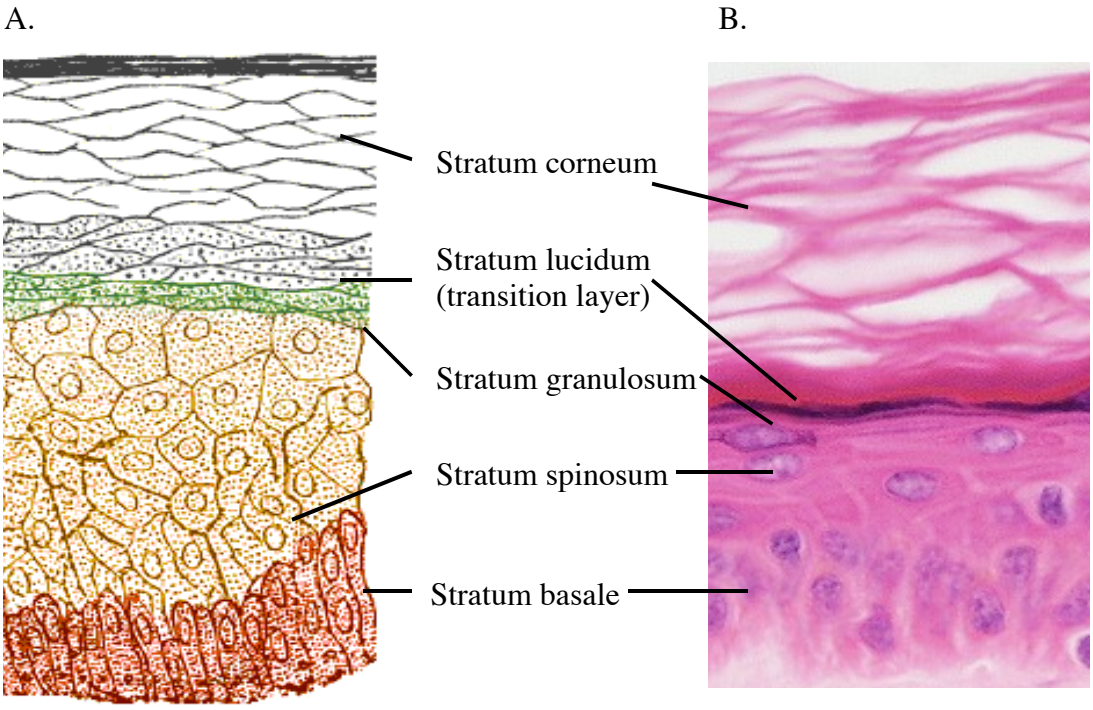


**Figure 1.3 The layers of the epidermis**

(A) a schematic and (B) an hematoxylin and eosin image of the epidermis. The diagram depicts the stratum basale where stem cells and transient amplifying keratinocytes reside. Once the keratinocytes have completed transient amplification, they undergo differentiation and migrate through the stratum spinosum, granulosum and lucidium. The stratum corneum is the site of terminal differentiation where lipids and proteins are released from the keratinocytes to form the skin barrier.

(modified from http://upload.wikimedia.org/wikipedia/commons/2/20/Skinlayers and www.etsu.edu/cpah/hsci/bowersjh/skin.html).

### 1.2.2 Atopic dermatitis

Atopic dermatitis (AD) is a common chronic inflammatory skin disease characterised by itchy, red, papulous, severely dry skin that is prone to cutaneous infections. The pathogenesis of AD is not fully characterised but there are clear environmental, immunologic and genetic contributions to the disease (Elias et al., 2008). Most AD patients also suffer from asthma and allergic rhinitis comorbidities, possibly due to IgE-sensitisation or low-grade systemic inflammation (Leung et al., 2004).

The histology of AD includes premature keratinocyte apoptosis throughout the epidermal layers, hyperproliferation, poor keratinocyte differentiation, disturbed barrier formation with increased trans-epidermal water loss (TEWL) and immune cell invasion (Elias et al., 2008; Leung et al., 2004). Classic hyperproliferation keratin markers are induced in lesional AD skin, including K6 and K16, K17 and a decrease in K10 expression (Jensen et al., 2004).

There are three different immune stages of atopic dermatitis; uninvolved, acute and chronic epidermal inflammation (Leung et al., 2004). Even uninvolved atopic dermatitis exhibits increased TEWL and a sparse perivascular T cell infiltrate that is not seen in normal healthy epidermis (Leung et al., 2004). Environmental factors such as irritating substances, climate, emotional stress or infection can exacerbate the disease triggering acute or chronic inflammation. The acute response activates keratinocytes to release proinflammatory cytokines and chemokines that facilitate immune cell infiltration into the epidermis resulting in a Th2 immune profile (IL-4, IL-5 and IL-13) (Leung et al., 2004).

Further irritation (e.g. by scratching the skin) stimulates IL-12 release that switches the immune response from a Th2 to Th1 profile with IFNγ expression (Trautmann et al., 2000). The secretion of IFNγ up regulates Fas-ligands, inducing Fas-mediated apoptosis in primary keratinocytes (Trautmann et al., 2000). Dysregulated apoptosis of keratinocytes is thought to be a key event in the development, severity and exacerbation of AD (Leung et al., 2004). Although apoptosis is commonly regarded as a form of cell death that does not release inflammatory mediators, apoptosis does appear to be coupled

with inflammation. It is thought that the inflammatory infiltrate is the cause rather than the consequence of keratinocyte apoptosis in AD (Leung et al., 2004; Trautmann et al., 2000).

Until recently, atopic dermatitis was primarily considered as an immunologic disorder, however, genetic screening identified that the *FLG* gene, which encodes filaggrin, is mutated in up to 20% of all Euro-American cases of AD (McGrath, 2008). Loss of filaggrin function in these patients may be responsible for the high TEWL loss of uninvolved atopic dermatitis (Seguchi et al., 1996).

In addition to filaggrin, involucrin and loricrin expression is also dysregulated in AD. Unlike filaggrin, normal involucrin levels were detected in uninvolved AD skin but expression was decreased in lesional regions (Seguchi et al., 1996). Loricrin was found to be decreased in both lesional and non-lesional AD relative to healthy skin. Involucrin and loricrin were suppressed by IL-4 and IL-13, thus the Th2 response could exacerbate dysregulated keratinocyte differentiation in acute AD (Kim et al., 2008). In addition, a recent mouse model with a triple knockout of involucrin, envoplakin and periplakin exhibited infiltration of $CD3^{+}CD4^{+}$ T cells, as observed in AD patients (Sevilla et al., 2007). It remains inconclusive as to whether inflammation or barrier defect is the primary cause of AD but both factors are able to influence the other to aggravate the disease.

AD skin is also prone to infection, particularly by *Staphylococcus aureus*. This is thought be due to the lack of inducible antimicrobial peptides, particularly the cathelicidin LL-37 and human beta-defensin 2 (HBD-2) which forms part of the innate immune system that targets *S. aureus* infection (Ong et al., 2002). In addition, defective epidermal pH regulation in AD provides an environment nearer to pH 7.4 rather than pH 5.5 that is optimum for most microbial growth (Elias et al., 2008).

Dry skin in AD is related to changes in epidermal lipid composition due to disturbed epidermal differentiation. This skin dehydration can be treated by topical application of an emollient cream containing lipids or lipid-like substances such as hydrocarbons, long chain alcohols, free fatty acids, cholesterol esters and triglycerides (Proksch et al.,

2003). Emollient treatment can reduce TEWL and in some cases even decrease mild inflammation (Proksch et al., 2003). Topical GC application is the mainstay anti-inflammatory therapy and is able to treat both acute and chronic AD (Proksch et al., 2003). Due to the associated skin thinning side-effects of GC, this treatment is not generally used for maintenance therapy. However, there is some evidence showing that once the initial disease is under control, long-term management can be achieved with twice-weekly GC therapy to prevent relapse. More recently, topical calcineurin inhibitors such as tacrolimus and pimecrolimus have been used to manage AD (Leung et al., 2004). Calcineurin inhibitors act by inhibiting nuclear factor of activated T cell protein (NF-ATp), providing an anti-inflammatory effect by preventing transcriptional activation of Th1 and Th2 cytokines (Leung et al., 2004).

### 1.2.3 Psoriasis

Psoriasis is a highly prevalent disease occurring worldwide and affecting approximately 2% population in the U.S. and Europe (Langley et al., 2005). This skin disorder can present at any stage of life, from birth to advanced age, however it is more likely to occur from the age of 15 to 20 years and then from 55 to 60 years (Langley et al., 2005). Psoriasis is described as a papulasquamous disease with scaling papules (raised lesions less than 1 cm in diameter) and plaques (raised lesions greater than 1 cm in diameter) (Langley et al., 2005). The distribution, morphology and severity can vary on a daily basis but the papules and plaques are generally distributed on the scalp, elbows, knees, lumbosacral area and in body folds (Langley et al., 2005). Histological features of psoriatic plaques include hyperproliferative keratinocytes with improper differentiation, immune cell infiltration and increased angiogenesis (Yu et al., 2007).

The underlying cause of psoriasis is unknown but it is regarded as a complex condition involving genetic, immunologic and environmental factors. Psoriasis is characterised by epidermal hyperplasia, increased keratin expression, recruitment of T cells and changes in the endothelial vascular system (Yu et al., 2007). Th1 cells secrete TNFα as part of the inflammatory response and inhibiting this process with anti-TNFα therapy offers a highly effective treatment for psoriasis (Albanesi et al., 2007).

However, it is clear that the disease also emanates from the skin itself and keratinocytes can release factors that initiate, propagate and exacerbate the disease (Albanesi et al., 2007). This is most elegantly described by the severe combined immunodeficiency (SCID) mouse xenograft model (Wrone-Smith and Nickoloff, 1996). Autologous immunocytes injected into the SCID mouse only produced psoriasis in xenograft skin from uninvolved psoriatic patients but not normal healthy human skin (Wrone-Smith and Nickoloff, 1996).

One of the hallmarks of psoriasis is hyperproliferation that corresponds with K6 and K16 expression in psoriatic lesions but not normal keratinocytes *in vivo* (Iizuka et al., 2004). Furthermore, high levels of the phosphorylated mitogen-activated protein kinases (MAPKs) ERK1/2 and p38, which are potent inducers of cell proliferation, are also upregulated in lesional psoriatic keratinocytes (Yu et al., 2007). Hyperproliferation also corresponded with poor differentiation and defective barrier formation in lesional psoriasis since K1, K10, loricrin and filaggrin were absent in the psoriatic lesion (Iizuka et al., 2004).

Cytokines released by infiltrating Th1 cells have been shown to promote keratinocyte hyperproliferation (Albanesi et al., 2007). The inflammatory cytokines TNFα, IL-1, IL-6 and IFNγ are released by Th1 cells and are elevated in lesional psoriatic skin (Albanesi et al., 2007). Interestingly, only IFNγ has been demonstrated to influence psoriatic stem cell proliferation and induce plaque development in pre-lesional psoriatic skin (Albanesi et al., 2007). However, the role of IFNγ in modulating epidermal hyperproliferation has recently been challenged since transgenic overexpression of IL-22 but not IFNγ was shown to induce a psoriatic skin phenotype in mice (Wolk et al., 2009). In addition, Th17 cells that secrete IL-22 and IL-17 are highly expressed in psoriatic lesions compared to AD where the Th17 response is absent (Guttman-Yassky et al., 2008). Psoriatic skin also demonstrated an upregulation of inducible antimicrobial peptides, which are absent in AD, accounting for the low prevalence of skin infections of psoriatic patients despite having a compromised immune barrier (Kim et al., 2005). Recently psoriasis has also been associated with comorbidities including arthritis, diabetes, atherosclerosis and coronary heart disease (Christophers, 2007).

These conditions have so far been attributed to persistent low-grade inflammation influencing other tissues in the body (Christophers, 2007).

High levels of apoptosis have also been detected by TUNEL assay in the epidermis of lesional psoriatic skin (Doger et al., 2007). This is partly thought to be an attempt to regulate the balance between cell proliferation and poor differentiation in lesional psoriatic skin (Doger et al., 2007). An aberrant patterning of apoptotic regulators was detected in psoriatic skin, where Fas, Bcl-xL, Bax and ICAD (inhibitor of caspase 3-related DNase) of the psoriatic involved epidermis were increased by 4.2-, 2.8-, 2.6- and 5.6-fold (Takahashi et al., 2002). In contrast Bcl-2 was down regulated by one third (Takahashi et al., 2002).

Consistent with observations of increased apoptosis, research has shown a disruption of NADPH levels, a compound intimately linked to apoptosis, in psoriatic skin. Analysis of NADPH and $NADP^+$ content of healthy versus psoriatic skin demonstrated an increase in $NADP^+$ content by approximately 75% in non-involved and involved areas of psoriatic skin compared to normal (Hammar, 1975). Since NADPH is a cofactor for many enzymes in steroid synthesis, this observation suggests that steroid synthesis could be dysregulated in psoriasis.

There is genetic evidence that links psoriatic susceptibility and poor steroid regulation. The Coiled-Coil alpha-Helical Rod protein 1 (CCHCR1) lies within the locus of the major psoriasis susceptibility locus PSORS1 and is regarded as a plausible candidate gene for risk effect (Tiala et al., 2007). CCHCR1 has been shown to regulate the expression of StAR and is linked to the potential aberrant regulation of steroid synthesis within psoriatic skin (Tiala et al., 2007). The expression pattern of CCHCR1 coincides with StAR in the basal layer of normal healthy epidermis and the CCHCR1 protein is able to promote steroid synthesis (Tiala et al., 2007). CCHCR1 mRNA was downregulated two fold in non-lesional psoriatic skin with an accompanying altered protein expression pattern lesional areas (Tiala et al., 2007). This suggests that StAR-mediated steroid synthesis could be dysregulated in psoriasis.

Other research has also implicated dysregulated localised HPA axis activity in psoriasis and AD. A localised HPA axis has been identified in hair follicles, and both CRH and the CRH-receptor have been identified in the epidermis (Ito et al., 2005; Kono et al., 2001; Slominski et al., 2001). As the end-point of the HPA axis, cortisol is able to negatively regulate CRH expression. If local cortisol synthesis is present in normal skin and ablated in psoriasis, then one would predict an increase in CRH and ACTH levels consistent with a block in HPA feedback response, as observed in congenital adrenal hyperplasia. Interestingly, CRH and CRH-R have been shown to be upregulated in psoriatic and atopic dermatitis skin (Kono et al., 2001; O'Kane et al., 2006). Synthetic cortisol analogues are able to rescue some of the abnormal phenotype of the psoriatic plaques and are one of the most widely prescribed drugs used to manage psoriasis.

### 1.2.4 Biological effects of GC on skin biology

The use of topical cortisol therapy was introduced in 1952 by Sulzberger and Witten to treat dermatological diseases such as psoriasis, atopic and seborrheic dermatitis, intertigo and eczema (Stojadinovic et al., 2007). Synthetic analogues of cortisol are still the treatment of choice for multiple skin disorders including psoriasis and atopic dermatitis. This powerful therapy is due to the profound effects that cortisol has on the epidermis since this steroid can influence keratinocyte cell fate, tissue remodelling, cell motility, differentiation and metabolism (Stojadinovic et al., 2007).

Cortisol is a potent inducer of keratinocyte differentiation. Microarray analysis of primary human keratinocytes demonstrated that dexamethasone (dex) induced transcription of *TGM1* (transglutaminase 1), *FLG* (filaggrin), *CDSN* (corneodesmosin), *SULT2B1* (sulfotransferase type 2 isoform B1) and *KLF4* (Kruppel-like factor 4) (Stojadinovic et al., 2007). All these genes contribute to driving late and terminal stages of keratinocyte differentiation. Interestingly this study found that dex inhibited involucrin expression while promoting filaggrin, suggesting that dex could inhibit early stages of differentiation in preference for late and terminal differentiation (Stojadinovic et al., 2007). Whilst there have been studies to show that dex can induce profilaggrin expression, other studies have shown that dex can induce rather than inhibit involucrin expression in immortalised keratinocytes (Monzon et al., 1996).

The role of cortisol-regulated keratinocyte differentiation was further supported by incomplete epidermal stratification of an embryonic GR knock out mouse model ($GR^{-/-}$) (Bayo et al., 2008). The $GR^{-/-}$ mouse displayed decreased filaggrin, loricrin and involucrin protein expression which was associated with poor granulosa and squamous cell differentiation (Bayo et al., 2008). The down regulated expression of filaggrin was due to decreased profilaggrin expression (Bayo et al., 2008). In addition, fewer desmosome connections were present and K10 and involucrin gene expression was decreased in $GR^{-/-}$ mouse skin (Bayo et al., 2008).

Concomitant with the induction of differentiation, cortisol appears to inhibit keratinocyte proliferation. Although some genes that promote the basal keratinocyte phenotype were induced by dex, activation of *DUSP1* was observed after 1 h treatment (Stojadinovic et al., 2007). DUSP1 dephosphorylates MAPKs, inhibiting MAPK-mediated induction of cell proliferation. Furthermore, cell counting assays showed that dex inhibited cell proliferation after 48 h (Stojadinovic et al., 2007). In addition, dex can inhibit the expression of K6 and K16 that are markers of hyperproliferating keratinocytes (Stojadinovic et al., 2007). Increased cell proliferation was also observed in the $GR^{-/-}$ mouse, where BrdU incorporation was increased in the basal and uniquely the suprabasal layers of the epidermis of the $GR^{-/-}$ but not $GR^{+/+}$ mouse (Bayo et al., 2008). Cultured keratinocytes from the $GR^{-/-}$ mouse also had constitutively active MAPK ERK1/2 activity (Bayo et al., 2008).

GC can also protect keratinocytes from apoptosis, whilst promoting differentiation and inhibiting proliferation. Primary neonatal foreskin keratinocytes co-cultured with T-cells to mimic an eczematous state were protected from Fas-induced apoptosis (Trautmann et al., 2000; Trautmann et al., 2001). In addition, skin from atopic dermatitis patients treated with prednicarbate (a synthetic cortisol analogue) exhibited significantly reduced keratinocyte apoptosis (Trautmann et al., 2001). Furthermore normal primary human keratinocytes were protected from U.V. induced apoptosis when treated with dex (Stojadinovic et al., 2007). Microarray analysis detected the induction of 12 anti-apoptotic genes such as *IkB, BCL6, SFP1, PTK2B* and *BAG* whereas pro-apoptotic genes such as *CASP1* and *–4, BAK1, TNSF10, TSSC3, MX1* and *TRADD* were

suppressed by dex (Stojadinovic et al., 2007). In addition, the IFNγ response was blocked by dex in primary keratinocytes predominantly by inhibiting STAT-1 activity (Stojadinovic et al., 2007). IFNγ released by infiltrating T-cells in chronic AD, triggers Fas-mediated apoptosis of primary keratinocytes leading to further barrier disruption (Leung et al., 2004). The $GR^{-/-}$ mouse displayed high levels of apoptosis throughout all the epidermis layers, whereas no apoptosis was observed in $GR^{+/+}$ mouse as detected by TUNEL assay (Bayo et al., 2008).

GC are also regarded as major anti-inflammatory agents as they suppress inflammation and regulate innate immunity. One of the key inducers of the inflammatory response is NFkB. Although GC are able to inhibit the NFkB pathway, microarray analysis did not detect down regulation of NFkB in primary human keratinocytes (Stojadinovic et al., 2007). Instead dex rapidly induced the negative NFkB regulator IkB, providing a mechanism for suppressing NFkB activity (Stojadinovic et al., 2007). Pro-inflammatory interleukin signalling was also down regulated as IL-1β, IL-4 receptor and IL-11 genes were inhibited (Stojadinovic et al., 2007).

Dex also affected keratinocyte lipid metabolism by suppressing fatty acid Δ-6-desaturase (*FADS2*) (Stojadinovic et al., 2007). This is the rate-limiting enzyme in the synthesis of long-chain polyunsaturated fatty acids such as arachidonic acid that plays a central role in regulating inflammation. In addition, dex has been reported to inhibit the synthesis of some lipids that form the epidermal barrier (Elias, 2005). Interestingly, dex upregulated 11βHSD2 transcription by 8-14-fold in keratinocytes (Stojadinovic et al., 2007). Unlike 11βHSD1, this enzyme acts irreversibly to inactivate cortisol to cortisone. Since dex is a potent steroid that cannot be deactivated by 11βHSD1 or 11βHSD2 activity, induction of 11βHSD2 could occur in response to hyper-GC stimulation.

Overall, dex appeared to predominantly act by suppressing gene activity rather than inducing transcription (Stojadinovic et al., 2007). This suggests that ligand-associated GR functions as a monomer rather than a dimer in keratinocytes since generally GR-monomer suppresses and GR-dimer activates gene transcription (Bayo et al., 2008). This also compliments findings observed in $GR^{dim/dim}$ mouse, where GR was mutated so

that it was unable to form a dimer (Bayo et al., 2008). Unlike the $GR^{-/-}$ mouse, keratinocyte differentiation was not impaired in the $GR^{dim/dim}$ mouse and the epidermis appeared normal (Bayo et al., 2008).

The affect of cortisol on skin is most apparent in patients with Cushing's syndrome. Cushing's syndrome can be caused by a pituitary adenoma that hyper secretes ACTH inducing elevated synthesis of cortisol by the adrenals. Alternatively, ACTH-independent Cushing's syndrome is caused by adrenal gland tumours, hyperplastic adrenal glands, or adrenal glands with nodular adrenal hyperplasia that secrete high levels of cortisol. This disease has a profound effect on the skin, causing skin thinning, dryness, fragility, facial acne and hirsutism. Milder forms of skin thinning/atrophy are observed in people suffering from psychological stress that increases cortisol circulatory levels. Studies in mice found that psychological stress and dex decreased lamellar body secretion and anti-microbial peptide synthesis, accounting for increased infection-related skin disorders of patients suffering from psychological stress. These Cushing's-like effects are also observed with prolonged cortisol therapy in patients suffering hyper proliferative skin diseases. Thus the correct balance of cortisol level in the skin is critical to regulating an effective epidermal barrier.

### 1.2.5 Steroid synthesis in the skin

Despite the effects that cortisol has on keratinocytes, local *de novo* synthesis of cortisol by these cells has not been reported. However, many regulators and enzymes required for steroidogenesis have been detected in the epidermis. In addition, some metabolic studies have identified androgen and oestrogen steroid metabolism by primary human keratinocytes (Figure 1.4).

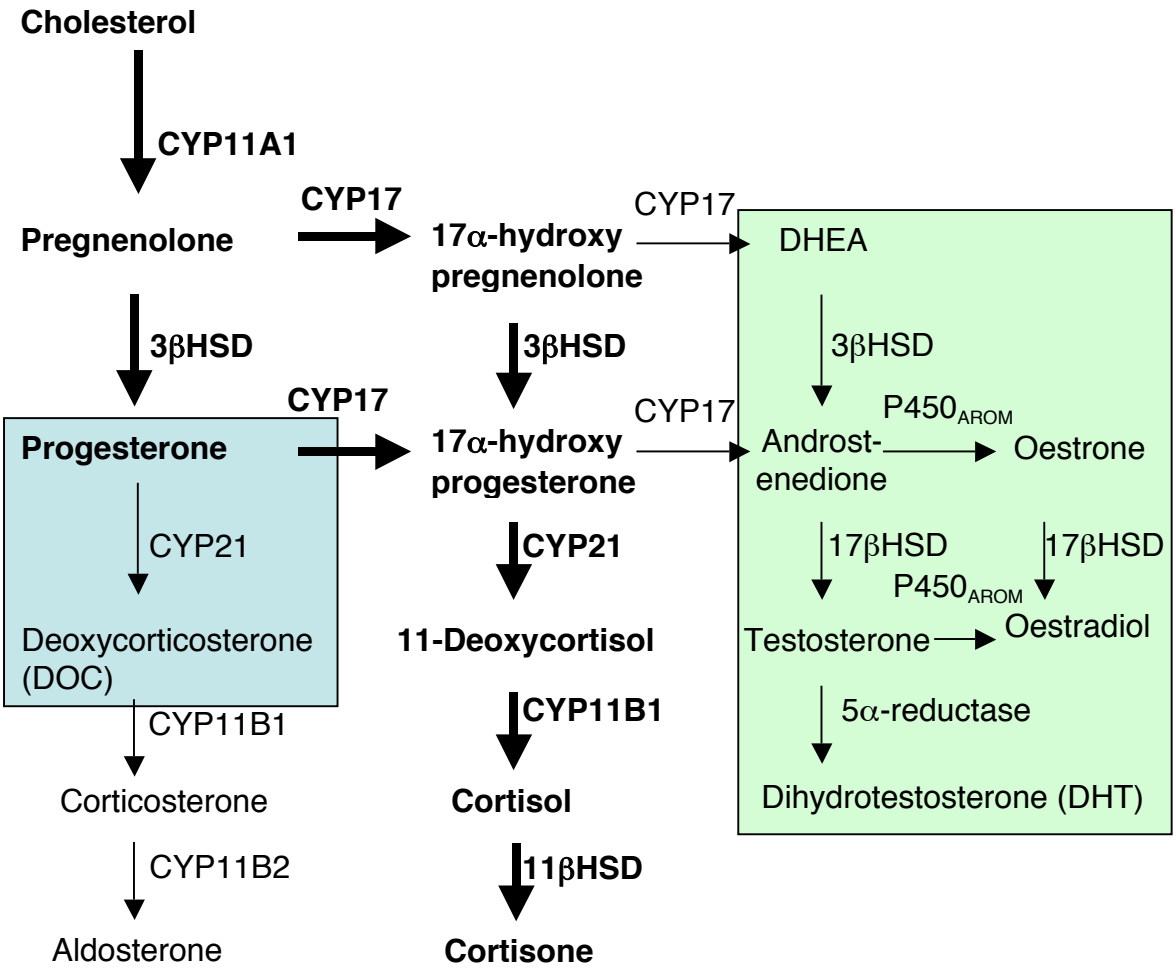


**Figure 1.4 Steroidogenesis previously reported in keratinocytes.**

Green box corresponds to androgen and oestrogen synthesis and metabolism identified in primary human keratinocytes (Milewich et al., 1988). Blue box corresponds to progesterone to deoxycorticosterone metabolism identified in HaCaT immortalised keratinocytes (Rogoff et al., 2001). Bold font and arrows depict *de novo* cortisol synthesis pathway of interest.

There is an abundant source of cholesterol in skin as keratinocytes are capable of synthesising cholesterol *de novo* (Menon et al., 1985). Cholesterol transporters associated with steroid synthesis have been identified in the skin. Immunohistochemistry detected StAR protein in the epidermis, sebocytes (more strongly in undifferentiated sebocytes), outer root sheath of hair follicles, eccrine sweat ducts but not eccrine sweat glands and vascular tissue in whole skin sections (Chen et al., 2006). MLN64 protein was serendipitously detected in whole skin extracts by western blotting when assessing for StAR expression, which was not detected in the study (Slominski et al., 2004). TSPO was also ubiquitously expressed throughout the epidermis with increasing intensity as keratinocytes differentiate (Stoebner et al., 1999). TSPO protein was distributed throughout the cytoplasm with selective expression on the mitochondrial membranes of epidermal cells (Stoebner et al., 1999).

Co-repressors and co-activators of StAR have also been identified in skin. DAX1, the negative regulator of StAR, was detected by immunohistochemistry in the epidermis, sebaceous glands, sweat glands and outer root sheath of the hair follicle with weaker expression in the inner root sheath, matrix cells, and dermal papilla cells (Patel et al., 2001). Immunohistochemistry discovered the presence of the StAR transcription activator SF-1/Ad4BP distributed with a scattered nuclear pattern throughout all epidermal layers (Patel et al., 2001; Thiboutot et al., 2003).

There have been several studies of steroid synthesis on skin and its appendages (Slominski et al., 2007) (Figure 1.5). For example, the hair follicle has been reported to express elements of the hypothalamic-pituitary-adrenal (HPA) axis and can synthesise cortisol (Ito et al., 2005). CYP11A1 and FDXR have been identified in the epidermis, hair follicles, sebaceous ducts and sebaceous glands of human facial skin, human sebocytes, and SEB-1 sebocytes (Thiboutot et al., 2003). The production of 17-hydroxypregnenolone from 22-hydroxycholesterol was detected at very low levels (0.008 pmol) in SEB-1 cells compared to normal theca cells (60-300 pmol) per $1x10^6$ cells over 72 h (Thiboutot et al., 2003). Melanocytes and dermal fibroblasts have also been shown to produce corticosterone and cortisol (Slominski et al., 2005a; Slominski et al., 2005b; Slominski et al., 2006).

**Total skin:** mRNA for CYP11A1, CYP17 and CYP21, MLN64 (Slominski *et al.*, 2004)

**Epidermal melanocytes** stimulated with CRH produce POMC, ACTH to synthesise cortisol (Slominski et al., 2005b)

**Primary human dermal fibroblasts** stimulated with CRH produce POMC, ACTH and can synthesise cortisol and corticosterone (Slominski et al., 2005a; Slominski et al., 2006)

**Primary human keratinocytes:** Androgen and oestrogen synthesis and metabolism (Milewich et al., 1988).

**HaCaT (immortalised keratinocytes):** mRNA for CYP11A1, CYP17 and CYP21, progesterone to corticosterone metabolism (Rogoff *et al.*, 2001)

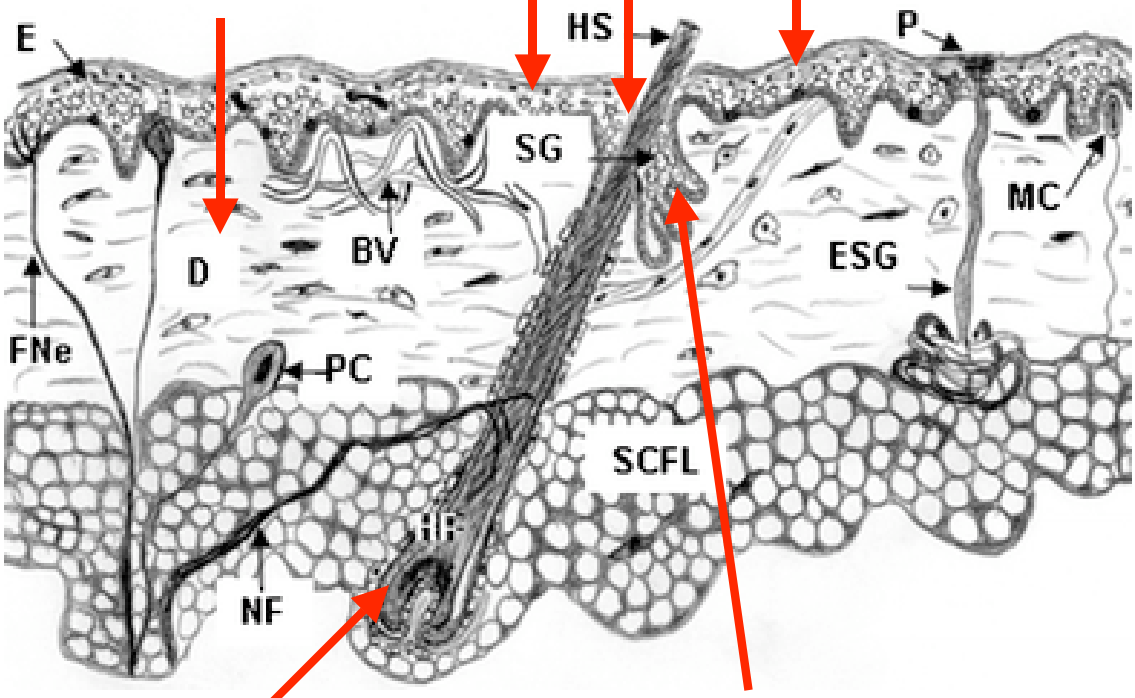


**Hair follicle:** responds to CRH to synthesise POMC, ACTH and cortisol. (Ito *et al.*, 2005).

**SZ95 (immortalised sebocytes):** mRNA for CYP11A1, CYP17 and CYP21, 17OH progesterone synthesis (Thioboutot *et al.*, 2003).

**Figure 1.5 Schematic representation of steroid enzymes and synthesis identified in the skin.** Modified from Tobin (2006).

BV: blood vessel, D: dermis, E: epidermis, FNe: free nerve ending, HF: hair follicle HS: hair shaft, MC: meissner's corpuscle, NF: nerve fibre, P: pore, PC: pacinian corpuscle, SCFL: subcutaneous fat layer, ESG: eccrine sweat gland, SC: sebaceous gland.

There has also been extensive research into keratinocyte steroid synthesis, although *de novo* steroid synthesis was not detected, androgens and oestrogens were effectively synthesised by the cells (Gingras et al., 2003; Milewich et al., 1988). Radiometric analysis of steroid metabolism in cultured primary keratinocytes revealed DHEA could be metabolised via androstenediol and testosterone to dihydrotestosterone (DHT). DHT could be further metabolised to 5α-androstane-3β, 17β-diol or 5α-androstane-3α,17β-diol by 3βHSD or 3αHSD respectively. Thus demonstrating 17βHSD, 3αHSD and 3βHSD activity in keratinocytes (Milewich et al., 1988). The synthesis of DHT is significant because it is at least five times more potent than testosterone due to higher affinity binding to androgen receptors (Hoffmann, 2001).

Oestrogen metabolism was also demonstrated in primary human keratinocytes. In skin, oestrogens can improve collagen content and quality, increase skin thickness, enhance vascularisation, increase the rate and quality of wound healing and protect the skin from photoaging in rats (Thornton, 2002). Oestrone (E1) to oestradiol (E2) metabolism by 17βHSD was demonstrated by radiometric assay. Similar to 11βHSD1, 17βHSD catalyses a reversible reaction, regulating the amount of active E2 relative to inactive E1. *In vitro* 17βHSD preferentially converts E2 to E1 by a factor of ten relative to the reverse reaction (Milewich et al., 1988). It has been postulated that E1 is unconventionally the biologically active oestrogen in skin, however it is possible that the preference for synthesising E1 over E2 is an *in vitro* phenomenon (Hughes et al., 1997).

Evidence of CYP19 aromatase activity, linking the DHEA pathway with E1/E2 metabolism is controversial, where some studies have not been able to identify the conversion of androstenedione to E1 (Milewich et al., 1988) but others have observed some CYP19 metabolic activity (Hughes et al., 1997).

The study by Milewich included radiometric analysis of pregnenolone and progesterone metabolism by primary human keratinocytes. Neither pregnenolone nor progesterone metabolism was detected (Milewich et al., 1988). However progesterone (but not pregnenolone) metabolism was demonstrated in HaCaT keratinocyte immortalised cells

but the metabolites were derivatives of deoxycorticosterone (DOC) (Slominski et al., 2002). Progesterone metabolism to DOC is a divergent pathway from the formation of cortisol from progesterone, where the latter proceeds via the synthesis of 17α-hydroxyprogesterone. Surprisingly, the synthesis of cortisol has yet to be functionally characterised in primary human keratinocytes.

**Aims and Objectives:**

To identify the expression of cholesterol transporters (StAR, TSPO and MLN64) and the negative regulator of steroidogenesis (DAX1) in normal human epidermis.

To determine whether the expression pattern of StAR, MLN64 and DAX1 is aberrant in skin disorders such as atopic dermatitis and psoriasis that are commonly treated with glucocorticoids.

To examine the expression of StAR, TSPO, MLN64 and DAX1 in cultured primary human keratinocytes.

To determine whether cultured normal primary human keratinocytes can synthesise cortisol.

To examine the affect of dexamethasone (a glucocorticoid analogue) on cell viability, proliferation and redox potential of cultured primary human keratinocytes.

# Chapter 2. Materials and methods

## 2.1 Cell culture methods

All cell culture was performed in a laminar flow hood under aseptic conditions in accordance with standard tissue culture technique. All sterile disposable tissue culture flasks, plates and dishes were purchased from Nunc (Roskilde, Denmark). For tissue culture all centrifuge steps were using an IEC Centra-3C Centrifuge (International Equipment company, Dunstable, U.K.), for sample analysis a SciQuip 1 – 15 K (Sigma-Aldrich, Poole, U.K.) centrifuge was used unless otherwise stated.

All primary human keratinocytes were used for experiments at passage 2 or less. RM+ culture medium was modified DMEM:Ham's F12, 3:1 (custom made, 3 parts DMEM to 1 part Ham's F12 containing 3.8 g/L D-glucose, 3.7 g/L sodium bicarbonate and 0.082 g/L sodium pyruvate; PAA laboratories GmbH, Pasching, Austria) supplemented with 10 % foetal bovine serum (FBS, Biowest, East Sussex, U.K.), 2 mM L-glutamine (PAA Laboratories GmbH, Pasching, Austria), 1X penicillin streptomycin (PAA laboratories GmbH, Pasching, Austria), 5 μg/ml apo-transferrin, 0.4 μg/ml hydrocortisone, 100 pM cholera toxin, 5 μg/ml insulin, 20 pM liothyronine, 10 ng/ml epidermal growth factor (EGF) (all from Sigma Aldrich, Poole, U.K.).

### 2.1.1 Immortalised mouse 3T3 fibroblasts

NIH/3T3 mouse fibroblast cells were purchased from ATCC (Manassas, VA, U.S.A.). This cell line was established from Swiss 3T3 cells that were originally isolated from disaggregated embryos of Swiss mouse and deposited by G. Todaro and H. Green in 1962. The cells were cultured in T75 or T175 $cm^2$ polystyrene culture flasks with Dulbecco's Modified Eagle's medium (DMEM) (PAA laboratories GmbH, Pasching, Austria) with 10% bovine calf serum (CS) (ATCC, Manassas, VA, U.S.A.), 2 mM L-glutamine (PAA Laboratories GmbH, Pasching, Austria) and 1x penicillin/streptomycin (PAA Laboratories GmbH, Pasching, Austria) at 37°C in an humidified chamber at 5% $CO_2$/95% atmospheric air. The culture medium was changed every two to three days and the cells were passaged (section 2.1.4) before reaching 70% confluency to prevent transformation.

### 2.1.2 Mitomycin C treatment of 3T3 mouse fibroblasts

Mouse 3T3 fibroblasts were used to support the growth of primary human keratinocytes. This is because 3T3 fibroblasts release nutrients that encourage keratinocyte proliferation and adhesion. In addition, the use of mouse 3T3 fibroblasts prevents the growth of potentially contaminating dermal fibroblasts. However, the 3T3 fibroblasts must first be treated with mitomcyin C (Sigma-Aldrich, Poole, U.K.) which intercalates with DNA to inhibit proliferation. This prevents the NIH/3T3 cells from outgrowing the keratinocytes but still allows the cells to support primary keratinocyte growth.

When mouse fibroblast NIH/3T3 cells were 60% confluent, they were treated with mitomycin C in the flask by removing spent media and adding 10 ml fresh media containing 10 μg/ml mitomycin C. The cells were incubated for 2 h at 37°C in an humidified chamber at 5% $CO_2$/95% atmospheric air. The cells were then washed three times in sterile PBS (PAA Laboratories GmbH, Pasching, Austria) to remove excess mitomycin C and trypsinised (as described in section 2.1.10).

Mitomycin C treated NIH/3T3 cells ($2x10^6$) were seeded per T75 $cm^2$ flask with 10 ml complete RM+ culture medium 24 h prior to adding primary keratinocytes. Seeding the fibroblasts 24 h in advance of the keratinocytes greatly increased keratinocyte growth and adhesion efficiency. If required, $5x10^5$ extra mitomycin C-treated 3T3 cells were added to top-up fibroblasts in existing primary keratinocyte culture.

### 2.1.3 Isolation of primary human keratinocytes

Human fronto-temporal scalp skin specimens were obtained with informed consent during routine face-lift surgery (Caucasian females over 40 years), approved by the East London and City Health Authority Research Ethics Committee for use of human redundant skin (T/01/034). The skin specimens were couriered from the theatre immediately after the operation in moist gauze. Upon arrival, the sample was transferred to a 100 mm cell culture dish containing complete RM+ culture medium and stored overnight at 4°C.

The keratinocytes were isolated based on the Rheinwald and Green method (Rheinwald and Green, 1975). The dermis and connective tissue was removed from the sample by scissors and a scalpel. This step is crucial for efficient isolation of primary keratinocytes since the keratinocytes can stick to fatty tissue, thus decreasing yield. The skin was washed twice in 1x versene (PAA Laboratories GmbH, Pasching, Austria) then chopped into small (approximately 4 mm by 4 mm) pieces in versene using a scalpel. Versene is an isotonic solution containing 0.53 mM ethylenediaminetetraacetic acid (EDTA) that chelates cationic ions which would otherwise inhibit trypsin enzymatic activity.

The tissue was then transferred into two 50 ml centrifuge tubes containing 30 ml 0.25% (v/v) trypsin (PAA laboratories GmbH, Pasching, Austria) and incubated at 37°C for 1 to 2 h and mixed well every 20 min. Trypsin acts by cleaving extracellular adhesion proteins that are responsible for cell to cell adhesion. Keratinocytes were among the cells that were shed into the trypsin during this process. Trypsinisation was deemed to be complete when the solution turned cloudy, the epidermis began to lift from the basement membrane and the tissue pieces floated to the surface of the liquid.

The solid material was transferred to a 100 mm cell culture dish and the cloudy trypsin solution was transferred to 50 ml centrifuge tubes and neutralised in complete RM+ culture medium in a 1:1 ratio. Using two needles, the epidermis was then separated from the basement membrane to release basal keratinocytes. The tissue clumps and cells were transferred to the centrifuge tubes containing the rest of the cells, the plate was rinsed with RM+ culture medium which was also then transferred to the centrifuge tubes. The samples were shaken vigorously to release any remaining cells. Excess skin clumps were removed by sieving the sample and retained for fibroblast isolation (see section 2.1.5). Equal volumes of complete RM+ culture medium was added to the filtrate (containing the keratinocytes) and centrifuged at 1,000 rpm for 5 min.

The supernatant was aspirated and the cell pellet was resuspended in 10 ml complete RM+ culture medium, 10 µl of this suspension was mixed with 10 µl 0.4% (w/v) trypan blue (Invitrogen, Paisley, UK) and the viable cells were counted using a

haemocytometer (Weber Scientific International Ltd, Middlesex, U.K.). Trypan blue is selective for membrane-damaged, non-viable cells. This is because Trypan blue has a negatively charged chromophore, which cannot penetrate an intact cell membrane. Therefore viable cells appeared bright and not stained when viewed under the microscope, whereas non-viable cells were dark blue. Cells were then washed again by centrifugation (1,000 rpm, 5 min at room temperature) and resuspended in 10 ml complete RM+ culture medium. Two million freshly isolated keratinocyte cells were seeded with 2 million mitomycin C treated 3T3 fibroblasts that had been seeded the previous day (as described in section 2.1.2). The cells were incubated at 37°C in a humid environment of 90% air, 10%$CO_2$ (RM+ culture medium sodium bicarbonate concentration buffers to pH 7.4 at 10% $CO_2$ rather than 5% $CO_2$). The culture medium was refreshed two days later. The cells were monitored daily with further addition of mitomycin C treated 3T3 cells if required.

### 2.1.4 Passaging primary human keratinocytes

Once keratinocytes were 60 to 70% confluent, the 3T3 fibroblast layer was removed by washing the cells twice with 5 ml PBS followed by incubating cells for 5 min in 5 ml 1x versene (Gibco, Paisley, U.K.) at 37°C, 90% air, 10% $CO_2$. The progress of 3T3 detachment was monitored every few minutes by checking the cells under a Leica DMIRB light microscope (Leica Microsystems, Germany); the flask was also tapped to encourage detachment. After all the fibroblasts had detached, the versene containing 3T3 fibroblasts was aspirated and the keratinocytes were washed twice with 5 ml PBS. The keratinocytes were then incubated overnight at 37°C, 90% air, 10% $CO_2$ in complete RM+ culture medium.

The next morning, keratinocytes were washed twice in 5 ml PBS, once in 5 ml 1x versene then incubated at 37°C, 90% air, 10%$CO_2$ in 5 ml pre-warmed 0.05% (v/v) trypsin/ 0.02% (v/v) versene (PAA laboratories GmbH, Pasching, Austria). The detachment process was encouraged by tapping the flasks every few minutes and was monitored using a light microscope. To prevent cell death of detached keratinocytes, cells that had lifted off the flask after 5 min were transferred to a 50 ml centrifuge tube containing 20 ml complete RM+ culture medium (containing 10% (v/v) FBS, to stop the

trypsinisation) and 5 ml fresh pre-warmed 0.05% (v/v) trypsin/ 0.02% (v/v) versene was added to the remaining keratinocytes in the flask. This process was repeated several times until all the keratinocytes were removed from the flask.

Once all the keratinocytes had been trypsinised, they were centrifuged at 1,000 rpm for 5 min at room temperature. The supernatant was discarded and the cell pellet was resuspended in 10 ml complete RM+ culture media and centrifuged again at 1,000 rpm for 5 min. The supernatant was aspirated and the cell pellet was resuspended in 10ml complete RM+ culture medium. Cells were counted using a haemocytometer and then plated out for experiments, transferred to new flasks for propagation (at $2x10^6$ per T75 $cm^2$ flask) or cryopreserved for storage (see section 2.1.12).

### 2.1.5 Isolation of human dermal fibroblasts

Human dermal fibroblasts were segregated from the solid material remaining after keratinocyte isolation. The material was incubated overnight in a 100 mm cell culture dish with 15 ml 0.5 mg/ml collagenase D (Roche Diagnostics GmbH, Mannheim, Germany) in a humid environment with 90% air, 10% $CO_2$ at 37°C.

The next day, any remaining solid material was removed by sieving the sample. The filtrate (containing dermal fibroblasts) was then centrifuged, 1,000 rpm, 5 min at room temperature. The cell pellet was resuspended in 10 ml DMEM medium and the cells were counted using a haemocytometer. The fibroblasts were then transferred to a T75 $cm^2$ flask and incubated overnight in 20 ml DMEM medium, 37°C, 90% air, 10% $CO_2$. The culture medium was refreshed every 2 – 3 days and cells were passaged according to section 2.1.10.

### 2.1.6 N/TERT immortalised keratinocytes

N/TERTs are telomerase immortalised human keratinocytes first deposited by J. Rheinwald and were obtained from the Centre for Cutaneous Research, (Institute of Cell and Molecular Science, London, U.K.). The cells are cultured in complete RM+ culture medium at 37°C in a humidified environment of 90% air, 10% $CO_2$. The culture

medium was refreshed every 2 – 3 days and cells were passaged according to section 2.1.10.

### 2.1.7 HaCaT immortalised keratinocytes

HaCaT cells are spontaneously immortalised human keratinocytes that were established by Boukamp (Boukamp et al., 1988) and obtained from the Centre for Cutaneous Research, (Institute of Cell and Molecular Science, London, U. K.). HaCaTs were cultured in DMEM with 10% (v/v) FCS (Biosera Ltd., East Sussex, U.K.), 2 mM L-glutamine, 1x penicillin/ streptomycin (both PAA Laboratories GmbH, Pasching, Austria) and incubated at 37°C in a humidified environment of 95% air, 5% $CO_2$. The culture medium was refreshed every 2 – 3 days and cells were passaged according to section 2.1.10.

### 2.1.8 H295R immortalised adrenocortical cells

H295R cells (ATCC, Manassas, U.S.A.) were adapted from the H295 pluripotent adrenal carcinoma cell line that was established by A.F. Gazdar from an adrenal carcinoma. Whereas H295 cells grow in suspension, H295R cells are an adherent cell line. Both cell lines have retained the ability to synthesise androgens. H295R cells were cultured in 35 ml DMEM:F12 medium supplemented with 2.5% (v/v) Nu-Serum I and 1x ITS+ premix (BD Biosciences, Belgium) which contains 0.00625 mg/ml insulin; 0.00625 mg/ml transferrin; 6.25 ng/ml selenium; 1.25 mg/ml bovine serum albumin; 0.00535 mg/ml linoleic acid. The cells were incubated in a humidity chamber at 5 % $CO_2$, 95% air, 37°C. Culture medium was refreshed every 2 – 3 days and cells were passaged according to section 2.1.10.

### 2.1.9 JEG-3 human choriocarcinoma cells

JEG-3 human choriocarcinoma cells were obtained from Professor V.K Chatterjee, (Department of Medicine, University of Cambridge, Cambridge, U.K.). The cells were cultured in DMEM (Sigma-Aldrich, Poole, U.K.) supplemented with 10% (v/v) FBS

(Biosera, East Sussex, U.K.) and 1% (v/v) L-glutamine at 37°C, 95% air, 5% $CO_2$ in a humidity chamber. The culture medium was refreshed every 2 – 3 days and cells were passaged according to section 2.1.10.

### 2.1.10 Passaging cells

Cells that were not grown on a feeder layer were passaged when they were 70% confluent by washing once in 5 ml PBS, once in 5 ml versene and incubating for approximately 5 min in 5 ml 0.05% (v/v) trypsin/ 0.02% (v/v) versene until all the cells had detached. The trypsinisation process was monitored under a Leica DMIRB light microscope and stopped by adding 5 ml culture medium containing 10% (v/v) serum (FBS or CS depending on cell type). The cells were centrifuged at 1,000 rpm, for 5 min at room temperature. The supernatant was aspirated, the cell pellet resuspended in 10 ml culture medium and the cells counted using a haemocytometer (see section 2.1.11). Cells were then seeded for experiments, propagated at 10-20% of their original density or cryopreserved.

### 2.1.11 Cell counting

After trypsinisation, cells (10µl of cell suspension) were counted using a haemocytometer (Weber Scientific International Ltd, Middlesex, UK). To count live cells, a 10 µl aliquot of cells was diluted 1:2 with trypan blue (Sigma-Aldrich, Poole, U.K.) and 10 µl of this solution was deposited on the haemocytometer. The haemocytometer grid arrangement had four primary squares, each containing sixteen squares. The cells in one of the major squares were counted, those that lay inside the square or touched the top or left boundary were included; those that lay outside the square, or touched the lower or right boundary were excluded. Cells in another major grid were counted and an average of the two counts was taken. The average count was then multiplied by $1x10^4$ to give the value of cells per ml. If the cells had been counted in trypan blue for cell viability (section 2.3), then the average count was multiplied by two to allow for the 1 in 2 trypan blue to cell dilution factor.

### 2.1.12 Cryopreservation

Trypsinised cells were centrifuged at 1,000 rpm at room temperature and resuspended in freezing medium (10% (v/v) diethyl sulphoxide (DMSO) (Fisher, Leicestershire, U.K.), 90% (v/v) complete culture medium containing serum) to a concentration of $2x10^6$ cells per ml. DMSO was included in the freezing medium to prevent the formation of crystals during the freezing process that would otherwise lyse the cells. The cell suspension (1ml) was transferred into each cryovial and frozen slowly to –80°C. After 1 – 3 days, the cell vials were transferred and stored in liquid nitrogen until required.

When cryopresereved cells were required, the vial was removed from liquid nitrogen storage and thawed rapidly at 37°C in a waterbath. As soon as the cell aliquot had thawed, the cells were transferred to a 50 ml centrifuge tube containing 10 ml complete culture medium (relevant to the cell type) and centrifuged at 1,000 rpm for 5 min to remove the DMSO. The supernatant was aspirated and the cell pellet was resuspended in complete culture medium and cells were seeded in T75 $cm^2$ flasks at 2 million per flask.

### 2.1.13 NEB-1 organotypic raft preparation

Frozen sections of NEB-1 organotypic rafts were kindly donated by Dr. Anna Thomas (Institute of Cell and Molecular Science, London, U.K.) and prepared as follows:
Glycerol preserved skin was obtained from the European skin bank in Denmark. The skin was washed three times in PBS and incubated in PBS containing an antibiotic mix (600units/ml penicillin-G, 600 $\mu$g/ml streptomycin sulphate, 250 $\mu$g/ml gentamycin and 2.5 Mg/ml of fungizone; all from Sigma-Aldrich, Poole, U.K.) at 37ºC for 10 days. Following incubation, the epidermis was removed from the dermis with a pair of sterile forceps. The dermis was cut into 1.5 x 1.5 cm squares and placed into a well of a 6 well dish with a sterilised stainless steel ring placed on the reticular side of the dermis. Human dermal fibroblasts ($2x10^5$) were seeded on to the DED in the ring in RM+ culture medium. Additional RM+ culture medium was added around the ring to keep the DED moist. The preparation was incubated overnight in a humidity chamber at 10% $CO_2$, 90% atmospheric air, 37°C.

Following incubation, the medium and ring was removed from the DED, the DED was inverted and the ring was placed on the papillary surface of the DED. NEB-1 immortalised keratinocytes ($2x10^5$) were seeded on to the DED within the ring in RM+ culture medium. Additional RM+ culture medium was added around the ring to keep the DED moist. The preparation was incubated overnight in a humidity chamber at 10% $CO_2$, 90% atmospheric air, 37°C. The ring was removed and the preparation was incubated for a further 2 days submerged in RM+ culture medium in a humidity chamber at 10% $CO_2$, 90% atmospheric air, 37°C.

Following this incubation, the DED was raised and placed on steel grids with medium underneath so that the keratinoycte cultures were at an air-liquid interface. The raft preparation was incubated in a humidity chamber at 10% $CO_2$, 90% atmospheric air, 37°C for a further 14 days with the media changed every 2 – 3 days. After this time, the organotypic raft preparation was cryopreserved and cut into sections for histological analysis.

## 2.2 Immunofluorescence histochemistry and immunofluorescence cytochemistry

Immunofluorescence histochemistry (tissue) and cytochemistry (cells) is a technique using a fluorescent secondary antibody to detect a primary antibody bound to an antigen (i.e. protein of interest) within a tissue or cell sample. This identifies the expression pattern of a specific protein within the sample.

All primary and secondary antibodies were diluted in 1% (w/v) BSA TBS-T (50 mM Tris base, 140 mM NaCl, 0.1% (v/v) Tween-20, pH 7.6) and all incubations were carried out in a humidified chamber at room temperature.

### 2.2.1 Sample preparation and method for immunofluorescence histochemistry

Immunofluorescence histochemistry was used to determine the protein expression pattern of MLN64, DAX1, TSPO and StAR in human skin sections. Skin from normal facelift and breast reduction patients were cut into 1 cm x 1 cm pieces, transferred into cryovials and snap frozen in liquid nitrogen for 1 h. Psoriatic skin sections were a kind

gift from Dr. Paul Bowden (Cardiff University, Cardiff, U.K.) and Dr. Catherine Harwood (Institute of Cell and Molecular Science, London, U.K), atopic dermatitis skin sections were donated from Dr. Wei-Li Di (Institute of Child Health, London, U.K.) and Professor Arne Akbar (UCL, London, U.K.). Professor David Kelsell (Institute of Cell and Molecular Science, London, U.K) generously gave sections from harlequin ichthyosis biopsies.

Samples were stored at –80°C prior to being cut into sections by Alex Brown (ICMS Pathology, London, U.K.). Skin biopsies were cut by cryostat into 6 μm sections and mounted onto Superfrost ® Plus microscope slides (Knittel Glaser, Germany) and stored at –80°C. When required, skin sections were removed from –80°C storage and allowed to thaw for 20 min at room temperature. The tissue sections were then fixed by submerging in ice-cold methanol: acetone 1:1 (v/v) for 10 min.

Tissue sections were washed three times in TBS-T for 5 min per wash before incubating in blocking solution, 1% (w/v) bovine serum albumin (BSA) (Sigma-Aldrich, Poole, U.K.) TBS-T, for 30 min. The blocking solution was removed and 20 μl of primary antibody (either rabbit polyclonal StAR (10 μg/ml), rabbit polyclonal MLN64 (10 μg/ml), chicken polyclonal PBR (5 μg/ml) all from Abcam, Cambridge, U.K. or rabbit polyclonal DAX1 (K-17) (2 μg/ml) (Santa Cruz, California, U.S.A) was added to the sections for 1 h.

Samples were washed three times for 5 min per wash in TBS-T and then incubated for 1 h in the dark with 200 μl Alexa Fluor ® 488 goat anti-rabbit IgG (H+L) 2 μg/ml (Molecular Probes, Invitrogen, Paisley, UK) with the exception of samples treated with PBR antibody, which were incubated with 200 μl Alexa Fluor ® 594 goat anti-chicken IgG (H+L) 2μg/ml (Molecular Probes, Invitrogen, Paisley, UK). The sections were washed once in TBS-T and then once in TBS (without Tween-20, since Tween-20 can auto-fluoresce) for 5 min per wash. Samples were then washed in TBS containing 2 μg/ml 4',6-diamidion-2-phenylindole dihydrochloride (DAPI) (Sigma-Aldrich, Poole, UK).

The skin sections were sealed with a drop of fluorescent mounting medium (DakoCytomation, Glostrup, Denmark) and a 22 mm x 22 mm coverslip (VWR, Leicestershire, U.K.) and allowed to set overnight in the dark at 4°C. The fluorescent signal was observed using a Carl Zeiss Laser Scanning Microscope LSM 510 META (Carl Zeiss Ltd., Hertfordshire, U.K.) and analysed using Zeiss LSM Image Browser software (Carl Zeiss Ltd., Hertfordshire, U.K.).

### 2.2.2 Sample preparation and method for immunofluorescence cytochemistry

Primary keratinocytes ($5x10^4$) were seeded onto sterile 19 cm diameter coverslips (VWR, Leicestershire, U.K.) that had been pre-seeded with mitomcycin C-treated 3T3 mouse fibroblasts ($5x10^4$) 24 h earlier in complete RM+ culture medium. Keratinocytes were incubated for a period of time as indicated in the figure legend of the specific experiment, 24 h prior to analysis the fibroblasts were removed with 1x versene (described in section 2.1.4) and the keratinocytes were incubated overnight in complete RM+ culture medium. Cells were then washed twice in PBS and fixed and permeabilised in ice-cold methanol:acetone (1:1 (v/v); Fisher, Leicestershire, U.K) for 2 min.

Cells were washed three times in TBS-T for 5 min per wash before incubating in blocking solution, 1% (w/v) BSA (Sigma-Aldrich, Poole, U.K.) TBS-T, for 30 min. The blocking solution was removed and 20 µl of primary antibody either rabbit polyclonal StAR (10 µg/ml), rabbit polyclonal MLN64 (10 µg/ml), chicken polyclonal PBR (5 µg/ml) (all Abcam, Cambridge, U.K.) or rabbit polyclonal DAX1 (K-17) (2 µg/ml; Santa Cruz, California, U.S.A) was added to the sections for 1 h.

Cells were washed three times for 5 min per wash in TBS-T and then incubated for 1 h in the dark with 200 µl Alexa Fluor ® 488 goat anti-rabbit IgG (H+L) 2 µg/ml (Molecular Probes, Invitrogen, Paisley, UK), with the exception of samples treated with PBR antibody, which were incubated with 200 µl Alexa Fluor ® 594 goat anti-chicken IgG (H+L) 2µg/ml (Molecular Probes, Invitrogen, Paisley, UK). Cells were washed once in TBS-T and then once in TBS (without tween, since tween can auto-fluoresce)

for 5 min per wash. Samples were then washed in TBS containing 2 μg/ml 4',6-diamidion-2-phenylindole dihydrochloride (DAPI) (Sigma-Aldrich, Poole, UK).

The coverslips (that the cells were seeded on) were inverted and mounted with a drop of fluorescent mounting medium (DakoCytomation, Glostrup, Denmark) onto Superfrost ® Plus microscope slides (Knittel Glaser, Germany) and allowed to set overnight in the dark at 4°C. The fluorescent signal was observed using a Carl Zeiss Laser Scanning Microscope LSM 510 META (Carl Zeiss Ltd., Hertfordshire, U.K.) and analysed using Zeiss LSM Image Browser software (Carl Zeiss Ltd., Hertfordshire, U.K.).

### 2.3 Protein isolation

Protein was isolated from cells and whole skin to be used for western analysis. Two methods, one using a RIPA buffer and the other a urea buffer, were used to isolate protein as outlined below.

#### 2.3.1 Total protein isolation

Cells seeded in 6 well plates were washed twice in ice-cold 1 ml PBS (PAA laboratories GmbH, Pasching, Austria) and then incubated in ice-cold 300 μl RIPA buffer (Tris 50 mM, pH 7.3, NaCl 150 mM, SDS 0.1% (w/v), NP-40 0.1% (v/v) (all from Sigma-Aldrich, Poole, U.K.) and 1X Complete Protease Cocktail Inhibitor (Roche Diagnostics GmbH, Mannheim, Germany) for 20 min. The protein was harvested in 1.5 ml microfuge tubes and pulse sonicated twice for 3 sec (Vibra Cell, Sonic and Material Incs, Danbury, CT, USA). The samples were then centrifuged for 5 min, 4°C, 10,000 x g to remove cell debris. The protein concentration of the supernatant was determined using a Bradford assay (section 2.4) and samples were stored at –80°C.

Alternatively, cells seeded in 6 well plates were washed twice in ice-cold 1 ml PBS and then incubated in 300 μl of 8 M urea buffer (8 M urea, 1 M thiourea, 0.5% (w/v) 3-[(3-cholamidopropyl)dimethylammonio]-1-propanesulfonate (CHAPS), 50 mM dithiothreitol (DTT), 24 mM spermine) for 5 min at room temperature. This is a strong buffer which rapidly lyses the cells and denatures all protein. The sample suspension

was harvested in 1.5 ml microfuge tubes and centrifuged at 10,000 x g for 5 min at 4°C. The supernatant (containing protein isolate) was transferred to fresh microfuge tubes and protein concentration was determined by Bradford assay (section 2.4) and samples were stored at –80°C if they were not used immediately.

### 2.3.2 Total protein isolation from human skin

Human fronto-temporal scalp skin specimens were obtained with informed consent during routine face-lift surgery (all Caucasian females over 40 years). The skin was cut into 10 x 5 mm pieces, individually transferred to cryovials and snap frozen in liquid nitrogen. A frozen skin section was then smashed to a powder using a metal pestle and mortar pre-chilled with liquid nitrogen. The skin powder was scraped up and transferred to a 5 ml bijoux tube (Fisher, Leicestershire, U.K.) containing 1 ml of RIPA buffer. The sample was homogenised on ice for 1 min at speed 5 using an Ultra-Turrax, x120 Status homogeniser. The sample was left in RIPA buffer for 20 min on ice, then sonicated for 3 x 3 sec pulses and centrifuged for 10 min at 10,000 x g at 4°C. The supernatant, containing the protein was transferred to a fresh 1 ml microfuge tube and stored at –80°C before being analysed for the protein concentration and used for western blot analysis (see Section 2.5).

### 2.3.3 Mitochondrial protein enrichment

Cells (JEG3, dermal fibroblasts, HaCaTs, primary human keratinocytes) were seeded at $1.5x10^6$ in 10 ml of their respective culture medium in 100 mm diameter cell culture dishes and incubated overnight in a humidity chamber, 37°C, 90% air, 10% $CO_2$. The media was refreshed and cells were treated with or without 1 mM dibutyryl cAMP (D0260, Sigma, Poole, UK) for 4 h 30 min.

Cells in 100 mm diameter Petri dishes were washed twice in ice cold 5 ml PBS and then harvested in 300 µl mitochondrial enrichment buffer pH 7.4 (20 mM HEPES-KOH, 10 mM KCl, 1.5 mM $MgCl_2$, 0.5 mM EGTA, 0.5 mM EDTA, 1M DTT) supplemented with 250 mM sucrose and 1X complete protease cocktail inhibitor (Roche Diagnostics GmbH, Mannheim, Germany). Cells were homogenised with approximately 60 stokes

of a 1 ml Dounce glass homogeniser with a tight pestle (Wheaton, Fisher Scientific, Leicestershire, UK). To remove the nuclear fraction and unlysed cells, the homogenate was centrifuged at 600 x g at 4°C for 5 min. The supernatant was transferred to a fresh tube and re-centrifuged at 600 x g at 4°C for 5 min. The supernatant was transferred to a fresh tube and centrifuged at 10,000 x g for 30 min at 4°C. The pellet, containing enriched mitochondrial protein, was resuspended in 50 µl mitochondrial enrichment buffer supplemented with 1X complete protease cocktail inhibitors but not sucrose. The protein concentration was determined using a BCA kit and stored at –80°C.

**2.4 Protein quantification**

The concentration of isolated protein was estimated using a Bio-Rad protein assay kit (Bio-Rad Laboratories, Hertfordshire, UK) based on the Bradford assay (Bradford, 1976). A protein standard curve was generated using 0.1 to 0.8 mg/ml BSA that had been reconstituted in the same buffer as the samples to be analysed. Protein standard or sample (10 µl) was pipetted in triplicate into well of a clear, flat bottomed 96-well plate (Fisher, Leicestershire, U.K.). To this, 200 µl of Bio-Rad protein assay solution was added and mixed well. The intensity of the solution colour in each well, which was proportional to the amount of protein, was measured using a spectrophotometer plate reader measuring absorbance at 600 nm (Victor 1420 Multi-Label Counter, Wallac, PerkinElmer, MA, USA). A standard curve was plotted (intersecting the y-axis at 0 since the value of the blank was subtracted from all readings) and the protein concentration of each sample was calculated according the equation of the straight line from the standard graph (Figure 2.1).

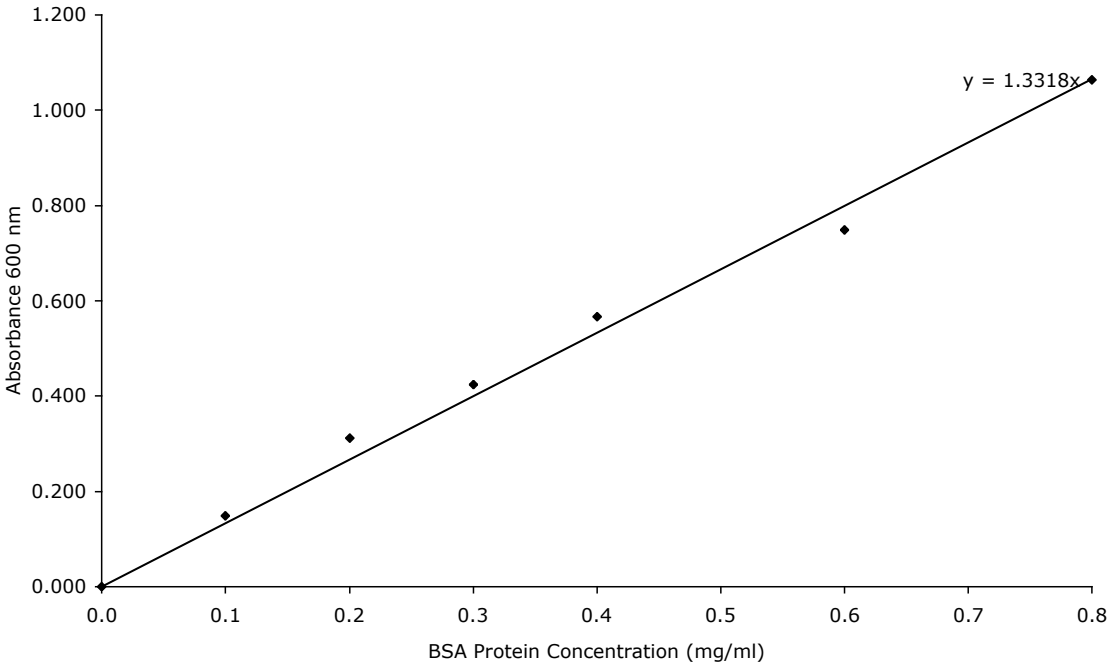


**Figure 2.1 Example of a Bio-Rad Bradford assay protein standard curve.**

## 2.5 Western blotting

Western blotting can be used to estimate the expression of a specific protein in cell lysates. Protein isolated from the cell is first denatured and then separated according to size by sodium dodecyl sulphate (SDS) gel electrophoresis. SDS applies a negative charge to any positive ion on the protein, thus allowing the protein to be transferred to a nitrocellulose membrane by electrophoresis. A specific protein is then detected on the membrane using a primary antibody, which a secondary antibody that is coupled to horseradish peroxidase (HRP) binds to. Bound secondary antibody can be detected by luminescence due to a chemical reaction with HRP upon the addition of ECL plus (GE Healthcare, Buckinghamshire, U.K.). The resulting light emission is detected using an autoradiography film.

### 2.5.1 Sodium dodecyl sulphate - polyacrylamide gel electrophoresis

Protein samples were adjusted to 1 mg/ml protein according to the outcome of the Bradford assay. Protein was reduced and denatured by adding 1:4 Laemmli buffer (Invitrogen Ltd, Paisley, U.K.), 2% (v/v) β-mercaptoethanol (VWR, Leicestershire, U.K.) and heating for 5 min at 95°C. A NuPAGE 10% Bis-Tris gel (Invitrogen, Paisley, U.K.) was assembled into a Novex Mini-cell gel electrophoresis tank (Invitrogen, Paisley, U.K.) according to manufacturers instructions and the tank was filled with 1X MOPS Running buffer (Invitrogen, Paisley, U.K.). Equal protein concentration and volume of each sample was loaded into the wells of the gel. In addition 10 µl of SeeBlue Plus Two protein standard molecular weight marker (Inivtrogen, Paisley, U.K.) was loaded into one well of the gel. The proteins were separated at 200 V for 50 min until the dye front reached the base of the gel.

### 2.5.2 Western blotting

Proteins were transferred from the polyacrylamide gel to a 45 micron Hybond C Extra nitrocellulose membrane (GE Healthcare, Buckinghamshire, U.K.) in 1X NuPAGE transfer buffer (Invitrogen, Paisley, U.K.) including 10% (v/v) methanol (Fisher, Leicestershire, U.K.) at 150 V, 250 mA for 90 min at 4°C. The membrane was

removed and immediately immersed in blocking solution and incubated according to table 2.1. The success of the transfer was estimated by checking the protein marker was present on the membrane. The membrane was then incubated in 10 ml of primary antibody (see Table 2.1 for the conditions of each antibody) on a rocking platform.

The membrane was washed three times for 5 min in TBS-T and then transferred into 10 ml 0.05 mM swine anti-rabbit HRP secondary antibody (DakoCytomation, Glostrup, Denmark) (Table 2.1), unless the primary antibody was mouse anti-β-actin, for which 10 ml 0.05 mM goat anti-mouse HRP secondary antibody (DakoCytomation, Glostrup, Denmark), or chicken anti-PBR (peripheral benzodiazepine receptor also known as TSPO), for which 10 ml 2 μg/ml goat anti-chicken IgY HRP secondary antibody (Abcam, Cambridge, U.K.) was used. All secondary antibodies were diluted 1:1000 in the same buffer as the primary antibody and incubated on a rocking platform for 1 h at room temperature. After 1 h the membrane was washed three times for 5 min in TBS-T. The protein of interest was detected by covering the membrane in 1 ml ECL-Plus chemiluminesence solution (GE Healthcare, Buckinghamshire, U.K.). The blot was wrapped in cling film. The resulting luminescence was observed by exposing the blot to light-sensitive Hyperfilm (GE Healthcare, Buckinghamshire, U.K.) for 1 – 30 min, depending on signal intensity, in a dark room and the film was developed using a Hyperprocessor automatic Autoradiography Film Processor (GE Healthcare, Buckinghamshire, U.K.).

| Protein | Blocking conditions | Primary antibody supplier and concentration or dilution | Primary antibody dilution buffer and incubation |
|---|---|---|---|
| StAR | 5% milk TBS-T, overnight, 4°C | StAR (ab3433, Abcam, Cambridge, UK) 1 μg/ml | 1% milk TBS-T, overnight, 4°C |
| DAX1 | 5% milk TBS-T, overnight 4°C | DAX1 (sc-841, Santa Cruz) 1 μg/ml | 1% milk TBS-T, 1 h, RT |
| MLN64 | 5% milk TBS-T, overnight 4°C | MLN64 (ab3478, Abcam, Cambridge, UK) 1 μg/ml | 1% milk TBS-T, 1 h, RT |
| TSPO | 5% milk TBS-T, overnight 4°C | PBR (ab37884, Abcam, Cambridge, UK) 5 μg/ml | 1% milk TBS-T, 1 h, RT |
| DUSP1 | 5% milk TBS-T, overnight 4°C | MKP1 (sc-1102, Santa Cruz) 1 μg/ml | 1% milk TBS-T, 1 h, RT |
| ERK 1/2 | 5% BSA TBS-T, 1 h, RT | p44/42 MAP kinase 1:1,000 (Cell Signalling, Danvers, MA. U.S.A.) | 5% BSA TBS-T, overnight, 4°C |
| pERK 1/2 | 5% BSA TBS-T, 1 h, RT | phospho- p44/42 MAP kinase, 1:2,000 (Cell Signalling, Danvers, MA. U.S.A.) | 5% BSA TBS-T, overnight, 4°C |
| pMEK | 5% BSA TBS-T, 1 h, RT | phospho MEK 1:1,000 (Cell Signalling, Danvers, MA. U.S.A.) | 5% BSA TBS-T, overnight, 4°C |
| β-Actin | 5% milk TBS-T, 1 h RT | β-Actin, 1:10,000 (Sigma-Aldrich, Poole, UK) | 1% milk TBS-T, 1 h RT |

**Table 2.1 Antibodies and conditions for western blotting.**

All primary antibodies listed are rabbit polyclonal antibodies, except for β-actin which is a mouse monoclonal antibody and TSPO which is a chicken polyclonal antibody.

### 2.5.3 Western blot membrane stripping and reprobing

Western blots can be reprobed for another protein of interest by stripping the membrane of primary and secondary antibodies and repeating the detection step with different antibodies. Thus a housekeeping gene, such as β-actin, can be detected to check equal loading between samples or, in the case of mitogen activated protein kinases (MAPK), phosphorylated versus total protein levels can be compared.

Membranes were stripped by incubation with stripping buffer (62.5 mM Tris pH 6.8, 2% (w/v) SDS, 100 mM β-mercaptoethanol, all from Sigma-Aldrich, Poole, U.K.) for 30 min at 60°C in an oven on a rocking platform. The blot was then washed three times in TBS-T for 5 min at room temperature and then blocked and re-probed with primary and secondary antibody according to Section 2.5.2 and Table 2.1.

## 2.6 Reverse transcriptase - polymerase chain reaction

Reverse transcriptase-polymerase chain reaction (RT-PCR) is a method to detect genes that are synthesised into RNA in cells or tissue. Extracted RNA is converted into DNA by reverse transcriptase. The presence of a specific DNA sequence is then targeted and amplified by PCR with the aid of oligonucleotide primers that are complementary to the flanking DNA regions of interest. The PCR product is separated by size by running the sample on an ethidium bromide-agarose gel that can be visualised with ultra violet (U.V.) light. If the size of the PCR product correlates with the expected size, the product can be extracted and authenticated with DNA sequencing.

### 2.6.1 Total RNA extraction from cultured cells

Cells were trypsinised as described in section 2.1.4 or 2.1.10 (depending on whether cells were cultured with 3T3 feeders) and centrifuged for 5 min at 1,000 rpm at room temperature. The cells were then washed twice in ice cold PBS and centrifuged for 5 min at 1,000 rpm. The work surface and pipettes were prepared with RNase Zap (Ambion, Cambridgeshire, U.K.) to remove enzymes that digest RNA. RNA extraction

was carried out using an RNeasy Mini Kit (Qiagen, West Sussex, U.K.). All centrifugation steps were at 13,000 rpm for 15 sec at room temperature unless stated otherwise. All flow-throughs were also discarded unless stated otherwise.

The supernatant was aspirated and the cell pellet was resuspended in 600 µl RLT buffer. The RLT buffer acts to lyse the cells and contains guanidine isothiocyanate, which deactivates RNase enzymes.

The cell lysate was transferred and passed through a QIAshredder Mini Spin column by centrifugation at 13,000 rpm for 2 min. The flow through solution was retained and mixed with 600 µl of 70% (v/v) ethanol. The sample was then transferred into an RNeasy Mini Spin column and RNA (and DNA) within the sample was adhered to the column by centrifugation.

RW1 wash buffer (350 µl) was added and the column was centrifuged. Genomic DNA was digested by adding 80 µl 1:5 (v/v) DNase: RDD buffer (RNase Free DNase Set, Qiagen, Crawley, West Sussex, U.K.) to the column and incubating for 15 min at room temperature.

The digested DNA was washed from the column with 350 µl RW1 following centrifugation. The column was then washed with 700 µl RPE buffer (part of RNeasy Mini kit) and centrifuged. The column was washed again with 500 µl RPE buffer and centrifuged for 2 min at 13,000 rpm. Finally, the column was transferred to a fresh RNase-free microfuge tube and the RNA was eluted by addition of 30 µl RNase free water to the column followed by centrifugation at 10,000 rpm for 1 min. The RNA was stored at -80°C until required.

### 2.6.2 RNA quantification

Isolated RNA was quantified using a NanoDrop ND-1000 Spectrophotometer (Labtech International Ltd, East Sussex, U.K.). The instrument was blanked against 1.5 µl diethyl-pyrocarbonate (DEPC)-treated water (Sigma-Aldrich, Dorset, U.K.). The

sample RNA content and quality was estimated from a 1.5 µl aliquot on the spectrophotometer measured at 260 to 280 nm.

### 2.6.3 Reverse transcriptase complementary DNA synthesis

Reverse transcriptase is an enzyme that transcribes single-stranded RNA into double-stranded DNA. Reverse transcriptases were first identified from tumour viruses by Temin and Baltimore in 1970 (Baltimore, 1970; Temin and Mizutani, 1970). Complimentary DNA synthesis from the RNA sample was achieved using SuperScript III First-Strand Synthesis SuperMix (Invitrogen, Paisley, U.K.). Firstly, the following reagents (10 µl 2x RT Reaction Mix, 2 µl RT Enzyme Mix, DEPC-treated water (all from Invitrogen, Paisley, U.K.) and 1 µg of sample RNA (final volume 20 µl) were mixed together and incubated for 10 min at 25°C. The tube was then incubated for 30 min at 50°C. The cDNA synthesis reaction was terminated by heating the sample to 85°C for 5 min, followed by chilling on ice. Finally, 1 µl (2 units) of *E. coli* RNase H was added to the mix and incubated for 20 min at 37°C to remove the RNA template. The cDNA sample was stored at –20°C until required.

To generate two negative controls for PCR, the reverse transcriptase reaction was carried out as described above but with the omission of (a) sample RNA or (b) RT Enzyme Mix.

### 2.6.4 Primer selection and sequences

Sense and anti-sense oligonucleotide primer sequences for StAR were designed using Primer 3 using the StAR gene sequence from the ensembl database (http://www.ensembl.org/index.html). Primer sequences for GAPDH were chosen from a previously published paper (Alexander and Klibanski, 1994). All primers were checked for non-specific binding using NCBI genebank BLAST analysis (http://blast.ncbi.nlm.nih.gov/Blast.cgi).

StAR Primer sequences:
Sense strand: 5'- GCATCCTTAGCAACCAAGAG-3'
Anti-sense strand: 5'- CCAGCTCGTGAGTAATGAATG-3'
Predicted PCR product size: 333 bp

GAPDH Primer sequences:
Sense strand: 5'-GAGCCACATCGCTCAGAC-3'
Anti-sense strand: 5'-TTCTCCATGGTGGTGAAG-3'
Predicted PCR product size: 340 bp

### 2.6.5 Polymerase chain reaction

Polymerase chain reaction (PCR) was conducted by combining 2 μl of cDNA with 0.5 μl of sense primer, 0.5 μl of anti-sense primer, 44 μl 1.1X ReddyMix PCR Master Mix (ABgene, Epsom, Surrey, U.K.) and 3 μl DEPC-treated water in a PCR tube and subjecting the sample to thermal cycling conditions as described in Table 2.2 and 2.3. The 1.1x ReddyMix PCR Master Mix contained 1.25 units of Taq DNA polymerase, 75 mM Tris HCl (pH 8.8 at 25°C), 20 mM $(NH_4)_2SO_4$, 1.5 mM $MgCl_2$, 0.01% Tween 20, 0.2 mM deoxyadenosine 5'-triphosphate (dATP), 0.2 mM deoxycytosine 5'-triphosphate (dCTP), 0.2 mM deoxyguanine 5'-triphosphate (dGTP), 0.2 mM deoxythymine 5'-triphosphate (dTTP), an inert red dye and gel loading precipitant. Thus the 1.1x ReddyMix was a simple one-step master mix for PCR and also allowed the PCR product to be loaded directly onto an agarose gel without further addition of a loading dye.

Two negative controls (RNA-free and reverse transcriptase enzyme-free) generated from the reverse transcriptase reaction (see Section 2.6.3) were concurrently subjected to the PCR. cDNA from H295R immortalised adrenal cells was used as a positive control for StAR. Equal loading was confirmed by GAPDH.

| Stage | Function | Temperature (°C) | Time | Number of cycles |
|---|---|---|---|---|
| 1 | Initial denaturation | 95 | 60 sec | 1 |
| 2 | Denaturation | 95 | 15 sec | 30 |
| | Annealing | 56 | 30 sec | |
| | Extension | 72 | 30 sec | |
| 3 | Final extension | 72 | 5 min | 1 |
| | Hold | 4 | Indefinite | |

**Table 2.2 Conditions used during thermal cycling for StAR PCR.**

| Stage | Function | Temperature (°C) | Time | Number of cycles |
|---|---|---|---|---|
| 1 | Initial denaturation | 94 | 60 sec | 1 |
| 2 | Denaturation | 94 | 60 sec | 35 |
| | Annealing | 55 | 60 sec | |
| | Extension | 72 | 60 sec | |
| 3 | Final extension | 72 | 5 min | 1 |
| | Hold | 4 | Indefinite | |

**Table 2.3 Conditions used during thermal cycling for GAPDH PCR.**

### 2.6.6 Agarose gel electrophoresis

PCR products (10 μl) were loaded on to a 1% (w/v) agarose-tris-acetate ethylediamine-tetra-acetic acid (TAE) gel containing 1 mg/ml ethidium bromide (Sigma-Aldrich, Poole, U.K.) in a gel tank with TAE running buffer. Ethidium bromide intercalates with

DNA, the intercalation causes the ethidium bromide molecule to strongly fluoresce when exposed to U.V. light. This allows for the location of DNA to be visualised on the gel under U.V. light. The samples were run against 10 µl Trackit 1 kB DNA ladder (Invitrogen, Paisley, U.K.), to estimate the product size, and separated by electrophoresis for 30 min at 120 V. Finally the PCR products were visualised by U.V. light and the gel was photographed using a Multi Image Light Cabinet (Alpha Innotech Corporation, San Leandro, CA, U.S.A.).

### 2.6.7 DNA sequencing

If the PCR product matched the predicted size, the remaining PCR sample (100 ng minimum) and StAR primers (10 pmol of each) were sent to the Genome Centre (Barts and The London, Charterhouse Square, London, U.K.) for PCR purification and sequencing to determine the authenticity of the product.

## 2.7 Pregnenolone radioimmunoassay

Radioimmunoassay (RIA) is an extremely sensitive method for detecting the concentration of a specific substance such as a peptide or non-peptide hormone, drug, vitamin, cyclic nucleotide, virus or protein. The assay was developed by Rosalyn Yalow, who observed that intravenously administered $^{131}$I-labelled insulin radioactivity disappeared more slowing from plasma of patients that had received insulin treatment compared to those that had not (Yalow and Berson, 1959). Yalow suspected that this was due to increased binding of $^{131}$I-labelled insulin to antibodies which had been produced in response to exogenous insulin treatment (Yalow, 1977). Yalow developed the observation into an assay that allowed concentrations of plasma insulin and other molecules to be quantified, even at low (pmole) concentrations, and later was awarded the Nobel Prize for her efforts (Yalow, 1977). The technique was then developed to measure steroid molecules. This revolutionised endocrinology because of its increased specificity and sensitivity over previous analytical methods (Hillier, 2007).

RIA quantitatively analyses pregnenolone synthesis by assessing competitive binding of cold pregnenolone (endogenous steroids released by cells) against radiolabeled

pregnenolone to a pregnenolone antibody. Any non-bound steroid is removed with dextran-coated charcoal. Thus the detected radioactive signal correlates inversely to the amount of pregnenolone synthesised by the cells. The concentration of pregnenolone released by the cells is quantified against a standard curve generated using known concentrations of cold pregnenolone.

### 2.7.1 Cell preparation for RIA

For RIA, primary keratinocytes (passage 1) were plated at $2x10^5$ cells per well in 24-well plates, grown in 3:1 DMEM:Hams F12 complete media and incubated in a humid atmosphere with 10% $CO_2$, 90% air at 37°C for 24 h in the absence of 3T3 fibroblasts. Keratinocytes were washed twice with serum free DMEM supplemented with 1% (v/v) glutamine and then incubated in serum free DMEM supplemented with 1% (v/v) glutamine, 100 μM trilostane (an 3βHSD inhibitor) and 10 μM ketoconazole (a CYP17 inhibitor) for 2 h in a humidity chamber with 95% air/5% $CO_2$ at 37°C. Control cells were incubated for 2 h as described above but without the 3βHSD/CYP17 inhibitors.

Following incubation, fresh serum free DMEM supplemented with 1% (v/v) glutamine, 100 μM trilostane and 10 μM ketoconazole was added to all cells, except control cells which had medium without the 3βHSD/CYP17 inhibitors. In addition, some cells were treated in triplicate with 5 μM 25R-OH cholesterol and/or EGF 60 ng/ml (Sigma-Aldrich, Poole, U.K.), 50 ng/ml TNFα, 1 μM dex and/or 50 ng/ml TNFα combined with 1 μM dex (all from Sigma-Aldrich, Poole, U.K.) in the presence of 3βHSD/CYP17 inhibitors. All cells were incubated in a humid atmosphere with 95% air/ 5% $CO_2$ for 24 h.

### 2.7.2 Pregnenolone RIA

Culture medium from cells treated as described above was collected in borosilicate glass tubes (Jencons-Pls, Leighton Buzzard, U.K.) and stored at –20°C prior to assay. Borosilicate glass was chosen since steroids can adhere to plastic and soda lime glass. Culture samples were thawed and centrifuged at 250 x g, 4°C for 5 min and 100 μl of

the supernatants were transferred in triplicate to clean glass tubes. An anti-pregnenolone antibody (diluted 1:3000) and 1.50 pmol [7-$^{3}$H]-pregnenolone (specific activity = 11.5 Ci/mmol; PerkinElmer, Boston, MA) were added to each sample. Non-bound pregnenolone was removed with a charcoal-dextran (T500 buffer Dextran T500 0.025% (w/v), charcoal 0.25% (w/v), 40mM $NaH_2PO_4.2H_2O$, 70 mM $NaHPO_4$, 75 mM NaCl, 0.1% (w/v) Gelatin pH 7.2; all compounds from Sigma Aldrich, Poole, U.K.). Unknown samples were compared to concurrently run standards and adjusted for non-specific binding (determined in the presence of an excess of non-radioactive pregnenolone) to calculate pregnenolone concentrations. All measured pregnenolone levels were standardised per ml culture medium. The working range of this RIA was 15.6 – 250 nmol/L with an assay sensitivity of 3.91 nmol/L.

**2.8 Radiometric steroid metabolism assays**

Primary keratinocytes (passage 2) were plated at $2x10^5$ cells per well in 24-well plates and incubated for 2 days in keratinocyte defined media (KDM) (Invitrogen, Paisley, U.K.) supplemented with 1.2 mM $CaCl_2$. All cells were washed twice in serum free DMEM supplemented with 1% (v/v) glutamine prior to treatment. Cells used to assess pregnenolone metabolism were pre-treated with 100 μM trilostane and 10 μM ketoconazole for 2 h in a humidity chamber with 5% $CO_2$ in air at 37°C. Triplicate wells of cells were incubated at 37°C for 24 h in a humid atmosphere of 5% (v/v) $CO_2$ in air with 0.037 MBq of [$^{3}$H]-steroid. This equated to 90.0 pmol [7-$^{3}$H]-pregnenolone (with or without 100 μM trilostane and 10 μM ketoconazole), 11.0 pmol [1,2,6,7-$^{3}$H]-progesterone or 13.7 pmol [1,2,6,7-$^{3}$H]-cortisol per ml of culture medium. Assay blanks were set up and incubated as described above but in the absence of cells.

Steroids released into the culture medium by keratinocytes were extracted by vigorous mixing with two volumes of chloroform (HPLC grade, Fisher, Leicestershire, U.K.). After centrifugation at 1,000 x g for 30 min at 4°C the aqueous phase was removed and the remaining chloroform was evaporated under nitrogen gas at 45°C. Steroid extracts were reconstituted in up to 50 μl ethyl acetate, from which 20 μl was transferred onto a thin layer chromatography (TLC) plate (Merck, Damstadt, Germany). The remaining 30 μl was reserved to be run with authentic standards (10 mM pregnenolone,

progesterone or cortisol, all purchased from Sigma-Aldrich, Poole, U.K.). Migration of reference steroids was monitored by spiking aliquots of each sample with 0.037 MBq [$^3$H] cortisol, [$^3$H] progesterone or [$^3$H] pregnenolone. TLC plates were developed in a tank in a pre-equilibrated atmosphere of 92:8 (v/v) chloroform: 95% (v/v) ethanol. Resolution of [$^3$H]-steroid metabolites was quantified using an AR2000 Bioscan radiochromatogramme scanner (Lablogic Ltd, Sheffield, U.K.) and Laura Lite software (version 3.0; Lablogic Ltd, U.K.).

**2.9 Liquid chromatography-mass spectrometry**

Liquid chromatography-mass spectrometry (LC-MS) was used to confirm the results generated from TLC analysis and to authenticate the formation of cortisol by primary keratinocytes.

Primary human keratinocytes were seeded at $1x10^6$ cells in a total volume of 3 ml 3:1 DMEM:Hams F12 complete media into a 12-well plate and allowed to adhere to the plate by incubating in a humidity chamber at 37°C, 10% $CO_2$, 90% atmospheric air overnight. The primary keratinocytes were treated for 24 h in serum-free DMEM supplemented with 1% (v/v) glutamine with or without 1 μM progesterone (Sigma-Aldrich, Poole, U.K.) in a humidified chamber at 37°C in 5% (v/v) $CO_2$ in air. Assay blanks were set up and incubated as described above but in the absence of cells.

10 ng of each internal standard (see below) were added to 2.5 ml culture medium. Steroids were then extracted from the culture medium by vigorously mixing the sample with 1.5 ml diethylether. The organic phase was transferred to a fresh borosilicate glass tube and evaporated under nitrogen gas, then reconstituted by vortexing in 100 μl of 50% (v/v) methanol and filtered through 0.45 μm. An ultra pressure liquid chromatography system (Waters, Milford, MA, USA) was used for sample separation with an Acquity BEH Phenyl reverse phase column, 100 mm length x 2.1 mm bore with 1.7 μm pore size. Mobile phase A was 0.1% (v/v) formic acid in water and mobile phase B was 0.1% (v/v) formic acid in acetonitrile. Separation was performed at the following gradients: 22% (v/v) B (0 – 5 min), 22%-52% (v/v) B (5 – 15 min, linear gradient), 52%-100% (v/v) B (15 – 16 min), 100% (v/v) B (16 – 20 min), 100%-22%

(v/v) B (20 – 21 min), 22% (v/v) B (21 – 25 min), while maintaining the flow rate at 0.4 ml/min. A Micromass quadruple Q-TOF Premier mass spectrometer (Waters, Milford, MA, USA) was used for detection. The instrument was set to ESP+ ionization mode, V-mode for 250 – 500 Da range. Cortisone [4-Pregnen-17α,21-diol-3,11,20-trione] (MW 360.44, m/z 361.20), Cortisol [4-Pregnene-11β,17α,21-triol-3,20-dione] (MW 362.46, m/z 363.22), Progesterone [4-Pregnene-3,20-dione] (MW 314.46, m/z 315.23) and Pregnenolone [5-Pregnen-3β-ol-20-one] (MW 316.48, m/z 299.24 + 317.25); (Sigma-Aldrich, Poole, U.K.) were used for calibration. Cortisone D2 (MW 362.46, m/z 363.21), Cortisol D4 (MW 366.49, m/z 367.24), Progesterone D9 (MW 323.52, m/z 324.28) and Pregnenolone D4 (MW 320.51, m/z 303.26 + 321.27); (C/D/N Isotopes Inc., Quebec, Canada) were used as internal standards. All steroid concentrations were standardised to $1x10^6$ cells.

**2.10 Cortisol enzyme-linked immunosorbent assay**

Primary human keratinocytes were seeded at $2x10^5$ cell/ml in 12-well plates in DMEM, RM+ culture medium, Keratinocyte defined medium (Gibco, Invitrogen Coporation, Paisley, U.K.) or EpiLife complete culture medium (Gibco, Invitrogen Coporation, Paisley, U.K.) (1ml/well) with supplements and allowed to adhere overnight in a humidified chamber, 37°C, 95% air, 5% $CO_2$. The cells were then washed three times in basal culture medium (respective culture medium with no supplemental additions) before being incubated for 24 h at 37°C in respective basal culture medium (with the exception of RM+(+sup) that contained 2 mM L-glutamine, 1X penicillin streptomycin, 5 μg/ml apo-transferrin, 100 pM cholera toxin, 5 μg/ml insulin, 20 pM liothyronine and 10 ng/ml EGF) in a humidified chamber, 37°C, 95% air, 5% $CO_2$. An assay blank was set up and incubated as described above but in the absence of cells.

The supernatant was analysed for cortisol using an enzyme-linked immunosorbent assay (ELISA) kit purchased from R&D Systems (Minneapolis, U.S.A.). The ELISA was conducted according to the manufacturer's instructions with the exception that the supernatants were not diluted. Standards and non-specific binding controls for the ELISA were therefore prepared in respective basal medium to account for this alteration to the assay.

## 2.11 MTT assay

The MTT (3-(4,5-dimethylthiazol-2-yl)-2,5-diphenyl tetrazolium bromide) assay is a rapid colorimetric analysis of mitochondrial reductase activity in metabolically active cells. Therefore the MTT assay generally corresponds to the number of proliferating cells. The soluble yellow tetrazolium salt (MTT) is reduced to purple insoluble formazan crystals by mitochondrial dehydrogenases that normally act to reduce nicotinamide adenine dinucleotide ($NAD^+$) and nicotinamide adenine dinucleotide phosphate ($NADP^+$) to NADH and NADPH respectively in active cells. The purple formazan crystals are solublised by DMSO/isopropanol and quantified using spectrophotometry by measuring the absorbance at 570 nm.

Primary keratinocytes were seeded at 5 x $10^4$ cells per well of a 24-well plate in modified RM+ culture medium (without cortisol and 1% FCS) and incubated overnight at 37°C, 10%$CO_2$, 90% air in a humidified chamber. The following day, the keratinocytes were washed twice in PBS then incubated in triplicate with treatments as described in Chapter 5. After three days, the culture media was aspirated from the wells and the cells were washed twice in PBS. MTT (500 µl of 0.5 mg/ml in PBS) (Sigma-Aldrich, Dorset, U.K.) was added to each well and incubated for 1 h at 37°C. The MTT solution was then aspirated and the cells were washed once in PBS before 300 µl of 10% (v/v) DMSO in propan-2-ol was added to each well to dissolve the formazan crystals. After 10 min the plate was agitated to ensure complete solubilisation of the crystals and 200 µl of the solution from each well was transferred to a well of a clear, flat bottomed 96-well plate. The optical density was measured at 570 nm using a 96-well plate reader (Victor 1420 Multi-Label Counter, Wallac, PerkinElmer, MA, USA).

## 2.12 Flow cytometry

Flow cytometry utilises cell size, granularity and fluorescent markers to sort discrete populations of cell types. Thus early apoptotic cells were detected by an annexin V antibody conjugated with fluorescein isothiocyanate (FITC) and propidium iodide (PI). Dead cells were detected as they were labelled with PI but did not bind the annexin V

antibody. Cell debris was also positively labelled for PI but was sorted by size, proliferating cells were negative for both markers. Basal keratinocytes were FACS sorted using a β1 integrin allophycocyanin (APC)-conjugated antibody.

### 2.12.1 Cell proliferation and apoptosis by flow cytometry

Primary keratinocytes were seeded at $1x10^6$ cells per 60 mm cell culture dish without 3T3 mouse fibroblasts in RM+ culture medium and incubated overnight at 37°C in a humidified chamber at 10% $CO_2$, 90% air. The next day the cells were washed three times in PBS and treated with one of the following conditions all made in modified RM+ culture medium (1% FCS, without cortisol): vehicle control (ethanol/methanol), 1 μM dex, 1 μM RU486 or 1 μM dex and 1 μM RU486. Alternatively, cells were exposed to 20 mJ U.V.B. at 0.2 $mV/cm^2$ for a negative control of apoptosis. The U.V. irradiation was carried out on cells that were in PBS with the cell culture dish lid removed (to ensure complete U.V. exposure). After U.V. exposure, the PBS was aspirated and the cells were bathed in modified RM+ (1% FCS, without cortisol). The cells were incubated for 72 h in a humidified chamber at 90% air, 10% $CO_2$.

After 72 h, the culture media was aspirated and the cells were washed once in PBS, once in versene and trypsinised until all the cells had detached. The trypsin reaction was inhibited by transferring the trypsinised cells to centrifuge tubes containing RM+ with 10% FCS at a ratio of 1:1 (v/v) cells to culture medium. The cells were washed twice in ice cold PBS with a series of centrifugation steps (1,300 rpm, 5 min at room temperature) in between each wash. The final cell pellet was resuspended in 500 μl annexin V binding buffer solution (BD Pharmingen, Franklin Lakes, NJ, U.S.A.) and transferred to a 5 ml round-bottomed polystyrene tube (BD Bioscience Discovery Labware, Bedford, MA, U.S.A.). To each sample, except the compensation control, 4 μl of annexin V-FITC antibody (BD Pharmingen, Franklin Lakes, NJ, U.S.A.) was added and the tubes were tapped gently to mix the solution. The samples were incubated in the dark for 15 min at room temperature. Finally, PI (5 μg/ml, Molecular Probes), was added per sample (except the compensation control) before the cells were analysed using a BD LSRII flow cytometer (BD Biosciences, San Jose, CA, U.S.A.) and data analysed using BD FACSDiva Software. Annexin V was excited by a red

HeNe laser of 633 nm, emission collected at 660 nm and the machine was fitted with a 660 nm/20 nm differential filter (DF). PI was excited by an argon laser of 488 nm, emission collected at 575 nm and the machine fitted with a 575 nm/26 nm DF.

### 2.12.2 β-Integrin cell sorting by flow cytometry

Primary keratinocytes (at least 4 million) were trypsinised as described in section 2.1.4 and resuspended in 6 ml 1% BSA in PBS. Cell suspension (1 ml) was transferred to a fresh tube to provide a negative control for flow cytometry analysis and both tubes were centrifuged and resuspended in 500 µl 1% BSA PBS. To the sample (but not negative control), 10 µl of APC anti-human CD29 (BD Pharmingen, Franklin Lakes, NJ, U.S.A.) was added and the tubes were incubated for 15 min on ice in the dark. The cells were washed twice in PBS with centrifugation at 1300 rpm and resuspended in 500 µl 1% BSA/PBS.

After the final wash, the cells were transferred to fresh, sterile 5 ml round-bottomed polystyrene tube (BD Bioscience Discovery Labware, Bedford, MA, U.S.A.). Using a BD FACS Aria I (BD Biosciences, San Jose, CA, U.S.A.) fitted with a 130 µm nozzle at 20 psi, cells were sorted according to emission spectra analysed by FlowJo version 7.2 Software. APC was excited by a red HeNe laser of 633 nm, emission collected at 660 nm and the machine was fitted with a 660 nm/20 nm differential filter (DF). The sorted enriched basal cells (APC conjugated CD29 positive) and suprabasal cells (APC conjugated CD29 negative) were immediately seeded for experiments or used for protein extraction.

## 2.13 Cell counting assay

Primary keratinocytes were seeded in T75 flask at $1x10^6$ cells per flask which were seeded with $1x10^6$ mitomycin C-treated NIH/3T3 fibroblasts the previous day. The keratinocytes were grown in complete RM+ culture media until 40% confluent. To remove the 3T3 fibroblasts cells were washed twice in PBS and then incubated with 1x versene for 2 – 5 min at 37°C. When all the fibroblasts were detached, the keratinocytes were washed three times in PBS and incubated for a further three days in

modified RM+ culture medium (1% serum but without cortisol) with either $1x10^{-6}$ M dex, 1:50,000 (v/v) methanol (as a vehicle control) or no further addition.

After 72 h, the culture medium was removed and the keratinocytes were trypsinised as described in Section 2.1.4. All washes, culture medium and trypsin solutions were kept and combined in a 50 ml centrifuge tube. The cell suspension was centrifuged at 1,000 rpm for 5 min at room temperature. Viable cells were then counted using trypan blue as described in section 2.1.11.

### 2.14 $NADP^+$/NADPH quantification assay

Primary keratinocytes were seeded and treated with dex as described in the MTT assay in section 2.10. After 72 h treatment (with or without dex), cells were washed twice in ice-cold PBS. $NADP^+$/NADPH was measured using an $NADP^+$/NADPH Quantification kit (BioVision, Mountain View, CA, U.S.A.) as described in the following passage.

Cells were lysed by adding 1 ml $NADP^+$/NADPH extraction buffer to each flask and subjecting the flasks to two freeze-thaw cycles (20 min on dry ice, 10 min at room temperature). The samples were then vortexed for 10 s. A 10 µl aliquot of the cell suspension was set aside for protein analysis. The remaining cell debris was removed by centrifuging at 13,000 rpm at 4°C for 5 min. To remove NADPH digesting enzymes, cell lysates were filtered by centrifugation through 10 kDa molecular weight cut off filters (BioVision, Mountain View, CA, U.S.A) at 14,000 rpm for 15 min at 4°C.

The total $NADP^+$/NADPH cell extraction sample (50 µl) was seeded in duplicate in a flat-bottomed 96-well plate. Another 150 µl aliquot of the sample was heated to 60°C for 30 min to degrade $NADP^+$. This provided the NADPH only reading of each sample. The samples were then cooled on ice and 50 µl was transferred in duplicate to a 96-well plate.

A standard curve was generated by diluting 10 µl of stock NADPH (1 nmol/µl) in 990 µl $NADP^+$/NADPH extraction buffer. In duplicate, 0, 2, 4, 6, 8, 10 µl of the diluted NADPH standard was added to wells of a 96-well plate so that the final concentration

of the standards was 0, 20, 40, 60, 80 and 100 pmol/well. The final volume of each standard was made up to 50 µl with $NADP^+$/NADPH extraction buffer and mixed vigorously.

An $NADP^+$ cycling mix was made by combining $NADP^+$ cycling enzyme mix with $NADP^+$ cycling buffer mix, 1:50 (v/v) and 100 µl was added and mixed well with each sample and standard. The plate was incubated at room temperature for 5 min to convert $NADP^+$ to NADPH, then 10 µl NADPH developer was added to each well. The reaction was incubated at room temperature allowed to develop for 1 h, then stopped with 10 µl stop solution and analysed at OD 450 nm using a spectrophotometer (Victor2 1420 Multilabel counter, Wallac, Perkin Elmer Life Sciences, Wellesley, MA, U.S.A.).

**2.15 Statistical analysis**

Statistical analysis was determined using an unpaired-t test or one-way analysis of variance (ANOVA) followed by a Tukey *post-hoc* test where appropriate. All statistical evaluations were performed using GraphPad Prism 4.0 software (San Diego, CA, U.S.A.). Significance was assessed in all experiments as a probability value of $*P < 0.05$, $**P < 0.01$, $***P < 0.001$.

# Chapter 3. Expression Analysis of Steroidogenic Regulatory Proteins in Skin

## 3.1 Introduction

Cholesterol transporters are crucial for steroid synthesis, as the transport of cholesterol is reported as the first and rate limiting step of steroid synthesis (Stocco and Sodeman, 1991). The ability of a cell or tissue to synthesise steroids is partly classified by the expression of mitochondrial cholesterol transporters and their regulators. Therefore, if the epidermis is capable of synthesising steroids, it is expected that the tissue would express critical cholesterol transporters associated with steroid synthesis.

StAR was the first protein identified as a cholesterol transporter for steroidogenesis. Pulse-chase experiments and the use of protein synthesis inhibitors identified the relationship between StAR phosphoprotein isoforms (37-, 32- and 30kDa) and steroid synthesis (Stocco and Sodeman, 1991). StAR is initially transcribed as a 37 kDa pre-protein associated with the outer mitochondrial membrane. The pre-protein is then modified to 32 kDa before being cleaved into the mature 30 kDa isoform expressed in the inner mitochondrial membrane (Stocco and Sodeman, 1991).

Protein synthesis inhibitors demonstrated the short half-life (less than 15 min) of 37 kDa StAR, which corresponded to a reduction in steroidogenesis and the appearance of 32 and 30 kDa phosphoproteins (Stocco and Sodeman, 1991). Therefore continual *de novo* synthesis of StAR is required to maintain acute steroidogenesis. StAR protein synthesis is tightly regulated and a potent inhibitor of StAR transcription is DAX1. DAX1 is a nuclear receptor that primarily acts by inhibiting StAR transcription (Zazopoulos et al., 1997). Therefore, for DAX1 to directly inhibit StAR transcription, it must reside in the nucleus of the cell.

The exact mechanism adopted by StAR to transport cholesterol has not been fully elucidated. Since StAR does not form a complete channel across both mitochondrial membranes, it is likely that StAR functions with a complex of proteins to transport cholesterol. For example, there is a close functional interaction with TSPO and StAR to facilitate cholesterol transport into the mitochondria (Liu et al., 2006).

MLN64 is another putative cholesterol transporter able to promote steroid synthesis (Watari et al., 1997). MLN64 shares a homologous START domain with StAR that is capable of accommodating one cholesterol molecule (Bose et al., 2000b; Watari et al., 1997). However, MLN64 has also been shown to localise to late endosomes rather than mitochondria, so the exact function of MLN64 in steroid synthesis remains controversial (Alpy et al., 2001).

The primary aim of this chapter was to identify the expression of steroid cholesterol transporters in the epidermis and cultured primary human keratinocytes. The presence of StAR, MLN64 and/or TSPO and the absence or non-nuclear localisation of DAX1 would suggest that keratinocytes could be steroidogenic cells. The secondary aim was to identify whether these proteins were aberrantly expressed in skin disorders that are commonly managed with GC, including psoriasis, atopic dermatitis and harlequin ichthyosis.

To characterise the expression pattern of StAR, DAX1, TSPO and MLN64 in epidermis, immunofluorescence histochemistry was carried out on normal human skin sections. Immunofluorescence cytochemistry, western blotting (and RT-PCR for StAR) were used to assess the protein expression in normal primary human keratinocytes. In addition, since many skin disorders are treated with analogues of cortisol, biopsies from atopic dermatitis, psoriasis and harlequin ichthyosis were analysed for the expression pattern of steroid synthesis regulators and compared to normal skin.

## 3.2 Results

### 3.2.1 StAR, MLN64, TSPO and DAX1 expression in normal human skin

StAR, the cholesterol transporter required for steroid synthesis in most steroidogenic tissues, was expressed in the basal layer of normal human epidermis (Figure 3.1). However, StAR was not detected in suprabasal layers of the epidermis. In some instances, a signal was observed in the cornified layer, although this is more likely to be attributed to non-specific antibody interactions as this patterning was also observed in negative (no primary antibody) controls. Non-specific antibody interactions are a common problem in the stratum corneum of the epidermis since it is highly rich in lipids to which antibodies can adhere.

In contrast to StAR, the StAR homologue MLN64 was completely absent in basal epidermal keratinocytes but present in suprabasal layers where keratinocytes differentiate (Figure 3.1). The signal for MLN64 appeared to intensify with differentiation. Of the cells that expressed either StAR or MLN64, protein was localised to the cytoplasm or an organelle within the cytoplasm since, as expected, there was no signal in nucleus of the cells.

DAX1, a nuclear receptor that acts as a suppressor of StAR was expressed throughout all epidermal layers but only in the cytoplasm of the cells rather than the nucleus. The expression appeared to be consistent throughout the layers since the intensity of the signal did not vary from the basal to cornified layer. TSPO was also detected throughout the layers of the epidermis with a particularly strong expression signal in the granular layer just prior to cornification. TSPO showed punctate nuclear or peri nuclear expression in the basal, spinous and granular layer that could be considered to colocalise with the nucleus or surround the nucleus of the cells. Both DAX1 and TSPO were also detected in fibroblasts of the dermis whereas StAR and MLN64 were absent from the dermis.

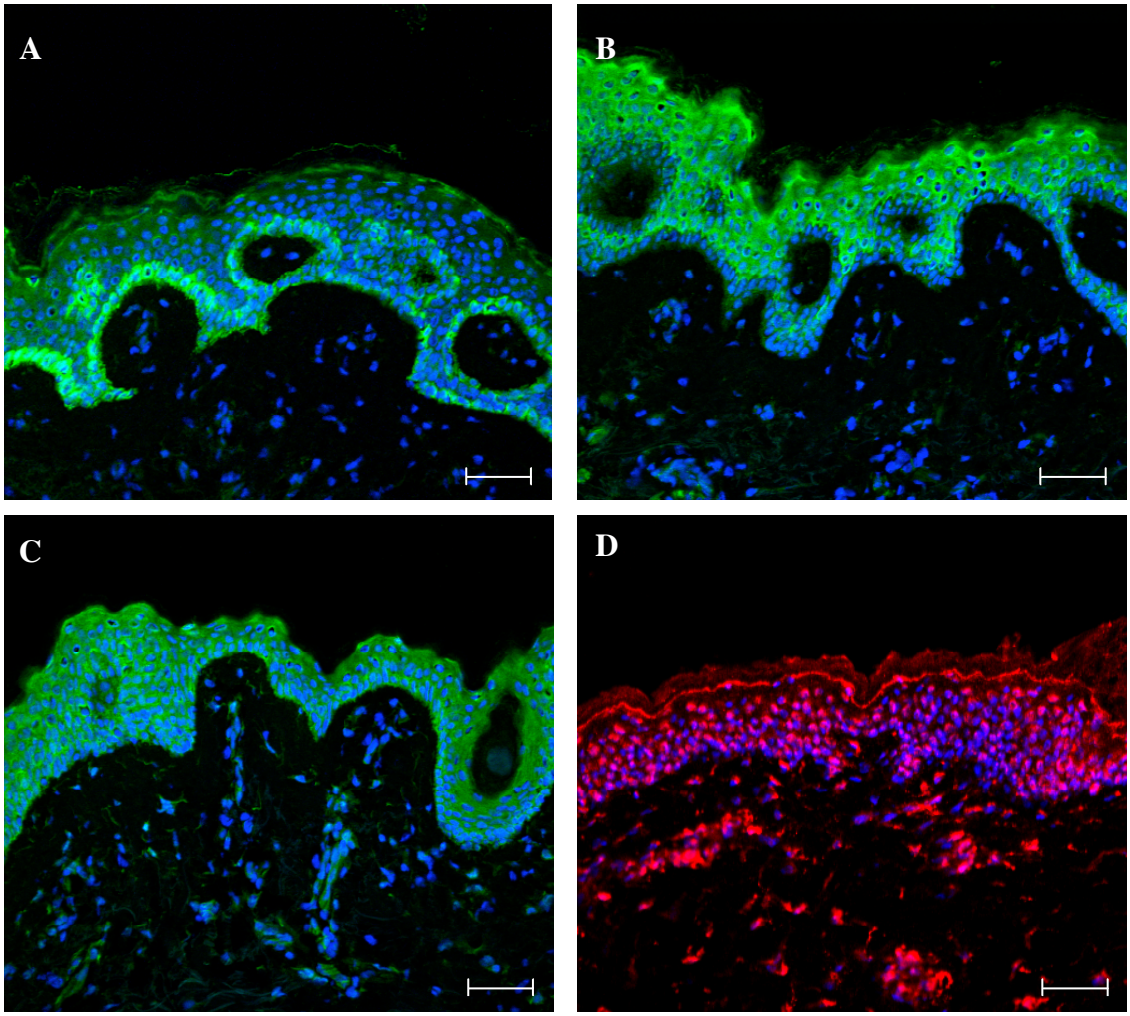


**Figure 3.1 StAR, MLN64 DAX1 and TSPO expression in normal human skin.** Immunofluorescence histochemistry of whole skin facelift sections from Caucasian females (over 40 years) probed with DAPI (blue nuclear stain) and rabbit polyclonal antibody to (A) StAR, (B) MLN64, (C) DAX1 and (D) TSPO and detected with (A-C) Alexafluor 488 secondary antibody (green) or (D) Alexafluor 594 secondary antibody (red). Each panel depicts a representative image of at least fifteen observations, each made in skin samples from a different individual, scale bar 50 μm.

### 3.2.2 StAR, MLN64 and DAX1 expression pattern in psoriatic skin

StAR was not detected in non-lesional psoriatic skin biopsies. This was in complete contrast to normal human skin where StAR was present in the basal epidermal layer. Low levels of StAR were observed in basal regions of the epidermis of lesional psoriatic skin but the signal did not appear to be as intense compared to normal skin (Figure 3.2). In contrast to cytoplasmic expression of DAX1 in normal human skin, DAX1 was localised to the nucleus in all layers of non-lesional psoriatic epidermis. However, in lesional psoriatic skin, DAX1 was localised to the cytoplasm in a similar manner to that seen in normal epidermis (Figure 3.2). The pattern of MLN64 expression was the same as normal skin in non-lesional psoriatic samples (Figure 3.2). However, MLN64 expression was detected several cell layers above the basal layer in lesional areas of psoriatic skin as opposed to the observed expression one layer above basal cells in normal skin. In addition the intensity of the signal appeared less in the involved regions of the skin diseases compared to normal epidermis (Figure 3.2).

### 3.2.3 StAR, MLN64 and DAX1 expression pattern in atopic dermatitis skin

Similar to non-lesional psoriatic skin, StAR was not detected in uninvolved atopic dermatitis biopsies (Figure 3.3). Unlike lesional psoriatic or normal skin, StAR was also not detected in involved epidermal regions of atopic dermatitis.

Similar to non-lesional psoriatic skin, DAX1 expression was identified in the nucleus of uninvolved atopic dermatitis skin. However, DAX1 also localised to the nucleus of all epidermal layers in involved regions of atopic dermatitis skin (Figure 3.3). The presence of DAX1 in the nucleus may account for maintained down-regulation of StAR expression in both involved and non-involved atopic dermatitis skin.

The MLN64 expression pattern was the same in uninvolved atopic dermatitis skin compared to normal skin (Figure 3.3). However, the expression pattern of MLN64 was comparable to psoriatic skin in involved regions of atopic dermatitis since MLN64 signal was detected several cell layers above the basal layer in lesional areas of atopic dermatitis and appeared to be less intense in atopic dermatitis biopsies compared to

normal skin. The intensity of MLN64 signal did not appear to increase as keratinocytes differentiated to the uppermost layer of the epidermis. This was in contrast to normal and lesional psoriatic epidermis where MLN64 signal intensified with differentiation.

### 3.2.4 StAR and MLN64 expression pattern in harlequin ichthyosis skin

Similar to lesional psoriatic skin, StAR expression was observed in the basal layer of the epidermis in harlequin ichthyosis but the signal appeared to be less intense compared to normal and lesional psoriatic epidermis (Figure 3.4). MLN64 expression was also observed in suprabasal regions of the epidermis, although it is difficult to determine the expression pattern since the section was unfortunately folded on the slide (Figure 3.4). Due to the rarity of harlequin ichthyosis and scarcity of sections, it was not possible to repeat the experiment.

### 3.2.5 StAR, MLN64 and DAX1 expression in NEB1 organotypic rafts

An epidermal raft model using NEB1 immortalised keratinocyte cells demonstrated an expression pattern of DAX1 and MLN64 similar to that of normal skin. DAX1 signal was observed in the cytoplasm throughout the layers but was completely absent from cell nuclei. MLN64 was also present in all suprabasal layers but again, MLN64 signal was completely absent within the basal layer of the system (Figure 3.5). However, unlike normal skin, StAR was not detected in any layer of the raft including the basal layer (Figure 3.5). This is in contrast with psoriatic and atopic dermatitis biopsies where the absence of StAR signal was associated with nuclear localisation of DAX1.

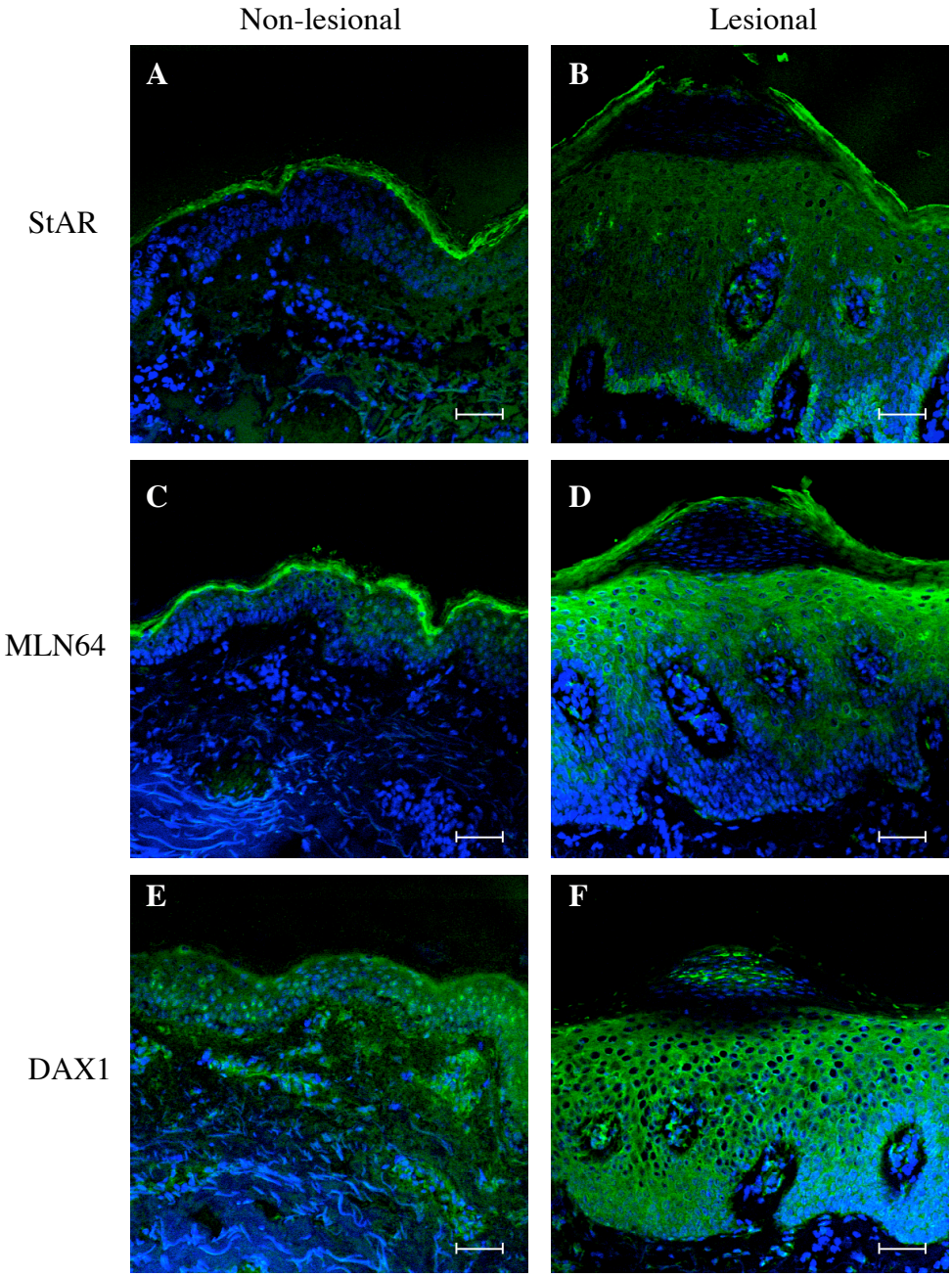


**Figure 3.2 StAR, MLN64 and DAX1 expression in psoriatic skin.**

Immunofluorescence histochemistry of matched non-lesional (A, C and E) and lesional (B, D and F) whole skin biopsies from psoriatic patients probed with DAPI (blue nuclear stain) and rabbit polyclonal antibody to (A and B) StAR, (C and D) MLN64 or (E and F) DAX1 that was detected with Alexafluor 488 secondary antibody (green). Each panel depicts a representative image of four observations, each made in paired lesional and non-lesional skin samples from a different individual scale bar 50 μm.

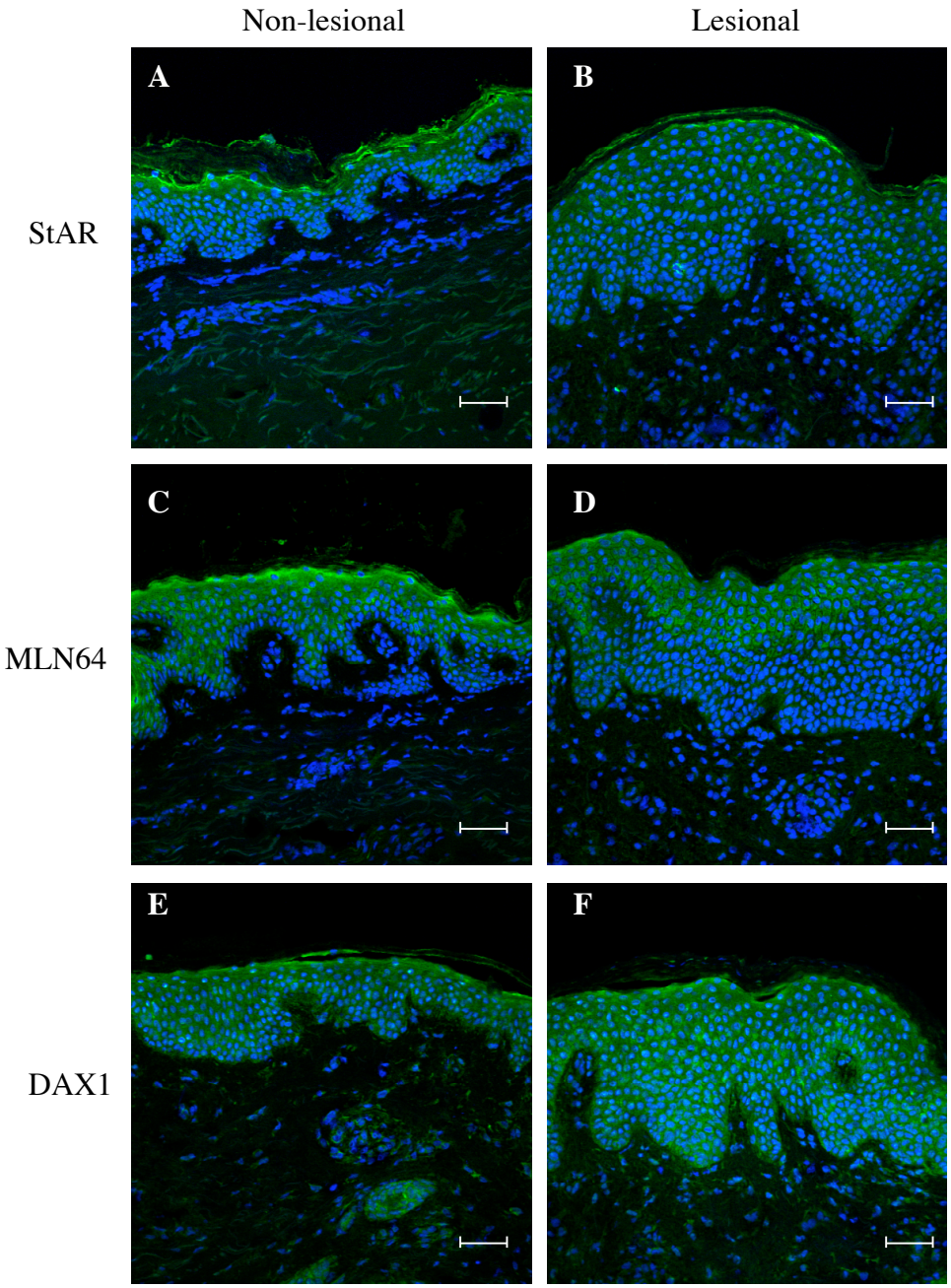


**Figure 3.3 StAR, MLN64 and DAX1 expression in atopic dermatitis skin.**
Immunofluorescence histochemistry of matched lesional (A, C and E) and non-lesional (B, D and F) whole skin biopsies from atopic dermatitis patients probed with DAPI (blue nuclear stain) and rabbit polyclonal antibody to (A and B) StAR, (C and D) MLN64 or (E and F) DAX1 that was detected with Alexafluor 488 secondary antibody (green). Each panel depicts a representative image of three observations, each made in paired involved and non-involved skin samples from a different individual, scale bar 50 μm.

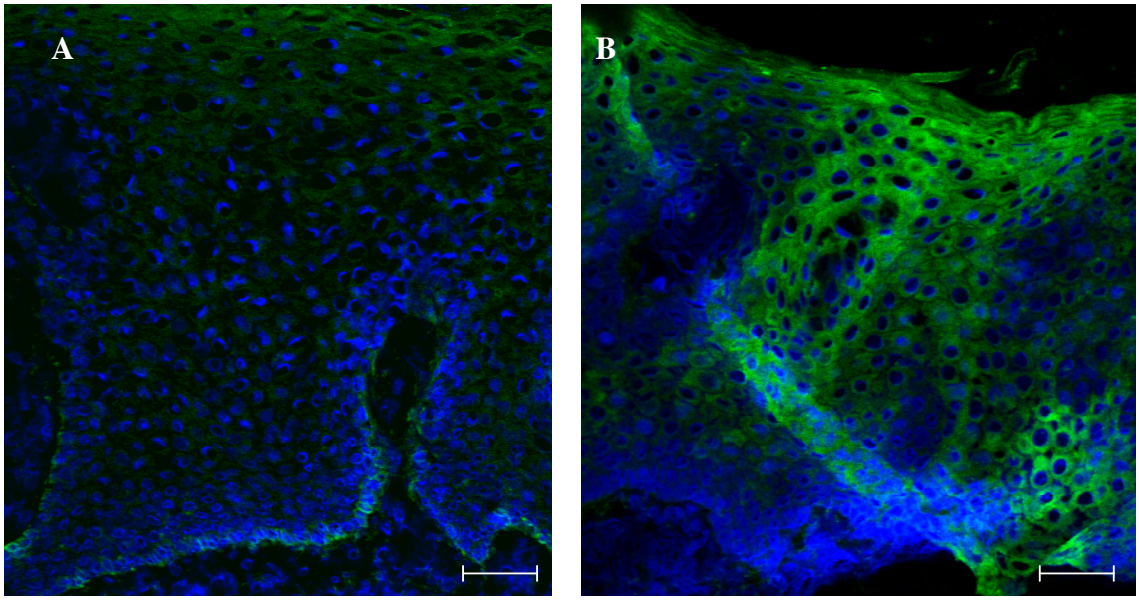


**Figure 3.4 StAR and MLN64 expression in harlequin ichthyosis skin.**
Immunofluorescence histochemistry of a whole skin biopsy from a harlequin ichthyosis patient probed with DAPI (blue nuclear stain) and rabbit polyclonal antibody to (A) StAR or (B) MLN64 that was detected with Alexafluor 488 secondary antibody (green). Due to the rarity of the disease and scarcity of skin sections, each panel is only from one observation, scale bar 50 μm.

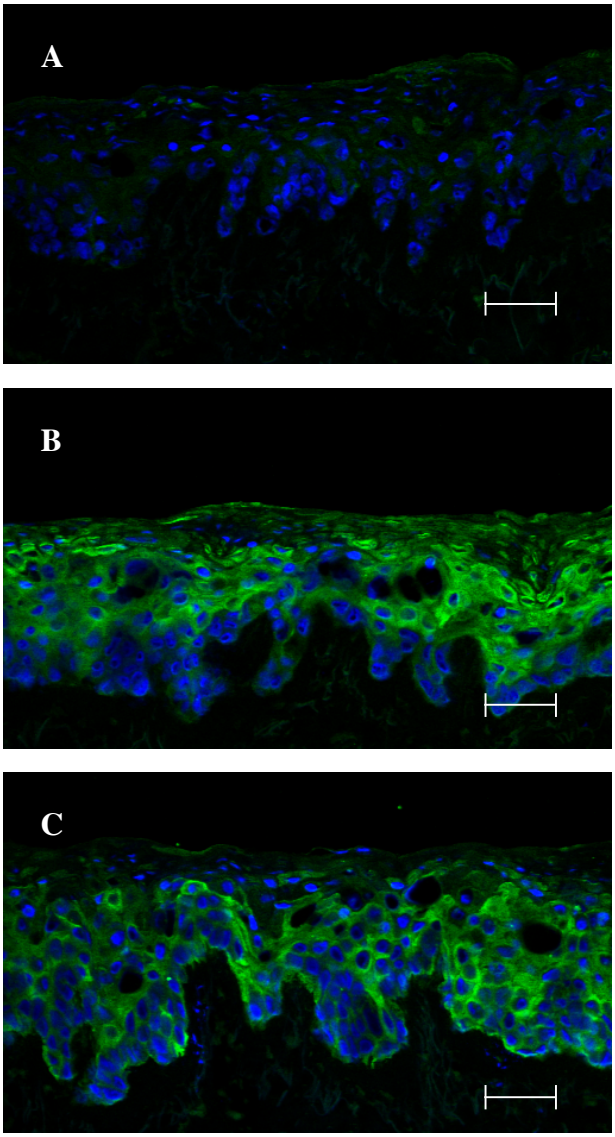


**Figure 3.5 StAR, MLN64 and DAX1 expression in NEB1 organotypic rafts.**
Immunofluorescence histochemistry of organotypic NEB1 rafts probed with DAPI (blue nuclear stain) and rabbit polyclonal antibody to (A) StAR, (B) MLN64 or (C) DAX1 that was detected with Alexafluor 488 secondary antibody (green). Each panel depicts a representative image of three observations, each made in different individual rafts, scale bar 50 μm.

### 3.2.6 Western blot analysis of StAR, MLN64, TSPO and DAX1 in skin cells

Cholesterol transport regulating proteins were identified in normal human skin by immunofluorescence histochemistry. To complement this data, expression of StAR, DAX1, TSPO and MLN64 was measured in protein isolates of cultured skin cells using western blotting (Figure 3.6). Despite detecting StAR in the basal layer of the normal epidermis (Figure 3.1), StAR was not detected by western blotting in primary keratinocytes, immortalised keratinocytes (HaCaTs and N/TERTS), primary dermal fibroblasts or immortalised sebocytes (SZ95). However, the StAR antibody was effective since a strong, single band was detected at approximately 30kDa in the H295R (positive control) protein isolate lane corresponding to the predicted size of StAR protein.

DAX1 was detected by western blotting in all cell samples tested, including keratinocytes and fibroblasts, supporting the data generated from previous immunohistochemistry analysis. MLN64 was also identified in all cells except dermal fibroblasts, in agreement with previous data showing MLN64 was absent from dermal fibroblasts in immunohistochemical analysis.

Multiple bands for TSPO were detected in all cell samples tested, consistent with the TSPO phenomenon of denaturation resistant dityrosine cluster formation (Delavoie et al., 2003). TSPO did not reside as an 18 kDa monomer in the cells since no band was detected below 39 kDa. The predominant band was approximately 64 kDa in N/TERT, HaCaT, H295R and JEG3 cells, whereas two bands (at 97 kDa and above 97 kDa) were the predominant TSPO clusters in primary keratinocytes.

In other cell systems, StAR protein has been shown to increase after 4 h with dbcAMP stimulation (Stocco and Sodeman, 1991). Therefore skin cells were incubated with 1 mM dbcAMP to determine whether this could induce StAR protein expression. In addition, since StAR is reported to be located to the outer mitochondrial membrane, mitochondrial protein enrichment was used in an attempt to enhance StAR protein

concentration. Figure 3.7 demonstrates by western analysis that dbcAMP did not promote StAR protein expression in the skin cells tested at the chosen time point.

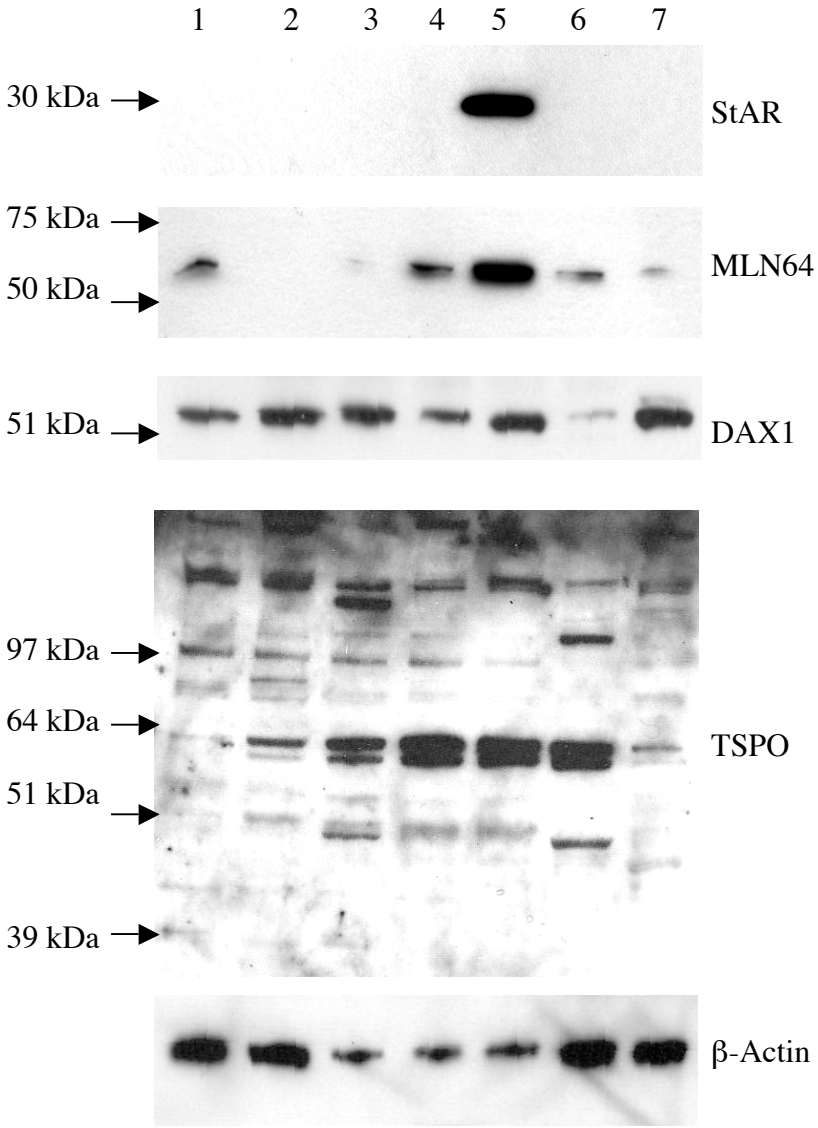


**Figure 3.6 Western blot analysis of StAR, MLN64, DAX1 and TSPO in skin-derived cells.**

(1) Primary human keratinocytes, (2) primary human dermal fibroblasts, (3) N/TERTS, (4) HaCaTs, (5) H295R immortalised adrenal cells (positive control for StAR), (6) JEG3 immortalised placenta cells (positive control for MLN64), (7) SZ95 immortalised sebocytes. Protein was loaded at 10 μg per lane for DAX1, MLN64, TSPO and 20 μg per lane for StAR. β-Actin was used to determine protein loading.

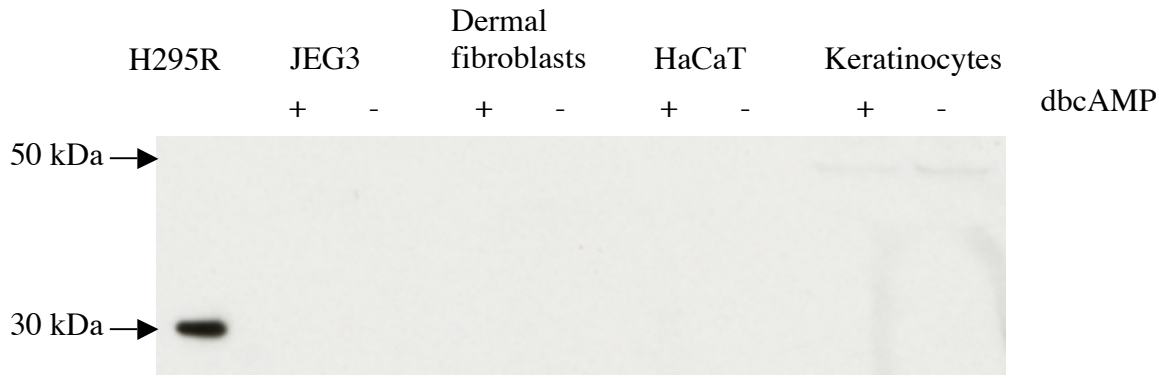


**Figure 3.7 Western blot analysis of StAR in skin cells treated with dbcAMP.**
Cells (JEG3, dermal fibroblasts, HaCaTs, primary human keratinocytes) were treated with or without 1 mM dbcAMP for 4 h 30 min. Protein was isolated with mitochondrial encrichment. Protein was loaded at 20 μg per lane with the exception of H295R cells (used to provide a positive control for StAR protein expression) where 10 μg of protein was loaded.

### 3.2.7 RT-PCR of StAR in primary human keratinocytes and skin extracts

Since StAR protein was not detected in protein isolates from skin cells, RT-PCR was used to check for StAR mRNA in the cells. Figure 3.8 demonstrates that StAR mRNA was present in primary human keratinocytes as well as in extracts from normal facelift skin. However, the level of StAR mRNA was lower in primary keratinocytes and skin compared to the H295R adrenal positive control. There was also a variation of StAR intensity between different whole skin biopsies even though equal amounts of cDNA were used for the PCR reaction and PCR products were loaded equally on the gel, as demonstrated by the GAPDH controls. The RT-PCR product was sequenced and confirmed as StAR in each of the samples tested. This shows that the mRNA transcript was present in the cells despite the absence of StAR protein by western analysis and low level expression identified by immunofluorescence histochemistry.

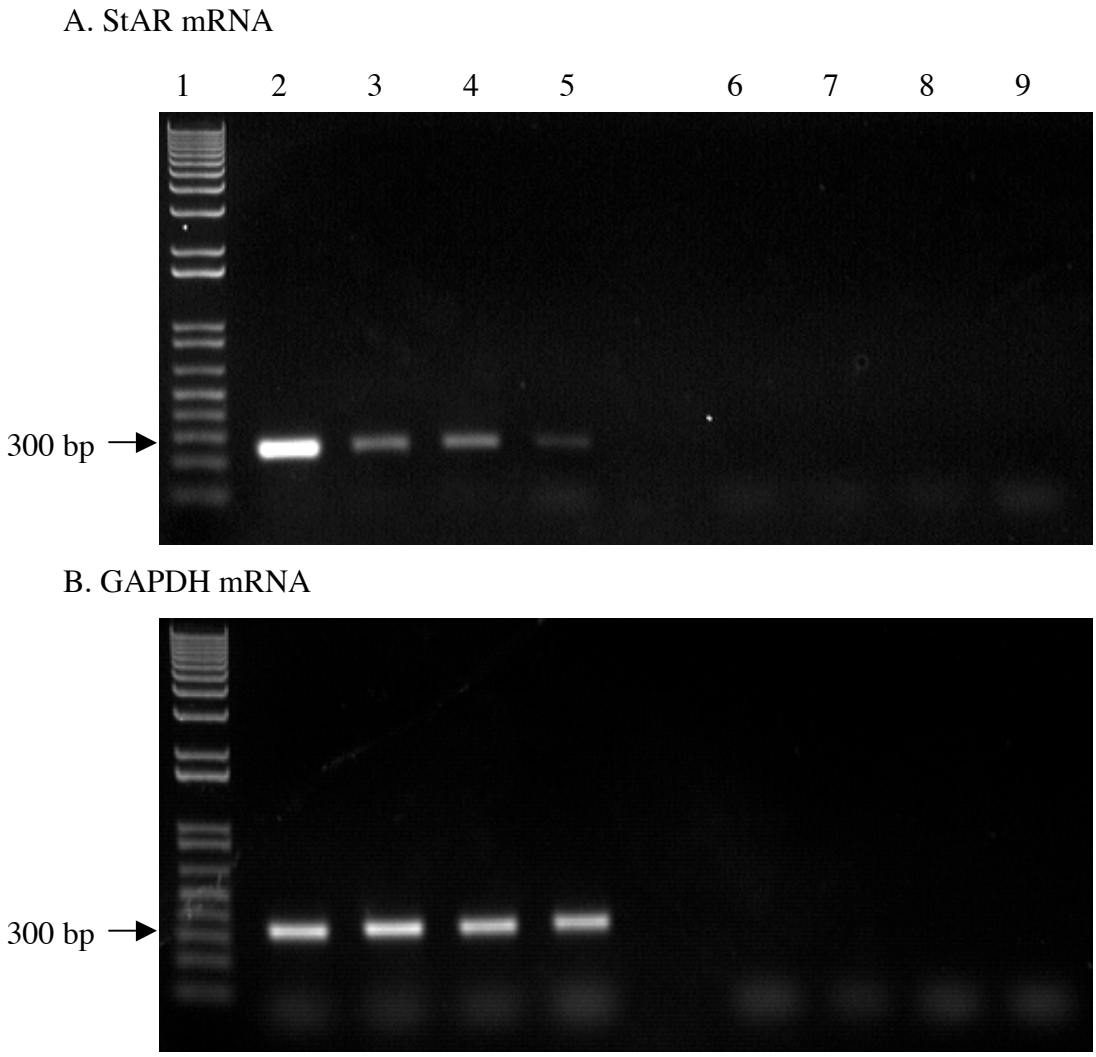


**Figure 3.8 RT-PCR analysis of StAR in primary human keratinocytes and skin.** RT-PCR result using primers specific for (A) StAR or (B) GAPDH. (1) 1 kb DNA ladder, (2) H295R positive control, (3) primary human keratinocytes, (4) facelift skin donor 1, (5) facelift skin donor 2. Lanes 6 – 9 negative controls generated from RNA sample extracts lacking the enzyme for cDNA synthesis for (6) H295R, (7) primary human keratinocytes, (8) facelift skin donor 1, (9) facelift skin donor 2. A single PCR product was detected in each lane matching the predicted product size for StAR (333 bp) or GAPDH (340 bp). Authenticity of the StAR product was confirmed by DNA sequencing. The figure is a representative of three separate experiments.

### 3.2.8 Influence of oxygen and dermal fibroblasts on StAR and MLN64 expression in keratinocytes

Keratinocyte culture conditions were manipulated to promote a basal cell keratinocyte environment. An oxygen gradient of 2 – 17% spans the epidermis from 2% $O_2$ in the basal layer to 17% in the stratum corneum (Ngo et al., 2007). Basal keratinocytes (particularly stem cells) isolated from mouse epidermis have been shown to apoptose more readily when cultured at atmospheric oxygen. In contrast, when cultured at 2% $O_2$ less apoptosis was observed (Fozia Chaudry, personal communication). Therefore primary human keratinocytes were cultured at 2% $O_2$ to investigate if this promoted the maintenance of a basal cell population and StAR expression. In addition keratinocytes were cultured with either human dermal fibroblasts or conventional 3T3 mouse fibroblasts. This is because the factors released by dermal fibroblasts are essential for keratinocyte function and growth and can vary between species. The use of human dermal fibroblasts was an attempt to replicate the human system to investigate whether this would encourage StAR expression in keratinocyte culture. Primary keratinocytes were also FACS sorted to enrich for the basal cell population using a β-integrin (CD29) antibody (Figure 3.9), since StAR was identified in the basal layer of the epidermis by immunofluorescence histochemistry. Figure 3.10 shows that StAR was not detected by western analysis in CD29+ or CD29- keratinocytes cultured at 2% $O_2$ or atmospheric oxygen, with either human dermal fibroblasts or mouse 3T3 fibroblasts. However, MLN64 was present in basal enriched (CD29+) cells and the expression of MLN64 increased in suprabasal cells (CD29-) cells.

A

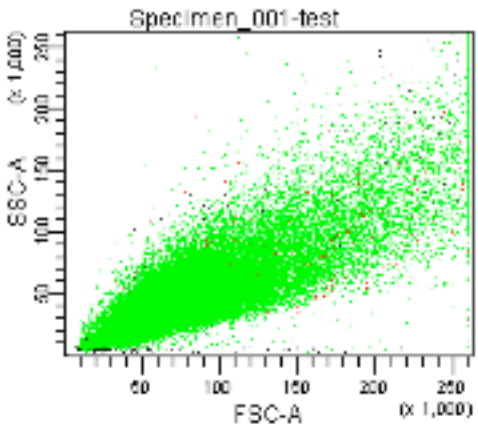


B

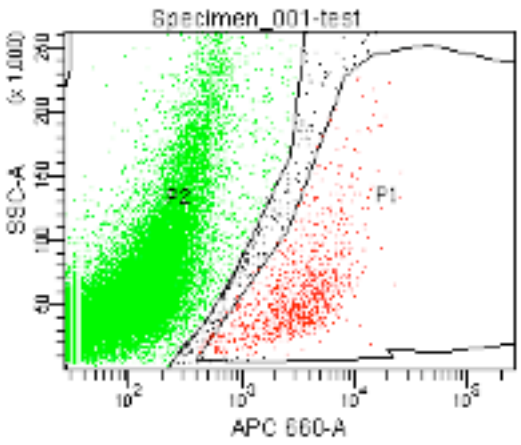


**Figure 3.9 Example of gating plots used for β1 integrin (CD29) cell sorting by flow cytometry.**

Basal cell keratinocyte enrichment was achieved with a FITC conjugated antibody to β1 integrin. The cells were separated for CD29 positive and negative labeling. A dot plot of the total cell population (A) is shown with gating for CD29 positive cell, P1 in (B), and CD29 negative cells, P2 in (B).

A. Ambient $O_2$

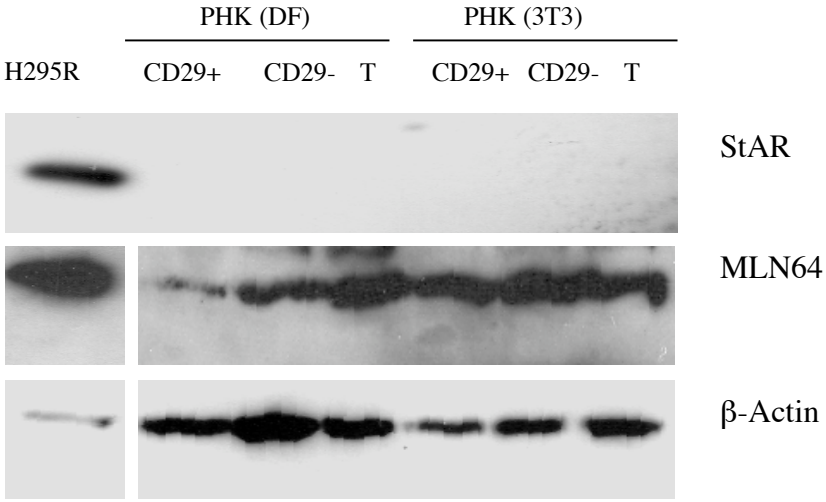


B. 2% $O_2$

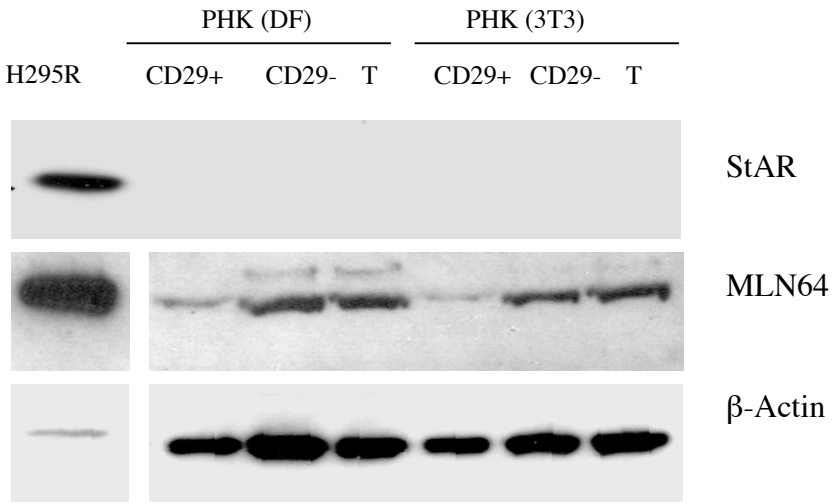


**Figure 3.10 Western blot analysis of StAR and MLN64 in primary human keratinocytes grown in modified oxygen and fibroblast conditions.**

Protein was isolated from primary human keratinocytes (PHK) that were FACS sorted for CD29+ (basal) and CD29- (suprabasal) cell enrichment or unsorted total population (T) and cultured for 24 h at (A) atmospheric oxygen or (B) 2% oxygen. PHK cultured with 3T3 mouse fibroblasts (3T3) or primary human dermal fibroblasts (DF). Protein was loaded at 25 μg per lane except for H295R cells where 10 μg protein was loaded. β-Actin was used to determine equal protein loading.

### 3.2.9 Immunofluorescence cytochemistry of StAR, DAX1 and MLN64 in primary human keratinocytes

The cellular expression pattern of StAR, DAX1 and MLN64 was assessed by immunofluorescence cytochemistry in keratinocytes that were cultured for five days (Figure 3.11). In tissue culture, DAX1 had a cytosolic expression pattern in every cell and was absent from the nucleus, matching the DAX1 expression pattern observed in normal human skin. MLN64 was detected with punctate patterning surrounding cell nuclei. It is likely that this patterning corresponds with endosome localisation since MLN64 has been associated with this organelle in other cell types (Alpy et al., 2001). MLN64 was not detected in every cell, suggesting differential expression in the cell population. This could correspond to differentiating keratinocyte versus stem/transit amplifying keratinocyte populations as observed by immunohistochemistry.

StAR expression was not detected in the majority of cells after five days of tissue culture (Figure 3.11), which corresponded with the absence of StAR signal in protein isolates from cultured keratinocytes (Figure 3.6). StAR expression was then measured in primary human keratinocytes over a five day time course (Figure 3.12). StAR was detected in all the primary keratinocytes after one day in tissue culture. The proportion of cells that expressed StAR decreased with time so that by day 5, StAR signal was absent in the majority of the cell population (Figure 3.12). In StAR positive cells, the protein was observed to form a ring-like mesh surrounding cell nuclei, which corresponds to patterning expected for mitochondrial localisation.

In summary, regulators of steroid synthesis were identified in normal human epidermis and the localisation of these proteins were aberrant in diseased skin (summary Table 3.1). StAR was present in the basal layer of normal epidermis but expression was reduced or not detected in hyperproliferative skin conditions. In culture, MLN64, TSPO and DAX1 were detected by western blotting and/or immunofluorescence cytochemistry, however StAR expression diminished with time in culture even though StAR message could still be detected.

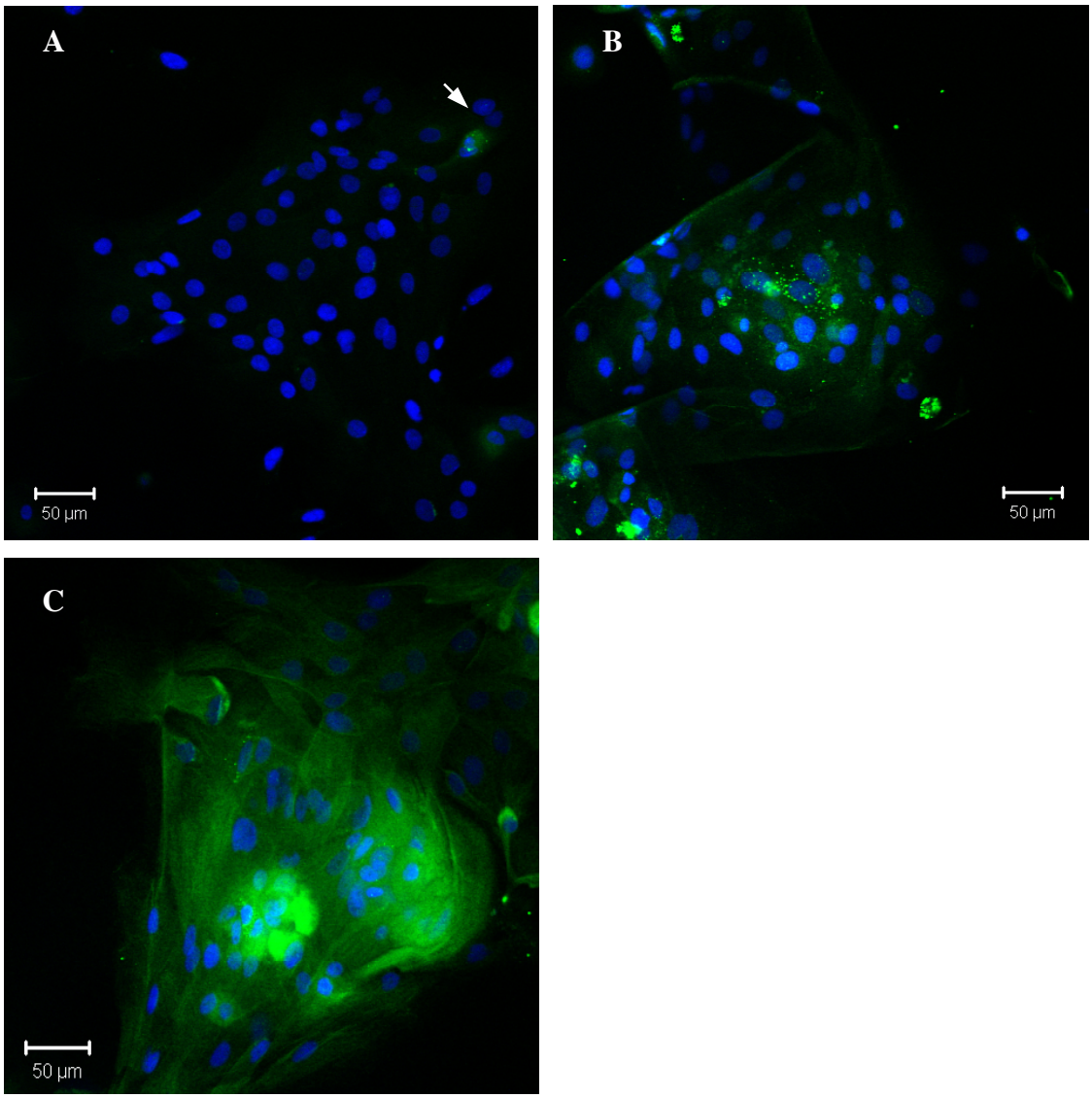


**Figure 3.11 Immunofluorescence cytochemistry of StAR, MLN64 and DAX1 in primary human keratinocytes.**

Expression pattern of (A) StAR, (B) MLN64 and (C) DAX1 after 5 d in tissue culture. The white arrow in (A) indicates a positive signal for StAR. Images are representative of three separate experiments.

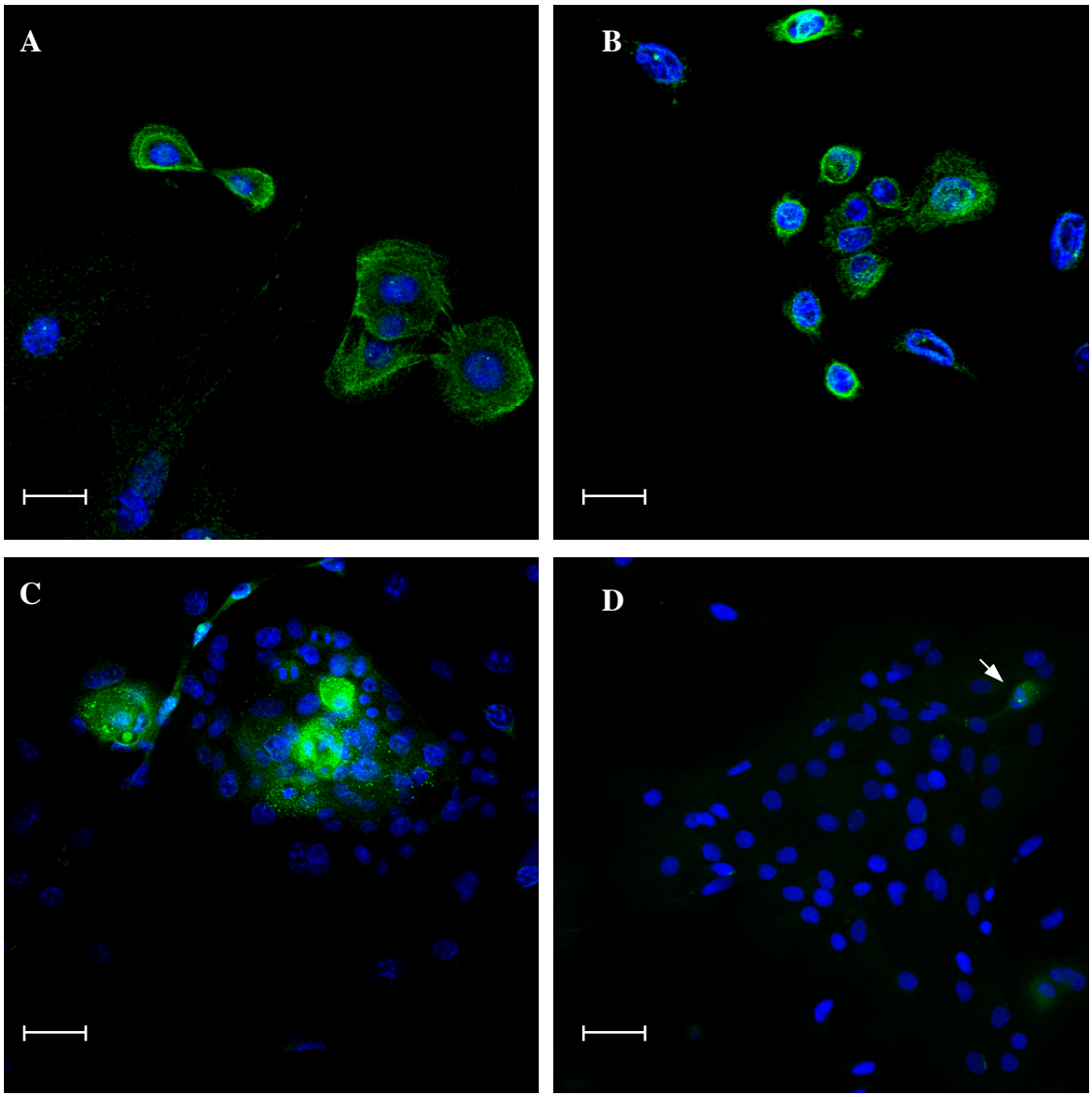


**Figure 3.12 Immunofluorescence cytochemistry of StAR expression over time in cultured primary human keratinocytes.**

Primary keratinocytes were cultured for (A) 1 day, (B) 2 days (C) 3 days or (D) 5 days prior to being subjected to immunofluorescence cytochemistry to detect StAR expression (green). The cell nuclei were detected with DAPI (blue). The white arrow in (D) indicates a StAR positive cell in a keratinocyte colony after 5 days in culture. Images are representative of three separate experiments, scale bar 50 μm.

| | StAR | MLN64 | DAX1 |
|---|---|---|---|
| Normal epidermis | Basal layer | Suprabasal layers | All layers, cytoplasm |
| Non-lesional psoriatic epidermis | Not detected in basal layer | Suprabasal layers | All layers, nucleus |
| Lesional psoriatic epidermis | Low level in basal layer | Upper suprabasal layers | All layers, cytoplasm |
| Non-lesional atopic dermatitis epidermis | Not detected in basal layer | Suprabasal layers | All layers, nucleus |
| Lesional atopic dermatitis epidermis | Not detected in basal layer | Upper suprabasal layers | All layers, nucleus |
| NEB-1 organotypic rafts | Not detected | Suprabasal layers | All layers, cytoplasm |
| Normal cultured primary human keratinocytes | Low level of expression decreasing with time in culture | Most cells, putative late endosome expression | All cells, cytoplasm |

**Table 3.1 Summary of StAR, MLN64 and DAX1 expression in human epidermis and keratinocyte culture detected by immunofluorescence histochemistry and cytochemistry respectively.**

### 3.3 Discussion

The expression pattern of the cholesterol transporters StAR, MLN64 and TSPO together with a negative regulator of StAR, DAX1 was examined in normal human skin by immunofluorescence histochemistry. StAR, the cholesterol transporter required for acute steroid synthesis in most steroidogenic tissues, was exclusively expressed in the basal layer of normal epidermis. This StAR expression pattern concurs with previously published research that identified StAR protein in skin by immunocytochemistry (Chen et al., 2006; Tiala et al., 2007). The presence of StAR in the tissue suggests that the epidermis could have steroidogenic potential since StAR expression is regarded as an indicator of steroid synthesis. The expression of StAR was restricted to the basal layer suggesting that acute regulation of steroid synthesis is only present in stem or proliferating keratinocytes and is absent in differentiating keratinocytes. Analysis of StAR expression in sebocytes also found the most intense StAR signal in undifferentiated sebocytes (Chen et al., 2006).

Previous reports detected MLN64, a protein that has also been implicated in cholesterol transport for steroidogenesis, in whole skin extracts by western blot analysis (Slominski et al., 2004). In this chapter, MLN64 was detected only in the suprabasal layers of the epidermis where keratinocytes differentiate and, in contrast to StAR, was absent from the basal layer. This is consistent with MLN64 analysis in the brain that identified the protein in glia and neurones but did not co-localised with steroidogenic cells of the brain (King et al., 2006). Unfortunately it was not possible to perform co-localisation studies since at the time of the experiments, only rabbit polyclonal antibodies for StAR and MLN64 were commercially available.

MLN64 is also present in the placenta, a steroidogenic tissue which is not thought to express StAR, where MLN64 has been linked to steroid synthesis (Tuckey, 2005). The protein is also highly expressed in human breast carcinomas with expression being linked to the Her 2 receptor and the relative aggressiveness of the cancer (Alpy et al., 2003; Vinatzer et al., 2005). In addition, MLN64 has been identified in the prostate, where upregulation of MLN64 expression was significantly associated with CYP17

expression and late stages of prostate cancer (Stigliano et al., 2007). Progression of breast and prostate carcinoma is a hormone dependent process and it has been suggested that there is a role for MLN64 with intra-neoplastic autonomous steroidogenesis (Stigliano et al., 2007). Future studies to determine MLN64 changes in skin cancer would be beneficial.

TSPO is reported to act synergistically with StAR to promote steroid synthesis when associated with the mitochondria (Liu et al., 2006). Similar to previous studies, TSPO was expressed throughout the tissue but was particularly intense in the granulosa layer just prior to keratinocyte stratification (Stoebner et al., 1999). However, in this chapter the TSPO expression pattern was predominantly perinuclear rather than mitochondrial as described previously (Stoebner et al., 1999). TSPO has also been detected in cell nuclei of breast cancers and this localisation was associated with increased cell proliferation (Hardwick et al., 1999). Therefore, the localisation of TSPO identified by this research suggests that the protein may be involved in regulating cell proliferation. However, localisation according Stoebner *et al*. (1999) suggests that TSPO maybe coordinating StAR-mediated cholesterol transport in the basal layer of the epidermis. In suprabasal layers where StAR is absent, TSPO could be functioning to coordinate StAR-independent steroidogenesis or regulating apoptosis as reported in other systems (Veenman et al., 2007).

In agreement with previous studies, DAX1, a negative regulator of StAR, was detected in the cytoplasm of all epidermal layers in normal skin (Patel et al., 2001). The absence of DAX1 from epidermal cell nuclei implies that DAX1 is not directly repressing StAR transcription at the point of analysis. In addition, the expression of DAX1 throughout all epidermal layers but absence of StAR in suprabasal layers, implies that there is an alternative mechanism for inhibiting StAR protein expression in suprabasal keratinocytes. Cytoplasmic DAX1 can also inhibit StAR expression by acting as an antagonist to SF1, preventing SF1 from initiating StAR transcription (Iyer and McCabe, 2004). The balance of DAX1 to SF1 has been shown to mediate steroidogenesis by regulating StAR expression (Iyer and McCabe, 2004). SF1 has been identified throughout the epidermis (Patel et al., 2001) therefore changes in StAR expression

pattern from basal to suprabasal layers could be mediated via DAX1:SF1 interactions, however this remains to be clarified.

Following the identification of StAR, DAX1, MLN64 and TSPO in normal skin, the expression of these proteins was investigated in cultured skin cells using western blotting and immunofluorescence cytochemistry. Western blot analysis revealed that DAX1 and MLN64 were expressed in all the cells tested (primary keratinocytes, primary dermal fibroblasts, HaCaTs and N/TERTS immortalised keratinocyte cell lines, SZ95 immortalised sebocytes, JEG3 immortalised placenta cells, H295R immortalised adrenal cells).

Whilst TSPO monomer (18 kDa) was not identified, a series of higher molecular weight bands were detected in all cells suggesting that TSPO was arranged in polymeric clusters (Delavoie et al., 2003). These clusters are formed by ROS-mediated dityrosine bond formation and cannot be broken back down to monomers by heat, urea buffer, SDS or reducing agents (Delavoie et al., 2003). The role of TSPO cluster formation remains to be defined but the TSPO monomer has been reported to promote cholesterol binding for steroid synthesis (Delavoie et al., 2003). Upon induction of steroidogenesis by hCG a concomitant rapid (30 sec) formation of cluster topography is observed in Leydig cells (Boujrad et al., 1996). In addition, large cluster formation is associated with cell proliferation, consistent with the environment of cell culture that is designed to promote cell growth (Delavoie et al., 2003).

In contrast, StAR was not detected by western blot in any of the cells tested except H295R adrenal cells that were used for a positive control. Even the addition of dbcAMP that has been shown to enhance StAR protein expression in MA-10 mouse Leydig cells did not lead to the detection of StAR protein in the skin cells tested. Due to the basal localisation of StAR and that the basal layer oxygen levels are physiologically closer to 2% $O_2$ rather than atmospheric $O_2$, keratinocytes were FACS sorted for basal cell enrichment (β1-integrin) and cultured at 2% $O_2$ (Ngo et al., 2007; Watt, 1998). Western blot analysis still failed to identify StAR protein under these culture conditions.

However, StAR mRNA was identified by RT-PCR in keratinocytes that had been cultured for 5 days, demonstrating that StAR transcription was present in the cells. This is consistent with the finding that the nuclear receptor DAX1 was localised to the cytoplasm of cultured cells rather than nucleus, suggesting that DAX1 is not directly repressing StAR transcription.

In addition, a time course of StAR expression in cultured keratinocytes showed that after 24 h, most keratinocytes were detected as expressing StAR. However, by day 5, the expression of StAR was virtually absent in all primary keratinocytes. This suggests that StAR protein was unstable and degraded in cultured keratinocytes or that StAR mRNA translation to protein was inhibited.

Recently, A-kinase anchoring protein (AKAP) 121 has been implicated in anchoring StAR mRNA and PKA to the outer mitochondrial membrane in mouse Leydig cells (Dyson et al., 2008). The research demonstrated that AKAP121 could provide a site for StAR mRNA translation coupled with rapid activation of the newly synthesised StAR protein (Dyson et al., 2008). Interestingly, knockdown of AKAP121 had no effect on StAR transcript levels but dramatically decreased StAR protein levels and prevented acute steroidogenesis. Due to the high turnover of StAR, proteosome inhibitors (MG132 and *clasto*-lactacystin β-lactone) have also been shown to increase StAR signal by preventing protein degradation in rat adrenal cortex, COS cells and primary granulosa cells (Granot et al., 2007b; Rucinski et al., 2008). Further analysis of AKAP149 (the human orthologue of AKAP121) and use of proteosome inhibitors is required to confirm the above findings.

MLN64 was expressed in the majority of cultured keratinocytes and detected both by western blotting and immunofluorescence cytochemistry. The MLN64 patterning that was displayed would be more similar to endosomal rather than mitochondrial localisation. This corresponds with other reports that have localised MLN64 to the late endosomes of neurones, glia MCF7 human breast cancer cell lines and SK-OV-3 human ovarian cancer cell lines (Alpy et al., 2001; King et al., 2006). The precise role of MLN64 remains to be defined, however current theory suggests that MLN64 functions

to supply cholesterol to StAR and/or TSPO for steroidogenesis, rather than delivering cholesterol across mitochondrial membranes to CYP11A1 (Rone et al., 2009).

The expression pattern of StAR, DAX1 and MLN64 were also investigated in psoriasis, harlequin ichthyosis and atopic dermatitis. This was to assess whether regulators of steroid synthesis were disrupted in these diseases since cortisol therapy is still the treatment of choice for psoriasis and atopic dermatitis (Stojadinovic et al., 2007).

Low level StAR expression was detected in the basal layer of the epidermis of harlequin ichthyosis skin. The intensity of StAR protein expression was less than normal skin consistent with the hypothesis that acute steroidogenesis is limited in hyperproliferative skin conditions. It is inconclusive as to whether MLN64 expression was moderated in the harlequin ichthyosis epidermis.

StAR was not detected in both non-lesional psoriatic and atopic dermatitis biopsies. However, low levels of StAR were observed in basal regions of the epidermis of lesional psoriatic and harlequin ichthyosis skin. Previously published research also demonstrated that StAR was absent or down regulated in non-lesional psoriasis (Tiala et al., 2007). In this study, lower StAR expression was associated with decreased levels of coiled-coil alpha helical rod protein 1 (CCHCR1); a gene that is located in the major psoriasis susceptibility locus PSORS1 and has been shown to regulate StAR expression (Tiala et al., 2007).

DAX1 was expressed in the cell nuclei of uninvolved atopic dermatitis, involved atopic dermatitis and non-lesional psoriatic skin but was in the cytoplasm of lesional psoriasis. The nuclear localisation of DAX1 could account for decreased StAR expression in uninvolved atopic dermatitis, involved atopic dermatitis and non-lesional psoriatic biopsies (Zazopoulos et al., 1997). Conversely, cytoplasmic expression of DAX1 in lesional regions of psoriasis could partly account for the slight increase in StAR expression observed in lesional versus non-lesional regions of the skin disease.

The MLN64 expression pattern was unchanged between non-lesional psoriatic, atopic dermatitis and normal skin. However, MLN64 was only expressed in upper suprabasal

layers and appeared to be less intense in lesional areas of psoriatic and atopic dermatitis biopsies when compared to normal skin. This could be because keratinocytes in involved regions of psoriasis and atopic dermatitis skin display hyperproliferation and poor differentiation. Markers of differentiation such as involucrin and filaggrin are downregulated in psoriasis, possibly due to increased rate of early apoptosis (Iizuka et al., 2004). Atopic dermatitis is also associated with loss of function mutations in the FLG gene, which encodes filaggrin (Palmer et al., 2006). Therefore the expression pattern of MLN64 could be related to poor regulation of keratinocyte differentiation in these skin diseases.

Reduced StAR expression patterning in involved and non-involved regions of psoriasis, atopic dermatitis and harlequin ichthyosis suggests that acute steroid synthesis is disrupted in diseased tissue. The MLN64 expression pattern also corresponds with the poor differentiation characteristic of psoriasis and atopic dermatitis. The altered expression pattern of StAR, DAX1 and MLN64 in both uninvolved and involved regions of the skin disorders is indicative of suppressed steroidogenic cholesterol transport. It also demonstrates that uninvolved regions of psoriatic and atopic dermatitis skin are not equivalent to normal skin.

In summary, the data presented here shows that normal human epidermis express the cholesterol transporters StAR, MLN64 and TSPO that are associated with steroid synthesis. The expression pattern of these proteins are aberrant in hyperporliferative skin disorders that are commonly managed with cortisol-based treatments. This suggests that normal epidermis could be capable of acute steroid synthesis and that this process is disrupted in the diseased skin tested. Although StAR expression was not stable in cultured keratinocytes, the cells did express MLN64 and TSPO and demonstrated cytoplasmic patterning of DAX1. Taken together, the evidence suggests that normal keratinocytes might be capable of *de novo* steroid synthesis.

# Chapter 4. Investigating Cortisol Synthesis by Primary Human Keratinocytes

## 4.1 Introduction

Cortisol has a profound effect on the epidermis. This steroid can induce keratinocyte differentiation, as well as decrease keratinocyte lipid formation, apoptosis and inflammation (Elias, 2005). Cortisol is therefore used as a potent anti-inflammatory agent and cortisol derivatives are the treatment of choice for multiple skin disorders including psoriasis and atopic dermatitis. Despite the broad clinical benefit of cortisol analogues, the ability of normal human keratinocytes to endogenously synthesise cortisol has not been reported.

There have been several studies of steroid synthesis within the skin (Slominski et al., 2007). For example, in humans the hair follicle has been reported to express a functional hypothalamic pituitary adrenal (HPA) axis to synthesise cortisol (Ito et al., 2005; Kauser et al., 2005). Sebocytes can convert 22R-hydroxycholesterol to 17-hydroxypregnenolone (Thiboutot et al., 2003), whilst melanocytes and fibroblasts have also been shown to produce corticosterone and cortisol through localised HPA axis stimulation (Slominski et al., 2005a; Slominski et al., 2005b; Slominski et al., 2006). There has also been extensive research into androgen and oestrogen metabolism by primary keratinocytes (Gingras et al., 2003; Milewich et al., 1988). Keratinocytes have also been shown to process POMC proteins including ACTH (Rousseau et al., 2007). In addition, progesterone metabolism was demonstrated in HaCaT keratinocyte cell lines but the metabolites were derivatives of deoxycorticosterone (Slominski et al., 2002). Progesterone metabolism to deoxycorticosterone is a divergent pathway from the formation of cortisol from progesterone, which proceeds via the synthesis of 17α-hydroxyprogesterone. Despite these advances, synthesis of cortisol from cholesterol has not previously been functionally characterised in primary keratinocytes.

Chapter 3 demonstrated that the epidermis expresses cholesterol transporters that are associated with the first step of steroid synthesis, including StAR, TSPO and MLN64. In addition, published research has shown that keratinocytes are capable of *de novo* synthesis of cholesterol, the precursor of all steroids (Menon et al., 1985). Finally, the complete P450 scc system, including CYP11A1, FDXR and FDX, is present in human

skin (Slominski et al., 2004; Thiboutot et al., 2003), although the functional capacity of these elements has not been determined in primary human keratinocytes.

The first step of steroidogenesis involves the conversion of cholesterol to pregnenolone, which is then metabolised to progesterone. Progesterone influences keratinocyte biology by enhancing keratinocyte cell proliferation and aiding moisture retention in the dermis (Kanda and Watanabe, 2005). The effect of progesterone on skin health is most apparent during menopause, where skin rapidly ages as the systemic progesterone concentration deceases (Kanda and Watanabe, 2005).

The epidermis responds rapidly to environmental stressors and can be profoundly modulated by steroids. Therefore, the aim of this chapter was to identify whether normal primary human keratinocytes are able to synthesise pregnenolone, progesterone and cortisol. Radioimmunoassay (RIA) was used to investigate endogenous pregnenolone synthesis by primary human keratinocytes. Radiometric was employed to assess the ability of keratinocytes to metabolise pregnenolone, progesterone and cortisol and liquid chromatography-mass spectrometry (LC-MS) was used to verify the synthesis of cortisol from progesterone by the cells. Finally ELISA was used to quantify cortisol synthesis by primary human keratinocytes.

## 4.2 Results

### 4.2.1 Optimising the pregnenolone RIA

The principle of RIA is based on tritiated labelled pregnenolone of known concentration competing for the binding of a pregnenolone antibody against endogenous (non-labelled) pregnenolone. The relative displacement of tritiated pregnenolone can be measured and thus the concentration of endogenous pregnenolone can be calculated comparatively against a standard curve. The concentration of both labelled pregnenolone and pregnenolone antibody must be optimised to provide sensitive displacement when cold (sample) pregnenolone is added to the system.

Figure 4.1 shows the optimisation process for generating a standard curve that lies within range for accurate pregnenolone displacement and therefore quantification. Figures 4.1 A and B show that at these antibody concentrations the assay is too sensitive since [$^3$H] pregnenolone is completely displaced even at the lowest concentration of cold pregnenolone in 4.1 A. Although the assay is still too sensitive in 4.1 B, the lowest concentration of cold pregnenolone (3.91 nM) did not completely displace [$^3$H] pregnenolone. In Figure 4.1 C the assay is not sensitive enough since effective displacement of [$^3$H] pregnenolone only occurred beyond 31.5 nM cold pregnenolone. Figure 4.1 D is an example of the optimised standard curve where [$^3$H] pregnenolone is effectively displaced from 3.91 nM to 1000 nM so that measurements of unknown pregnenolone could be calculated at any point within this range of pregnenolone concentrations.

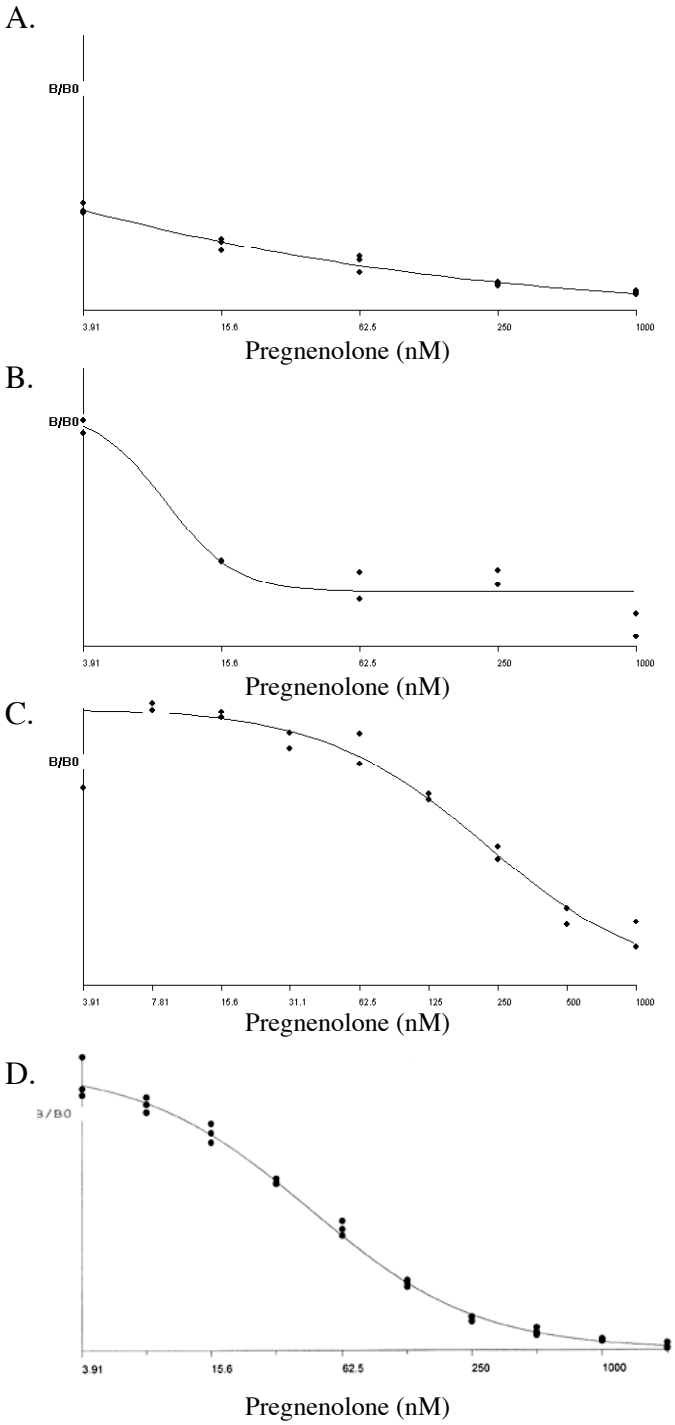


**Figure 4.1 Optimisation of the pregnenolone RIA.**

Concentrations of pregnenolone antibody and tritiated pregnenolone were optimised so that known concentrations of unlabelled pregnenolone would displace tritiated pregnenolone to generate a standard curve between 3.91 and 1000 nM pregnenolone. (A) antibody dilution 1:3000, [$^3$H]pregnenolone 1:8000 (B) antibody dilution 1:4000, [$^3$H]pregnenolone 1:8000 (C) antibody dilution 1:8000, [$^3$H]pregnenolone 1:4000 (D) antibody dilution 1:3000, [$^3$H]pregnenolone 1:6000.

### 4.2.2 Pregnenolone synthesis detected by RIA

RIA was used to quantify pregnenolone concentration in primary human keratinocyte culture media. Since pregnenolone was not detected in cell-free culture medium, it is assumed that any pregnenolone detected was due to endogenous synthesis by the cells. It was also predicted that the level of pregnenolone synthesis would be low, therefore two compounds, trilostane (T) and ketokonazole (K), were used to inhibit further metabolism of pregnenolone (Figure 4.2 B). T is an inhibitor of 3βHSD, the enzyme which metabolises pregnenolone to progesterone. K is an inhibitor of CYP17, the enzyme which converts pregnenolone to 17-OH pregnenolone.

Keratinocytes treated with T and K displayed a significant (3.7 ± 0.4 fold) increase of pregnenolone detection relative to untreated cells (Figure 4.2A). This demonstrated that primary human keratinocytes are able to synthesise pregnenolone. In addition to T and K, 25-OH cholesterol and EGF were incubated with the cells (Figure 4.3). 25-OH cholesterol was predicted to promote steroid synthesis by bypassing StAR, which is considered as the rate determining step of steroid synthesis, and providing abundant substrate to the system. EGF was predicted to upregulate pregnenolone synthesis since it has been shown to increase StAR promoter activity more effectively than dbcAMP in keratinocytes (MV Patel, 2002). Neither compound alone was able to promote pregnenolone synthesis above basal T and K levels (T and K: 24.42 ± 3.8 nM, EGF with T and K: 22.8 ± 11.7 nM, 25-OH cholesterol with T and K: 24.9 ± 9.0 nM pregnenolone, Figure 4.3). Only the combination of all four compounds, 25-OH cholesterol, EGF with T and K, produced a significant increase in pregnenolone above the untreated baseline (untreated: 5.0 ± 5.0, 25-OH cholesterol, EGF with T and K 44.6±18.0 nM pregnenolone, $P<0.001$), but this increase was not significantly greater than that achieved with T and K alone.

The only treatment tested that independently promoted pregnenolone synthesis above T and K levels was dex (T and K: 24.4 ± 3.8 nM, dex with T and K: 52.2 ± 7.8 nM pregnenolone, $P<0.05$, Figure 4.4). The addition of 25-OH cholesterol to dex with T

and K did not further promote pregnenolone synthesis (60.7 ± 12.7 nM), as would be predicted of this compound that can bypass StAR.

Primary keratinocytes were incubated with TNFα to measure the input of stress response on pregnenolone synthesis. TNFα with T and K did not significantly promote pregnenolone synthesis compared to T and K only treated cells (32.8 ± 12.5 nM versus 24.4 ± 3.8 nM respectively, Figure 4.4). However, when TNFα was added in combination with dex, 25-OH cholesterol, T and K pregnenolone synthesis was significantly increased compared to T and K levels (75.5 ± 19.7 nM). This demonstrated that dex was critical for the promotion of pregnenolone steroidogenesis.

Overall the results indicate that primary human keratinocytes are able to synthesise pregnenolone. In addition, since T and K can enhance the level of pregnenolone detected, it is likely that 3βHSD and CYP17 are able to actively metabolise pregnenolone. The addition of 25-OH cholesterol did not further promote steroidogenesis, suggesting there could be a different rate determining step for steroid synthesis in cultured primary human keratinocytes compared to most steroidogenic cells. Only the addition of dex appeared to significantly increase pregnenolone steroidogenesis.

A.

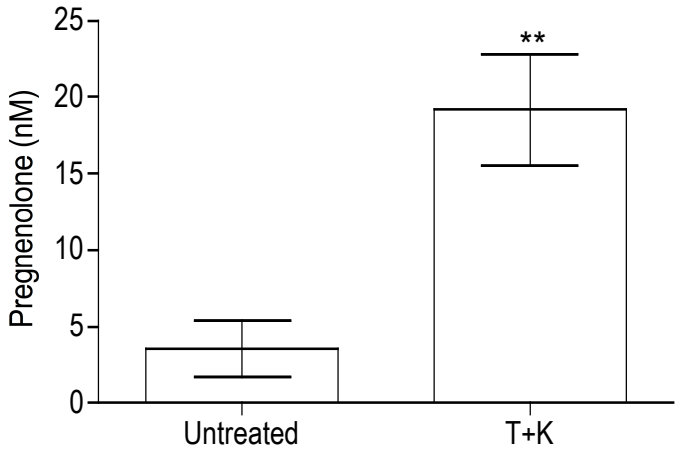


B.

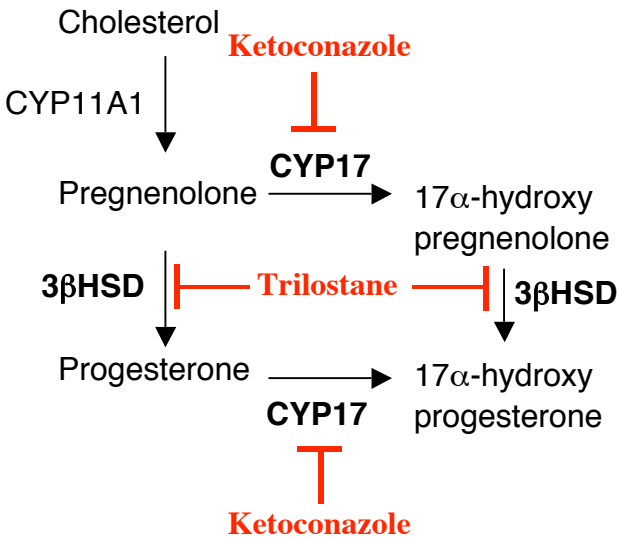


**Figure 4.2 Pregnenolone synthesis by primary human keratinocytes with T and K.** (A) Pregnenolone was detected by RIA from 1ml culture media of primary human keratinocytes (seeded at a density of $2.5x10^5$ in 12 well plates) after 24 h. T: 100 μM trilostane, K: 10 μM ketoconazole. The data are from three separate experiments, statistical differences were determine using an unpaired T-test (n=3, mean ± SEM, **P<0.01). (B) Illustration of 3βHSD inhibition by trilostane and CYP17 inhibition by ketoconazole.

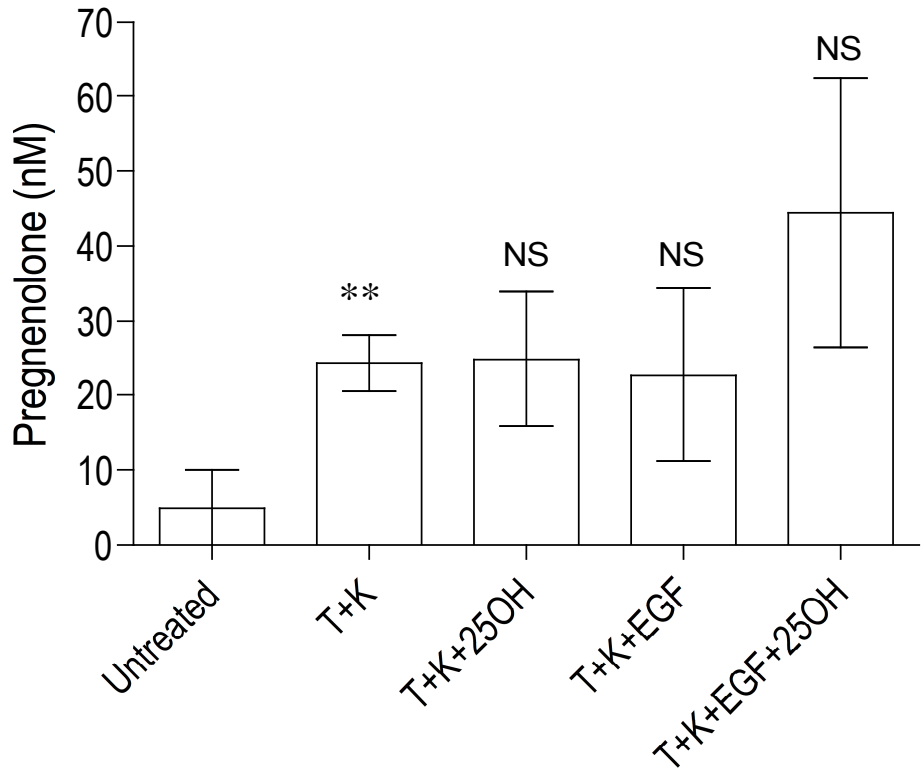


**Figure 4.3 Pregnenolone synthesis by primary human keratinocytes with EGF and 25OH cholesterol.**

Pregnenolone was detected by RIA from 1ml culture media of primary human keratinocytes (seeded at a density of $2.5x10^5$ in 12 well plates) after 24 h. T: 100 μM trilostane, K: 10 μM ketoconazole, EGF: 60 ng/ml epidermal growth factor, 25-OH: 5 μM 25-OH cholesterol. The data was normalised against cell density, statistical differences were determine using one-way ANOVA followed by a post-hoc Tukey test where appropriate (200,000 cell/ml, mean ±S.D., **P<0.01 relative to untreated cells, NS not significant relative to T+K).

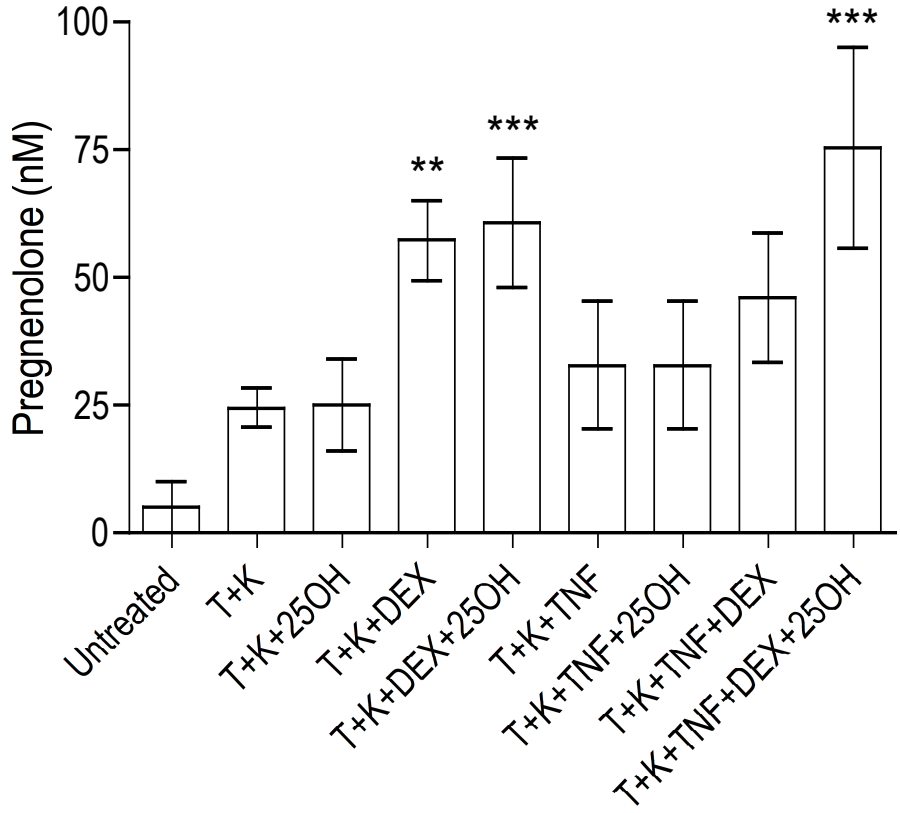


**Figure 4.4 Pregnenolone synthesis by primary human keratinocytes with dex and TNFα.**

Pregnenolone was detected by RIA from 1ml culture media of primary human keratinocytes (seeded at a density of $2.5x10^5$ in 12 well plates) after 24 h. T: 100 μM trilostane, K: 10 μM ketoconazole, dex: 1 μM dex, 25-OH: 5 μM 25-hydroxycholesterol, TNF: 60 ng/ml tumour necrosis factor-α. The data was normalised against total protein concentration, statistical differences were determine using one-way ANOVA followed by a post-hoc Tukey test where appropriate (mean ±S.D., *P <0.05, **P<0.01, ***P<0.001 relative to T+K).

### 4.2.3 Pregnenolone metabolism by radiometric assay

The ability of primary human keratinocytes to metabolise pregnenolone was then analysed by thin layer chromatography (TLC). The products of [$^3$H] pregnenolone metabolism by cultured keratinocytes after 24 h incubation is illustrated in Figure 4.5. The products of [$^3$H] pregnenolone metabolism co-migrated with progesterone, 17-OH progesterone and 17-OH pregnenolone, cortisol, cortisone, 11 desoxycortisol, and corticosterone together with some undetermined steroid metabolites. This therefore demonstrates that primary human keratinocytes are capable of synthesising cortisol from pregnenolone. [$^3$H] Pregnenolone metabolism was also analysed in the presence or absence of T and/or K (Figure 4.6). This was for two reasons; to demonstrate whether pregnenolone metabolism was mediated via 3βHSD and CYP17, and to identify the relative efficiency of the 3βHSD and CYP17 inhibitors. Therefore, if T were 100% effective, the expected TLC pattern would include peaks that co-migrate with pregnenolone and 17-OH pregnenolone but peaks co-migrating with progesterone and 17-OH progesterone would be absent. If K were 100% efficient, the predicted TLC pattern would include peaks co-migrating with pregnenolone and progesterone but no 17-OH pregnenolone and 17-OH progesterone peaks. Figure 4.6 demonstrates that T was efficient at inhibiting 3βHSD activity since upon its addition, the majority of pregnenolone was not further metabolised.

Likewise, K acts to inhibit CYP17, therefore with K treatment, the product of [$^3$H] pregnenolone metabolism was expected to be progesterone with little or no 17-OH derivatives of pregnenolone and progesterone. Figure 4.6 shows that, there was an efficient block of keratinocyte CYP17 [$^3$H] pregnenolone metabolism since no 17-OH derivatives were detected by radiometric assay in the presence of K. These data enhance the confidence that the metabolites of [$^3$H] pregnenolone are likely to be progesterone, 17-OH pregnenolone and 17-OH progesterone since their synthesis can be partially blocked by the 3βHSD and CYP17 inhibitors T and K.

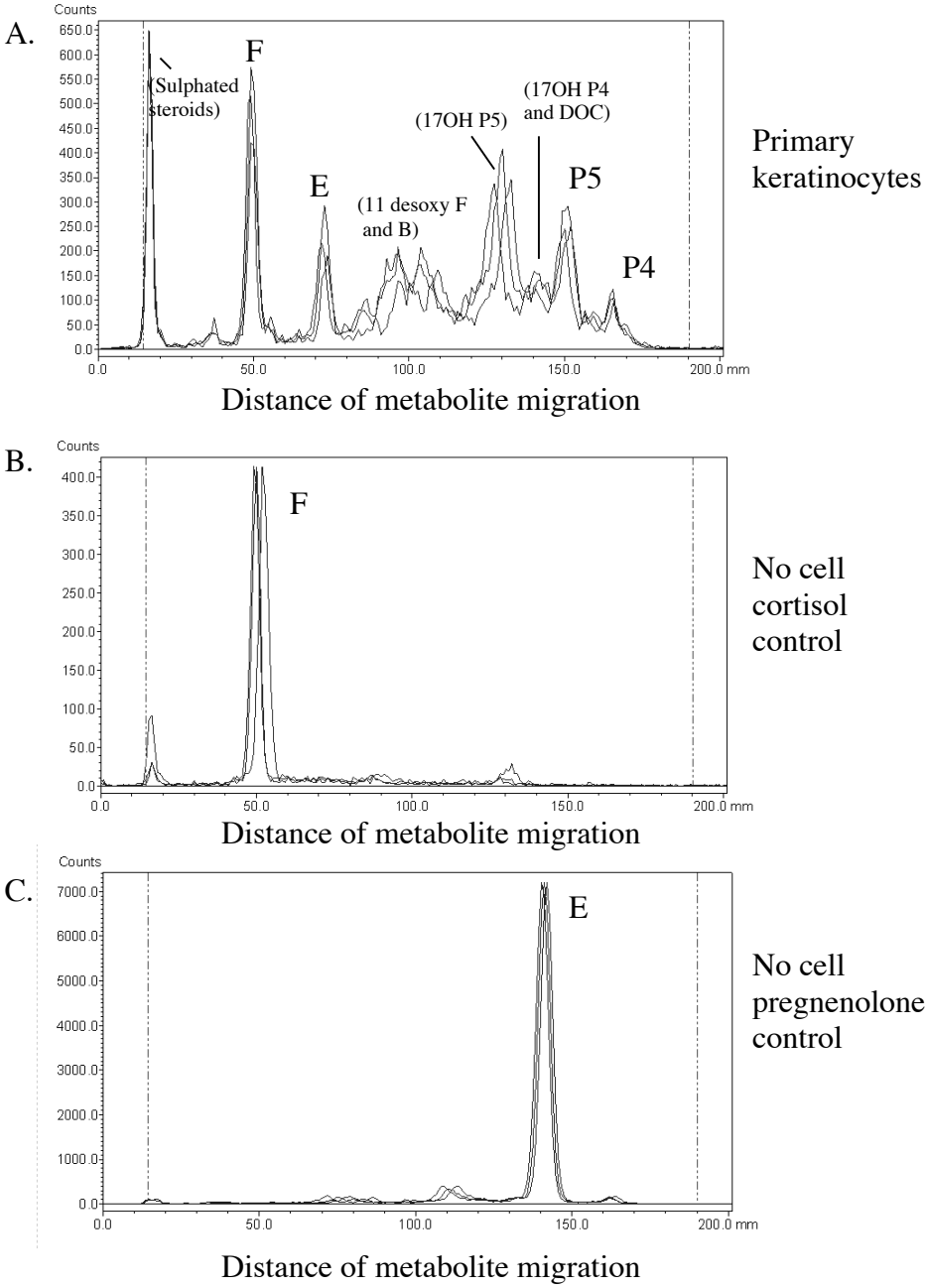


**Figure 4.5 Pregnenolone metabolism by primary human keratinocytes.**

(A) Cells (at a density of $2.5x10^5$ in 12 well plates) were incubated for 24 h with fresh serum free medium containing 0.037 MBq (90.0 pmol) of [$^3$H] pregnenolone in a volume of 1ml/well. Steroid metabolites were chloroform-extracted from culture medium and resolved by thin layer chromatography. (B) Authentic cortisol standard, (C) authentic pregnenolone standard demonstrate the hallmark migration of these metabolites. Chromatogram is a representative of three separate assays, each performed in triplicate (one triplicate depicted in each panel) using keratinocytes isolated from two different individuals. P5 = pregnenolone, P4 = progesterone, 17OHP5 = 17-hydroxypregnenolone, 17OHP4 = 17-hydroxyprogesterone. E = cortisone, F = cortisol, B = corticosterone, 11 desoxy F = 11 desoxycortisol.

A. [$^3$H] Pregnenolone with trilostane

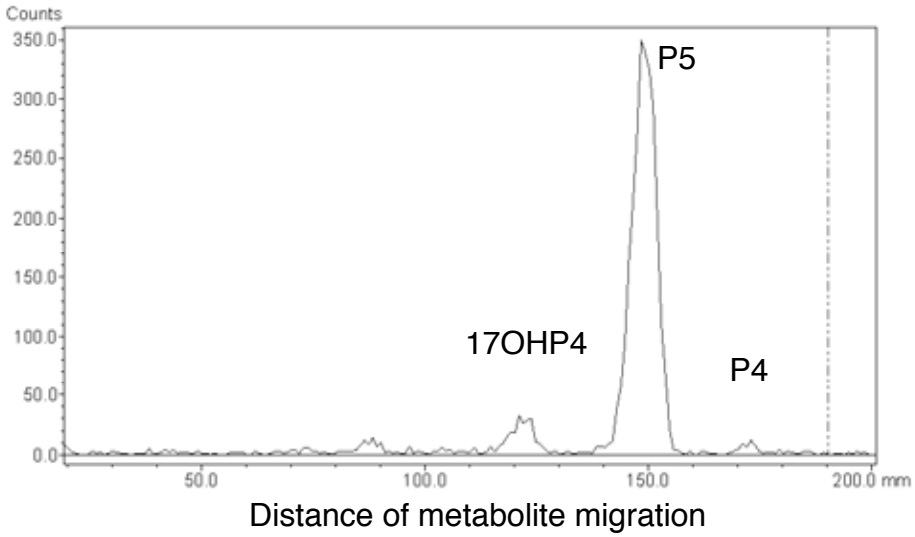


B. [$^3$H] Pregnenolone with ketoconazole

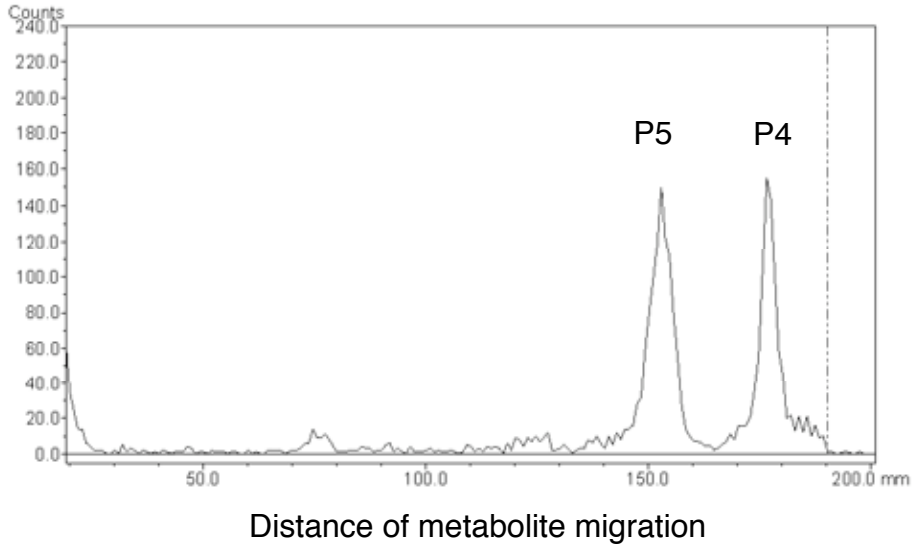


**Figure 4.6 Inhibition of pregnenolone metabolism by T and K in primary human keratinocytes.**

Cells (at a density of 2.5x10$^5$ in 12 well plates) were incubated for 24 h with 0.037MBq (90.0 pmol) of [$^3$H] pregnenolone and trilostane (T, 100 μM) or ketoconazole (K, 10 μM) in a volume of 1 ml/well. Steroid metabolites were chloroform-extracted from culture medium and resolved by thin layer chromatography. Chromatogram is a representative of three separate assays, each performed in triplicate using keratinocytes isolated from a different individual. P5 = pregnenolone, P4 = progesterone, 17OHP5 = 17-hydroxypregnenolone, 17OHP4 = 17-hydroxyprogesterone.

### 4.2.4 Progesterone metabolism by radiometric assay

The results of the radiometric assay to measure [$^{3}$H] progesterone metabolism by primary human keratinocytes after 24 h are shown in Figure 4.7. The major products migrated with Rf values that matched 17-OH progesterone (32.9 ± 2.5 % conversion) and cortisol (28.5 ± 1.9 % conversion). Production of cortisol from progesterone was confirmed by co-migration of progesterone metabolites with an authentic [1,2,6,7-$^{3}$H] cortisol standard (Figure 4.7 B). The metabolites 11-deoxycortisol and cortisone were not observed at the 24 h time point, however a small peak that migrated to a Rf value matching pregnenolone was detected. This would be consistent with reverse 3βHSD activity, causing progesterone to be reduced to pregnenolone.

A.

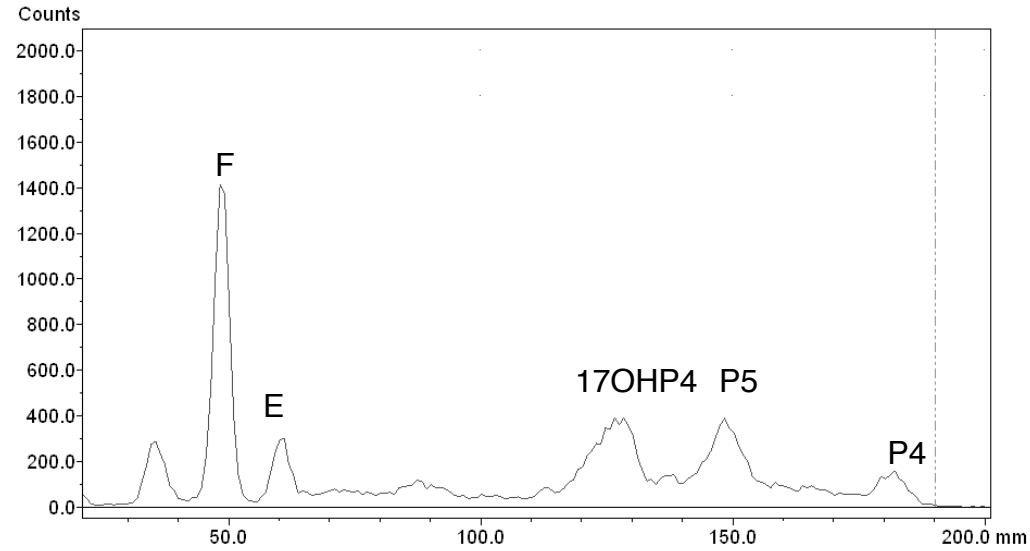


B.

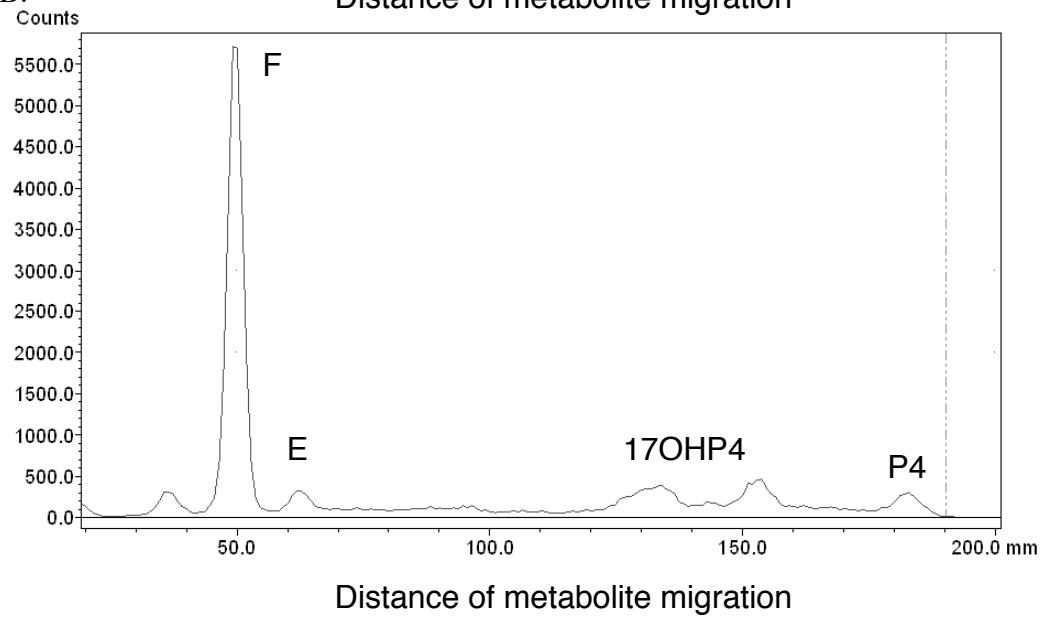


**Figure 4.7 Progesterone metabolism by primary human keratinocytes.**

Primary human keratinocytes (at a density of $2.5x10^5$ cells/well in 12 well plates) were incubated for 24 h with fresh serum free medium containing 0.037 MBq (11.0 pmol) of [$^3$H] progesterone in a total volume of 1 ml/well. Steroid metabolites were chloroform-extracted from culture medium and resolved by thin layer chromatography. (A) Progesterone metabolism by primary keratinocytes (B) Co-migration of progesterone metabolite with cortisol authentic standard (labelled F). Chromatogram is a representative of three separate assays, each performed in triplicate using keratinocytes isolated from a different individual. P4 = progesterone, 17OHP4 = 17-hydroxyprogesterone, F = cortisol, E = cortisone.

### 4.2.5 Cortisol metabolism by radiometric assay

Cortisol metabolism was assessed over 24 h using [$^{3}$H] cortisol and TLC. The results, as illustrated in Figure 4.8, showed that primary keratinocytes were also capable of metabolising cortisol into a product that co-migrated with cortisone. Over 70% of the cortisol available to the keratinocytes was oxidised to cortisone within 24 h (Table 1). This suggests that primary human keratinocytes possess 11βHSD activity and are able to inactivate cortisol to cortisone. It could also indicate a suboptimal $NADP^{+}$/NADPH ER ratio in cells cultured in a serum free environment, which would favour the metabolism of cortisol to cortisone.

In conclusion, the radiometric data demonstrates that primary human keratinocytes are able to metabolise pregnenolone, progesterone and cortisol. Pregnenolone was metabolised to products that were indicative of progesterone, 17-OH pregnenolone and 17-OH progesterone. Progesterone was metabolised to a product that co-migrated with a cortisol authentic standard and cortisol was metabolised to a product matching cortisone Rf migration.

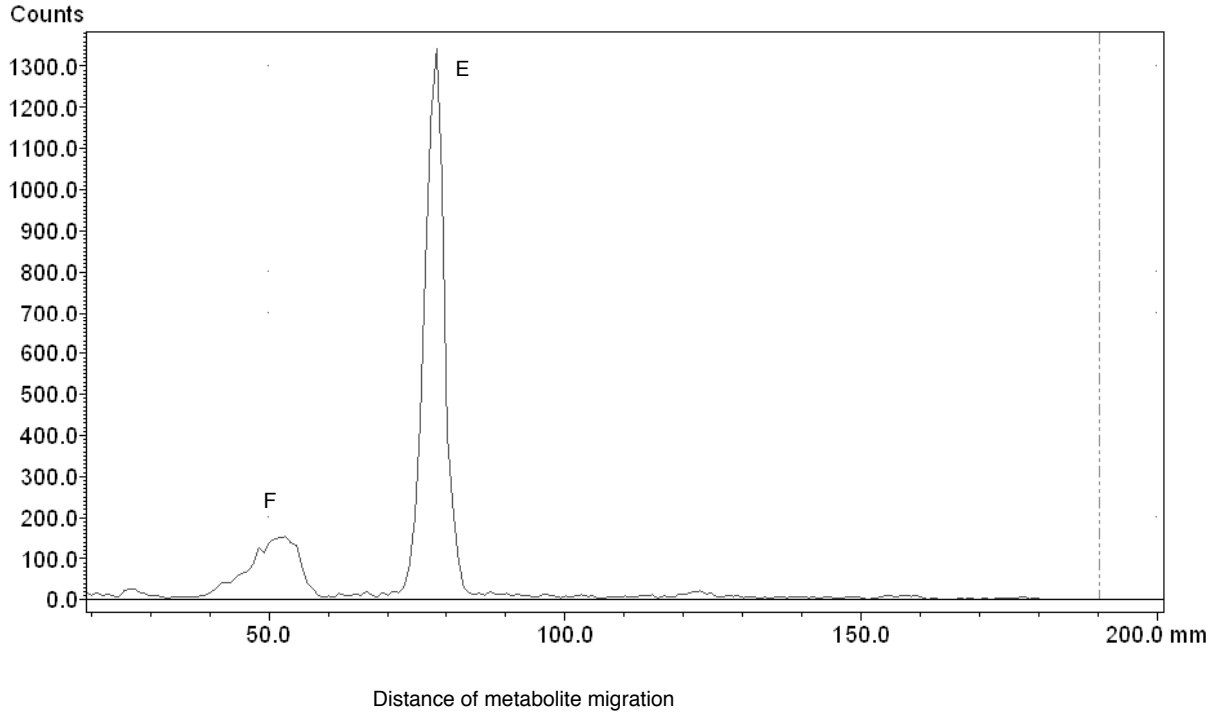


**Figure 4.8 Cortisol metabolism by primary human keratinocytes.**

Primary human keratinocytes (at a density of $2.5x10^5$ cells/well in 12 well plates) were incubated for 24 h with fresh serum free medium containing 0.037 MBq (13.7 pmol) of [$^3$H] cortisol in a total volume of 1 ml/well. Steroid metabolites were chloroform-extracted from culture medium and resolved by thin layer chromatography. Representative chromatogram for three separate assays, each performed in triplicate using keratinocytes isolated from a different individual. F = cortisol, E = cortisone.

### 4.2.6 LC-MS analysis of keratinocyte steroid synthesis

To confirm the formation of cortisol from progesterone, cell culture medium from keratinocytes incubated with progesterone (1 μM; 24 h) was analysed by LC-MS (Figure 4.9). In the absence of cells (i.e. in blank wells), the concentration of progesterone recovered after 24 h was 192.5 ± 23.0 nM, indicating an extraction efficiency of 19.3% relative to the total amount of progesterone added (since 192.5 nM is equivalent to 19.3% of the total 1 μM of progesterone added). In contrast, in the presence of cells, the concentration of progesterone detected after 24 h fell to 102.7 ± 7.8 nM. Concomitantly, 104.0 ± 33.6 nM cortisol was measured in the culture medium. In addition, pregnenolone became detectable in the culture medium at a concentration of 19.6 ± 4.4 nM. The presence of pregnenolone could reflect *de novo* synthesis. Alternatively, it could reflect the reduction of progesterone to pregnenolone via 3βHSD as previously observed in immortalised HaCaT keratinocytes (Slominski et al., 2002).

The LC-MS and radiometric analysis both demonstrated that progesterone could be metabolised to cortisol. To investigate the process, time courses of pregnenolone, progesterone and cortisol metabolism were analysed by LC-MS. When 1 μM pregnenolone was added to primary keratinocytes it was rapidly metabolised between 0 – 10 min but little metabolism was observed after 10 min (Figure 4.10). There was however, a large degree of variation in the distribution of the level of cortisol detected at t = 0, ranging from 120 nM to 420 nM, possibly due to poor extraction efficiency or low number of experimental replicates. This experiment would need to be repeated to confirm this rapid rate of pregnenolone metabolism at early time points. There was no change in progesterone or cortisol levels over this pregnenolone metabolism time course.

The data illustrated in Figure 4.11 showed that progesterone was metabolised by primary keratinocytes over a 240 min (four h) period, however, a concurrent increase in cortisol levels was not observed during this time course. Interestingly, there was a trend suggesting that treating keratinocytes with progesterone could promote progesterone synthesis, since there was an increase in progesterone detected above the baseline between 10 min and 30 min which returned to basal levels at 60 min. Progesterone was

steadily metabolised thereafter (from 60 min to 240 min) although a corresponding increase in cortisol was not detected. This may be because the time course was not sufficiently long enough for cortisol to be generated from progesterone as observed with other 24 h experiments. Future experiments should be conducted over a longer time course, and should include the measurement of other progesterone metabolites such as 17-OH progesterone and 11-deoxycortisol.

Cortisol metabolism was also measured over a 4 h (240 min) time course. Addition of 1 μM cortisol also appeared to induce a rapid peak in cortisol production, since the level of cortisol increased above time 0 at 10 min (Figure 4.12). The amount of cortisol detected then returned to basal (time 0 levels) and did not appear to change from 30 min to 240 min. There was no change in pregnenolone or progesterone levels over the cortisol time course.

LC-MS was also used to determine the efficiency of inhibition of 3βHSD and CYP17 activity by T and K. Although radiometric assay demonstrated almost complete inhibition of 3βHSD and CYP17 activity by T and K, LC-MS did not demonstrate the same efficiency. Table 4.1 displays the LC-MS results of pregnenolone detected in the culture medium of primary keratinocytes treated with T and K and 1 μM pregnenolone versus pregnenolone-treated cells. The data showed that the relative capabilities of the inhibitors to prevent further pregnenolone metabolism was as little as 7.81%.

LC-MS analysis was performed to analyse steroid synthesis by primary keratinocytes incubated with 25-OH cholesterol, TNFα and/or dex in the presence or absence of T and K over 24 h. This was to corroborate the pregnenolone RIA results and to provide a broader understanding of pregnenolone, progesterone, cortisol and cortisone synthesis by primary human keratinocytes. Unfortunately, there appeared to be a high level of sample degradation as indicated by the relative levels of progesterone and pregnenolone in the no cell control samples (Table 4.2). However, despite sample degradation, some progesterone and cortisol was detected in cells treated with the five compounds, T and K, TNFα, dex and 25-OH cholesterol (cortisol 3.7 ± 2.6 nM, progesterone 3.6 ± 4.6 nM; pregnenolone was not detected). This was the only treatment where cortisol and progesterone were detected above basal/quantification limits. The result correlates with

the RIA data which also showed that the highest production of steroid (pregnenolone) synthesis was with the same five compounds, T and K, TNFα, dex and 25-OH cholesterol treatment (Figure 4.4).

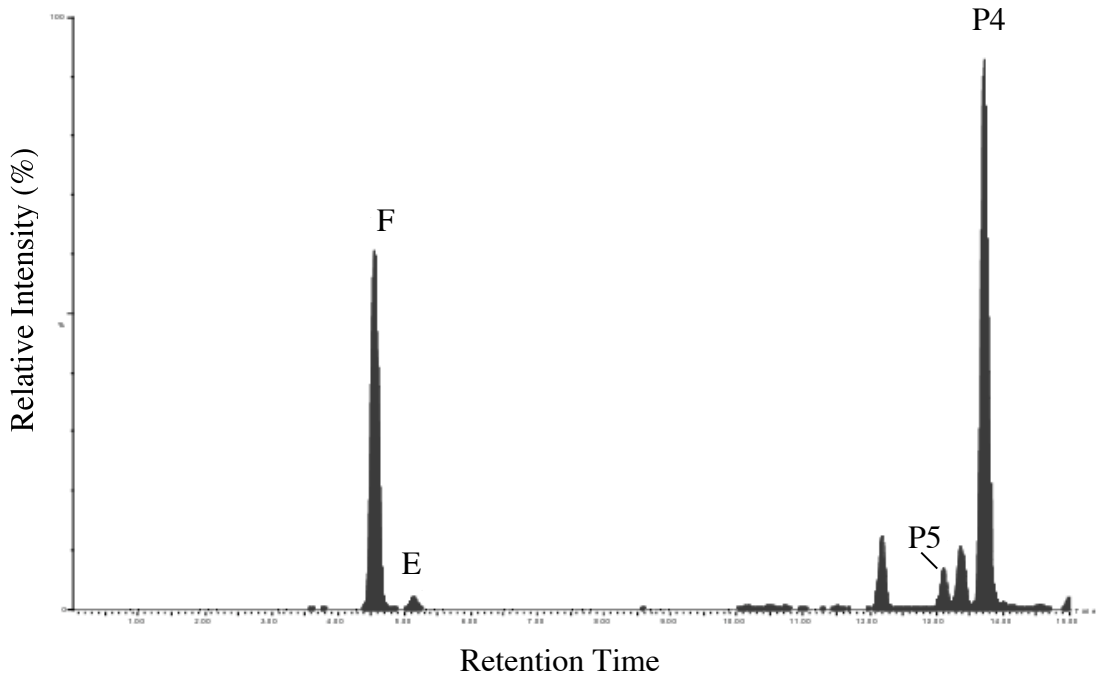


**Figure 4.9 LC-MS analysis of progesterone metabolism by primary human keratinocytes.**

LC-MS trace of cortisol peak detected from the culture medium of primary human keratinocytes treated with 1 μM progesterone for 24 h. The result is a representative trace of two separate experiments from keratinocytes isolated a single skin biopsy. P4 = progesterone, F = cortisol, E = cortisone.

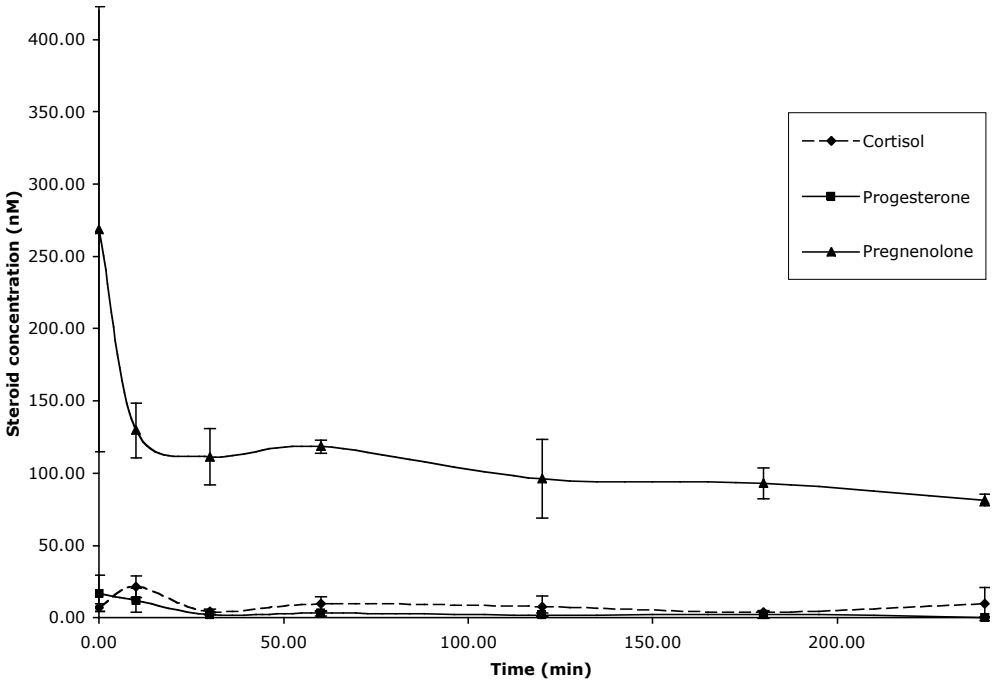


**Figure 4.10 Time course of pregnenolone metabolism analysed by LC-MS.**

Primary keratinocytes were treated with 1 μM pregnenolone. Steroids were extracted from culture medium after 0, 10, 30, 60, 120, 180 and 240 min and analysed by LC-MS for cortisol, progesterone and pregnenolone. The data represents a single experiment, taken from keratinocytes (isolated from one biopsy) treated in triplicate for each treatment and analysed by LC-MS (mean ± S.D).

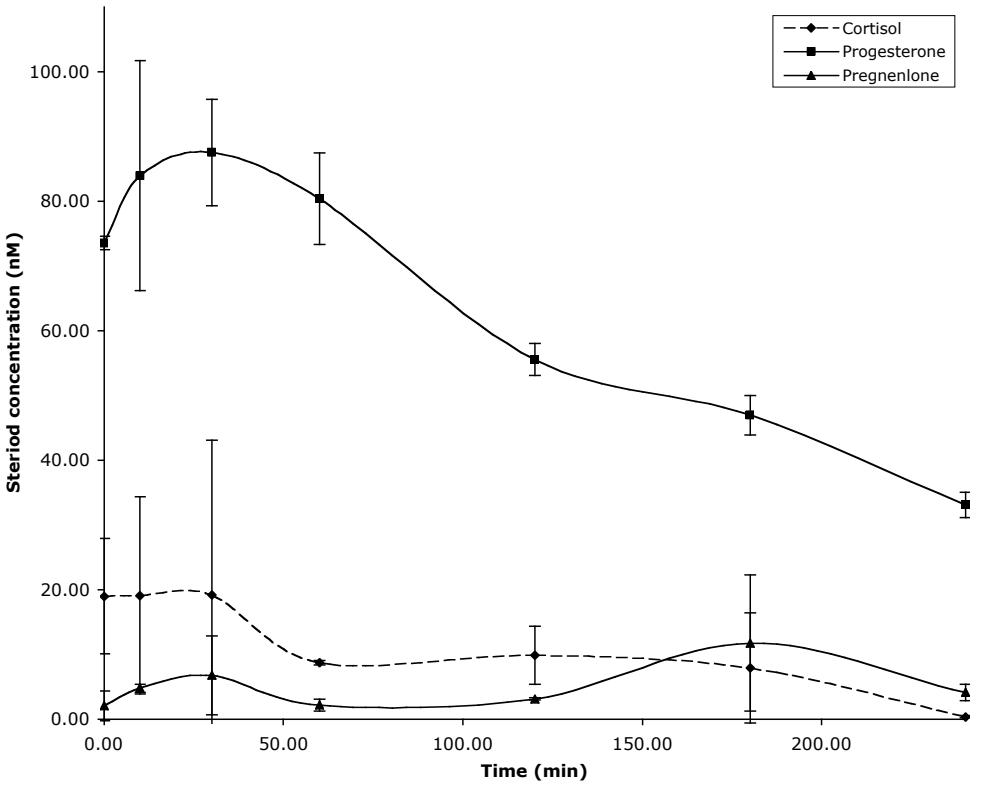


**Figure 4.11 Time course of progesterone metabolism analysed by LC-MS.**

Primary keratinocytes were treated with 1 μM progesterone. Steroids were extracted from culture medium after 0, 10, 30, 60, 120, 180 and 240 min and analysed by LC-MS for cortisol, progesterone and pregnenolone. The data represents a single experiment, taken from keratinocytes (isolated from one biopsy) treated in triplicate for each treatment and analysed by LC-MS (mean ± S.D).

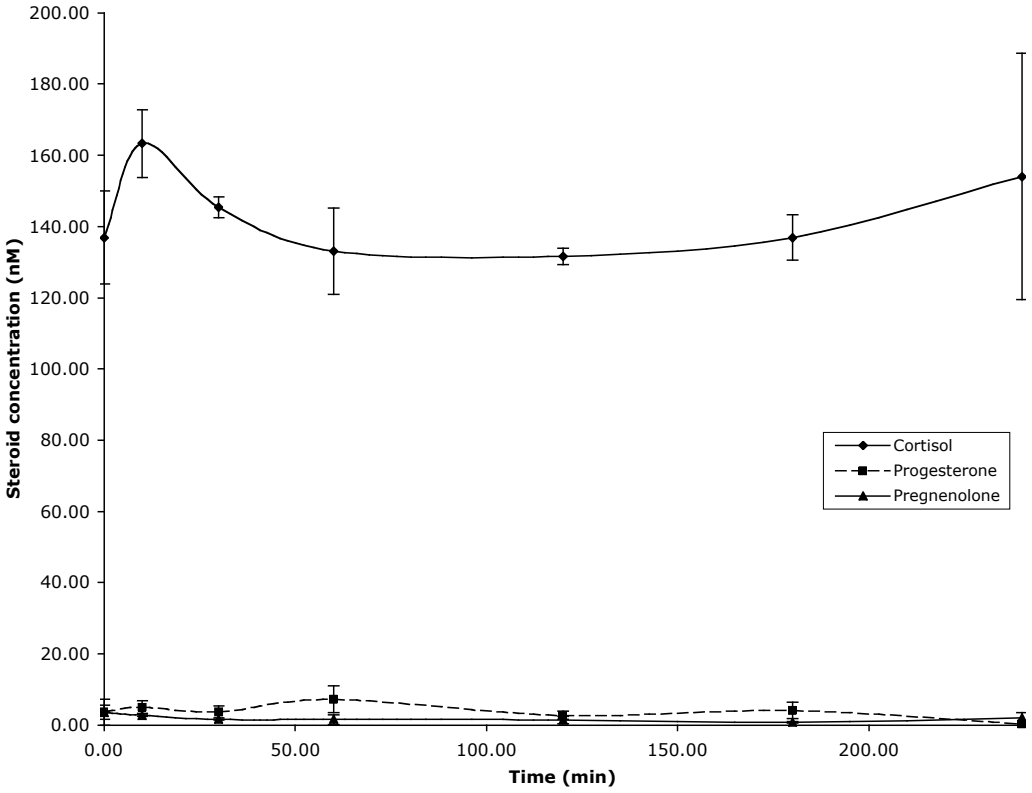


**Figure 4.12 Time course of cortisol metabolism analysed by LC-MS.**

Primary keratinocytes were treated with 1 μM cortisol. Steroids were extracted from culture medium after 0, 10, 30, 60, 120, 180 and 240 min and analysed by LC-MS for cortisol, progesterone and pregnenolone. The data represents a single experiment, taken from keratinocytes (isolated from one biopsy) treated in triplicate for each treatment and analysed by LC-MS (mean ± S.D).

| | Cell-free controls | Untreated cells | T and K | T, K and pregnenolone |
|---|---|---|---|---|
| | 247.7 | 1.6 | < 0.4 | 19.6 |
| | 253.6 | 1.8 | < 0.4 | 22.6 |
| | 329.7 | Traces | < 0.4 | 22.8 |
| **Average** | **277.0** | **1.7** | **< 0.4** | **21.7** |
| **SD** | 45.8 | 0.1 | - | 1.8 |

**Table 4.1 Pregnenolone (nM) concentration determined by LC-MS to assess relative efficiency of T and K to inhibit pregnenolone metabolism.**

The data was generated from a single LC-MS run of triplicate samples for each condition.

| **Cell-free controls** | **Cortisol** | **Progesterone** | **Pregnenolone** |
|---|---|---|---|
| Untreated | 0.00 | 0.21 (±0.17) | 1.43 (±0.47) |
| Pregnenolone | 0.05 (±0.00) | 0.00 (±0.00) | 92.37 (±27.46) |
| Progesterone | 0.11 (±0.14) | 0.10 (±0.17) | 0.00 |
| T, K, TNFα, dex and 25-OH cholesterol | 0.00 | 0.64 (±0.61) | 0.00 |
| **Cells** | **Cortisol** | **Progesterone** | **Pregnenolone** |
| Untreated | 0.30 (±0.22) | 0.97 (±0.68) | 0.00 |
| Pregnenolone | 0.10 (±0.17) | 0.00 | 1.30 (±0.90) |
| Progesterone | 0.52 (±0.91) | 2.08 (±2.67) | 3.35 (±3.02) |
| T and K | 0.08 (±0.13) | 0.50 (±0.51) | 0.00 |
| T, K, TNFα, dex and 25-OH cholesterol | 3.67 (±2.61) | 3.58 (±4.58) | 0.00 |

**Table 4.2 Sample degradation affected LC-MS steroid analysis.**

Primary human keratinocytes were incubated for 24 h with or without the following; progesterone (1 μM), pregnenolone (1μM), T (100 μM), K (10 μM), dex (1 μM), 25-OH cholesterol (5 μM), TNFα (50 ng/ml). Steroids from cell media were extracted and analysed (after more than three months storage at –80°C) by LC-MS, steroid concentrations are displayed in nM. The data represent average steroid concentration (nM ± S.D.) from a single LC-MS analysis of three separate samples per condition.

### 4.2.7 Keratinocyte cortisol synthesis detected by ELISA

A highly sensitive cortisol ELISA was utilised to quantify the production of cortisol by primary human keratinocytes and to determine which medium condition was optimal for cortisol synthesis. Figure 4.13 shows that different types of keratinocyte culture media affected the ability of the cells to synthesise cortisol. Culturing keratinocytes in EpiLife medium (without supplements) provided the highest cortisol levels detected by ELISA. Interestingly little or no cortisol was detected in cells that had been incubated in RM+ culture medium (without supplements) or DMEM. These experiments demonstrated that primary keratinocytes ($2x10^5$ cell/ml in 12-well plates) grown in EpiLife released 1.0 ± 0.2 nM cortisol over a 24 h period. The ELISA data demonstrate that primary human keratinocytes are able to synthesise cortisol without any exogenous stimulation. The basal level of cortisol synthesis was dependent upon culture conditions, with EpiLife keratinocyte culture medium providing the best conditions for the synthesis of the steroid. The complete formula of EpiLife is not publicly available so it is not possible to determine if there is a compound within the medium that is promoting cortisol synthesis.

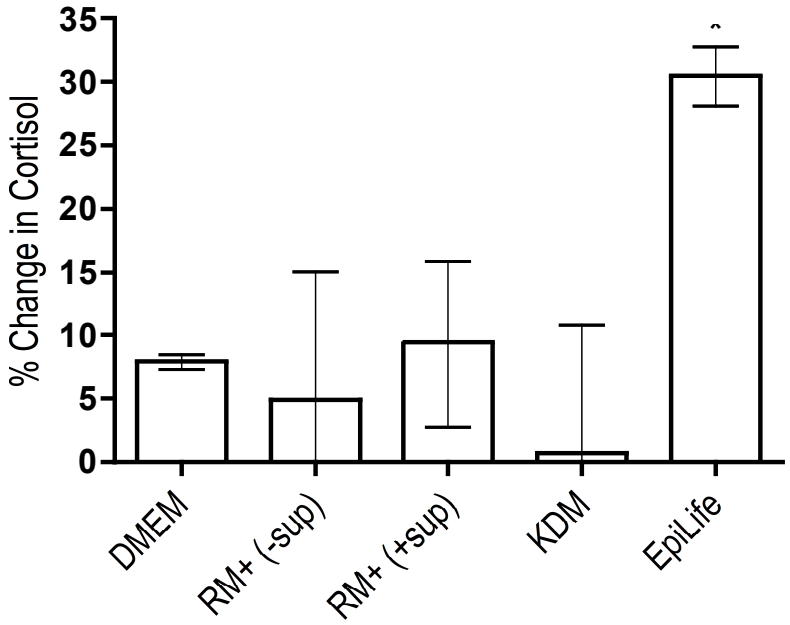


**Figure 4.13 Optimisation of culture media for cortisol analysis by ELISA.**
Primary human keratinocytes ($2x10^5$ cell/ml in 12-well plates) were cultured for 24 h in different culture. Cortisol levels from the culture media were then analysed by ELISA. The percentage increase in cortisol detection relative to cell-free controls for each condition was calculated. The results represents two separate experiments of primary keratinocytes isolated from a single biopsy, each measured in duplicate (mean ±S.D.).

## 4.3 Discussion

In the experiments described in this chapter, the ability of primary human keratinocytes to synthesise steroids *de novo* from cholesterol and produce cortisol was investigated. This pathway has not previously been reported in keratinocytes.

RIA demonstrated that primary keratinocytes were capable of producing pregnenolone, the first committing step of steroid synthesis. Previous research had detected CYP11A1, FDX and FDXR in whole skin by RT-PCR and western blotting, complementing the findings in this chapter (Slominski et al., 2004). The pregnenolone RIA results in this chapter suggest that there is a functionally active P450 side chain cleavage system in primary keratinocytes. Although pregnenolone synthesis has not been previously reported in whole cell primary keratinocytes, steroid synthesis has been detected by RIA in SEB-1 sebocytes (Thiboutot et al., 2003). Enzymes required for steroid synthesis were also identified in the hair follicle and cortisol was detected in spent medium of cultured hair follicles and dermal fibroblasts (Ito et al., 2005; Slominski et al., 2006). In addition metabolism of 7-dehydrocholesterol to 7-dehydropregnenolone via CYP11A1 has been detected in mitochondria isolated from skin cells (Slominski et al., 2009).

Although radiometric assay demonstrated that T and K were effective 3βHSD and CYP17 inhibitors, LC-MS data suggested that there was not a complete inhibition of pregnenolone metabolism by T and K. LC-MS demonstrated that the inhibitors were as little as 7% effective. This difference could be due to the amount of substrate used for the two assays, where only 90 pmol pregnenolone was used for radiometric assay whereas 1 μM (3 mmol) pregnenolone was used for LC-MS.

The RIA data generated some interesting findings since it showed that the addition of 25-OH cholesterol did not promote pregnenolone synthesis. In classic endocrine systems, this compound increases pregnenolone synthesis at least three fold (Dyson et al., 2008). This is because 25-OH cholesterol is more soluble than cholesterol and can bypass StAR transport, circumventing the rate determining step of steroidogenesis and

providing an abundant source of substrate to P45011A1. However, in keratinocytes no significant increase in steroidogenesis was detected when cells were treated with 25-OH cholesterol in the presence of T and K compared to keratinocytes only treated with T and K. This suggests that there could be an alternative rate determining step of steroid synthesis in primary human keratinocytes, such as cofactor availability and rodox potential.

The only compound that was able to independently promote pregnenolone synthesis above the level attained with T and K was dex. This was a serendipitous finding since dex was originally used to see whether there was a negative feedback mechanism present in keratinocytes similar to the HPA axis, where cortisol can suppress CRH activity to inhibit further steroid synthesis (Miller and O'Callaghan, 2002). However, there is evidence in the literature suggesting that GC can promote steroid synthesis. For example, Wistar rat Leydig cells treated with metyrapone to induce corticosterone deficiency showed impaired testosterone production which could be rescued with the addition of corticosterone (Parthasarathy and Balasubramanian, 2008). In addition, production of progesterone by immortalised human granulosa cells was at least four fold higher in dex treated cells (Sasson et al., 2001). This study showed that forskolin upregulated StAR and FDXR expression in immortalised human granulosa cells. Forskolin plus dex caused a significantly greater induction of steroid synthesis without further upregulation of StAR or FDXR. The authors did not discuss a mechanism by which dex enhanced steroid synthesis without further upregulation of key steroidogenic regulating proteins (Sasson et al., 2001). This is indicative of potential alternative mechanism for dex induced steroid synthesis by immortalised granulosa cells.

Radiometric analysis demonstrated that primary human keratinocytes could metabolise pregnenolone, forming compounds that migrated with a pattern matching 17OH progesterone, 17OH pregnenolone and progesterone. The enzyme responsible for converting pregnenolone into progesterone is 3βHSD (Berliner et al., 1962). Although this study is the first to report oxidation of pregnenolone to progesterone in primary cultures of human keratinocytes, 3βHSD enzyme activity has previously been reported in cultured keratinocytes demonstrated by the metabolism of DHEA to androstenedione (Milewich et al., 1988). The study by Milewich also treated primary human

keratinocytes with [$^3$H] pregnenolone but did not observe any metabolic activity. This could be due to the high concentration of [$^3$H] pregnenolone chosen or to limited sensitivity of the equipment used to measure the metabolites. Reverse (but not forward) 3βHSD activity, converting progesterone to pregnenolone was also identified in HaCaT immortalised keratinocytes (Slominski et al., 2002). Therefore this unusual reverse 3βHSD activity that was observed in HaCaT cells has also been detected in cultured primary keratinocytes as described in this chapter.

The presence of 17-hydroxy derivatives of pregnenolone and progesterone and functional inhibition of 17-hydroxy derivative synthesis by ketoconazole suggests that CYP17 is active in primary keratinocytes. One previous study has shown that CYP17 protein is present in skin, including the epidermis, and was found to be functionally active in SEB-1 sebocyte cells (Thiboutot et al., 2003). CYP17 can also convert 17-hydroxypregnenolone and 17-hydroxyprogesterone to DHEA and androstenedione respectively. Although DHEA and androstenedione metabolism has been described by Milewich, synthesis of androgens from 17OH progesterone or 17OH pregnenolone was not demonstrated by the results presented here or in previous reported studies of skin steroidogenesis (Milewich et al., 1988).

Further analysis of steroid metabolism showed that primary human keratinocytes converted pregnenolone to cortisol, including all obligate steroid intermediates. This is in contrast to the study of steroid metabolism in primary keratinocytes by Milewich that was unable to detect pregnenolone or progesterone metabolism (Milewich et al., 1988). More recently, the conversion of progesterone to deoxycorticosterone and a number of additional deoxycorticosterone metabolites was demonstrated in HaCaT keratinocyte immortalised cells, perhaps because this immortalised cell line has lost some endogenous steroidogenic pathways (Slominski et al., 2002). However, cortisol synthesis from progesterone was not detected in the HaCaT system (Slominski et al., 2002). Milewich et al, performed similar TLC analysis of pregnenolone and progesterone metabolism in keratinocytes with [$^3$H] steroids. However, neither pregnenolone nor progesterone metabolism by primary human keratinocytes was identified in their study (Milewich et al., 1988). This might be due to the concentration

of the [$^3$H] steroids affecting the relative sensitivity of the enzyme activity and the assay.

LC-MS analysis of progesterone metabolism confirmed the production of cortisol by primary human keratinocytes. In the absence of cells (i.e. in blank wells supplemented with 1 μM progesterone), the concentration of progesterone recovered after 24 h was 192.5 ± 23.0 nM, indicating an extraction efficiency of 19.2%. In contrast, in the presence of cells, the concentration of progesterone detected after 24 h fell to 102.7 ± 7.8 nM, and 104.0 ± 33.6 nM cortisol appeared in the culture medium. This suggests that approximately 50% of the available progesterone was metabolised to cortisol. In addition, pregnenolone was also detected in the culture medium at a concentration of 19.6 ± 4.4 nM. The presence of pregnenolone could either reflect *de novo* synthesis via StAR/MLN64 & CYP11A1, or the reduction of progesterone to pregnenolone via 3βHSD, which has previously been observed in immortalised HaCaT keratinocytes (Slominski et al., 2002). The 3βHSD enzyme requires $NAD^+$ as a cofactor for pregnenolone to be converted to progesterone, whilst NADH is required for the reverse reaction.

Further radiometric analysis also demonstrated that primary human keratinocyte can metabolise cortisol to cortisone. Inter-conversion of cortisol to cortisone is carried out by 11βHSD and is a common mechanism in mineralocorticoid sensitive tissues to prevent illicit occupation of mineralocorticoid receptors by cortisol (Monder, 1991; Tomlinson and Stewart, 2001; Tomlinson et al., 2004). 11βHSD1 activity has been observed in whole skin, epidermis, sweat gland ducts and dermal fibroblasts (Hammami and Siiteri, 1991; Hsia and Hao, 1966; Kenouch et al., 1994; Malkinson et al., 1959). However, 11βHSD1 activity is reported to be low in the epidermis in comparison with sweat gland ducts (Kenouch et al., 1994). The results presented in the radiometric assay demonstrate that keratinocytes possess the ability to inactivate cortisol. Potentially this would enable them to achieve a balance between the anti-inflammatory and pro-differentiation properties of cortisol and the necessity for cell proliferation. The high proportion (approximately 70%) of cortisol that was metabolised to cortisone potentially indicates that $NADP^+$ was abundantly available for 11βHSD1. Similar to 3βHSD, 11βHSD1 require $NADP^+$/NADPH as cofactors. When $NADP^+$ is abundant,

conversion of cortisol to cortisone is favoured. Alternatively, the cortisol metabolism could be due to 11βHSD2 activity that has been shown to be induced in primary keratinocytes treated with dex (Stojadinovic et al., 2007). Further experiments are required to determine 11βHSD1 and 11βHSD2 activity respectively.

Keratinocyte culture medium influenced the ability of cells to synthesise cortisol. The differences in the culture media and their effect on keratinocyte cortisol synthesis remain to be defined. This is mainly because the composition of commercially available keratinocyte culture media is not publicly available. However, the level of cortisol detected by ELISA from cells ($2x10^5$ cell/ml in 12-well plates) without any exogenous stimulation was 1.0 ± 0.2 nM when cultured in EpiLife medium over 24 h. This confirms that primary human keratinocytes can synthesise cortisol. Although this concentration of cortisol is a fraction of systemic levels, which range between 200 – 500 nM for total cortisol and 1-10 nM for free cortisol, it is of physiological relevance since between 1 – 10 nM cortisol is sufficient to activate glucocorticoid receptors (Charmandari et al., 2008; Dong et al., 2006). In addition, the actual levels of cortisol synthesised by primary keratinocytes maybe as high as 5 nM when taking into account the 70% oxidation of cortisol to cortisone as observed by radiometric assay. Cortisol production by keratinocytes is unlikely to make a significant impact on systemic cortisol levels since cortisol is negligible in serum from adrenalectomised mice (del Mar Grasa et al., 2007). However, it is likely to be important for cutaneous biology as the glucocorticoid receptor has been shown to be critical to maintain barrier competency and promotes normal keratinocyte differentiation (Bayo et al., 2008). In addition, the epidermis is avascular so may require a localised cortisol supply to maintain the skin barrier.

The combined analysis of RIA, radiometric assay and LC-MS suggest that the redox potential of cultured primary keratinocytes favours $NADP^+$ and NADH availability rather than NADPH and $NAD^+$. This is for a number of reasons; firstly RIA data did not increase with 25-OH cholesterol, suggesting an alternative rate determining step of steroid synthesis other than StAR-mediated cholesterol transport across mitochondrial membranes. An alternative rate determining step could involve the availability of the NADPH co-substrate required for the synthesis of pregnenolone from cholesterol.

Secondly, radiometric data of [$^{3}$H]cortisol metabolism showed that approximately 70% of cortisol was metabolised to cortisone. The cortisol to cortisone shuttle is a reversible reaction mediated by 11βHSD1. The direction of the reaction is regulated by the availability of the NADPH co-substrate, so when NADPH is abundant, the enzyme favours cortisone to cortisol conversion and when $NADP^{+}$ is abundant, cortisol metabolism to cortisone is favoured. Thus HSB11B1 activity could act as a sensor for NADPH redox potential of the endoplasmic reticulum (ER). Thirdly, putative progesterone metabolism to pregnenolone was identified by radiometric assay and LC-MS in primary human keratinocytes. Although 3βHSD is not generally regarded as a bi-directional enzyme, this reverse activity, generating pregnenolone from progesterone, has been described in HaCaT keratinocytes (Slominski et al., 2002). Since $NAD^{+}$ is required for the reaction to proceed in the direction of pregnenolone to progesterone synthesis, NADH would need to be abundant to the enzyme in order for the reverse reaction to occur. Finally, dex was able to promote pregnenolone synthesis. Dex has been shown to increase luminal NADPH availability (Piccirella et al., 2006). In addition, in reconstituted systems, cortisol has been shown to increase NADPH redox potential, whereas cortisone promotes $NADP^{+}$ redox potential (Piccirella et al., 2006).

Previous expression analysis of regulators of steroid synthesis in normal versus diseased epidermis demonstrated a disruption to the expression pattern of steroidogenic regulators, indicating dysregulated steroidogenesis in these hyperproliferative disorders (Chapter 3). Thus it is likely that disorders such as psoriasis and atopic dermatitis that are treated with cortisol analogues, have a disrupted local steroidogenesis pathway. Unfortunately it has not been possible to obtain keratinocytes isolated from psoriatic or atopic dermatitis skin to assess this hypothesis.

In summary, this chapter has demonstrated that primary human keratinocytes are capable of synthesising and metabolising pregnenolone, progesterone and cortisol. The levels of cortisol synthesised by primary keratinocytes without exogenous stimulation would be sufficient to activate glucocorticoid receptors. There is also evidence to suggest that the rate determining step of steroid synthesis in cultured keratinocytes could be regulated by cofactor availability rather than cholesterol transport.

# Chapter 5. Investigating the function of dexamethasone in primary human keratinocytes

## 5.1 Introduction

Despite the widespread use of GC for skin conditions such as psoriasis and atopic dermatitis, there is surprisingly limited analysis of the molecular function of cortisol in skin. The most common side-effect of prolonged GC treatment is skin atrophy (Stojadinovic et al., 2007). This effect of cortisol is also evident in patients with Cushing's syndrome who present with wafer-thin skin. Cushing's syndrome patients and patients who require chronic GC therapy also have increased incidence of bone fractures (Horsch et al., 2007). Moreover, some studies have found a correlation with bone density and skin thickness and the risk of osteoporosis (Cagle et al., 2007).

High doses of GC have been shown to inhibit osteoblast (MBA-15.4 mouse bone marrow stromal cells and MG-63) cell proliferation, and therefore decrease bone density, through activation of DUSP1. This leads to inhibition of the mitogen activated protein kinase ERK1/2 (Horsch et al., 2007). DUSP1 is a dual phosphatase that dephosphorylates and deactivates ERK1/2 activity at p42/44. Dex has been shown to promote DUSP1 transcription in primary human keratinocytes but the mechanism of GC mediated-skin atrophy has yet to be elucidated (Stojadinovic et al., 2007).

In contrast to inducing skin atrophy, cortisol has also been shown to protect specific types of cells from apoptosis, which has partly been attributed to the effect of cortisol on cellular redox potential in neurones (Du et al., 2009). Recently, dex was also shown to protect primary human keratinocytes from apoptosis by promoting anti-apoptotic and suppressing pro-apoptotic gene transcription (Stojadinovic et al., 2007). The anti-apoptotic nature of cortisol in skin was also demonstrated in GR knock out mice. Mice with $GR^{-/-}$ knockout had increased keratinocyte apoptosis throughout the layers of the epidermis together with hyperproliferation, decreased keratinocyte differentiation and barrier formation (Bayo et al., 2008). Therefore, as in neuronal cells, cortisol could also influence cellular redox potential in keratinocytes as part of a protective mechanism to prevent apoptosis.

Cortisol has been shown to promote cellular redox potential by increasing G6PDH and H6PDH activity to increase the availability of NADPH in rat hepatocytes and adipose cells (Piccirella et al., 2006). In addition, cortisol was able to increase NADPH even in the oxidative environment of the ER, making NADPH available to enzymes such as 11βHSD1 (Piccirella et al., 2006). All enzymes involved in steroidogenesis are dependent upon cofactors to deliver or receive electrons for the catalysis of steroids (Agarwal and Auchus, 2005; Sherbet et al., 2007). Depending on the steroid enzyme, these cofactors are NADPH or $NAD^+$ and their abundance determines the oxidative or reductive capacity of the cell (i.e. the redox potential) (Agarwal and Auchus, 2005; Sherbet et al., 2007). NADPH are $NAD^+$ are more abundant than steroid precursors by several orders of magnitude and are required for many metabolic processes (Agarwal and Auchus, 2005; Sherbet et al., 2007). Therefore the redox potential of the cell is regarded as a critical driver of steroid synthesis and subtle changes in cofactor availability can dramatically alter the steroidogenic potential of a cell (Agarwal and Auchus, 2005; Sherbet et al., 2007). This suggests that cortisol could enhance steroid synthesis by influencing cellular redox potential. Indeed, cortisol has been shown to promote steroidogenesis in Leydig and granulosa cells, which in granulosa cells, was independent of StAR, or steroid enzyme expression (Parthasarathy and Balasubramanian, 2008; Sasson et al., 2001).

The aim of this chapter was to investigate mechanisms of GC induced skin thinning by examining DUSP1 and pERK1/2 expression in keratinocytes after incubation with dex. Cell proliferation was measured by MTT assay. Cellular redox potential was measured by MTT and $NADP^+$/NADPH cycling assay. Cell viability was assessed using a trypan blue cell counting assay. Annexin V and PI labelling flow cytometry was used to investigate the influence of dex on cell cycle, apoptosis and cell death in primary human keratinocytes.

## 5.2 Results

### 5.2.1 Effect of dex on DUSP1 expression and ERK1/2

Dex (1 μM) induced DUSP1 expression over time in primary human keratinocytes (Figure 5.1). The protein expression increased from 3 h, peaking at 5 h then returned to basal levels at 7 h. This suggests that dex was able to activate DUSP1 expression which could have the ability to suppress MAPK activity.

Dex was able to rapidly decrease phospho-ERK1/2 (pERK1/2) after 30 min whilst total ERK1/2 expression remained constant (Figure 5.2). However, pERK1/2 increased after 30 min suggesting that induction of DUSP1 expression between 1 and 5 h was not responsible for the rapid alteration in pERK1/2 activity. In addition, phosphorylation of MEK, the upstream regulator of pERK1/2 remained unchanged by dex treatment (Figure 5.2).

DUSP1 is also able to influence other members of the MAPK pathway that regulate cell proliferation. Therefore a simple MTT assay was employed to assess keratinocyte cell proliferation in the presence of MAPK inhibitors (MEKi, JNKi, p38i) to determine if one MAPK pathway was predominant in regulating cell proliferation of primary human keratinocytes (Figure 5.3). All three MAPK inhibitors significantly reduced the MTT readout from primary human keratinocytes suggesting either all three MAPK are required for keratinocyte proliferation, although the inhibitors are not entirely specific or demonstrate cross-talk between the pathways. The most effective inhibitor was pJNKi, however it is worth noting that the cells appeared highly necrotic upon visual inspection implying some toxicity of the inhibitor. Rather unexpectedly, dex significantly increased the MTT readout.

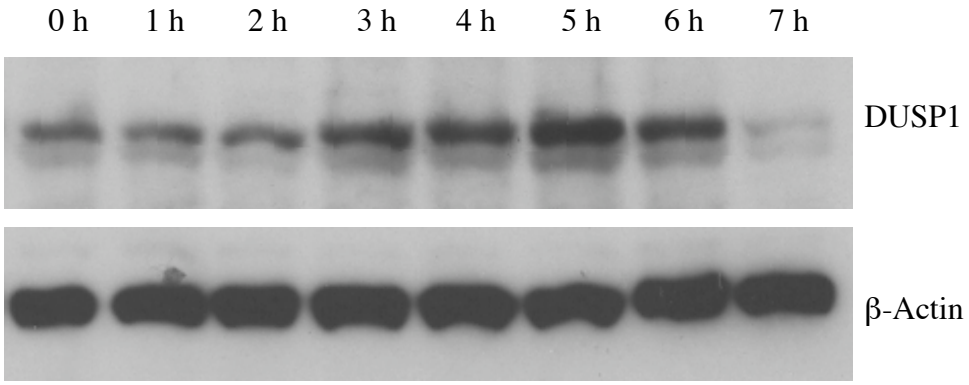


**Figure 5.1 Western blot analysis of DUSP1 expression (0 – 7 h) in primary keratinocytes incubated with 1 μM dex.**

Upper blot: DUSP1 protein detection, lower blot: β-actin loading control. Images are representative of three separate experiments.

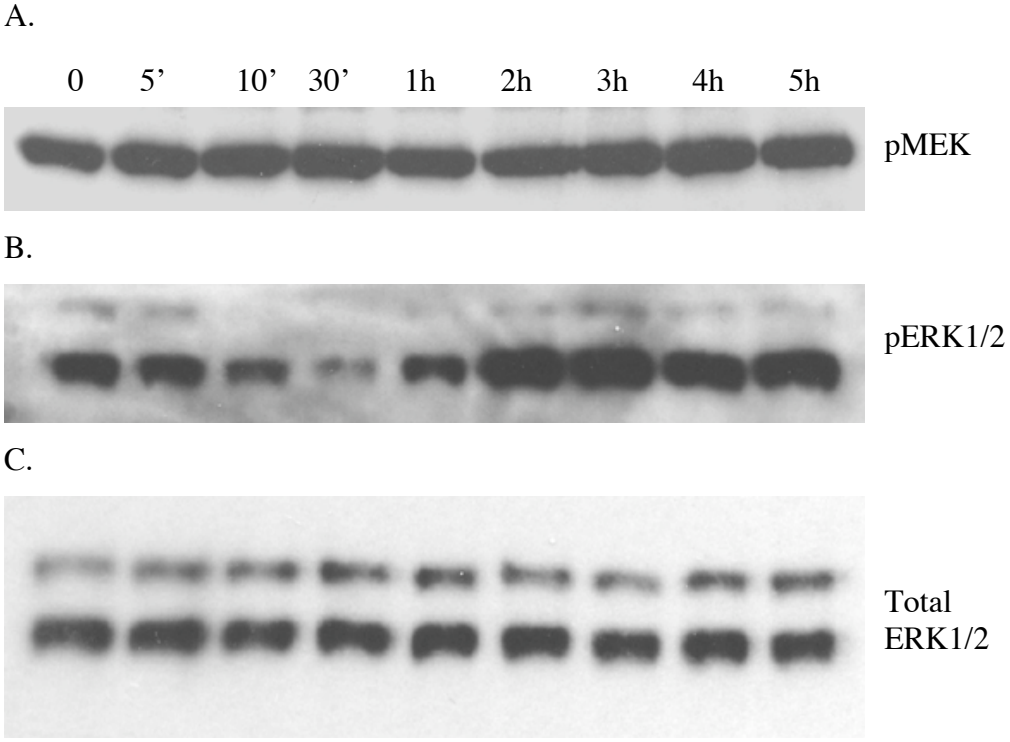


**Figure 5.2 Western blot analysis of pMEK, pERK1/2 and total ERK1/2 expression over time in primary keratinocytes treated with 1 μM dex.**

(A) pMEK, (B) pERK1/2, (C) total ERK1/2 expression. Images are representative of three separate experiments.

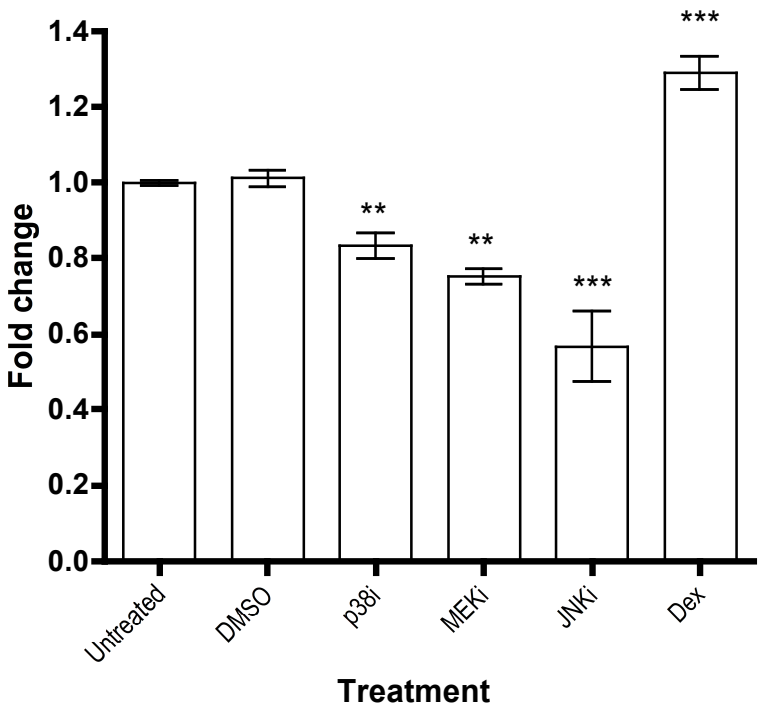


**Figure 5.3 MTT assay of primary human keratinocytes treated for 72 h with MAPK inhibitors or dex.**

Keratinocytes were incubated with 1 μM dex or MAPK inhibitors; p38i (SB203580 1 μM), JNKi (SP600125 10 μM), MEKi (U0126 10μM). The data represent the mean+/- S.E.M of three separate experiments. Statistical differences were obtained using one-way ANOVA followed by Tukey's multiple comparisons test where appropriate, * $P<0.05$, ** $P<0.01$, *** $P<0.001$.

### 5.2.2 Effect of dex on MTT reductive capacity of primary keratinocytes

The MTT assay is primarily used as an indicator of cell proliferation but the assay actually measures the reductive capacity of cells (for more information see Methods 2.11) (Bernas and Dobrucki, 2002). There are a number of factors that could influence an increase in MTT assay readout including increased cell proliferation, increased cellular redox capacity or decreased cell death.

Dex was able to induce a small but significant (approximately 1.3-fold) increase in MTT readout of primary human keratinocytes cultured in RM+ keratinocyte medium without serum (or cortisol) for 72 h. The effect of dex appeared to be dose-dependent, with maximal response occurring between 0.01 – 1 μM (Figure 5.4). The MTT readout between these doses was significantly higher than untreated or vehicle controls. In addition, there was a trend for reduced MTT readout (though not significantly) at the highest concentration of dex (100 μM). The keratinocyte response to dex decreased towards untreated levels at 0.001 μM. Since dex was used at 1 μM for pregnenolone RIA and provided maximal MTT response in the primary keratinocytes, 1 μM dex was chosen for all subsequent experiments.

Increased MTT signal following incubation with dex was unexpected since the MTT assay is primarily used to measure cell proliferation and dex is regarded as an inhibitor of keratinocyte proliferation (Stojadinovic et al., 2007). Visual inspection of cell morphology of dex treated keratinocytes showed that proliferating cells appeared to form smaller and in tighter colonies compared to untreated or vehicle control keratinocytes (Figure 5.7). There was not a noticeable visual difference in differentiating keratinocytes that are reported as having a larger, flatter morphology. However, more aggregates of apoptotic/necrotic cells were observed in untreated and vehicle control cells. Thus dex could influence MTT readout by maintaining cell viability, even in serum-free conditions.

The effect of serum on cultured primary human keratinocytes with and without dex was also investigated by MTT assay (Figure 5.5). Low serum culture conditions are reported to inhibit cell cycle (Cooper, 2003). Therefore as expected there was a

sequential increase in MTT readout with increasing serum conditions, 0 % (v/v), ≤ 1% (v/v) and < 10% (v/v). Dex also significantly increased MTT readout detected from the keratinocytes at each of the different serum concentrations. Since serum also contains cortisol, all experiments were consequently performed in serum-free medium.

The effect of dex on keratinocyte MTT assay was inhibited by the GR inhibitor RU486 (Figure 5.6). Cells incubated with RU486 for 72 h had an MTT readout similar to untreated keratinocytes. Moreover, the inhibitor completely blocked the effect of dex since the combined treatments also matched basal levels. Therefore dex is likely to be exerting its effects on keratinocytes via the GR in this instance.

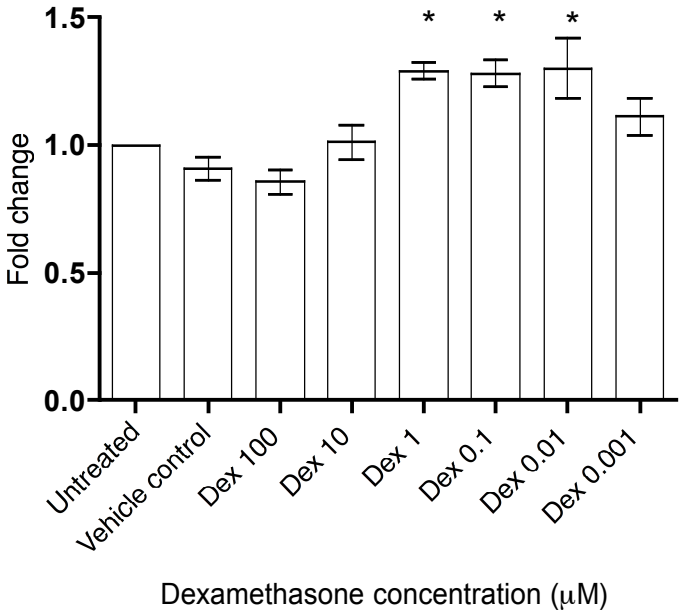


**Figure 5.4 MTT assay concentration-response of primary keratinocytes incubated with dex.**

Primary human keratinocytes were incubated with dex ($1x10^{-9}$ M – $1x10^{-4}$ M) in serum-free and cortisol-free keratinocyte culture medium for 72 h. Statistical differences were obtained using one-way ANOVA followed by Tukey's multiple comparisons test where appropriate, * $P<0.05$.

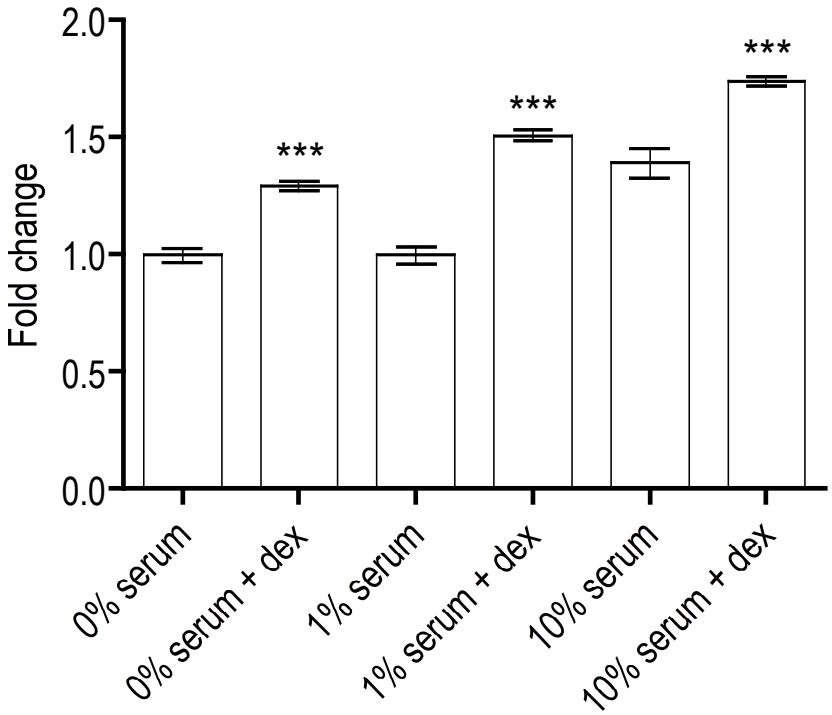


**Figure 5.5 MTT assay of primary keratinocytes cultured in different concentrations of serum with or without dex.**

Primary human keratinocytes were incubated for 72 h in serum-free medium (SFM), 1% serum or 10% serum in the absence or presence of 1μM dex. The data represent the mean +/- S.E.M of three separate experiments. Statistical differences were obtained using one-way ANOVA followed by Tukey's multiple comparisons test where appropriate, *** $P<0.001$.

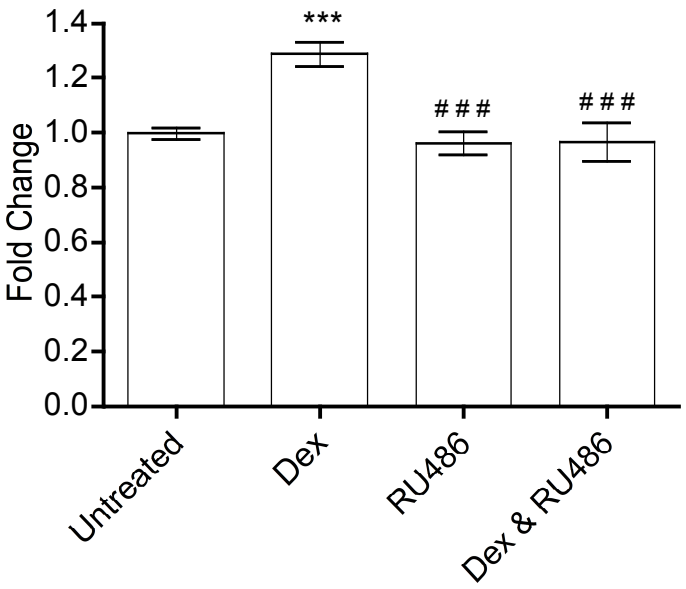


**Figure 5.6 MTT assay of primary human keratinocytes incubated with dex and/or RU486 for 72 h.**

Keratinocytes were incubated with 1 μM dex and/or 1 μM RU486. The data represent the mean +/- S.E.M of three separate experiments. Statistical differences were obtained using one-way ANOVA followed by Tukey's multiple comparisons test where appropriate, *** P<0.001 versus untreated; # # # P<0.001 versus dex.

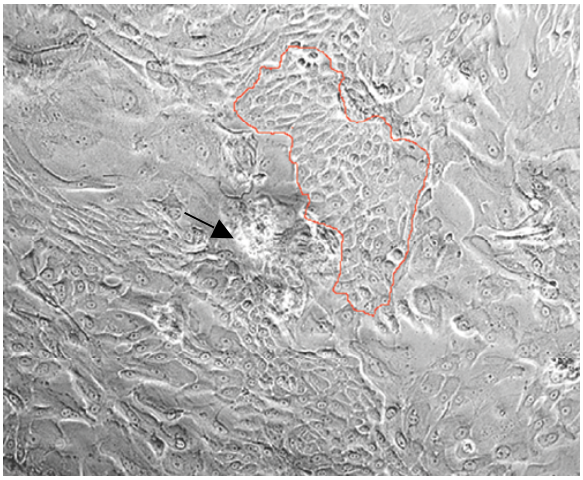

A. Untreated

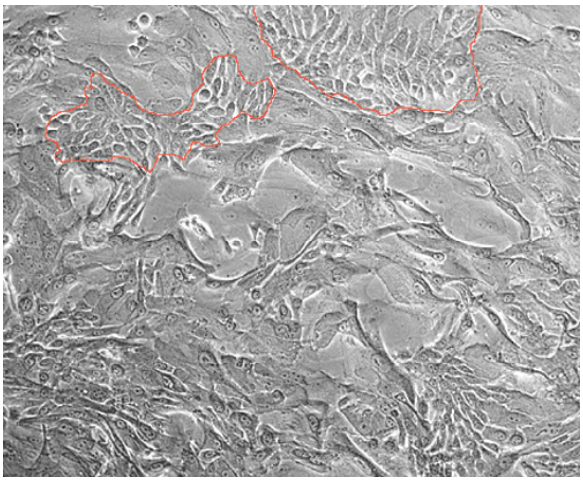

B. Vehicle control

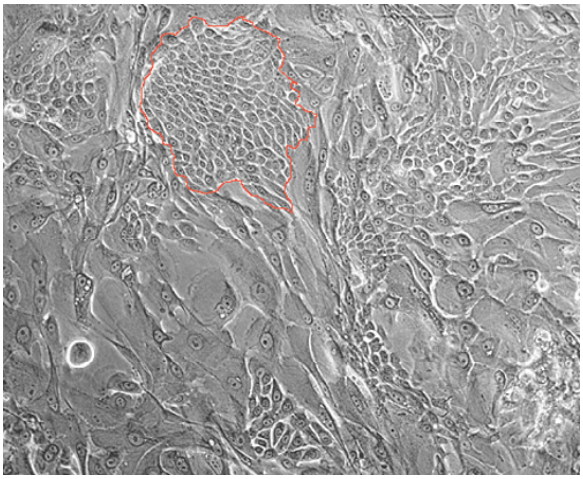

C. Dex

**Figure 5.7 Morphological effects of dex on primary human keratinocytes.**

(A) Untreated, (B) vehicle control, (C) dex 1 μM incubated for 72 h in RM+ culture medium without serum. Proliferating cells (example colonies are highlighted with a red outline) formed tighter colonies when treated with dex. Arrow depicts apoptotic/necrotic cell cluster. Images are representative of at least three separate experiments.

### 5.2.3 Effect of dex on keratinocyte cell viability

Primary human keratinocytes were also analysed for cell viability since this could also explain the changes in MTT readout. A trypan blue cell counting assay was used to determine the number of viable keratinocytes (Figure 5.8). Cell number was significantly increased (over two-fold) in keratinocytes incubated with dex compared to untreated or vehicle control samples. There was no significant difference between the number of viable cells in untreated and vehicle control samples, suggesting that the solvent (methanol) that dex was dissolved in did not influence keratinocyte viability. However, the data does not indicate whether increased cell viability was due to an up regulation of cell proliferation or inhibition of cell death.

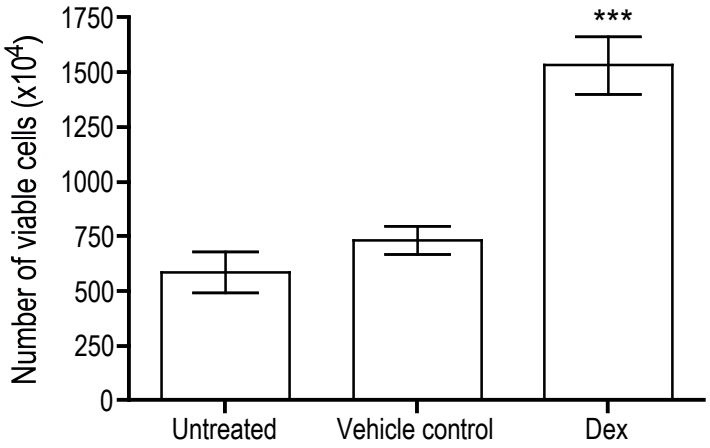


**Figure 5.8 Trypan blue cell viability assay of primary human keratinocytes incubated with dex for 72 h.**

Keratinocytes were incubated with 1 μM dex. The data represent the total number of viable cells in a T75 flask counted using a haemocytometer, mean +/- S.E.M of three separate experiments. Statistical differences were obtained using one-way ANOVA followed by Tukey's multiple comparisons test where appropriate, *** $P<0.001$.

### 5.2.4 Effect of dex on live, early apoptotic and dead keratinocytes

To determine whether increased cell viability and MTT readout were due to changes in keratinocyte proliferation or cell death, cells were assessed using annexin V and PI FACS analysis. Figure 5.9 is an example of the controls and gates used to determine the subdivision of live, early apoptotic, dead cells and cell debris that had been detected by annexin V and PI labelling. U.V. light was used as a positive control for cell death. The controls showed a clear difference in the distribution of subpopulations, however there was some autofluoresence detected during analysis, thus the division between subpopulations was not as discrete as expected.

Figure 5.10 displays the results of live cells determined from annexin V and PI FACS analysis. There was no significant difference between any of the treatments except U.V. exposure, which induced a 50% decrease in cell viability. Neither dex nor RU486 affected the number of viable cells using this technique of analysis. In addition there was no significant difference in early apoptosis between any of the treatments except for U.V. exposure, where annexin V positive cells increased more than 2 fold (Figure 5.10). Moreover, there was no significant difference between dead (PI positive and annexin V positive) cells for any of the treatments, although there was a trend for an increased cell death in U.V. exposed cells (Figure 5.11). Finally there was no significant difference in the amount of cell debris or total number of dead cells (cell debris and dead cells combined) between in any of the treatments. Therefore, in contrast to the trypan blue cell viability assay, annexin V FACS analysis did not detect a difference in live, early apoptotic, dead cells or cell debris in primary keratinocytes treated with dex and/or RU486.

An alternative to increased cell viability or decreased cell death that could account for the higher trypan blue reading would be a change in cell cycle. Annexin V/PI FACS analysis only accounts for a proportion of the cells within a given sample. However, changes in cell cycle can lead to an increase in cell number without necessarily altering the proportion of proliferating cells versus apoptotic or dead cells. To account for this, cell cycle was analysed using PI labelling (Figure 5.12). However, no difference in cell cycle was detected with the different treatments, except for U.V. exposed keratinocytes

that arrested in $G_2M$ phase of the cell cycle (Figure 5.13). One limitation of PI cell cycle analysis is that it does not account for cell stasis, where the cell stops cycling but is still metabolically active with an unchanged cell cycle profile. Further analysis using bromodeoxyuridine (BrdU) labelling would be required to measure cell stasis.

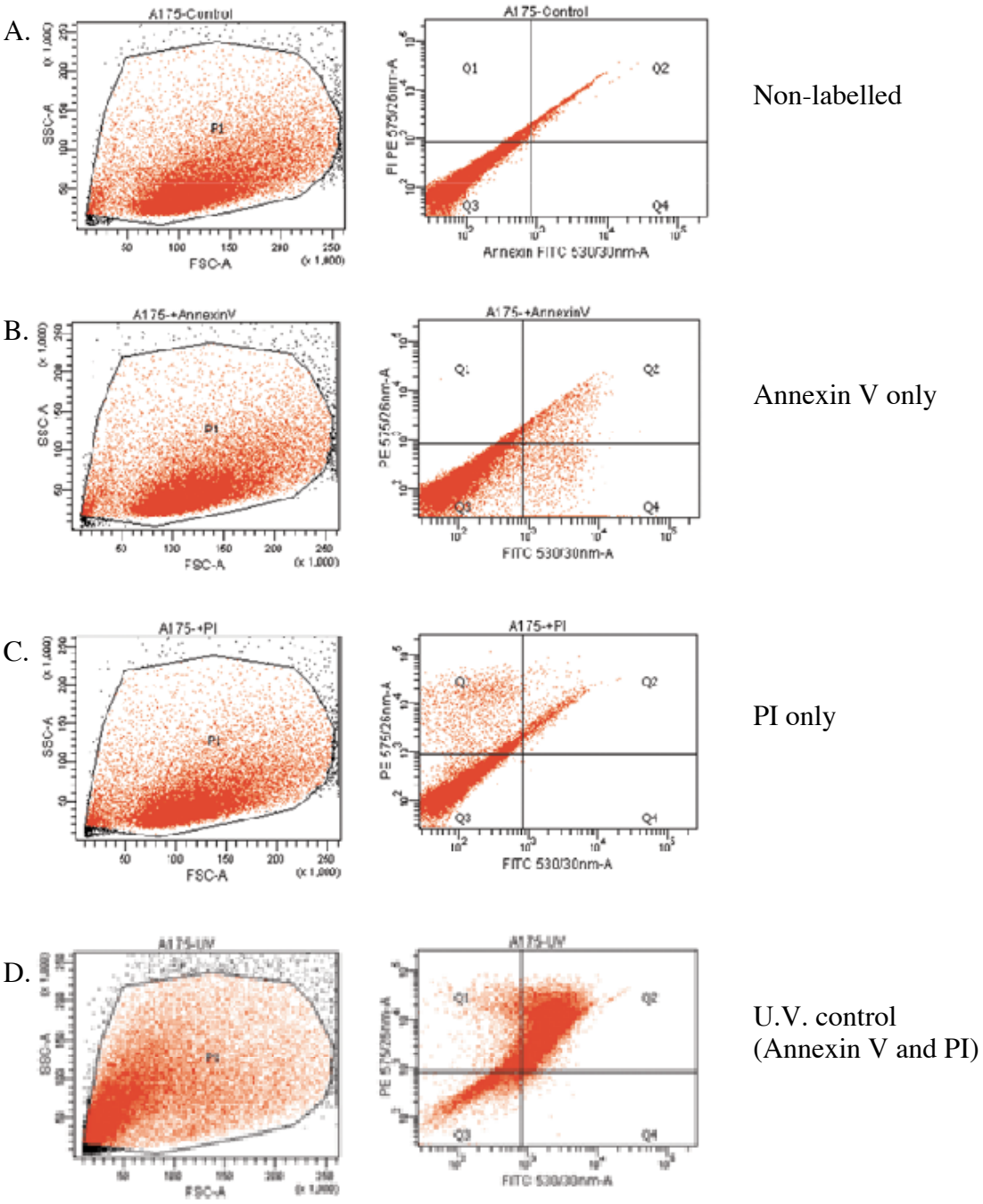


**Figure 5.9 Example of gated plots used for analysing cell viability, apoptosis and death.**

(A) Total non-labelled cell population, (B) Annexin V labelled cells display apoptotic cells in Q4, (C) PI labelled cells display cell debris in Q1 and dead cells in Q2, (D) U.V. treated cells were used as a positive control for cell death. Left-hand plots depict total cell population, right-hand plots display gates used for subdividing cells from live, apoptotic, dead and cell debris.

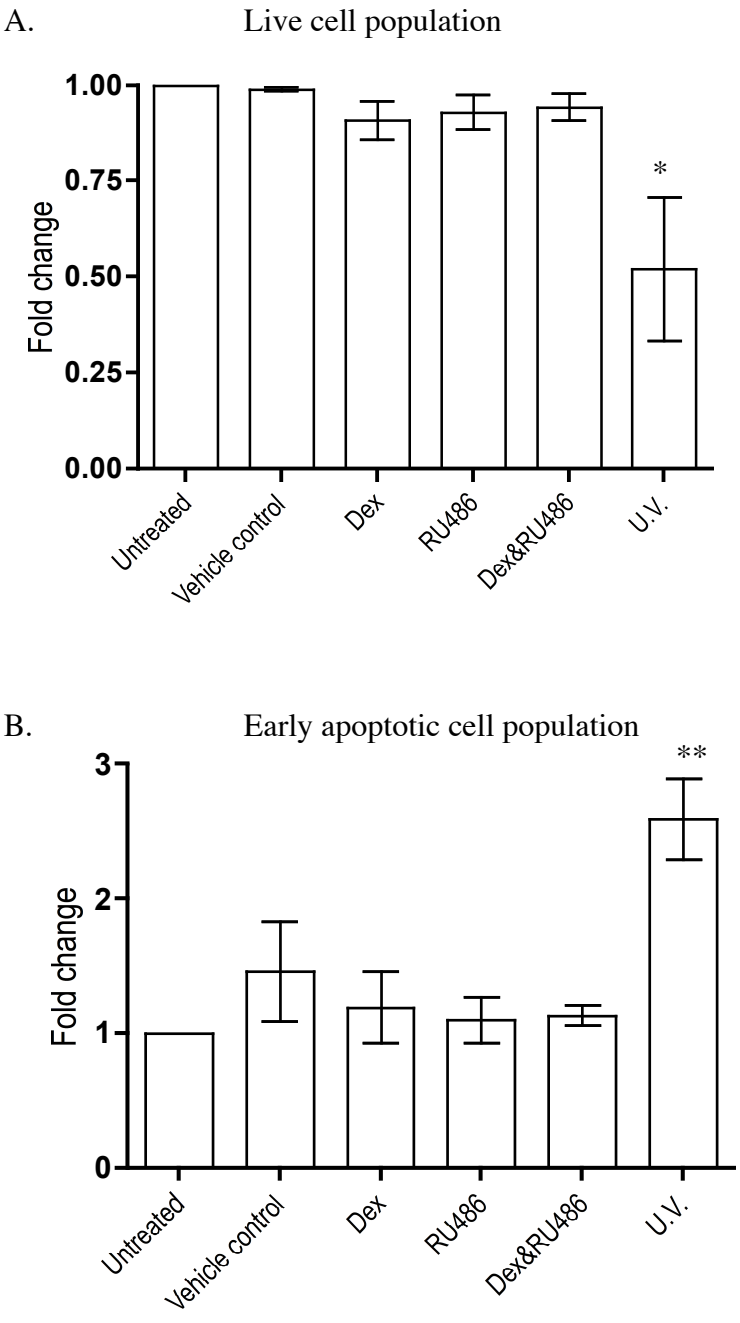


**Figure 5.10 Flow cytometry analysis of cell viability and apoptosis following treatment with dex and/or RU486.**

FACS analysis results of (A) PI and annexin V negative (live) cells, (B) annexin V positive (early apoptotic) cells. Dex 1 μM, RU486 1 μM, U.V. 20 mJ U.V.B. at 0.2 $mV/cm^2$. Data represents the mean ± SEM, n=3. Statistical differences were obtained using one-way ANOVA followed by Tukey's multiple comparisons test where appropriate, * P<0.05, ** P<0.01, ***P<0.001.

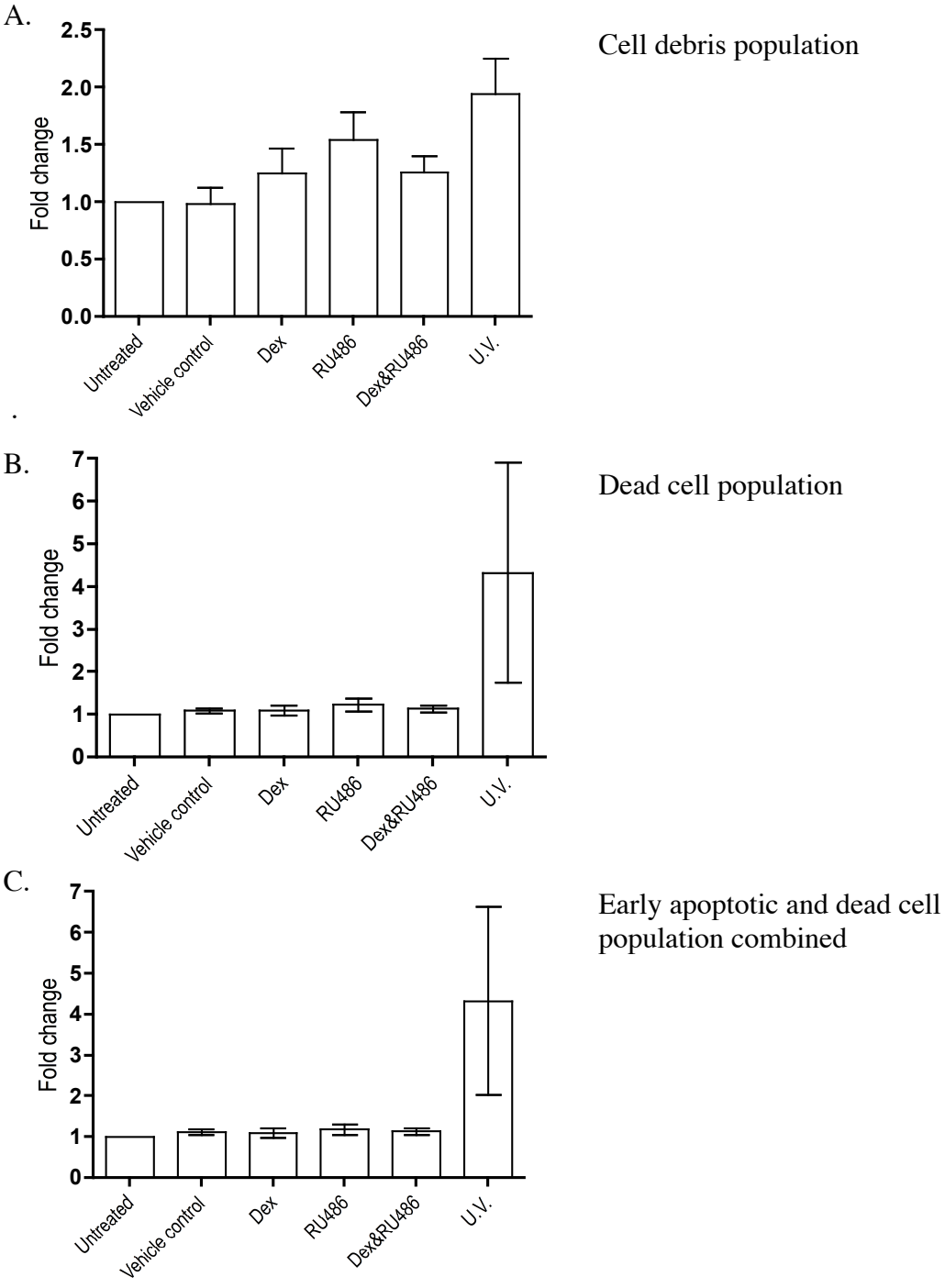


**Figure 5.11 Flow cytometry analysis of cell debris and dead cells following treatment with dex and/or RU486.**

FACS analysis results of (A) PI positive cell debris, (B) PI positive and annexin V positive (dead cells), (C) combined population of PI positive only (cell debris) and PI positive and annexin V positive (dead cells). Dex 1 μM, RU486 1μM, 20 mJ U.V.B. at 0.2 mV/cm$^2$. Data represents the mean ± SEM, n=3. Statistical differences were obtained using one-way ANOVA followed by Tukey's multiple comparisons test where appropriate.

| Treatment | Live cells | Early apoptotic cells | Dead cells | Cell debris | Early apoptotic & dead cells |
|---|---|---|---|---|---|
| Untreated | 76.3 +/- 4.6 | 9.7 +/- 8.7 | 12.2 +/- 5.3 | 2.9 +/-1.0 | 21.9 +/-14.0 |
| Vehicle control | 76.3 +/- 3.5 | 3.3 +/- 1.8 | 11.4 +/- 3.6 | 1.4 +/- 0.8 | 14.7 +/- 5.4 |
| Dex | 70.8 +/- 7.2 | 3.6 +/- 2.7 | 12.8 +/- 6.0 | 1.6 +/- 0.9 | 16.4 +/- 8.7 |
| RU486 | 72.1 +/- 6.9 | 3.2 +/- 2.2 | 14.4 +/- 7.0 | 2.2 +/- 1.3 | 17.6 +/- 9.2 |
| Dex and RU486 | 73.0 +/- 6.0 | 3.5 +/- 2.5 | 12.8 +/- 5.4 | 2.1 +/- 1.5 | 16.3 +/- 7.9 |
| U.V. | 40.0 +/- 14.9 | 8.4 +/- 5.7 | 34.5 +/- 13.3 | 4.0 +/- 3.1 | 42.9 +/- 12.2 |

**Table 5.1 Summary of annexin V/PI flow cytometry data.**

The table displays the percentage of live (annexin V and PI negative), early apoptotic (annexin V positive, PI negative), dead (annexin V and PI positive) cells and cell debris (PI positive, distinguished by side scatter distribution) of primary human keratinocytes treated with or without dex and RU486. Dex 1 μM, RU486 1μM, 20 mJ U.V.B. at 0.2 $mV/cm^2$. Data represents the % mean ± SEM, n=3.

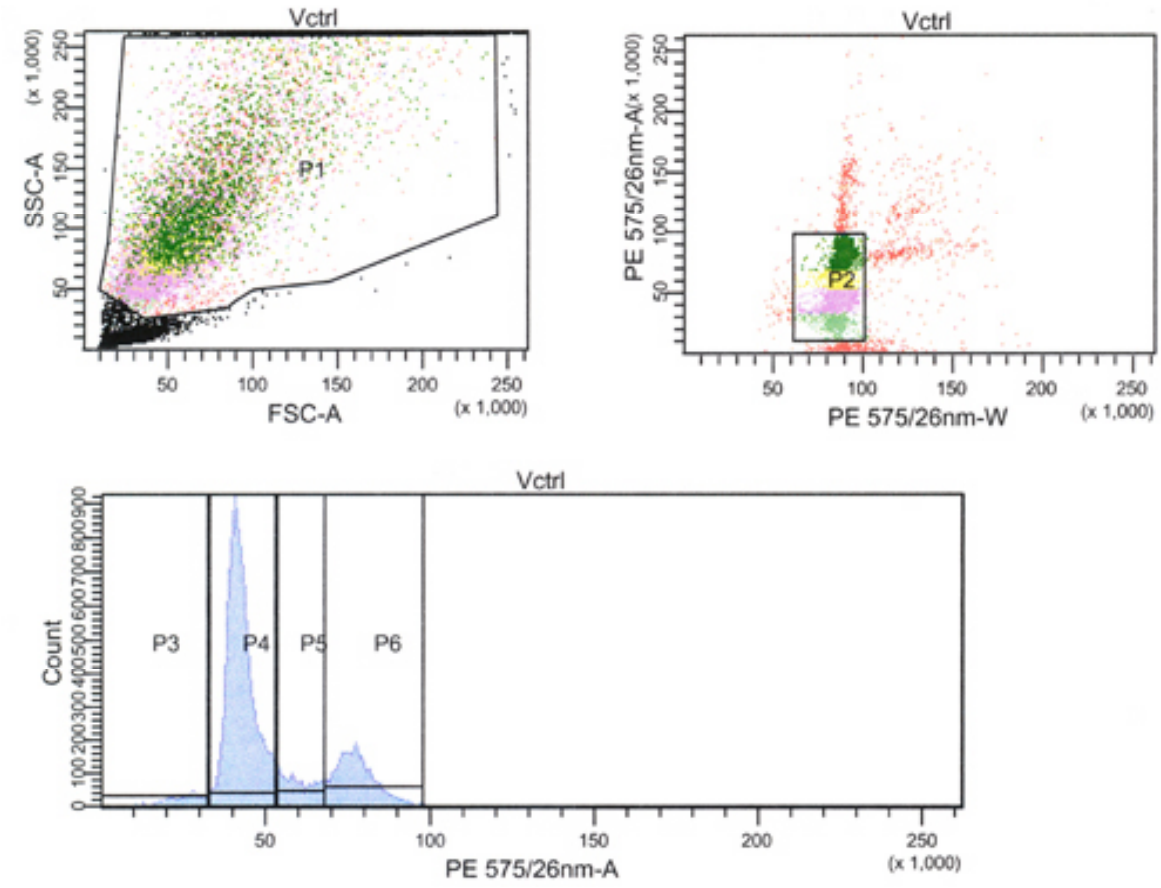


**Figure 5.12 Example of gated graphs used for analysing cell cycle.**

The total population was gated (P1) then live cells were gated (P2) and an area histogram was generated to determine the percentage of cells in sub $G_1$ (P3), $G_1$ (P4), S (P5) and $G_2M$ (P6) phases of the cell cycle.

A.

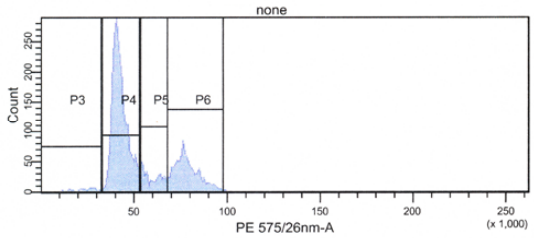


B.

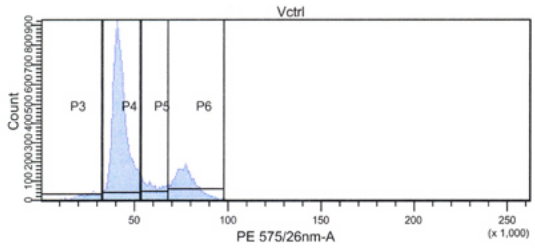


C.

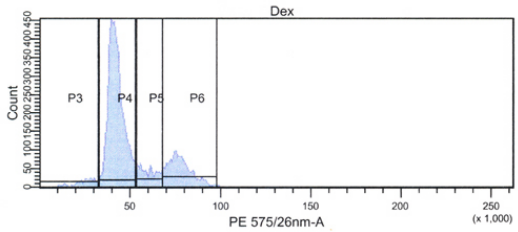


D.

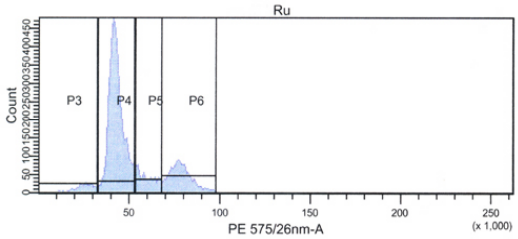


E.

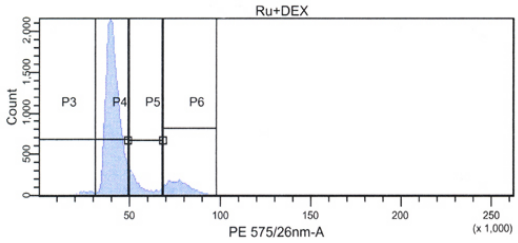


F.

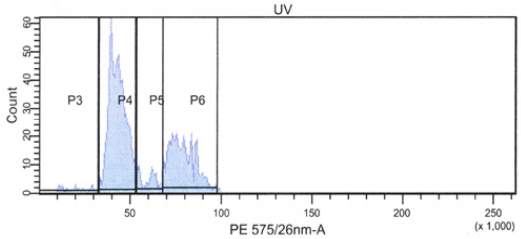


**Figure 5.13 Area parameter histograms representing cell cycle analysis of primary keratinocytes treated with dex and/or RU486 for 72 h.**

(A) untreated cells, (B) vehicle control, (C) dex, (D) RU486, (E) dex and RU486, (F) U.V. exposed cells. Dex 1μM, RU486 1μM, 20 mJ U.V.B. at 0.2 mV/cm2. Histograms are representative of two separate experiments.

### 5.2.5 Effect of dex on NADPH redox potential of keratinocytes

An alternative explanation for changes in MTT readout and pregnenolone synthesis (Section 4.3.2) could be through dex mediated changes in cellular redox potential. The influence of dex on cellular redox potential was further investigated by measuring $NADP^+$/NADPH ratio using a cell cycling assay. The cell cycling assay in Figure 5.14 demonstrated a trend for an increase of total ratio of NADPH relative to $NADP^+$ in primary human keratinocytes treated with dex for 72 h. However, the statistical analysis did not classify this difference as significant. Therefore it is currently inconclusive as to whether dex can influence total cellular NADPH availability in keratinocytes although the trend of the data lies in favour of this possibility.

Since dex appeared to improve cell viability in a serum-free media, the RIA data was also recalculated relative to total protein concentration to determine whether the observed increase of pregnenolone output by dex was due to changes in cell viability/ cell number. Figure 5.15 demonstrated that dex was able to induce significantly higher pregnenolone synthesis by primary human keratinocytes even when normalised to total cell protein. This suggests that the effects of dex on keratinocyte steroidogenic capacity was not just due to an increase in cell number.

In summary, dex has been shown to induce DUSP1 expression after 3 h and decrease pERK1/2 after 30 min. Unexpectedly, dex significantly enhanced MTT measured reductase capacity of untreated primary keratinocytes whereas MAPK inhibitors significantly reduced this activity. Dex treated keratinocytes were then analysed for cell viability, apoptosis, necrosis and influence on NADPH availability. No significant difference was detected in live cells, early apoptotic or dead cells by FACS analysis. There was also no difference in cell cycle. However, there was an increase in the number of viable cells tested by trypan blue assay. In addition, there was a trend for dex to enhance total NADPH levels, a shift that may explain the increase in pregnenolone synthesis induced by dex in primary human keratinocytes.

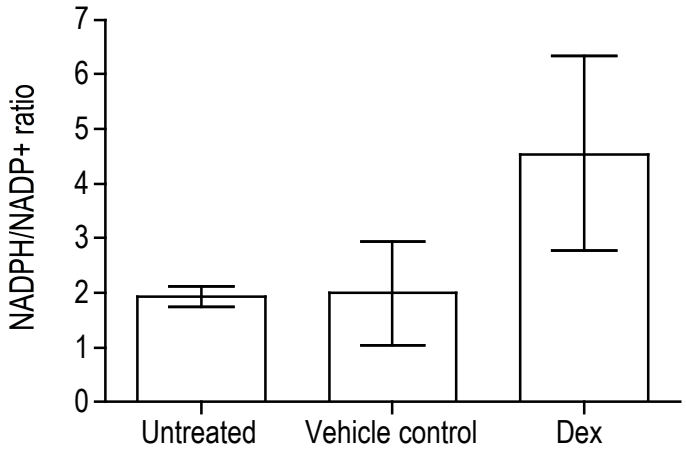


**Figure 5.14 Quantification of NADPH relative to $NADP^+$ in primary human keratinocytes treated with dex.**

Cells were incubated for 72 h with dex (1 μM), results are expressed as a ratio of NADPH relative to $NADP^+$. The data represents a two experiments (mean ±S.D.).

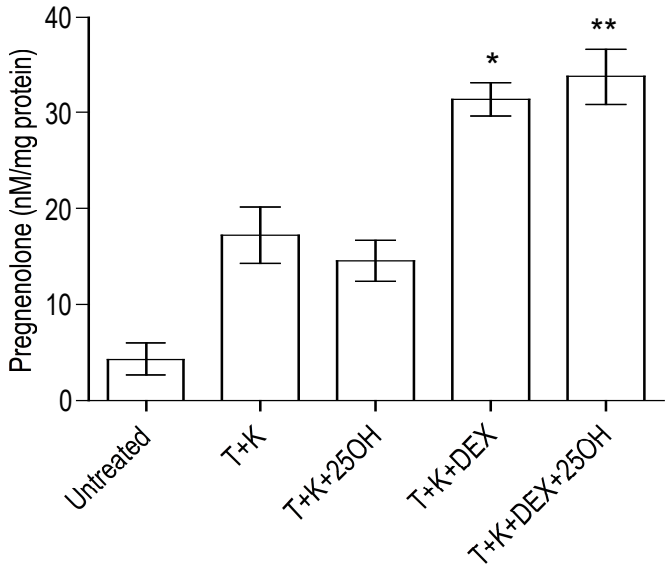


**Figure 5.15 Pregnenolone synthesis by primary human keratinocytes normalised to total protein concentration.**

Pregnenolone was detected by RIA from culture media of primary human keratinocytes after 24 h. T: 100 μM trilostane, K: 10 μM ketoconazole, dex: 1 μM dexamethasone, 25-OH: 5 μM 25-hydroxycholesterol. The data represents a single experiment, taken from keratinocytes treated in triplicate wells for each treatment and analysed in duplicate by RIA. Statistical differences were obtained using one-way ANOVA followed by Tukey's multiple comparisons test where appropriate (mean ± S.D., *P <0.05, **P<0.01).

## 5.3 Discussion

Dex gradually increased DUSP1 expression which peaked at 5 h and decreased after 7 h. This DUSP1 expression time course corresponds with dex-induced DUSP1 transcription detected between 1 and 4 h by microarray in primary human keratinocytes (Stojadinovic et al., 2007). In addition, DUSP1 expression was maximal after 5 h in MBA-15.4 and MG-63 osteoblasts and this was associated with a decreased level of pERK1/2 at this time point (Horsch et al., 2007). However, the same response was not observed in primary human keratinocytes where dex rapidly reduced pERK1/2 after 30 min but appeared to have no effect at 5 h. This suggests there was not the same prolonged suppression of pERK1/2 in keratinocytes relative to osteoblasts, although further time points would be required to confirm this finding.

The absence of prolonged pERK1/2 dephosphorylation suggests that in this culture system, dex might not be inhibiting cell proliferation. Although deactivation of other MAPK such as JNK and p38 might provide an alternative target for DUSP1 mediated inhibition of cell division, the MTT assay, FACS analysis and visual inspection of cell morphology did not identify a suppression of keratinocyte proliferation by dex.

In contrast, dex actually increased the MTT signal in both a concentration-dependent and GR-dependent manner in primary human keratinocytes. Although the MTT assay is classically used to assess cell proliferation it in fact measures cellular reductase activity. The MTT reaction was thought to be specific to the mitochondria but MTT reduction has recently been reported to localise to other organelles in the cell in addition to the mitochondria (Bernas and Dobrucki, 2002). Therefore there are a number of factors that could contribute to increased MTT signal including cell proliferation, decreased cell death or increased cellular redox potential.

Dex is regarded as an inhibitor of cell proliferation since it is used to suppress hyperproliferative skin disorders. Therefore, increased MTT signal by dex treatment was unexpected. Indeed, dex ($1x10^{-7}$M) was reported to induce a small but significant decrease in cell proliferation in primary human keratinocytes over 72 h (Stojadinovic et al., 2007). However, surprisingly the same study demonstrated that dex did not reduce

the transcription of genes associated with proliferation but rather induced those associated with differentiation (Stojadinovic et al., 2007). Differing cell culture conditions could account for the disparity between these results. Keratinocytes in this study were cultured in high calcium medium (supported with 3T3 fibroblasts prior to the assay) whereas keratinocytes in the Stojadinovik study were cultured in low calcium keratinocyte defined serum-free (and 3T3 fibroblast-free) medium. Primary human keratinocytes cultured in keratinocyte defined medium have been reported to have slower growth rate/expansion time, poorer adhesion, increased granulation and higher batch to batch variation with respect to keratinocytes grown in high calcium with 3T3 cells (Daniels et al., 1996). Therefore the difference in culture conditions could have a profound effect on cell proliferation assays.

Serum levels of culture medium also increased the MTT response of keratinocytes since low or no serum can inhibit the cell cycle (Cooper, 2003). Serum contains steroids, so all steroid analysis in this study was performed in the absence of serum. However, the data shows that serum can significantly alter the MTT signal, suggesting an increase in cell proliferation, redox potential and/or decrease in cell death. If redox potential is dysregulated by an absence of serum, it implies that conditions could be suboptimal for maximal steroidogenesis of keratinocytes in culture. Interestingly, the addition of dex was able to promote a further MTT response at each of the serum concentrations used, implying dex had a role beyond the serum effect alone.

Dex has been shown to promote granulosa cell viability by preventing apoptosis in a serum-free environment, so the increase in MTT signal could be due to protection from apoptosis (Sasson et al., 2001). Dex can also inhibit apoptosis in keratinocytes exposed to U.V. light (Stojadinovic et al., 2007). Therefore, the increased MTT signal could be due to increase in cell viability by preventing cell death. The trypan blue assay demonstrated that with no serum, dex could enhance keratinocyte cell viability. This matched the previous observations of keratinocyte morphology in cell culture with and without dex treatment and the MTT data.

In contrast, annexin V FACS analysis that was utilised to identify whether a difference in cell viability was due to changes in live, apoptotic or dead cells, failed to determine a

difference in dex treatment from untreated cells. Analysis of live, dead and apoptotic cells by flow cytometry did not demonstrate a significant difference between untreated, dex and/or RU486 treated cells. This could be because the assay was not sensitive enough to detect a difference between treatments. Alternatively annexin V may not have been the optimum marker for apoptotic cells in this instance. This is because during apoptosis there is a lag phase between phosphatidylserine (PS) positivity that is detected by annexin V and PI positivity (Krysko et al., 2008). Therefore a late apoptotic cell can appear positive for both annexin V and PI. In addition, some necrotic cells have been reported to be PI negative whilst externalising PS that would provide a false-positive signal of an early apoptotic cell (Krysko et al., 2008). Thus either the time point or the marker of apoptosis would need to be optimised if FACS were to be used for further analysis. However, since there was no significant difference between samples with apoptotic and dead cells combined, the data suggests that there was no change in overall cell death with dex treatment. Alternatively, due to the mechanics of FACS, only single cells are selected for analysis and cell aggregates are rejected. Primary keratinocytes commonly form aggregates upon trypsinisation, therefore a subpopulation of cell aggregates may have been disregarded which could provide essential information that could account for the differences between treatments.

An alternate method for analysing apoptosis is a terminal deoxynucleotidyl transferase dUTP nick end labelling (TUNEL) assay that measures DNA fragmentation as a result of the apoptotic signalling cascade. This assay can be performed *in vitro* without the use of trypsinisation and measures late rather than early stages of apoptosis. Therefore, future work to determine whether dex can protect keratinocytes from apoptosis should use TUNEL assay, since it will circumvent some of the limitations of FACS analysis.

The anti-apoptotic effects of dex on neuronal cells have been partly attributed to the treatments influence on cellular redox potential of the cells (Du et al., 2009). Changes in reduction capacity could also account for elevated MTT signal with dex treatment. Further analysis of cellular redox potential was investigated by $NADP^+$/NADPH cell cycling assay. Although the data did not reach significance (probably due to the low n number), there was a trend for increased amount of total NADPH in keratinocytes treated with dex. This suggests that dex could have the potential to increase NADPH

availability, an essential cofactor for many steroidogenic enzymes including CYP11A1 that regulates pregnenolone synthesis. Previous research has also demonstrated that dex and cortisol can promote NAPDH production even in an oxidative environment (Piccirella et al., 2006). Therefore, since cellular redox is an essential driver of steroidogenesis (Agarwal and Auchus, 2005; Sherbet et al., 2007), the potential effect of dex on redox potential could account for its potency for induction of steroidogenesis.

Overall, the data shows that dex could induce DUSP1 expression though a corresponding decrease in proliferation was not detected. The MTT assay and trypan blue assay imply that dex can enhance cell viability and mitochondrial reduction capacity of primary keratinocytes. Further analysis by FACS did not highlight a difference in proliferation, early apoptosis, dead cells or cell debris, potentially due to limitations of FACS analysis. Alternatively, the analysis could be correct and dex does not influence cell viability, although this conclusion does not correspond with visual observations, trypan blue assay or previous publications highlighting the ability of dex and the GR to protect keratinocytes from apoptosis (Bayo et al., 2008; Stojadinovic et al., 2007).

The $NADP^+$/NADPH cycling assay showed a trend for increased total NADPH upon dex treatment that may account for the changes in MTT signal observed. Moreover, changes in cellular redox potential in response to dex could account for the augmented level of pregnenolone synthesis described in chapter 4. However, this data does not determine whether dex can promote other factors that are required for pregnenolone synthesis such as CYP11A1 expression so further experiments are needed to examine this possibility.

Finally the chapter also highlights that culture conditions were suboptimal for steroid analysis since the absence of serum greatly affected the MTT response. Therefore the majority of steroid synthesis measured in previous chapters probably represents StAR independent basal level steroidogenesis that is restricted by the redox potential of the cultured cells.

# Chapter 6. Discussion and future research

## 6.1 Discussion

The research presented in this thesis demonstrates that primary human keratinocytes are capable of *de novo* synthesis of cortisol and intermediate steroids. Androgen and oestrogen metabolism have previously been identified in primary human keratinocytes and progesterone metabolism to corticosterone was described in immortalised HaCaT keratinocytes (Milewich et al., 1988; Slominski et al., 2002). However the synthesis of cortisol by primary human keratinocytes has not been previously published.

Local steroid synthesis has been identified in many non-classical endocrine cells including pancreatic cells, retinal pigment epithelium, chondrocytes, astrocytes, the hair follicle and sebocytes (Chen et al., 2006; Ito et al., 2005; Karri et al., 2007; Morales et al., 2008; Takeuchi et al., 2007; Zmijewski et al., 2007). Therefore the phenomenon of steroid (and cortisol synthesis) is not restricted to endocrine glands. It is likely that locally produced cortisol acts in an autocrine or paracrine fashion since levels corticosterone are negligible in the serum of adrenalectomised rodents (del Mar Grasa et al., 2007). However, the function for local cortisol production remains to be defined, particularly whether it serves a purpose that is independent of the adrenal supply.

Major regulators of steroidogenesis that are regarded as indicators of steroidogenic potential were also identified in the epidermis. StAR that regulates acute steroid production was localised specifically to the basal keratinocyte layer of the epidermis. This complements previous research that has also identified StAR in the basal layer of the epidermis (Tiala et al., 2007). In addition, StAR mRNA was detected in cultured primary keratinocytes, although StAR protein was not observed by western blot analysis. Using immunofluoresence cytochemistry the expression of StAR was shown to decrease with time in culture. Previous research also attempted to identify StAR in cultured primary human keratinocytes but serendipitously identified MLN64 rather than StAR when using an antibody to StAR (Slominski et al., 2004).

The loss of StAR expression in tissue culture suggests that acute steroidogenesis is disrupted in cultured primary keratinocytes. Moreover, 25OH cholesterol that can bypass StAR to circumvent the rate determining step of steroidogenesis, failed to

promote pregnenolone production. However, keratinocytes still retained some steroidogenic ability that was likely to be StAR-independent.

The necessity for StAR-independent steroidogenesis is exemplified by comparing patients suffering from CAH and LCAH. LCAH occurs due to loss of StAR function and therefore loss of acute steroidogenesis. Patients with LCAH have low levels of circulating cortisol but are able to survive for several months without steroid treatment (Miller, 2007). It is the secondary response to the build-up of lipids in the adrenals that causes complete ablation of steroidogenesis that would be fatal without GC treatment (Caron et al., 1997; Miller, 2007). Patients with severe CAH that commonly manifests due to loss of CYP21 activity have no ability to synthesise cortisol and do not survive without immediate GC treatment (Miller, 2007). A similar difference in viability was observed in mice where $StAR^{-/-}$ mice survived for up to 16 days without treatment whereas $GR^{-/-}$ mice died within hours of birth (Caron et al., 1997; Cole et al., 1995). This demonstrates that there is a clear difference in function between acute and background GC turnover. The steroidogenic potential measured in primary keratinocytes is likely to represent low-level StAR-independent steroidogenesis.

The cortisol analogue dex was the only single compound tested that could promote pregnenolone synthesis in primary human keratinocytes significantly above the basal T+K level. In the systemic system, cortisol ultimately suppresses steroidogenesis through negative feedback of the HPA axis. Therefore the ability of dex to promote pregnenolone synthesis was unexpected. However, there is evidence that cortisol can promote rather than suppress steroid synthesis in other cell types. Dex promoted progesterone synthesis by 8- or 4- fold in HO-23 granulosa cells incubated with forskolin at 37 or 32°C respectively (Sasson et al., 2001). This dex-mediated promotion of progesterone synthesis was independent of StAR and FDXR expression levels (Sasson et al., 2001). Furthermore, lack of cortisol was associated with decreased testosterone synthesis in Leydig cells (Parthasarathy and Balasubramanian, 2008). Thus dex and cortisol have been shown to promote steroidogenesis in other systems as well as primary human keratinocytes.

The absence of StAR, lack of steroidogenic response to 25OH cholesterol and the ability of dex to promote pregnenolone suggests that there could be an alternative rate determining step to steroid production in cultured primary keratinocytes. Changes in cellular redox potential may represent an alternative mechanism, since this dictates the level of cofactor available for steroidogenic enzymes (Agarwal and Auchus, 2005; Sherbet et al., 2007). Subtle changes in cellular redox that can be tolerated by cells can have a large impact on the cells steroidogenic capabilities, hence redox potential has been described as the driver of steroidogenesis (Agarwal and Auchus, 2005; Sherbet et al., 2007). The MTT assays detected a significant increase in mitochondrial reductase capacity of primary keratinocytes treated with dex. Moreover, there was a trend for increased total cellular NADPH relative to $NADP^+$. Cortisol has also been shown to induce NADPH production in microsomes, suggesting that cortisol can influence ER redox potential (Piccirella et al., 2006). In addition cortisol can promote G6PDH and H6PD activity to increase the availability of cytosolic and ER-localised NADPH. Finally dex was shown to act in a biphasic manner where low concentrations of dex protected neuronal cells from apoptosis by regulating redox potential, whereas high concentrations of dex had the opposite effect (Du et al., 2009). Therefore, although further investigations are required, there is evidence to suggest that dex could promote steroidogenesis in primary human keratinocytes by influencing cofactor availability.

Collectively the data suggests that the act of culturing primary keratinocytes creates a suboptimal environment for maintaining the steroidogenic potential of the cell. This is for several reasons. Firstly, normal primary keratinocytes express markers of hyperproliferation (K6 and K16) that are absent in normal epidermis but present in skin diseases including psoriasis and atopic dermatitis (Leigh et al., 1993). StAR expression was absent in these hyperproliferative conditions but StAR was detected in normal epidermis. This suggests that isolated normal keratinocytes acquire a phenotype that in some aspects is similar to hyperproliferative keratinocytes. Secondly, in order to measure steroidogenesis cells must be in a steroid-free environment. Primary keratinocytes are routinely cultured with cortisol and serum (or pituitary extract for serum-free culture media). Removing these components affects cell proliferation, viability and redox potential that could contribute to limiting steroidogenic capabilities. Thirdly, the ratio between cells that would reside in the basal, spinous, granular and

corneum layers is skewed in cultures relative to physiological ratios, where basal and spinous keratinocytes are encouraged to expand but few corneocytes are detected in culture. Organotypic keratinocyte cultures have also been reported to exhibit desquamation that is more representative of psoriatic rather than normal skin (Vicanova et al., 1996). Fourthly, the oxygen gradient that has been shown to regulate keratinocyte proliferation and differentiation is disrupted in cell culture (Horikoshi et al., 1986; Ngo et al., 2007). The ambient oxygen environment in which cells are cultured does not represent the physiological oxygen gradient across the epidermis, which could stress the keratinocytes. However culturing keratinocytes at low (2%) oxygen was still unable to maintain/upregulate StAR protein expression by western blot analysis. Finally, the calcium gradient that regulates keratinocyte differentiation is disrupted in cell culture, since cells are incubated in a homogeneous calcium environment. Homogenously low calcium levels throughout the epidermis are detected in hyperproliferative conditions such as atopic dermatitis (Proksch et al., 2008). Calcium signalling is a critical in coordinating cell viability, apoptosis and can affect steroidogenic potential (Yamazaki et al., 1995). All these components will limit the ability of normal primary human keratinocytes to synthesise steroids.

In light of the above observations, compounds that prevent apoptosis and regulate cellular redox potential might create a better environment for measuring steroid production in keratinocytes. Therefore an alternative target for manipulation is the TSPO protein. TSPO was identified throughout the epidermis, is present in keratinocyte culture and has been directly associated with regulating apoptosis and coordinating cholesterol transport for steroid synthesis (Veenman et al., 2007). Compounds that act on TSPO such as PK1115 might also enhance steroid production in primary human keratinocytes.

Regulators of steroidogenesis were shown to be disrupted in hyperproliferative skin disorders. This suggest that local steroid synthesis could be disrupted in skin conditions such as psoriasis and atopic dermatitis. Down regulation of StAR in psoriatic skin was previously linked to *CCHCR1* located on the major psoriasis susceptibility locus *PSORS1* (Tiala et al., 2007). DAX1 was localised to the nucleus rather than cytoplasm of atopic dermatitis and psoriatic (non-lesional only) skin. Since DAX1 is a nuclear

receptor that inhibits the transcription of StAR, this change in location could account for decreased StAR expression. In addition, $NADP^+$/NADPH ratio has been found to be aberrant in psoriatic skin suggesting that cofactor availability for steroid synthesis could be limited in this condition (Hammar, 1975). Therefore the results from this thesis suggest that there could be a novel endocrine component influencing the pathogenesis of atopic dermatitis and psoriasis that requires further investigation.

Cortisol analogues such as dex are one of the most widely prescribed treatments for hyperproliferative skin disorders but have the major side effect of inducing skin atrophy with chronic use. Dex was shown to induce DUSP1 expression, a protein that can suppress MAPK activity to inhibit cell proliferation. The DUSP1 pathway has been implicated in GC-mediated bone weakening by inhibiting ERK1/2 MAPK activity and cell proliferation of immortalised osteoblasts (Horsch et al., 2007). The activation of DUSP1 by dex in keratinocytes suggests that a similar pathway could be the cause of skin atrophy by GC treatment. However, inhibition of MAPK activity or cell division was not detected under the culture conditions. This is in contrast with an *in vivo* embryonic mouse model where $GR^{-/-}$ knockout led to increased keratinocyte proliferation by up regulating ERK1/2 MAPK activity (Bayo et al., 2008).

Although a decrease in keratinocyte apoptosis was not detected when keratinocytes were treated with dex, an increase in cell viability was observed. Recently dex has been shown to protect primary human keratinocytes from apoptosis when exposed to U.V. light (Stojadinovic et al., 2007). Moreover, the epidermis from $GR^{-/-}$ mouse embryos were shown to have elevated epidermal apoptosis (Bayo et al., 2008). This phenomenon of protection from cell death by GC has been observed in many other cell types including mammary gland epithelial cells, endometrium, hepatocytes, ovarian follicular cells, fibroblasts and neuronal cells (Du et al., 2009; Viegas et al., 2008). It appears to be concentration dependent (where high levels of dex can induce cell death), tissue specific and has been described as a novel anti-inflammatory component of GC (Du et al., 2009; Viegas et al., 2008). In addition increased apoptosis is a hallmark of hyperproliferative skin disorders that are treated with GC (Iizuka et al., 2004; Trautmann et al., 2001). Therefore the anti-apoptotic nature of GC action suggests that localised cortisol production could function to protect cells from apoptosis.

Ultimately the research in this thesis demonstrates that primary human keratinocytes are capable of *de novo* cortisol synthesis, that dex (an analogue of cortisol) can promote further pregnenolone production and that this response is potentially due to the influence of dex on redox potential. It remains to be shown whether dex alters keratinocyte proliferation and differentiation, or protects cells from apoptosis, however these actions of dex have been demonstrated in other studies (Bayo et al., 2008; Stojadinovic et al., 2007). In addition, steroidogenic regulators were identified in the epidermis but their expression was dysregulated in hyperproliferative skin diseases. This suggests that acute steroid production could be ablated in these conditions. Many hallmarks of hyperproliferative keratinocytes are detected in normal keratinocytes when they are isolated and cultured *in vitro,* including the down regulation of StAR expression. Therefore steroidogenesis measured in this thesis is likely to be StAR-independent.

The function of local *de novo* cortisol synthesis remains to be defined, however from these data and the published literature, I hypothesise that localised *de novo* cortisol synthesis acts by a feedback mechanism to regulate cellular redox and prevent keratinocyte death. Local cortisol synthesis could increase NADPH and $NAD^+$ availability that in turn promotes steroid synthesis. The local production of cortisol could also act on Bcl-2 proteins to prevent MPTP opening and maintain the cholesterol transport function of TSPO for steroidogenesis rather than the apoptotic role of the protein.

The system suggests that an apoptotic or necrotic cell would be incapable of synthesising cortisol. Whilst apoptosis is considered a form of cell death that does not release inflammatory signals, an increasing number of reports have associated apoptosis with inflammation (Schwarz, 2000). This model would imply that an apoptotic cell loses its anti-inflammatory signal rather than releases an inflammatory signal. The local production of cortisol of a healthy cell would inhibit infiltration of immune cells to protect the tissue from inflammation. Whilst each of the components of the system have been described individually in many cell types, coordination of the system has not been

reported. In addition the nature of this system to act as a sensor and signal of tissue health would require steroid production to act locally and not systemically.

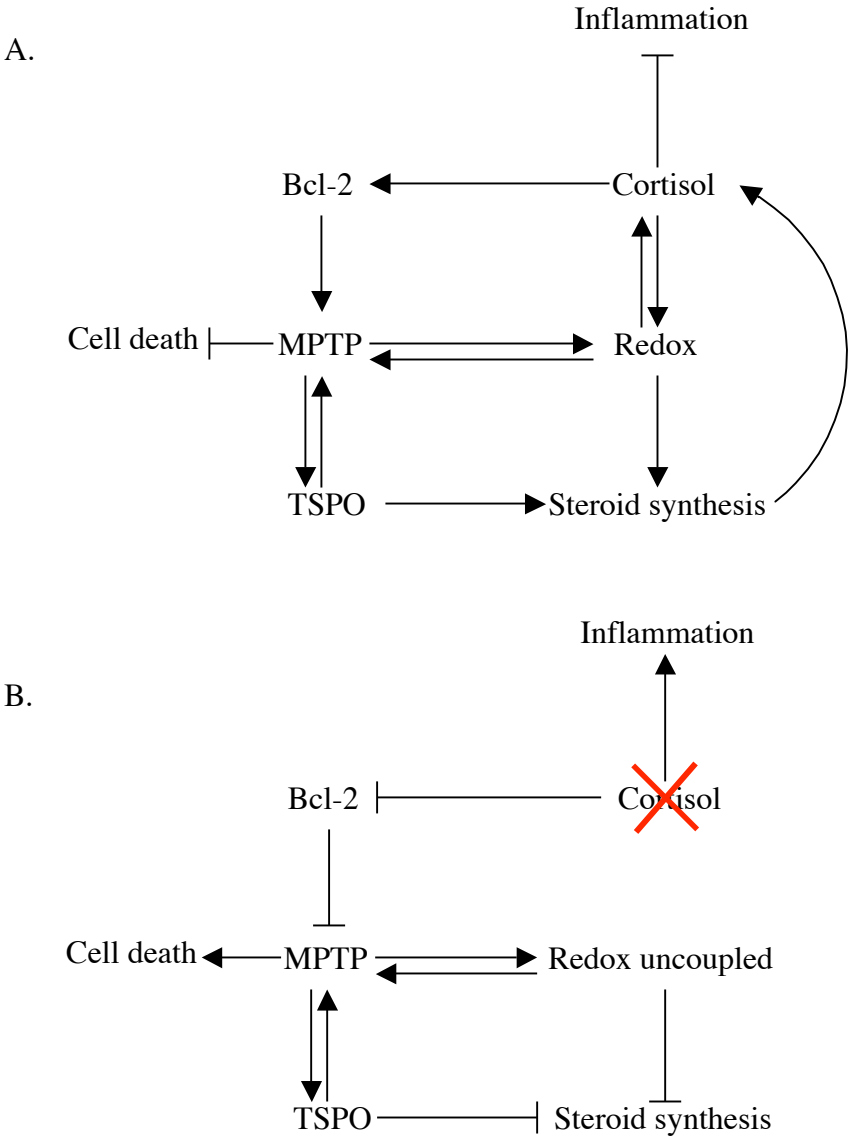


**Figure 6.1 Hypothesis for the function of *de novo* cortisol synthesis to prevent keratinocyte inflammation and premature cell death.**

(A) Normal keratinocytes synthesise cortisol that acts as a local signal to prevent inflammation. Production of cortisol is regulated by, and able to regulate cellular redox potential that, via TSPO maintains MPTP in a conformation that would facilitate further steroid synthesis and prevent the induction of cell death. (B) Loss of cortisol through uncoupled redox potential causes the release of Bcl-2 that leads to MPTP and TSPO to induce cell death and prevents TSPO-mediated steroid synthesis. Although not depicted here, StAR could promote acute steroid synthesis in cells that require a boosted system (e.g. stem cells and proliferating keratinocytes) to protect the cells from oxidative stress and prevent premature apoptosis.

## 6.2 Future Research

This thesis has identified the *de novo* cortisol synthesis pathway in normal primary human keratinocytes. However, there are two fundamental elements that need to be addressed in order to demonstrate the physiological relevance of this research. Firstly, local production of cortisol needs to be shown to have functional relevance in addition to the systemic cortisol supply. Secondly, a different model that can overcome the limitations of steroidogenesis in cultured keratinocytes needs to be identified.

A collaboration with Professor Rod Flower (Barts and The London, London, U.K.) has been organised to provide an animal model to separate local from systemic GC supply as follows: Adrenalectomised rats (to remove systemic corticosterone) or sham operated as controls will have local steroid production or corticosterone response blocked by daily topical application of (a) T and K or (b) GR inhibitor RU486 to one ear of the animal for 72h. The other ear will be treated with a vehicle control. This time point was chosen since changes in keratinocyte biology in response to dex were observed after 72h (Stojadinovic et al., 2007). Rats will be housed in separate cages to prevent grooming that could remove or redistribute the treatment to other parts of the body.

Skin sections of rat ears will be compared by measures of (a) hematoxylin and eosin for histology, (b) Ki67 for proliferation, (c) filaggrin, involucrin and loricrin for differentiation, (d) TUNEL assay for apoptosis, (e) JC-1 for mitochondrial membrane potential, (f) TSPO expression and localisation, (g) oil red-O analysis for identifying lipid accumulation, (h) histochemistry of GR location for assessing RU486 inhibition, (i) CRH, CRH receptor and ACTH to determine if there is an upregulation of local expression as would be expected with a block in GC feedback. In addition the rat serum will be analysed for corticosterone to validation of complete adrenalectomy. These analyses should help identify the function for local GC synthesis, whether it regulates cell viability, proliferation, differentiation apoptosis and cellular redox potential.

In addition, MALDI imaging is a new technique that can measure small molecules including steroids *in situ*. Therefore a complete steroid profile together with

localisation can be generated from whole tissue using this technique. This method of analysis will also overcome limitations that the cell culturing process appears to have on steroidogenesis. MALDI imaging will be employed to measure the *in situ* localisation of steroids in the rat skin (from sham operated and adrenalectomised animals) to confirm local production relative to the systemic supply and whether trilostane and ketoconazole have effectively blocked the pathway. The technique will also be used on organotypic models of keratinocytes (also treated with or without RU486 or T and K) to identify whether *in vitro* levels of steroidogenesis are equivalent to *in situ* levels. Finally freshly isolated psoriatic and atopic dermatitis will also be analysed using this method to identify whether there is a decrease of local cortisol levels relative to normal skin.

These experiments could therefore address the hypothesis that local *de novo* cortisol synthesis is required to maintain the epidermal barrier, where ablation of the system leads to premature apoptosis, poor differentiation, immune cell infiltration and hyperproliferation. Many tissues that are not regarded as steroidogenic glands have been found to have steroidogenic potential, this research may eventually be translated to other tissues and conditions where cortisol provides a potent therapy.

**References**

Agarwal AK, Auchus RJ. 2005. Minireview: cellular redox state regulates hydroxysteroid dehydrogenase activity and intracellular hormone potency. Endocrinology 146(6):2531-2538.

Albanesi C, De Pita O, Girolomoni G. 2007. Resident skin cells in psoriasis: a special look at the pathogenetic functions of keratinocytes. Clin Dermatol 25(6):581-588.

Alexander JM, Klibanski A. 1994. Gonadotropin-releasing hormone receptor mRNA expression by human pituitary tumors in vitro. J Clin Invest 93(6):2332-2339.

Alpy F, Boulay A, Moog-Lutz C, Andarawewa KL, Degot S, Stoll I, *et al*. 2003. Metastatic lymph node 64 (MLN64), a gene overexpressed in breast cancers, is regulated by Sp/KLF transcription factors. Oncogene 22(24):3770-3780.

Alpy F, Stoeckel ME, Dierich A, Escola JM, Wendling C, Chenard MP, *et al*. 2001. The steroidogenic acute regulatory protein homolog MLN64, a late endosomal cholesterol-binding protein. J Biol Chem 276(6):4261-4269.

Alpy F, Tomasetto C. 2005. Give lipids a START: the StAR-related lipid transfer (START) domain in mammals. J Cell Sci 118(Pt 13):2791-2801.

Amri H, Ogwuegbu SO, Boujrad N, Drieu K, Papadopoulos V. 1996. In vivo regulation of peripheral-type benzodiazepine receptor and glucocorticoid synthesis by Ginkgo biloba extract EGb 761 and isolated ginkgolides. Endocrinology 137(12):5707-5718.

Arakane F, Sugawara T, Nishino H, Liu Z, Holt JA, Pain D, *et al*. 1996. Steroidogenic acute regulatory protein (StAR) retains activity in the absence of its mitochondrial import sequence: implications for the mechanism of StAR action. Proc Natl Acad Sci U S A 93(24):13731-13736.

Baltimore D. 1970. RNA-dependent DNA polymerase in virions of RNA tumour viruses. Nature 226(5252):1209-1211.

Bayo P, Sanchis A, Bravo A, Cascallana JL, Buder K, Tuckermann J, *et al.* 2008. Glucocorticoid receptor is required for skin barrier competence. Endocrinology 149(3):1377-1388.

Berliner DL, Cazes DM, Nabors CJ, Jr. 1962. Adrenal 3beta-hydroxysteroid dehydrogenase activity on C17-hydroxylated delta5-pregnenes, C21-hydroxylated delta5-pregnenes, or both. J Biol Chem 237:2478-2480.

Bernard P, Ludbrook L, Queipo G, Dinulos MB, Kletter GB, Zhang YH, *et al.* 2006. A familial missense mutation in the hinge region of DAX1 associated with late-onset AHC in a prepubertal female. Mol Genet Metab 88(3):272-279.

Bernas T, Dobrucki J. 2002. Mitochondrial and nonmitochondrial reduction of MTT: interaction of MTT with TMRE, JC-1, and NAO mitochondrial fluorescent probes. Cytometry 47(4):236-242.

Bogan RL, Davis TL, Niswender GD. 2007. Peripheral-type benzodiazepine receptor (PBR) aggregation and absence of steroidogenic acute regulatory protein (StAR)/PBR association in the mitochondrial membrane as determined by bioluminescence resonance energy transfer (BRET). J Steroid Biochem Mol Biol 104(1-2):61-67.

Borthwick F, Taylor JM, Bartholomew C, Graham A. 2009. Differential regulation of the STARD1 subfamily of START lipid trafficking proteins in human macrophages. FEBS Lett.

Bose HS, Sato S, Aisenberg J, Shalev SA, Matsuo N, Miller WL. 2000a. Mutations in the steroidogenic acute regulatory protein (StAR) in six patients with congenital lipoid adrenal hyperplasia. J Clin Endocrinol Metab 85(10):3636-3639.

Bose HS, Sugawara T, Strauss JF, 3rd, Miller WL. 1996. The pathophysiology and genetics of congenital lipoid adrenal hyperplasia. International Congenital Lipoid Adrenal Hyperplasia Consortium. N Engl J Med 335(25):1870-1878.

Bose HS, Whittal RM, Baldwin MA, Miller WL. 1999. The active form of the steroidogenic acute regulatory protein, StAR, appears to be a molten globule. Proc Natl Acad Sci U S A 96(13):7250-7255.

Bose HS, Whittal RM, Bose M, Debnath D. 2009. Hydrophobic Core of the Steroidogenic Acute Regulatory Protein for Cholesterol Transport (dagger). Biochemistry.

Bose HS, Whittal RM, Huang MC, Baldwin MA, Miller WL. 2000b. N-218 MLN64, a protein with StAR-like steroidogenic activity, is folded and cleaved similarly to StAR. Biochemistry 39(38):11722-11731.

Bose M, Whittal RM, Miller WL, Bose HS. 2008. Steroidogenic activity of StAR requires contact with mitochondrial VDAC1 and phosphate carrier protein. J Biol Chem 283(14):8837-8845.

Boujrad N, Vidic B, Papadopoulos V. 1996. Acute action of choriogonadotropin on Leydig tumor cells: changes in the topography of the mitochondrial peripheral-type benzodiazepine receptor. Endocrinology 137(12):5727-5730.

Boukamp P, Petrussevska RT, Breitkreutz D, Hornung J, Markham A, Fusenig NE. 1988. Normal keratinization in a spontaneously immortalized aneuploid human keratinocyte cell line. J Cell Biol 106(3):761-771.

Bradford MM. 1976. A rapid and sensitive method for the quantitation of microgram quantities of protein utilizing the principle of protein-dye binding. Anal Biochem 72:248-254.

Braestrup C, Squires RF. 1977. Specific benzodiazepine receptors in rat brain characterized by high-affinity (3H)diazepam binding. Proc Natl Acad Sci U S A 74(9):3805-3809.

Bratland E, Bredholt G, Mellgren G, Knappskog PM, Mozes E, Husebye ES. 2009. The purification and application of biologically active recombinant steroid cytochrome P450

21-hydroxylase: The major autoantigen in autoimmune Addison's disease. J Autoimmun.

Brownie AC, Simpson ER, Jefcoate CR, Boyd GS, Orme-Johnson WH, Beinert H. 1972. Effect of ACTH on cholesterol side-chain cleavage in rat adrenal mitochondria. Biochem Biophys Res Commun 46(2):483-490.

Cagle PE, Dyson M, Gajewski B, Lukert B. 2007. Can dermal thickness measured by ultrasound biomicroscopy assist in determining osteoporosis risk? Skin Res Technol 13(1):95-100.

Caron KM, Soo SC, Wetsel WC, Stocco DM, Clark BJ, Parker KL. 1997. Targeted disruption of the mouse gene encoding steroidogenic acute regulatory protein provides insights into congenital lipoid adrenal hyperplasia. Proc Natl Acad Sci U S A 94(21):11540-11545.

Cauet G, Balbuena D, Achstetter T, Dumas B. 2001. CYP11A1 stimulates the hydroxylase activity of CYP11B1 in mitochondria of recombinant yeast in vivo and in vitro. Eur J Biochem 268(14):4054-4062.

Chapman JC, Polanco JR, Min S, Michael SD. 2005. Mitochondrial 3 beta-hydroxysteroid dehydrogenase (HSD) is essential for the synthesis of progesterone by corpora lutea: an hypothesis. Reprod Biol Endocrinol 3:11.

Charmandari E, Ichijo T, Jubiz W, Baid S, Zachman K, Chrousos GP*, et al*. 2008. A novel point mutation in the amino terminal domain of the human glucocorticoid receptor (hGR) gene enhancing hGR-mediated gene expression. J Clin Endocrinol Metab 93(12):4963-4968.

Chen W, Tsai SJ, Liao CY, Tsai RY, Chen YJ, Pan BJ*, et al*. 2006. Higher levels of steroidogenic acute regulatory protein and type I 3beta-hydroxysteroid dehydrogenase in the scalp of men with androgenetic alopecia. J Invest Dermatol 126(10):2332-2335.

Cherradi N, Capponi AM. 1998. The Acute Regulation of Mineralocorticoid Biosynthesis: Scenarios for the StAR System. Trends Endocrinol Metab 9(10):412-418.

Christenson LK, Strauss JF, 3rd. 2001. Steroidogenic acute regulatory protein: an update on its regulation and mechanism of action. Arch Med Res 32(6):576-586.

Christophers E. 2007. Comorbidities in psoriasis. Clin Dermatol 25(6):529-534.

Clark BJ, Wells J, King SR, Stocco DM. 1994. The purification, cloning, and expression of a novel luteinizing hormone-induced mitochondrial protein in MA-10 mouse Leydig tumor cells. Characterization of the steroidogenic acute regulatory protein (StAR). J Biol Chem 269(45):28314-28322.

Cole TJ, Blendy JA, Monaghan AP, Krieglstein K, Schmid W, Aguzzi A*, et al*. 1995. Targeted disruption of the glucocorticoid receptor gene blocks adrenergic chromaffin cell development and severely retards lung maturation. Genes Dev 9(13):1608-1621.

Cooper S. 2003. Reappraisal of serum starvation, the restriction point, G0, and G1 phase arrest points. Faseb J 17(3):333-340.

Daniels JT, Kearney JN, Ingham E. 1996. Human keratinocyte isolation and cell culture: a survey of current practices in the UK. Burns 22(1):35-39.

Davies E, MacKenzie SM. 2003. Extra-adrenal production of corticosteroids. Clin Exp Pharmacol Physiol 30(7):437-445.

del Mar Grasa M, Serrano M, Fernandez-Lopez JA, Alemany M. 2007. Corticosterone inhibits the lipid-mobilizing effects of oleoyl-estrone in adrenalectomized rats. Endocrinology 148(8):4056-4063.

Delavoie F, Li H, Hardwick M, Robert JC, Giatzakis C, Peranzi G*, et al*. 2003. In vivo and in vitro peripheral-type benzodiazepine receptor polymerization: functional significance in drug ligand and cholesterol binding. Biochemistry 42(15):4506-4519.

Doger FK, Dikicioglu E, Ergin F, Unal E, Sendur N, Uslu M. 2007. Nature of cell kinetics in psoriatic epidermis. J Cutan Pathol 34(3):257-263.

Dong DD, Jewell CM, Bienstock RJ, Cidlowski JA. 2006. Functional analysis of the LXXLL motifs of the human glucocorticoid receptor: association with altered ligand affinity. J Steroid Biochem Mol Biol 101(2-3):106-117.

Du J, Wang Y, Hunter R, Wei Y, Blumenthal R, Falke C, *et al.* 2009. Dynamic regulation of mitochondrial function by glucocorticoids. Proc Natl Acad Sci U S A 106(9):3543-3548.

Dyson MT, Jones JK, Kowalewski MP, Manna PR, Alonso M, Gottesman ME, *et al.* 2008. Mitochondrial A-kinase anchoring protein 121 binds type II protein kinase A and enhances steroidogenic acute regulatory protein-mediated steroidogenesis in MA-10 mouse leydig tumor cells. Biol Reprod 78(2):267-277.

Eckert RL. 1989. Structure, function, and differentiation of the keratinocyte. Physiol Rev 69(4):1316-1346.

Elias LL, Clark AJ. 2000. The expression of the ACTH receptor. Braz J Med Biol Res 33(10):1245-1248.

Elias PM. 2005. Stratum corneum defensive functions: an integrated view. J Invest Dermatol 125(2):183-200.

Elias PM, Hatano Y, Williams ML. 2008. Basis for the barrier abnormality in atopic dermatitis: outside-inside-outside pathogenic mechanisms. J Allergy Clin Immunol 121(6):1337-1343.

Gavish M, Bachman I, Shoukrun R, Katz Y, Veenman L, Weisinger G, *et al.* 1999. Enigma of the peripheral benzodiazepine receptor. Pharmacol Rev 51(4):629-650.

Gingras S, Turgeon C, Brochu N, Soucy P, Labrie F, Simard J. 2003. Characterization and modulation of sex steroid metabolizing activity in normal human keratinocytes in primary culture and HaCaT cells. J Steroid Biochem Mol Biol 87(2-3):167-179.

Golani I, Weizman A, Leschiner S, Spanier I, Eckstein N, Limor R, *et al*. 2001. Hormonal regulation of peripheral benzodiazepine receptor binding properties is mediated by subunit interaction. Biochemistry 40(34):10213-10222.

Granot Z, Kobiler O, Melamed-Book N, Eimerl S, Bahat A, Lu B, *et al*. 2007a. Turnover of mitochondrial steroidogenic acute regulatory (StAR) protein by Lon protease: the unexpected effect of proteasome inhibitors. Mol Endocrinol 21(9):2164-2177.

Granot Z, Melamed-Book N, Bahat A, Orly J. 2007b. Turnover of StAR protein: roles for the proteasome and mitochondrial proteases. Mol Cell Endocrinol 265-266:51-58.

Green DR, Reed JC. 1998. Mitochondria and apoptosis. Science 281(5381):1309-1312.

Guarneri P, Papadopoulos V, Pan B, Costa E. 1992. Regulation of pregnenolone synthesis in C6-2B glioma cells by 4'-chlorodiazepam. Proc Natl Acad Sci U S A 89(11):5118-5122.

Guttman-Yassky E, Lowes MA, Fuentes-Duculan J, Zaba LC, Cardinale I, Nograles KE, *et al*. 2008. Low expression of the IL-23/Th17 pathway in atopic dermatitis compared to psoriasis. J Immunol 181(10):7420-7427.

Hammami MM, Siiteri PK. 1991. Regulation of 11 beta-hydroxysteroid dehydrogenase activity in human skin fibroblasts: enzymatic modulation of glucocorticoid action. J Clin Endocrinol Metab 73(2):326-334.

Hammar H. 1975. Epidermal nicotinamide adenine dinucleotides in psoriasis and neurodermatitis (lichen simplex hypertrophicus). Arch Dermatol Forsch 252(3):217-227.

Hardwick M, Fertikh D, Culty M, Li H, Vidic B, Papadopoulos V. 1999. Peripheral-type benzodiazepine receptor (PBR) in human breast cancer: correlation of breast cancer cell aggressive phenotype with PBR expression, nuclear localization, and PBR-

mediated cell proliferation and nuclear transport of cholesterol. Cancer Res 59(4):831-842.

Hewitt KN, Walker EA, Stewart PM. 2005. Minireview: hexose-6-phosphate dehydrogenase and redox control of 11{beta}-hydroxysteroid dehydrogenase type 1 activity. Endocrinology 146(6):2539-2543.

Hillier SG. 2007. Diamonds are forever: the cortisone legacy. J Endocrinol 195(1):1-6.

Hodge T, Colombini M. 1997. Regulation of metabolite flux through voltage-gating of VDAC channels. J Membr Biol 157(3):271-279.

Hoffmann R. 2001. Enzymology of the hair follicle. Eur J Dermatol 11(4):296-300.

Holtta-Vuori M, Alpy F, Tanhuanpaa K, Jokitalo E, Mutka AL, Ikonen E. 2005. MLN64 is involved in actin-mediated dynamics of late endocytic organelles. Mol Biol Cell 16(8):3873-3886.

Horikoshi T, Balin AK, Carter DM. 1986. Effect of oxygen on the growth of human epidermal keratinocytes. J Invest Dermatol 86(4):424-427.

Horsch K, de Wet H, Schuurmans MM, Allie-Reid F, Cato AC, Cunningham J*, et al.* 2007. Mitogen-activated protein kinase phosphatase 1/dual specificity phosphatase 1 mediates glucocorticoid inhibition of osteoblast proliferation. Mol Endocrinol 21(12):2929-2940.

Hsia SL, Hao YL. 1966. Metabolic transformations of cortisol-4-[14C] in human skin. Biochemistry 5(5):1469-1474.

Hughes SV, Robinson E, Bland R, Lewis HM, Stewart PM, Hewison M. 1997. 1,25-dihydroxyvitamin D3 regulates estrogen metabolism in cultured keratinocytes. Endocrinology 138(9):3711-3718.

Iida S, Papadopoulos V, Hall PF. 1989. The influence of exogenous free cholesterol on steroid synthesis in cultured adrenal cells. Endocrinology 124(5):2619-2624.

Iizuka H, Takahashi H, Honma M, Ishida-Yamamoto A. 2004. Unique keratinization process in psoriasis: late differentiation markers are abolished because of the premature cell death. J Dermatol 31(4):271-276.

Ishimura K, Fujita H. 1997. Light and electron microscopic immunohistochemistry of the localization of adrenal steroidogenic enzymes. Microsc Res Tech 36(6):445-453.

Ito N, Ito T, Kromminga A, Bettermann A, Takigawa M, Kees F, *et al*. 2005. Human hair follicles display a functional equivalent of the hypothalamic-pituitary-adrenal axis and synthesize cortisol. Faseb J 19(10):1332-1334.

Iyer AK, McCabe ER. 2004. Molecular mechanisms of DAX1 action. Mol Genet Metab 83(1-2):60-73.

Jensen JM, Folster-Holst R, Baranowsky A, Schunck M, Winoto-Morbach S, Neumann C, *et al*. 2004. Impaired sphingomyelinase activity and epidermal differentiation in atopic dermatitis. J Invest Dermatol 122(6):1423-1431.

Johansson AS, Mannervik B. 2001. Human glutathione transferase A3-3, a highly efficient catalyst of double-bond isomerization in the biosynthetic pathway of steroid hormones. J Biol Chem 276(35):33061-33065.

Kanda N, Watanabe S. 2005. Regulatory roles of sex hormones in cutaneous biology and immunology. J Dermatol Sci 38(1):1-7.

Karri S, Dertien JS, Stocco DM, Syapin PJ. 2007. Steroidogenic acute regulatory protein expression and pregnenolone synthesis in rat astrocyte cultures. J Neuroendocrinol 19(11):860-869.

Kauser S, Thody AJ, Schallreuter KU, Gummer CL, Tobin DJ. 2005. A fully functional proopiomelanocortin/melanocortin-1 receptor system regulates the differentiation of human scalp hair follicle melanocytes. Endocrinology 146(2):532-543.

Kawabe K, Shikayama T, Tsuboi H, Oka S, Oba K, Yanase T, *et al*. 1999. Dax-1 as one of the target genes of Ad4BP/SF-1. Mol Endocrinol 13(8):1267-1284.

Kenouch S, Lombes M, Delahaye F, Eugene E, Bonvalet JP, Farman N. 1994. Human skin as target for aldosterone: coexpression of mineralocorticoid receptors and 11 beta-hydroxysteroid dehydrogenase. J Clin Endocrinol Metab 79(5):1334-1341.

Kim BE, Leung DY, Boguniewicz M, Howell MD. 2008. Loricrin and involucrin expression is down-regulated by Th2 cytokines through STAT-6. Clin Immunol 126(3):332-337.

Kim JE, Kim BJ, Jeong MS, Seo SJ, Kim MN, Hong CK, *et al*. 2005. Expression and modulation of LL-37 in normal human keratinocytes, HaCaT cells, and inflammatory skin diseases. J Korean Med Sci 20(4):649-654.

King SR, Smith AG, Alpy F, Tomasetto C, Ginsberg SD, Lamb DJ. 2006. Characterization of the putative cholesterol transport protein metastatic lymph node 64 in the brain. Neuroscience 139(3):1031-1038.

Kishida T, Kostetskii I, Zhang Z, Martinez F, Liu P, Walkley SU, *et al*. 2004. Targeted mutation of the MLN64 START domain causes only modest alterations in cellular sterol metabolism. J Biol Chem 279(18):19276-19285.

Kono M, Nagata H, Umemura S, Kawana S, Osamura RY. 2001. In situ expression of corticotropin-releasing hormone (CRH) and proopiomelanocortin (POMC) genes in human skin. Faseb J 15(12):2297-2299.

Krueger KE, Papadopoulos V. 1990. Peripheral-type benzodiazepine receptors mediate translocation of cholesterol from outer to inner mitochondrial membranes in adrenocortical cells. J Biol Chem 265(25):15015-15022.

Krysko DV, Vanden Berghe T, D'Herde K, Vandenabeele P. 2008. Apoptosis and necrosis: detection, discrimination and phagocytosis. Methods 44(3):205-221.

Lambeth JD, McCaslin DR, Kamin H. 1976. Adrenodoxin reductase-adrenodexin complex. J Biol Chem 251(23):7545-7550.

Lambeth JD, Seybert DW, Kamin H. 1979. Ionic effects on adrenal steroidogenic electron transport. The role of adrenodoxin as an electron shuttle. J Biol Chem 254(15):7255-7264.

Langley RG, Krueger GG, Griffiths CE. 2005. Psoriasis: epidemiology, clinical features, and quality of life. Ann Rheum Dis 64 Suppl 2:ii18-23; discussion ii24-15.

Leigh IM, Purkis PE, Whitehead P, Lane EB. 1993. Monospecific monoclonal antibodies to keratin 1 carboxy terminal (synthetic peptide) and to keratin 10 as markers of epidermal differentiation. Br J Dermatol 129(2):110-119.

Leung DY, Boguniewicz M, Howell MD, Nomura I, Hamid QA. 2004. New insights into atopic dermatitis. J Clin Invest 113(5):651-657.

Liu J, Rone MB, Papadopoulos V. 2006. Protein-protein interactions mediate mitochondrial cholesterol transport and steroid biosynthesis. J Biol Chem.

Ludbrook LM, Harley VR. 2004. Sex determination: a 'window' of DAX1 activity. Trends Endocrinol Metab 15(3):116-121.

Malkinson FD, Lee MW, Cutukovic I. 1959. In vitro studies of adrenal steroid metabolism in the skin. J Invest Dermatol 32(2, Part 1):101-107.

Manna PR, Chandrala SP, Jo Y, Stocco DM. 2006. cAMP-independent signaling regulates steroidogenesis in mouse Leydig cells in the absence of StAR phosphorylation. J Mol Endocrinol 37(1):81-95.

Manna PR, Dyson MT, Jo Y, Stocco DM. 2009a. Role of dosage-sensitive sex reversal, adrenal hypoplasia congenita, critical region on the X chromosome, gene 1 in protein kinase A- and protein kinase C-mediated regulation of the steroidogenic acute regulatory protein expression in mouse Leydig tumor cells: mechanism of action. Endocrinology 150(1):187-199.

Manna PR, Dyson MT, Stocco DM. 2009b. Role of basic leucine zipper proteins in transcriptional regulation of the steroidogenic acute regulatory protein gene. Mol Cell Endocrinol 302(1):1-11.

Markova NG, Marekov LN, Chipev CC, Gan SQ, Idler WW, Steinert PM. 1993. Profilaggrin is a major epidermal calcium-binding protein. Mol Cell Biol 13(1):613-625.

McEnery MW, Snowman AM, Trifiletti RR, Snyder SH. 1992. Isolation of the mitochondrial benzodiazepine receptor: association with the voltage-dependent anion channel and the adenine nucleotide carrier. Proc Natl Acad Sci U S A 89(8):3170-3174.

McGrath JA. 2008. Filaggrin and the great epidermal barrier grief. Australas J Dermatol 49(2):67-73; quiz 73-64.

Menon GK, Feingold KR, Moser AH, Brown BE, Elias PM. 1985. De novo sterologenesis in the skin. II. Regulation by cutaneous barrier requirements. J Lipid Res 26(4):418-427.

Milewich L, Shaw CB, Sontheimer RD. 1988. Steroid metabolism by epidermal keratinocytes. Ann N Y Acad Sci 548:66-89.

Miller DB, O'Callaghan JP. 2002. Neuroendocrine aspects of the response to stress. Metabolism 51(6 Suppl 1):5-10.

Miller WL. 2005. Disorders of androgen synthesis--from cholesterol to dehydroepiandrosterone. Med Princ Pract 14 Suppl 1:58-68.

Miller WL. 2007. Steroidogenic acute regulatory protein (StAR), a novel mitochondrial cholesterol transporter. Biochim Biophys Acta 1771(6):663-676.

Monder C. 1991. Corticosteroids, receptors, and the organ-specific functions of 11 beta-hydroxysteroid dehydrogenase. Faseb J 5(15):3047-3054.

Monzon RI, LaPres JJ, Hudson LG. 1996. Regulation of involucrin gene expression by retinoic acid and glucocorticoids. Cell Growth Differ 7(12):1751-1759.

Morales A, Vilchis F, Chavez B, Morimoto S, Chan C, Robles-Diaz G, *et al*. 2008. Differential expression of steroidogenic factors 1 and 2, cytochrome p450scc, and steroidogenic acute regulatory protein in human pancreas. Pancreas 37(2):165-169.

MV Patel RF, JM Burrin. The regulation of steroidogenic acute regulatory (StAR) protein gene in human epidermal keratinocytes; 2002 2002; Birmingham, UK. p OC20.

Ngo MA, Sinitsyna NN, Qin Q, Rice RH. 2007. Oxygen-dependent differentiation of human keratinocytes. J Invest Dermatol 127(2):354-361.

Niakan KK, McCabe ER. 2005. DAX1 origin, function, and novel role. Mol Genet Metab 86(1-2):70-83.

O'Kane M, Murphy EP, Kirby B. 2006. The role of corticotropin-releasing hormone in immune-mediated cutaneous inflammatory disease. Exp Dermatol 15(3):143-153.

Ong PY, Ohtake T, Brandt C, Strickland I, Boguniewicz M, Ganz T, *et al*. 2002. Endogenous antimicrobial peptides and skin infections in atopic dermatitis. N Engl J Med 347(15):1151-1160.

Palmer CN, Irvine AD, Terron-Kwiatkowski A, Zhao Y, Liao H, Lee SP, *et al*. 2006. Common loss-of-function variants of the epidermal barrier protein filaggrin are a major predisposing factor for atopic dermatitis. Nat Genet 38(4):441-446.

Papadopoulos V, Berkovich A, Krueger KE. 1991a. The role of diazepam binding inhibitor and its processing products at mitochondrial benzodiazepine receptors: regulation of steroid biosynthesis. Neuropharmacology 30(12B):1417-1423.

Papadopoulos V, Berkovich A, Krueger KE, Costa E, Guidotti A. 1991b. Diazepam binding inhibitor and its processing products stimulate mitochondrial steroid biosynthesis via an interaction with mitochondrial benzodiazepine receptors. Endocrinology 129(3):1481-1488.

Papadopoulos V, Guarneri P, Kreuger KE, Guidotti A, Costa E. 1992. Pregnenolone biosynthesis in C6-2B glioma cell mitochondria: regulation by a mitochondrial diazepam binding inhibitor receptor. Proc Natl Acad Sci U S A 89(11):5113-5117.

Papadopoulos V, Mukhin AG, Costa E, Krueger KE. 1990. The peripheral-type benzodiazepine receptor is functionally linked to Leydig cell steroidogenesis. J Biol Chem 265(7):3772-3779.

Parthasarathy C, Balasubramanian K. 2008. Effects of corticosterone deficiency and its replacement on Leydig cell steroidogenesis. J Cell Biochem 104(5):1671-1683.

Patel MV, McKay IA, Burrin JM. 2001. Transcriptional regulators of steroidogenesis, DAX-1 and SF-1, are expressed in human skin. J Invest Dermatol 117(6):1559-1565.

Peters A, Schweiger U, Pellerin L, Hubold C, Oltmanns KM, Conrad M, *et al*. 2004. The selfish brain: competition for energy resources. Neurosci Biobehav Rev 28(2):143-180.

Piccirella S, Czegle I, Lizak B, Margittai E, Senesi S, Papp E, *et al*. 2006. Uncoupled redox systems in the lumen of the endoplasmic reticulum. Pyridine nucleotides stay reduced in an oxidative environment. J Biol Chem 281(8):4671-4677.

Proksch E, Brandner JM, Jensen JM. 2008. The skin: an indispensable barrier. Exp Dermatol.

Proksch E, Jensen JM, Elias PM. 2003. Skin lipids and epidermal differentiation in atopic dermatitis. Clin Dermatol 21(2):134-144.

Raffalli-Mathieu F, Orre C, Stridsberg M, Hansson Edalat M, Mannervik B. 2008. Targeting human glutathione transferase A3-3 attenuates progesterone production in human steroidogenic cells. Biochem J 414(1):103-109.

Reitz J, Gehrig-Burger K, Strauss JF, 3rd, Gimpl G. 2008. Cholesterol interaction with the related steroidogenic acute regulatory lipid-transfer (START) domains of StAR (STARD1) and MLN64 (STARD3). Febs J 275(8):1790-1802.

Rheinwald JG, Green H. 1975. Serial cultivation of strains of human epidermal keratinocytes: the formation of keratinizing colonies from single cells. Cell 6(3):331-343.

Rogoff D, Gomez-Sanchez CE, Foecking MF, Wortsman J, Slominski A. 2001. Steroidogenesis in the human skin: 21-hydroxylation in cultured keratinocytes. J Steroid Biochem Mol Biol 78(1):77-81.

Rone MB, Fan J, Papadopoulos V. 2009. Cholesterol transport in steroid biosynthesis: Role of protein-protein interactions and implications in disease states. Biochim Biophys Acta.

Roostaee A, Barbar E, Lehoux JG, Lavigne P. 2008. Cholesterol binding is a prerequisite for the activity of the steroidogenic acute regulatory protein (StAR). Biochem J 412(3):553-562.

Rousseau K, Kauser S, Pritchard LE, Warhurst A, Oliver RL, Slominski A, *et al*. 2007. Proopiomelanocortin (POMC), the ACTH/melanocortin precursor, is secreted by human epidermal keratinocytes and melanocytes and stimulates melanogenesis. Faseb J 21(8):1844-1856.

Rucinski M, Tortorella C, Ziolkowska A, Nowak M, Nussdorfer GG, Malendowicz LK. 2008. Steroidogenic acute regulatory protein gene expression, steroid-hormone secretion and proliferative activity of adrenocortical cells in the presence of proteasome inhibitors: in vivo studies on the regenerating rat adrenal cortex. Int J Mol Med 21(5):593-597.

Sasson R, Tajima K, Amsterdam A. 2001. Glucocorticoids protect against apoptosis induced by serum deprivation, cyclic adenosine 3',5'-monophosphate and p53 activation in immortalized human granulosa cells: involvement of Bcl-2. Endocrinology 142(2):802-811.

Schwarz T. 2000. No eczema without keratinocyte death. J Clin Invest 106(1):9-10.

Seguchi T, Cui CY, Kusuda S, Takahashi M, Aisu K, Tezuka T. 1996. Decreased expression of filaggrin in atopic skin. Arch Dermatol Res 288(8):442-446.

Sevilla LM, Nachat R, Groot KR, Klement JF, Uitto J, Djian P, *et al.* 2007. Mice deficient in involucrin, envoplakin, and periplakin have a defective epidermal barrier. J Cell Biol 179(7):1599-1612.

Sherbet DP, Papari-Zareei M, Khan N, Sharma KK, Brandmaier A, Rambally S, *et al.* 2007. Cofactors, redox state, and directional preferences of hydroxysteroid dehydrogenases. Mol Cell Endocrinol 265-266:83-88.

Silvestre JS, Robert V, Heymes C, Aupetit-Faisant B, Mouas C, Moalic JM, *et al.* 1998. Myocardial production of aldosterone and corticosterone in the rat. Physiological regulation. J Biol Chem 273(9):4883-4891.

Simard J, Ricketts ML, Gingras S, Soucy P, Feltus FA, Melner MH. 2005. Molecular biology of the 3beta-hydroxysteroid dehydrogenase/delta5-delta4 isomerase gene family. Endocr Rev 26(4):525-582.

Slominski A, Wortsman J, Foecking MF, Shackleton C, Gomez-Sanchez C, Szczesniewski A. 2002. Gas chromatography/mass spectrometry characterization of corticosteroid metabolism in human immortalized keratinocytes. J Invest Dermatol 118(2):310-315.

Slominski A, Wortsman J, Pisarchik A, Zbytek B, Linton EA, Mazurkiewicz JE, *et al.* 2001. Cutaneous expression of corticotropin-releasing hormone (CRH), urocortin, and CRH receptors. Faseb J 15(10):1678-1693.

Slominski A, Wortsman J, Tuckey RC, Paus R. 2007. Differential expression of HPA axis homolog in the skin. Mol Cell Endocrinol 265-266:143-149.

Slominski A, Zbytek B, Semak I, Sweatman T, Wortsman J. 2005a. CRH stimulates POMC activity and corticosterone production in dermal fibroblasts. J Neuroimmunol 162(1-2):97-102.

Slominski A, Zbytek B, Szczesniewski A, Semak I, Kaminski J, Sweatman T, *et al*. 2005b. CRH stimulation of corticosteroids production in melanocytes is mediated by ACTH. Am J Physiol Endocrinol Metab 288(4):E701-706.

Slominski A, Zbytek B, Szczesniewski A, Wortsman J. 2006. Cultured human dermal fibroblasts do produce cortisol. J Invest Dermatol 126(5):1177-1178.

Slominski A, Zjawiony J, Wortsman J, Semak I, Stewart J, Pisarchik A, *et al*. 2004. A novel pathway for sequential transformation of 7-dehydrocholesterol and expression of the P450scc system in mammalian skin. Eur J Biochem 271(21):4178-4188.

Slominski AT, Zmijewski MA, Semak I, Sweatman T, Janjetovic Z, Li W, *et al*. 2009. Sequential metabolism of 7-dehydrocholesterol to steroidal 5,7-dienes in adrenal glands and its biological implication in the skin. PLoS ONE 4(2):e4309.

Stigliano A, Gandini O, Cerquetti L, Gazzaniga P, Misiti S, Monti S, *et al*. 2007. Increased metastatic lymph node 64 and CYP17 expression are associated with high stage prostate cancer. J Endocrinol 194(1):55-61.

Stocco DM. 2001a. StAR protein and the regulation of steroid hormone biosynthesis. Annu Rev Physiol 63:193-213.

Stocco DM. 2001b. Tracking the role of a star in the sky of the new millennium. Mol Endocrinol 15(8):1245-1254.

Stocco DM, Clark BJ. 1996. Role of the steroidogenic acute regulatory protein (StAR) in steroidogenesis. Biochem Pharmacol 51(3):197-205.

Stocco DM, Sodeman TC. 1991. The 30-kDa mitochondrial proteins induced by hormone stimulation in MA-10 mouse Leydig tumor cells are processed from larger precursors. J Biol Chem 266(29):19731-19738.

Stoebner PE, Carayon P, Penarier G, Frechin N, Barneon G, Casellas P, *et al*. 1999. The expression of peripheral benzodiazepine receptors in human skin: the relationship with epidermal cell differentiation. Br J Dermatol 140(6):1010-1016.

Stojadinovic O, Lee B, Vouthounis C, Vukelic S, Pastar I, Blumenberg M, *et al*. 2007. Novel genomic effects of glucocorticoids in epidermal keratinocytes: inhibition of apoptosis, interferon-gamma pathway, and wound healing along with promotion of terminal differentiation. J Biol Chem 282(6):4021-4034.

Storbeck KH, Swart P, Swart AC. 2007. Cytochrome P450 side-chain cleavage: insights gained from homology modeling. Mol Cell Endocrinol 265-266:65-70.

Sugawara T, Holt JA, Driscoll D, Strauss JF, 3rd, Lin D, Miller WL, *et al*. 1995. Human steroidogenic acute regulatory protein: functional activity in COS-1 cells, tissue-specific expression, and mapping of the structural gene to 8p11.2 and a pseudogene to chromosome 13. Proc Natl Acad Sci U S A 92(11):4778-4782.

Suzuki T, Kasahara M, Yoshioka H, Morohashi K, Umesono K. 2003. LXXLL-related motifs in Dax-1 have target specificity for the orphan nuclear receptors Ad4BP/SF-1 and LRH-1. Mol Cell Biol 23(1):238-249.

Takahashi H, Manabe A, Ishida-Yamamoto A, Hashimoto Y, Iizuka H. 2002. Aberrant expression of apoptosis-related molecules in psoriatic epidermis. J Dermatol Sci 28(3):187-197.

Takeuchi S, Mukai N, Tateishi T, Miyakawa S. 2007. Production of sex steroid hormones from DHEA in articular chondrocyte of rats. Am J Physiol Endocrinol Metab 293(1):E410-415.

Tee MK, Lin D, Sugawara T, Holt JA, Guiguen Y, Buckingham B, *et al*. 1995. T-->A transversion 11 bp from a splice acceptor site in the human gene for steroidogenic acute regulatory protein causes congenital lipoid adrenal hyperplasia. Hum Mol Genet 4(12):2299-2305.

Temin HM, Mizutani S. 1970. RNA-dependent DNA polymerase in virions of Rous sarcoma virus. Nature 226(5252):1211-1213.

Thiboutot D, Jabara S, McAllister JM, Sivarajah A, Gilliland K, Cong Z, *et al*. 2003. Human skin is a steroidogenic tissue: steroidogenic enzymes and cofactors are expressed in epidermis, normal sebocytes, and an immortalized sebocyte cell line (SEB-1). J Invest Dermatol 120(6):905-914.

Thomson M. 2003. Does cholesterol use the mitochondrial contact site as a conduit to the steroidogenic pathway? Bioessays 25(3):252-258.

Thornton MJ. 2002. The biological actions of estrogens on skin. Exp Dermatol 11(6):487-502.

Tiala I, Suomela S, Huuhtanen J, Wakkinen J, Holtta-Vuori M, Kainu K, *et al*. 2007. The CCHCR1 (HCR) gene is relevant for skin steroidogenesis and downregulated in cultured psoriatic keratinocytes. J Mol Med 85(6):589-601.

Tichauer JE, Morales MG, Amigo L, Galdames L, Klein A, Quinones V, *et al*. 2007. Overexpression of the cholesterol-binding protein MLN64 induces liver damage in the mouse. World J Gastroenterol 13(22):3071-3079.

Tobin 2006. Biochemistry of human skin--our brain on the outside. Chem Soc Rec 35(1):52-67

Tomlinson JW, Stewart PM. 2001. Cortisol metabolism and the role of 11beta-hydroxysteroid dehydrogenase. Best Pract Res Clin Endocrinol Metab 15(1):61-78.

Tomlinson JW, Walker EA, Bujalska IJ, Draper N, Lavery GG, Cooper MS, *et al*. 2004. 11beta-hydroxysteroid dehydrogenase type 1: a tissue-specific regulator of glucocorticoid response. Endocr Rev 25(5):831-866.

Trakakis E, Loghis C, Kassanos D. 2009. Congenital adrenal hyperplasia because of 21-hydroxylase deficiency. A genetic disorder of interest to obstetricians and gynecologists. Obstet Gynecol Surv 64(3):177-189.

Trautmann A, Akdis M, Kleemann D, Altznauer F, Simon HU, Graeve T, *et al*. 2000. T cell-mediated Fas-induced keratinocyte apoptosis plays a key pathogenetic role in eczematous dermatitis. J Clin Invest 106(1):25-35.

Trautmann A, Akdis M, Schmid-Grendelmeier P, Disch R, Brocker EB, Blaser K, *et al*. 2001. Targeting keratinocyte apoptosis in the treatment of atopic dermatitis and allergic contact dermatitis. J Allergy Clin Immunol 108(5):839-846.

Tsujimoto Y, Shimizu S. 2000. VDAC regulation by the Bcl-2 family of proteins. Cell Death Differ 7(12):1174-1181.

Tsujishita Y, Hurley JH. 2000. Structure and lipid transport mechanism of a StAR-related domain. Nat Struct Biol 7(5):408-414.

Tuckey RC. 2005. Progesterone synthesis by the human placenta. Placenta 26(4):273-281.

Veenman L, Papadopoulos V, Gavish M. 2007. Channel-like functions of the 18-kDa translocator protein (TSPO): regulation of apoptosis and steroidogenesis as part of the host-defense response. Curr Pharm Des 13(23):2385-2405.

Vicanova J, Mommaas AM, Mulder AA, Koerten HK, Ponec M. 1996. Impaired desquamation in the in vitro reconstructed human epidermis. Cell Tissue Res 286(1):115-122.

Viegas LR, Hoijman E, Beato M, Pecci A. 2008. Mechanisms involved in tissue-specific apopotosis regulated by glucocorticoids. J Steroid Biochem Mol Biol 109(3-5):273-278.

Vinatzer U, Dampier B, Streubel B, Pacher M, Seewald MJ, Stratowa C, *et al*. 2005. Expression of HER2 and the coamplified genes GRB7 and MLN64 in human breast cancer: quantitative real-time reverse transcription-PCR as a diagnostic alternative to immunohistochemistry and fluorescence in situ hybridization. Clin Cancer Res 11(23):8348-8357.

Watari H, Arakane F, Moog-Lutz C, Kallen CB, Tomasetto C, Gerton GL, *et al*. 1997. MLN64 contains a domain with homology to the steroidogenic acute regulatory protein (StAR) that stimulates steroidogenesis. Proc Natl Acad Sci U S A 94(16):8462-8467.

Watt FM. 1998. Epidermal stem cells: markers, patterning and the control of stem cell fate. Philos Trans R Soc Lond B Biol Sci 353(1370):831-837.

West LA, Horvat RD, Roess DA, Barisas BG, Juengel JL, Niswender GD. 2001. Steroidogenic acute regulatory protein and peripheral-type benzodiazepine receptor associate at the mitochondrial membrane. Endocrinology 142(1):502-505.

Wolk K, Haugen HS, Xu W, Witte E, Waggie K, Anderson M, *et al*. 2009. IL-22 and IL-20 are key mediators of the epidermal alterations in psoriasis while IL-17 and IFN-gamma are not. J Mol Med.

Wrone-Smith T, Nickoloff BJ. 1996. Dermal injection of immunocytes induces psoriasis. J Clin Invest 98(8):1878-1887.

Yalow R. Radioimmunoassay: A probe for fine structure of biologic systems; 1977 08/12/1977.

Yalow RS, Berson SA. 1959. Assay of plasma insulin in human subjects by immunological methods. Nature 184 (Suppl 21):1648-1649.

Yamazaki T, Kowluru R, McNamara BC, Jefcoate CR. 1995. P450scc-dependent cholesterol metabolism in rat adrenal mitochondria is inhibited by low concentrations of matrix Ca2+. Arch Biochem Biophys 318(1):131-139.

Ying W. 2008. NAD+/NADH and NADP+/NADPH in cellular functions and cell death: regulation and biological consequences. Antioxid Redox Signal 10(2):179-206.

Yu XJ, Li CY, Dai HY, Cai DX, Wang KY, Xu YH, *et al*. 2007. Expression and localization of the activated mitogen-activated protein kinase in lesional psoriatic skin. Exp Mol Pathol 83(3):413-418.

Zanaria E, Muscatelli F, Bardoni B, Strom TM, Guioli S, Guo W, *et al*. 1994. An unusual member of the nuclear hormone receptor superfamily responsible for X-linked adrenal hypoplasia congenita. Nature 372(6507):635-641.

Zazopoulos E, Lalli E, Stocco DM, Sassone-Corsi P. 1997. DNA binding and transcriptional repression by DAX-1 blocks steroidogenesis. Nature 390(6657):311-315.

Zmijewski MA, Sharma RK, Slominski AT. 2007. Expression of molecular equivalent of hypothalamic-pituitary-adrenal axis in adult retinal pigment epithelium. J Endocrinol 193(1):157-169.